NASA SP-395

SECOND NASA CONFERENCE ON LASER ENERGY CONVERSION

A conference held at

NASA AMES RESEARCH CENTER

Moffett Field, California

January 27–28, 1975

NATIONAL AERONAUTICS AND SPACE ADMINISTRATION

NASA SP-395

SECOND NASA CONFERENCE ON LASER ENERGY CONVERSION

Proceedings of a conference held at the
NASA Ames Research Center, Moffett Field,
California, on January 27–28, 1975

Edited by
Kenneth W. Billman

Scientific and Technical Information Office 1976
NATIONAL AERONAUTICS AND SPACE ADMINISTRATION
Washington, D.C.

For sale by the National Technical Information Service
Springfield, Virginia 22161
Price – $7.00

PREFACE

Approximately 75 scientists gathered at Ames Research Center, NASA, Moffett Field, California on 27-28 January 1975 to attend the 2nd NASA Conference on Laser Energy Conversion. They heard the presentations of 18 technical papers and participated enthusiastically in the discussions that followed. It was generally agreed, and evidenced by comments made during the final summary discussion, that they were both informed and stimulated by the results of initial studies and developments made in certain converter areas, by the advances made in ancillary devices and techniques, and by the possibilities of the more speculative approaches to this newly developing area of advanced technology.

Why hold a laser energy conversion conference? To answer this we must first answer another question: why is NASA interested in laser power transmission? Quite simply because it may ultimately allow space missions which would be impossible by other means. For example, it could lower costs – an important consideration for the acceptance of a new mission. Space solar cell systems now cost between $2,000 to $5,000 per electrical watt delivered and there is also a large launch weight of about 0.05 kg/W associated with large solar arrays. Furthermore, the low available solar engery makes solar cell systems impractical for outer planet missions – thus requiring radioisotope thermoelectric generators. These are even more expensive, about $20,000/W, have low efficiency (which translates into large mass for a given power delivered – and perhaps less experimental payload as a consequence) of 5-6 percent, and their radioactive emission can adversely affect some payloads. Nevertheless, partly because of these constraints, most satellites of the 1970s and 1980s will only need 1-3 kW and these sources will be adequate. But for direct broadcast and manned laboratory craft, and especially in the late 1980s and onward, the necessary larger power demands will probably require nuclear reactors.

Hence, it seems logical to ask whether a laser system, either ground-based or in orbit, offers a practical solution to some of these problems of cost, weight, radioactivity, and perhaps even propulsion. The laser system would generate power in the form of low-divergence electromagnetic waves that would be transmitted sequentially to a number of satellites where the laser energy would be converted to the form – electrical, storable chemical, shaft horsepower, or propulsion – necessary for the satellite operation. In addition, one might also ask whether such a laser system would provide entirely new possibilities in space science or application, beyond its task of transmitting power.

Clearly, these possibilities must be considered within the harsh reality of engineering feasibility and cost comparison with the aforementioned alternatives. It is necessary to study possible laser power transmission missions and to accurately predict the advanced technology necessary for them. Initial studies indicated that such power transmission would be competitive. Of course, it had to meet the obvious specifications: the overall system efficiency (which determines the necessary launch weight for a given transmitted power) had to be reasonable, and it had to function reliably in the hostile temperature and radiation environment of space. Early assessment of the essential components of such a system indicated where advanced technology development was necessary. The laser required improvement in several areas: output power; efficiency (ratio of output electromagnetic energy to input energy) without resorting to cryogenic cooling; closed-cycle, long-term operation; and, hopefully, shorter wavelength to minimize the beam divergence ($\simeq$ laser wavelength/diameter of transmitting optics) or the size of the transmitting and receiving optics.

Fortunately, this "wish list" did not need fulfillment in entirety for some missions. It was foreseen, and indeed it is happening, that definite progress is being made on most of these items. A second component, the transmitting optics, also required development, but just as was true for the laser, some prior work in the area made this tenable. However, in the final component – the laser energy converter – the picture was not bright. The high intensity laser radiation, certainly much greater than solar intensity (Ca. 0.14 W/cm^2), possibly at infrared wavelengths, such as 10.6 μ for the CO_2 laser, presented new requirements and possibilities, such as coherence and narrow wavelength spread, that did not appear consistent with existing optical detectors. There was speculation on various fronts, such as simply using the laser beam like a fossil fuel, that is, to supply raw heat to a thermopile or a steam engine, or to convert it with photovoltaic devices such as advanced p/n junction solar cells or HgCdTe diodes. Indeed on one item all agreed: if laser power transmission was to succeed, either in space or on Earth, a new converter technology needed development and sponsorship.

Thus the first conference on this topic was held at Ames in January 1973. Its dual purpose was first, to acquaint the scientific community of NASA's interest in this area, and secondly, to have experts in the various disciplines of electromagnetic detection and energy related areas assess the existing status and point out the directions in which the efforts should move. The present meeting was designed to examine some hard engineering data on subsequent pursuits, and to again examine some potential new areas needing investigation. Of course, concurrent developments in the other elements of the laser power transmission system can significantly influence the necessary converter characteristics. Thus, limited conference time was devoted to papers presenting the outlook in these areas.

The success of the conference was assured by the expertise and energy that all of the participants brought to it, but it was achieved more easily because of guidance provided by many individuals. Among these, special mention should be made of Dr. Hans Mark (Director, Ames), Mr. C. Frederick Hansen (Ames), and Carl Schwenk (NASA Headquarters). Finally, we wish to acknowledge the secretarial assistance of Mrs. Kay Lemon whose skills contributed greatly to the smooth operation and enjoyment of the conference.

Dr. Kenneth W. Billman
Assistant Chief, Physical
Gasdynamics and Lasers Branch
Ames Research Center, NASA

TABLE OF CONTENTS

TABLE OF CONTENTS (Continued)

CONFERENCE PARTICIPANTS

Dr. Winfield H. Arata, Jr.
Northrop Corporation
1701 No. Ft. Myer Drive, Suite 1208
Arlington, Virginia 22209

Dr. M.L. Bhaumik
Northrop Corporation
3401 W. Broadway
Hawthorne, California 90250

Dr. Kenneth W. Billman
NASA-Ames Research Center
Mail Stop 230-3
Moffett Field, California 94035

Professor William R. Bottoms
School of Engineering and Applied Sciences
Princeton University
Princeton, New Jersey 08540

Dr. Stuart W. Bowen
NASA-Ames Research Center
Mail Stop 230-3
Moffett Field, California 94035

Dr. Ernest G. Brock
Los Alamos Scientific Laboratory
P.O. Box 1663
Los Alamos, New Mexico 87544

Dr. Philip S. Brody
Department of the Army
Harry Diamond Laboratories
2800 Powder Mill Road
Adelphi, Maryland 20783

Dr. N.E. Buholz
Lockheed Missiles and Space Company
B-151
P.O. Box 504
Sunnyvale, California 94086

Professor Robert Byer
Stanford University
Applied Physics Department
Stanford, California 94305

Dr. George E. Caledonia
Physical Sciences, Inc.
18 Lakeside Office Park
Wakefield, Massachusetts 01880

Dr. Dean R. Chapman
NASA-Ames Research Center
Mail Stop 200-4
Moffett Field, California 94035

Dr. Arthur Cohn
Electric Power Research Institute
3412 Hillview Avenue
Palo Alto, California 94304

David M. Cooper
NASA-Ames Research Center
Mail Stop 230-3
Moffett Field, California 94035

Gerald Dzakowic
Lawrence Livermore Laboratory
Box 808
Livermore, California 94550

Dr. Don Eckstrom
Stanford Research Institute
333 Ravenswood
Menlo Park, California 94025

Dr. James E. Etter
Hughes Research Laboratories
3011 Malibu Canyon Road
Malibu, California 90265

S.M. Faris
University of California – Berkeley
Berkeley, California 94720

Dr. Max Garbuny
Westinghouse Research Laboratories
Pittsburgh, Pennsylvania 15235

Dr. Kenya Goto
Toshiba Research and Development Center
1, Komukai Toshiba-Cho
Saiwai-ku, Kawasaki-City
Kanagawa, 210, Japan

Dr. Malcolm Gower
NASA-Ames Research Center
Mail Stop 230-3
Moffett Field, California 94035

Professor T. Kenneth Gustafson
Department of Electrical Engineering and
Computer Sciences
University of California – Berkeley
Berkeley, California 94720

C. Frederick Hansen
NASA-Ames Research Center
Mail Stop 230-3
Moffett Field, California 94035

Dr. Lorin K. Hanson
Rasor Associates
420 Persian Drive
Sunnyvale, California 94086

Professor Abraham Hertzberg, Director
Aerospace Research Laboratory FL-10
University of Washington
Seattle, Washington 98195

Dr. Robert V. Hess
NASA-Langley Research Center
Mail Code 193-A
Hampton, Virginia 23365

Dr. Robert M. Hill
Stanford Research Institute
Building 106-B
Menlo Park, California 94025

Joseph Horwath
Lockheed Missiles and Space Company
Department 6230
Building 151
P.O. Box 504
Sunnyvale, California 94086

Dr. Cheng-Chung Huang
Lockheed Missiles and Space Company
Department 6230
Building 151
Sunnyvale, California 94086

Dr. L.K. Isaacson
Electric Power Research Institute
P.O. Box 10412
Palo Alto, California 94304

Tatsuo Izawa
University of California – Berkeley
Berkeley, California 94720

Dr. Gareth M. Janney
Hughes Research Laboratories
3011 Malibu Canyon Road
Malibu, California 90265

Professor Ali Javan
Physics Department
Massachusetts Institute of Technology
Cambridge, Massachusetts 02139

Dr. Thomas W. Karras
General Electric Space Sciences
Box 8555
Philadelphia, Pennsylvania

Donald M. Kuehn
NASA-Ames Research Center
Mail Stop 230-3
Moffett Field, California 94035

Dr. Gary Langford
Stanford Research Institute
Menlo Park, California 94025

George Lee
NASA-Ames Research Center
Mail Stop 230-3
Moffett Field, California 94035

Dr. Michael Lieber
University of Arkansas
Physics Department
Fayetteville, Arkansas 72701

Dr. Kenneth Lincoln
NASA-Ames Research Center
Mail Stop 234-1
Moffett Field, California 94035

Randy Linebarger
Lockheed Missiles and Space Company
Department 6230
Building 151
Sunnyvale, California 94088

Homer Lohr
Lawrence Livermore Laboratory
Box 808
Livermore, California 94550

John Lundell
NASA-Ames Research Center
Mail Stop 234-1
Moffett Field, California 94035

Dr. Joseph Lundholm
NASA Headquarters
Code RR
Washington, D.C. 20546

Robert L. McKenzie
NASA-Ames Research Center
Mail Stop 230-3
Moffett Field, California 94035

Professor Richard B. Miles
School of Engineering and Applied Sciences
Princeton University
Princeton, New Jersey 08540

Daryl Monson
NASA-Ames Research Center
Mail Stop 230-3
Moffett Field, California 94035

Donald L. Nored
NASA-Lewis Research Center
Mail Stop 500-318
21000 Brookpark Road
Cleveland, Ohio 44135

Dr. Thomas Olson
Maxwell Laboratories
9244 Balboa Avenue
San Diego, California 92123

Dr. John Osmundson
Lockheed Missiles and Space Company
Department 6230
Building 151
Sunnyvale, California 94043

Professor Richard Pantell
Stanford University
McCullough Building, Room 308
Stanford, California 94305

Dr. Demos Papailiou
Jet Propulsion Laboratory
Mail Stop 122-123
4800 Oak Grove Drive
Pasadena, California 91103

Dr. Martin Pechersky
Westinghouse Research Laboratories
Pittsburgh, Pennsylvania 15235

Dr. Ned S. Rasor
Rasor Associates
420 Persian Drive
Sunnyvale, CAlifornia 94086

Dr. James K. Rice
Sandia Laboratories
P.O. Box 5800, Division 5216
Albuquerque, New Mexico 87115

Robert E. Ricles
W.J. Schafer Associates
14 Lakeside Office Park
Wakefield, Massachusetts 01880

Paul D. Rowley
NASA-Ames Research Center
Mail Stop 230-3
Moffett Field, California 94035

Dr. Gary R. Russell
Jet Propulsion Laboratory
4800 Oak Grove Drive
Pasadena, California 91103

C. Tim Ryan
University of California – Berkeley
Berkeley, California 94720

Walter J. Schafer
W.J. Schafer Associates
14 Lakeside Office Park
Wakefield, Massachusetts 01880

Dr. Chiao-Yao She
Colorado State University
Physics Department
Fort Collins, Colorado 80523

Dr. K. Shimada
Jet Propulsion Laboratory
Mail Stop 198-326
4800 Oak Grove Drive
Pasadena, California 91103

Dr. Sandra H. Slivinsky
Lockheed Missiles and Space Company
Department 6230
Building 151
Sunnyvale, California 94088

Dr. G. Srinivasan
NASA-Ames Research Center
Mail Stop 230-3
Moffett Field, California

James R. Stallcop
NASA-Ames Research Center
Mail Stop 230-3
Moffett Field, California 94035

Dr. Richard Stirn
Jet Propulsion Laboratory
Mail Stop 198-326
4800 Oak Grove Drive
Pasadena, Californai 91103

Dr. George Sutton
AVCO Everett Research Laboratory
Everett, Massachusetts 02149

Dr. Leroy Thielman
Lockheed Missiles and Space Company
Department 6230
Building 151
Sunnyvale, California 94088

Dr. Karlheinz Thom
NASA Headquarters
Code RR
Washington, D.C. 20546

Norman L. Thomas
NASA-Ames Research Center
Mail Stop 244-13
Moffett Field, California 94035

Dr. Kurt L. Wray
Physical Sciences, Incorporated
18 Lakeside Office Park
Wakefield, Massachusetts 01880

Dr. Mark S. Wrighton
Department of Chemistry
Massachusetts Institute of Technology
Cambridge, Massachusetts 02139

Dr. Chung-Yung Robert Wu
Department of Chemistry
University of Southern California
Los Angeles, California 90007

Dr. S.V. Yadavalli
Stanford Research Institute
333 Ravenswood Avenue
Menlo Park, California 94025

BRIEF OVERVIEW OF THE CONFERENCE

Kenneth Billman, Ames Research Center

In an overview of the NASA High Intensity Laser Program, Joseph Lundholm, NASA Headquarters, outlined the general objective: to examine the possible transmission of high power laser beams over long distances and their conversion to thrust, electricity, or other useful forms of work. Each NASA Center is providing the necessary technology base to evaluate the potential for NASA missions and applications. Selected system technology studies are to begin in 1978 and, if these warrant it, prototype development is to begin in 1980.

A new area of conversion – laser-induced chemistry – was considered by two groups. The common goal was to effect a means of converting laser energy to storable chemical energy, namely hydrogen and oxygen. Initial experimental results and theoretical considerations make this approach appear feasible and worthy of continued research.

Significant developments in photovoltaics were reported. Modification of the Schottky barrier device has increased efficiency up to 30 percent for 0.5-μm laser radiation. Cost may be reduced; however, the potential wavelength coverage of 0.4–1.5 μm will not overlap the high efficiency IR lasers. Another novel report was the generation of high voltage emf's by laser irradiation of piezoelectric ceramics.

Solid progress in the optical diode area was also reported, especially in the areas of theoretical modeling, measurement of antenna characteristics, and initial attempts at array fabrication. Although the possible ultimate practicality of this detector for laser power transmission is not yet certain, the scientific spin-off into many areas is impressive.

Mission studies based on laser energy conversion to either electricity or thrust were reported by Donald Nored. Optical dimensions and mass remain a severe problem for long range (e.g. 36,000 km) transmission of the IR laser wavelengths usually considered for power transmission. Various laser-rocket propulsion missions were discussed, as well as the areas that need investigation in the engine itself. A companion paper pointed out the advantages of using a high pressure molecular absorber as an effective means of converting laser radiation to gas translational energy for generation of shaft horsepower or propulsion over inverse bremsstrahlung absorption.

The initial studies on the thermo electronic laser energy converter (TELEC) are encouraging. This device is a form of thermionic converter in which the laser heats the plasma by inverse bremsstrahlung absorption. Although bulky, without folded optics, the calculated efficiencies are about 45 percent using state-of-the-art materials and fabrication. Another paper, on an LPD converter, seems to indicate that this device holds little promise for reasonable efficiency.

A series of short papers examined the "outlook" for various techniques and devices that can influence the necessary characteristics of the laser energy converter. The extremely interesting possibility of constructing an optical klystron that provides large power optical gain was the first of these. Certainly the possiblities, for an Earth-based laser mission, warrant a continued examination of this concept. A possibility of harmonic conversion of IR laser radiation in molecular gases was considered in a second paper. Very reasonable efficiencies (10-30 percent) were predicted and

experimentation should proceed. The NASA/Langley group, pointed to a recent study showing enhanced vertical and horizontal atmospheric transmission by tuning ($\simeq$ 5 GHz) a CO_2 laser off the CO_2 absorption lines, and reported on the development of such a tunable laser for experimental confirmation. Gary Russell reported on the recent, significant advances in the metallic vapor laser. He has achieved 1 percent efficiency with a copper halide lasant (λ = 5107 Å), achieving power output per pulse of 1.7 kW/cm^3 of discharge volume. Finally, the recent success in direct nuclear pumping of a Xe:He mixture in a joint NASA/LASL experiment was reported. Overall efficiency is not high, although it will undoubtedly improve, and nuclear-pumped devices may be competitive with more efficient space-based lasers if one includes their necessary power source.

The session on photon engines was, as usual, very interesting. Professor Hertzberg has found his older photon engine concept (reversing laser action) to have little possibility of achieving high efficiency. However, in a new approach he uses the "Energy Exchanger" to essentially construct a heat engine operating at very high temperatures but with the engine walls only seeing the average temperature – thus high thermal efficiencies ($>$ 60 percent) are expected. Max Garbuny examined the general class of laser-driven engines and concluded that the piston engine offers many practical advantages. Again, under the known constraints of materials, absorbers, window materials (sapphire), etc. he predicts thermal efficiencies $>$ 60 percent for laser wavelengths less than 5.5 μ. Finally, Robert Byer reported on an actual set of preliminary experiments which he and his students carried out on a laser-driven Stirling engine.

In summary, the conference has shown encouraging developments in many areas. Clearly, for direct conversion to electrical energy, the Schottky barrier device holds a lead. However, it will not work for wavelengths exceeding about 1.5 μm. A second fact that was appreciated, for the TELEC, laser-driven engines, rockets, etc. is the need for a high strength optically transmissive window. Sapphire is satisfactory up to laser wavelengths of 5.5 μm; diamond will transmit CO_2 radiation but can only be obtained in small dimensions. Of course, if the harmonic conversion technique proves feasible for the CO_2 laser, it may alleviate this problem. Finally, the thermal efficiencies predicted for the laser engines look very impressive.

Certainly many concepts have reached the stage of demanding engineering design and laboratory tests. But to do this is an effective way, the necessary operating characteristics and constraints must be clearly defined. Although complicated by not knowing the "ultimate" laser to be used, the energy converter designers must now be provided this information from the mission studies.

AMES GREETING

2ND NASA CONFERENCE ON LASER ENERGY CONVERSION

Dr. Dean R. Chapman, Director, Astronautics Directorate

As Ken has indicated, in the absence of our Director, Hans Mark, it is my pleasure to extend to everyone a cordial welcome to the 2nd NASA Conference on Laser Energy Conversion. As he also mentioned, those of us who are on the NASA staff here will be very happy to do whatever we can to make your stay a pleasant one so don't hesitate to call on us.

At the first conference on laser energy conversion two years ago this month, I was able to attend only some of the sessions so I took the opportunity recently to look over the proceedings of that conference. There were four things that attracted my attention.

First was that, although the purpose of the NASA high intensity laser program was then stated to be to discover suitable applications in space, one particular application, namely long-range power transmission was singled out to focus on, recognizing that there was no specific NASA mission that requried such a system, and that the research done in this area would, therefore, be of rather long range or of basic character. I think it will be interesting to see if two years later at the end of this conference, we might be approaching more closely the definition of such a mission.

Second, I noticed that it was fully recognized two years ago, that a number of key elements would be involved in such a transmission system, such as highly efficient lasers with closed-cycle operation, short wavelengths, and good modal quality. But the one that was signaled out as being the bottleneck was efficient laser energy conversion, hence, the subject of the conference. I think it will be interesting to see if, two years later, this prospective is still the case.

Third, I noticed there was discussion of at least two or three different methods that appeared to offer the potential of achieving efficiencies approaching fifty percent. I think it will be interesting to see if our goals **now**, two years later, are about the same or if, perhaps, they are hopefully a little higher.

Fourth, and really of greatest interest to me as one involved in management of research at this Center, I noticed that in a number of the discussion sessions following the papers, there was, time and time again, the expression of concern over dwindling support for basic research. I think it will be interesting to see if during this conference similar expressions appear. From my own vantage point, I think the situation is at least no worse than it was two years ago. In one respect it may even be a little better. There have been, of course, two major changes that affected this situation in the last two years. The first, of course, is the energy crisis that started in the winter of 1973, and has been apparent to everybody and in a peripheral way to anyone working in energy related fields. Of course it also brought about the obvious second change – the effect on the economy of this country which, as we are all well aware, placed a lot of perspective on the federal budget and some pressure on NASA's budget, and hence pressure on the budget available for basic research. So, clearly I believe we are in an environment where we cannot work simultaneously on *all* aspects of interest in a research field. We have to be selective. I think that it is in this regard that the deliberations at this conference can be of great value to those of us who are in management at

NASA: making sure we are applying the best collective judgement of those who are working in this field in order to make the right selections.

In closing, I would like to again say welcome to the Ames Research Center. I hope you will enjoy your stay here and find the conference to be profitable.

OVERVIEW OF THE NASA HIGH POWER LASER PROGRAM

Joseph G. Lundholm

NASA Headquarters

Good Morning! It is a pleasure to take part in this Second Conference on Laser Energy Conversion. I will take the liberty of speaking for the audience in stating that we all appreciate the hospitality that Dean Chapman extended to us. We also appreciate the efforts that Fred Hansen and Ken Billman have expended in setting up this conference. I am sure that we are all looking forward to two days of interesting and challenging interchange between those of you who have been busy pushing back the frontiers in the laser field since the last conference. I hope that each of you will take an active part in this conference since I believe the success of this meeting is equally dependent on the speakers and the listeners. At the wrap-up panel discussion, I suspect that Ken Billman and I may be questioning many of you to obtain your opinion on how we should proceed and where we should place our efforts during the next two years.

A number of changes in personnel have occurred in the last two years. The most significant change is that Carl Schwenk, who was slated to give this talk, was named Director of the Research Division which was established in the Office of Aeronautics and Space Technology in August 1973. At the present time, Dr. Karl Thom, one of the speakers tomorrow, and I are program managers in this division. Dr. Thom manages the photonics and energetics programs and I manage the high power laser and thermionic power conversion systems programs.

At this point, I believe it is appropriate to reiterate the overall objectives of the *NASA* High Power Laser Program, to quickly review its structure and center responsibilities, make a few comments regarding present and future funding, and last but not least, to briefly examine the possible pace of the program.

Figure 1 shows the recommendations formulated by the AD HOC Laser Advisory Committee in 1971. We still believe that high power lasers will eventually prove useful for space missions.

Figure 2 lists the program objectives. In all cases, the overall thrust of our efforts is directed at the long range transmission of high power laser beams which are then converted to propulsive thrust or electrical power.

The next two figures 3 and 4 portray the elements of the laser power transmission program. You should note that the program is structured to provide for research on each of the key areas in order to build the required technology base which must exist in order to decide the essential issues before proceeding with prototype systems development for a space mission. This approach is illustrated in figure 5. We are able to take advantage of the DOD work, especially in the area of coherent adaptive optical technology (coat) and by attending DOD major planning and review meetings and by interacting with their contractors.

Figure 6 shows the major activity that each center is focusing on. We consider ARC the lead center for laser-energy conversion, LaRC the lead center for propagation research and LeRC the lead center for systems technology and large optical arrays.

Figure 7 shows the program targets as prepared for the FY 1976 budget and RTOP cycle. I believe it is important that you recongize the time frame we indicate we are working toward. Perhaps this aspect of the program plan should be considered in the panel summary discussion tomorrow afternoon[1].

Figure 8 lists six selected program highlights that I felt would be of special interest to you. One conclusion that I draw is that in the last few years we have gotten organized and proceeded to implement selected plans. We are now about to settle down to even more serious efforts, the success of which will be the major factor in decisions that are identified as being made around 1980.

Figure 9 is a gross schedule chart. It is a chart that is more than a year old and I deliberately did not update it. The chart indicates that by the end of this calendar year we would have narrowed down our efforts to selected systems technology. It may be necessary to do some narrowing in order to provide increased funding to concepts that appear most promising; however, I foresee this as a difficult step at this stage of the program.

The funding level for FY 1976 is presently stated to be at the same level as this year. Not until congress appropriates our funds later this year will we know how we fared.

At the present time, it appears our progess has been satisfactory. What we must all remember is that the years pass rather quickly and the 1980 time period will arrive before we realize it unless we continually assess our progress against our stated goals and schedules.

Now I am ready to listen to the researchers – the people who will have to do the work that we all hope will give us a successful program.

Ken, again we wish to thank you for getting us together for this conference. I hope all of us will pitch in with enthusiasm and help make the next two days both interesting and – perhaps – even a little exciting.

Thank You.

---

[1]With reference to figure 7, High Power Laser Systems Program Targets, the last item – "Complete Evaluation of Applications for High Power Laser Systems to Assess Progress, Goals, and Benefits to NASA Missions by FY 80", – could be interpreted incorrectly to mean that research and technology efforts would cease after FY 1980. Even if a NASA space mission application requiring a high power laser system has been identified and work is initiated on a prototype unit, it is presently believed that R&T efforts would continue at an appropriate funding level.

- HIGH-POWER LASERS WILL BE IMPORTANT TO NASA
  - NEED FOCUS FOR HIGH ENERGY LASER R&D AND APPLICATIONS STUDIES WITHIN NASA
  - NEED MAJOR EFFORT IN R&D PROGRAMS AND APPLICATIONS STUDIES
  - BOTH SPACE-BASED AND GROUND-BASED LASERS FOR POSSIBLE NASA APPLICATIONS
- DIRECT LINK TO DOD ACTIVITIES ON HIGH ENERGY LASERS IS CRUCIAL

Figure 1.– Recommendations (from Ad Hoc Laser Advisory Committee).

- EVALUATE TECHNICAL PROBLEMS OF CLOSED-LOOP CO_2 LASER SYSTEM. CONTINUE RESEARCH THROUGH FY 76
- INVESTIGATE POTENTIAL NEW LASER CONCEPTS THROUGH FY 76
- GENERATE AND INVESTIGATE NOVEL MEANS TO CONVERT LASER BEAMS INTO THRUST OR ELECTRICITY WITH AN EFFICIENCY GREATER THAN 50% THROUGH FY 76-79
- ESTABLISH LIMITS FOR TRANSMITTING LASER BEAMS THROUGH ATMOSPHERE UNDER ALL CONDITIONS BY FY 77
- COMPLETE EVALUATION OF APPLICATIONS FOR HIGH POWER LASER SYSTEMS TO ASSESS PROGRESS, GOALS, AND BENEFITS TO NASA MISSIONS BY FY 80

Figure 2.– High power laser systems technology.

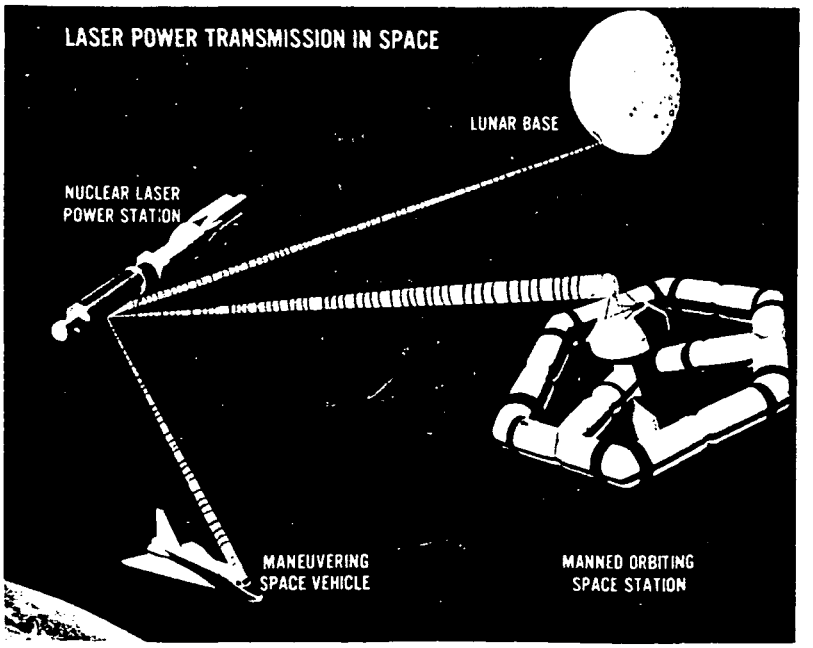

Figure 3.– Laser power transmission in space.

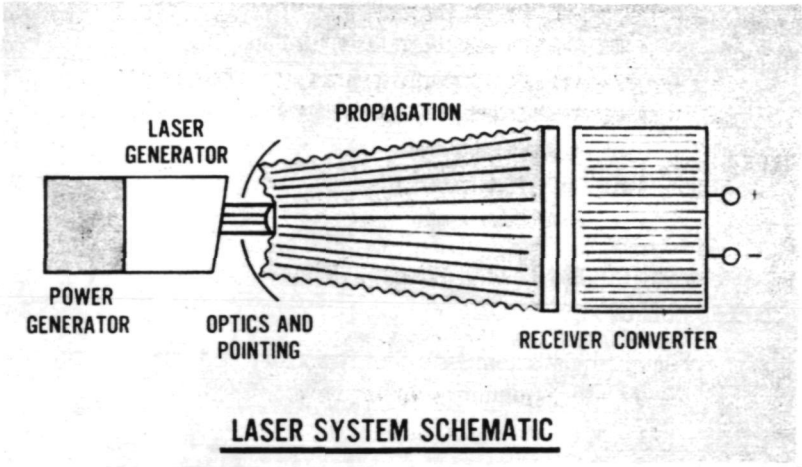

Figure 4.– Elements of laser power transmission system.

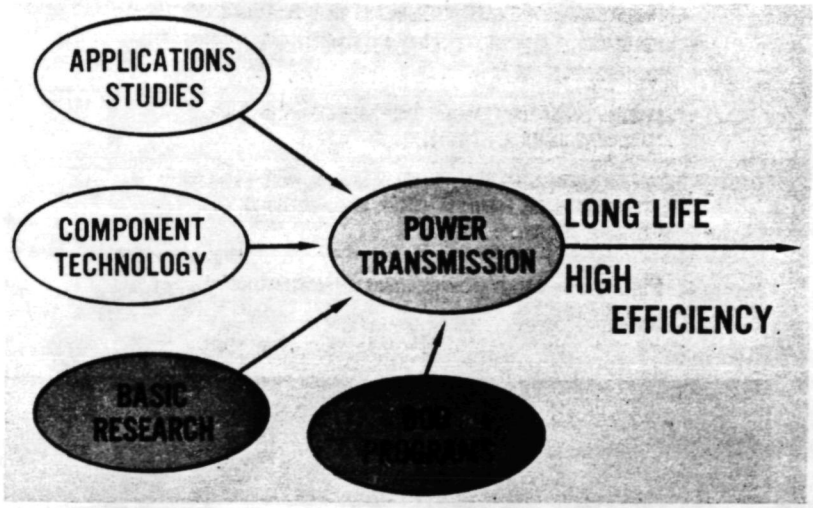

Figure 5.– Program perspective.

AMES RESEARCH CENTER
- NEW LASER CONCEPTS
- CONVERTER RESEARCH

LANGLEY RESEARCH CENTER
- PROPAGATION RESEARCH

LEWIS RESEARCH CENTER
- LASER SYSTEM TECHNOLOGY
- CONVERTER TECHNOLOGY
- NEW LASER CONCEPTS
- LARGE OPTICAL SYSTEMS TECHNOLOGY

JET PROPULSION LABORATORY
- NEW LASER CONCEPTS
- CONVERTER RESEARCH

Figure 6.– Center roles NASA high power laser systems program.

PROGRAM OBJECTIVE

THE TRANSMISSION OF HIGH POWER LASER BEAMS OVER LONG DISTANCES AND CONVERSION TO THRUST OR ELECTRICITY

- EVALUATE POTENTIAL OF HIGH POWER LASERS FOR NASA MISSIONS AND APPLICATIONS
  - PROVIDE TECHNOLOGY BASE NEEDED TO MAKE THIS EVALUATION
- DEMONSTRATE POTENTIAL UTILITY OF HIGH POWER LASERS FOR SELECTED APPLICATIONS

Figure 7.– High power laser systems program targets as listed in FY 76 (program and specific objectives document).

- LERC PILOT LASER LOOP EXPECTED TO BE OPERATING IN FEW MONTHS
- STUDY CONTRACTS ON 30 METER SPACE BASED AND 5-6 METER GROUND BASED ADAPTIVE OPTICAL ARRAYS INITIATED BY LERC
- COPPER LASER TECHNOLOGY ADVANCED BY RUSSELL OF JPL
- NUCLEAR-PUMPED LASER OPERATED AT LASL
- PULSED HIGH PRESSURE OPERATION OF CO_2 LASER PROVIDES BROADENING OF LASER LINES – PERMITS TUNING LASER "OFF" ATMOSPHERIC ABSORPTION LINES FOR IMPROVED ATMOSPHERIC TRANSMISSION PROPOSED BY HESS AND SEALS OF LARC
- SECOND CONFERENCE ON LASER-ENERGY CONVERSION AT ARC

Figure 8.– Selected high power laser systems program high-lights.

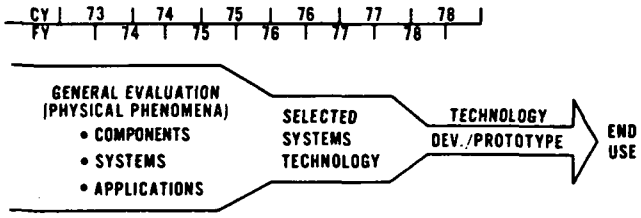

Figure 9.– Laser power system research and technology general schedule.

CONVERSION OF LASER ENERGY TO CHEMICAL ENERGY BY THE PHOTOASSISTED ELECTROLYSIS OF WATER

Mark S. Wrighton

Massachusetts Institute of Technology

ABSTRACT

Ultraviolet irradiation (351, 364 nm) of the n-type semiconductor TiO_2 crystal electrode of an aqueous electrochemical cell evolves O_2 at the TiO_2 electrode and H_2 at the Pt electrode. The gases are typically evolved in a 2:1 (H_2:O_2) volume ratio. The photo-assisted reaction seems to require applied voltages, but values as low as 0.25 V do allow the photo-assisted electrolysis to proceed. Prolonged irradiation in either acid or base evolves the gaseous products in amounts which clearly demonstrate that the reaction is catalytic with respect to the TiO_2. The wavelength response of the TiO_2 and the correlation of product yield and current are reported. The results support the claim that TiO_2 is a true photo-assistance agent for the electrolysis of water. Minimum optical storage efficiencies of the order of 1 percent can be achieved by the production of H_2.

INTRODUCTION

The efficient conversion of optical energy to chemical energy is a problem of great interest. Despite the fact that solid state solar cells have reached a high level of development there is still considerable merit in achieving the direct conversion of optical energy into chemical energy. The reasons for this are severalfold and include the desire to have abundant high energy chemicals for use as fuels and for use in industrial chemical synthesis. Additionally, in view of the rather limited amount of detailed knowledge concerning direct photoproduction of high-energy materials, it is appropriate to undertake fundamental research aimed toward establishing what can be done and how efficiently it can be done. The reaction indicated in (1) is among the many possible chemical reactions of importance in the conversion of optical energy to chemical energy. The standard heat of formation of liquid water is 68.3 kcal/mole

$$H_2O \rightarrow H_2 + 1/2\ O_2 \qquad (1)$$

and thus the reaction as written is substantially energetically uphill. The use of optical energy to run reaction (1) is practicable energetically, but H_2O absorbs little in that region of the electromagnetic spectrum commonly regarded as the optical energy region. Thus, irradiation to yield reaction (1) can only occur by an indirect excitation.

The most common mode of indirect excitation is triplet photosensitization as schemed in reactions (2)-(4) for the benzil sensitized *trans*→*cis* isomerization

$$\text{benzil} \xrightarrow{436\ \text{nm}} [\text{benzil}]^* \tag{2}$$

$$[\text{benzil}]^* + \textit{trans}\text{-4-styrylpyridine} \longrightarrow \text{benzil} + [\text{4-styrylpyridine}]^* \tag{3}$$

$$[\text{4-styrylpyridine}]^* \longrightarrow \alpha\ \textit{trans}\text{-4-styrylpyridine} + (1-\alpha)\textit{cis}\text{-4-styrylpyridine} \tag{4}$$

of 4-styrylpyridine. The benzil is the photoreceptor since the 4-styrylpyridine is transparent to 436 nm light, but the benzil excited state can transfer its excitation energy to *trans*-4-styrylpyridine which has a triplet state energetically below the triplet donor level in benzil[1] (ref. 3). Thus, the energetically uphill trans→cis 4-styrylpyridine isomerization can be achieved with lower energy light than possible without benzil present. The use of a photosensitizer for reaction (1) is conceivable, but in practice H_2O really has no low lying excited states accessible with even the highest energy sensitizers.

A second type of indirect excitation called transition metal photo-assistance (defined in ref. 4) might be more successfully applied to reaction (1). We have recently worked out a model photoassistance situation (ref. 5) and it is schemed in reactions (5) through (8) where *cis* and *trans* refer to *cis* and *trans*-4styrylpyridine, respectively.

$$\text{Cl Re(CO)}_3(\textit{trans})_2 \xrightarrow{436\ \text{nm}} \text{Cl Re(CO)}_3(\textit{trans})(\textit{cis}) \tag{5}$$

$$\text{Cl Re(CO)}_3(\textit{trans})(\textit{cis}) \xrightarrow{436\ \text{nm}} \text{Cl Re(CO)}_3(\textit{cis})_2 \tag{6}$$

$$\text{Cl Re(CO)}_3(\textit{cis})_2 + \textit{trans} \xrightarrow{\Delta} \text{Cl Re(CO)}_3(\textit{trans})(\textit{cis}) + \textit{cis} \tag{7}$$

$$\text{Cl Re(CO)}_3(\textit{trans})(\textit{cis}) + \textit{trans} \xrightarrow{\Delta} \text{Cl Re(CO)}_3(\textit{trans})_2 + \textit{cis} \tag{8}$$

The key points here are that (1) a transition metal complex present in catalytic quantities, serves as the photoreceptor and as the "template" for the desired chemical change; (2) continuous irradiation of the metal complex is required to sustain the uphill *trans→cis*-4-styrylpyridine isomerization, but the $\text{Cl Re(CO)}_3\text{L}_2$ photoassistance agent is not consumed; and (3) the reaction occurs with lower energy light than possible without the photoassistance agent. The use of the transition metal photoassistance technique to run reaction (1) and other valuable uphill chemical reactions merits serious consideration. In fact, it has been pointed out that the photooxidation and photoreduction of aquo transition metal ions can be coupled to the reduction and oxidation of water (ref. 6). The reactions (9) and (10) (ref. 7) together could, in principle, be used to run reaction (1),

[1]The triplet energy of *trans*-styrlpyridine is 50 kcal/mole and that of benzil is about 52 kcal/mole (ref. 3).

$$Ce^{3+} + H^{+} \xrightarrow{h\nu} Ce^{4+} + 1/2\ H_2 \tag{9}$$

$$Ce^{4+} + OH^{-} \xrightarrow{h\nu} Ce^{3+} + 1/4\ O_2 + 1/2\ H_2O \tag{10}$$

but actually only extremely small yields (and very low quantum yields of formation) of O_2 and H_2 can be obtained from irradiation of Ce^{3+}, Ce^{4+} aqueous solutions. Such reactions are still good models to demonstrate the principle, however. Another conceiveable path for the photoassisted reaction (1) is indicated in the series of reactions (11) through (13) where the metal complex, Ru(2,2'-bipyridine)$_3^{2+}$ becomes an extremely strong reducing agent upon electronic excitation, yielding the products indicated in reaction (12). The oxidized Ru complex is formed in its ground electronic state and may be unstable enough to oxidize OH^- (reaction (13)) and return to the original Ru(2,2'-bipyridine)$_3^{2+}$ complex. Note taht in the homogeneous reactions (11) through (13) only one quantum is required for the oxidation and reduction steps whereas in reactions (9) and (10) two quanta are required.

$$Ru(2,2'\text{-bipyridine})_3^{2+} \xrightarrow{h\nu} [Ru(2,2'\text{-bipyridine})_3^{2+}]^* \tag{11}$$

$$[Ru(2,2'\text{-bipyridine})_3^{2+}]^* + H^{+} \longrightarrow Ru(2,2'\text{-bipyridine})_3^{3+} + \frac{1}{2} H_2 \tag{12}$$

$$Ru(2,2'\text{-bipyridine})_3^{3+} + OH^{-} \longrightarrow Ru(2,2'\text{-bipyridine})_3^{2+} + \frac{1}{4} O_2 + \frac{1}{2} H_2O \tag{13}$$

Unfortunately, electronically excited Ru(2,2'-bipyridine)$_3^{2+}$ is unable to reduce H_+ to H^2 (ref. 8). But Ru(2,2'-bipyridine)$_3^{2+}$ has been shown to be an electron donor from its excited state reducing $Fe(OH_2)_6^{3+}$ (ref. 9), Co(III) complexes (ref. 10), and Tl^{3+} (ref. 11). Therefore, continued investigation in this area could prove very fruitful for other chemical transformations besides reaction (1).

Heterogeneous substances have recently shown some promise as photoassistance agents for reaction (1) (refs. 12 and 13). The observation of currents upon photolysis of an electrode in an electrochemical cell has been known for a very long time (ref. 14), but it has not been until recently that it has been claimed that the electrode reactions occurring could actually yield H_2 and O_2. The photolysis of an n-type TiO_2 single crystal electrode, in a cell like that depicted in figure 1a, was reported to yield current flow such that O_2 is evolved at the TiO_2 and H_2 at the Pt electrode (refs. 12 and 13). We report herein a detailed characterization of this system which shows for the first time that reaction (1) can be sustained with light using an electrode system as the photoassistance agent. Products have been unequivocally identified, and the efficiency of product formation based on current flow and incident optical energy are reported.

RESULTS AND DISCUSSION

Product Identification and Electrode Stability

The use of a metal oxide as a photoelectrode prompts the question of its stability to light in the electrolyte, especially as it may be a source of O_2. To answer this question two sets of experiments have been carried out in a photoelectrochemical cell, such as that shown in Figure 1a, using the 351.1, 363.8 nm doublet emission of a Spectra Physics Model 164 argon ion laser as the irradiation source. First, mass spectroscopic analyses have been carried out on the gases evolved at both the TiO_2 and the Pt electrode. When the TiO_2 is immersed in 1.0 M NaOH with $D_2{}^{18}O/D_2O$ (¼) as the solvent and the Pt is in 1 $\underline{N}$ H_2SO_4 with D_2O as solvent $^{18}O^{16}O$, $^{18}O_2$, and $^{16}O_2$ are evolved at TiO_2 and D_2 and a trace amount of HD is evolved at Pt. The ^{18}O ^{16}O: $^{16}O_2$ ratio is very close to the 1:2 value predicted based on the ratio of ^{18}O to ^{16}O present in the electrolyte. In a second series of experiments, electrodes prepared from pre-weighed crystals of TiO_2 were used in a photoelectrochemical cell and the amount of O_2 evolved was measured volumetrically. The crystal was then recovered and weighed. Typical data (table 1) show that within experimental error no weight loss obtains even when the number of moles of O_2 evolved surpasses the number of moles of TiO_2 initially present. The oxygen labeling experiment and the stability of the TiO_2 electrode under illumination prove that the O_2 comes from the H_2O and show that the reaction is catalytic with respect to TiO_2.

Stoichiometry and Efficiency of Product Formation

Some quantitative measurements have first been made with a photoelectrochemical cell as shown in figure 1a and the data are summarized in table 2. The data show that (1) the ratio of H_2:O_2 is generally close to 2:1, (2) approximately 2 moles of electrons flow per mole of H_2 evolved, and approximately 4 moles of electrons flow per mole of O_2 evolved; and (3) the quantum efficiency of H_2 formation at 351, 364 nm excitation is of the order 10^{-2} to 10^{-1}. Quantum efficiency is defined here to mean the number of moles of H_2 formed per einstein at 351, 364 nm striking the electrode. No correction has been made for losses due to reflection. Sustained currents of the order of 1-2 ma can be typically achieved using the laser (~50 mW) with a beam diameter of ~1 mm; thus, the current density is of the order of 10^2 ma per cm^2 of irradiated surface area. However, little or no hydrogen evolution can be detected in the two compartment cell in figure 1a when the electrolyte at Pt and TiO_2 is the same, although O_2 evolution and current flow is usually observed. Toward the aim of establishing the role of the diffusion barrier in the cell in figure 1a, we have undertaken an investigation of the photoelectrochemical cell depicted in figure 1b.

In the one compartment cell we have been able to observe photo-induced H_2 and O_2 evolution at applied voltages as small as 0.25 V and some quantitative data are given in table 3. Again the stoichimetry is fairly clean and quantum efficiencies are in the range 10^{-2} to 10^{-1} for H_2 evolution. As seen in table 3, the quantum efficiency does seem to depend on the applied voltage, and it is apparent then that the two compartment cell (fig. 1a) works without an external power supply because the acid in the Pt compartment and the base on the TiO_2 side provide the bias necessary for the reaction to occur. However, when the electrolysis of H_2O can be carried out at less than 1.23 V, energy must be supplied from an external source, which in this case is the light. Some indications of the optical storage efficiency are given in table 4. The storage efficiency is calculated with the assumption that H_2 can be used to generage heat and is worth 68 kcal/mole.

These minimum storage efficiencies are seen to be of the order of 1 percent at 351, 364 nm excitation.

Wavelength Response

The n-type TiO_2 has a band gap of ~3.0 eV (ref. 15). If the photoassistance activity observed for TiO_2 is associated with an electronic transition from the valence band to the conduction band, we expect that the minimum light energy required will correspond the band-gap energy. The relative current as a function of irradiation wavelength for a cell such as that shown in figure 1b is given in figure 2 for a TiO_2 electrode and a tungsten-doped TiO_2 electrode. The wavelength response is independent of the applied voltage, and, at least for the TiO_2, the onset of activity does correspond closely to that expected, based on the band gap. The difference in the response for the tungsten-doped TiO_2 electrode is remarkable despite the fact that the shift of the onset is toward higher energy compared to the TiO_2 itself. Understanding of the origin of this effect may make it possible to design tuned response systems.

SUMMARY

These data are the first to show that reaction (1), the conversion of H_2O to H_2 and O_2, can be sustained using optical energy. The TiO_2 electrode system is a true photoassistance agent serving to absorb light and to dissipate the excitation energy in such a way as to achieve the desired chemical change. Importantly, the electrode system is itself photoinert, and therefore the production of H_2 and O_2 is catalytic with respect to TiO_2. The merit of the results disclosed here rests in the demonstration that the photoassisted electrolysis of H_2O can be achieved. Further studies are underway and are directed toward more efficient utilization of the optical energy as well as a confident understanding of the mechanism of the processes involved.

Acknowledgement – I wish to thank my collaborators D. S. Ginley, P. G. Wolczanski, A. B. Ellis, D. L. Morse and A. Linz for their contributions to the work discussed. The financial support of the National Aeronautics and Space Administration is gratefully acknowledged.

REFERENCES

1. Moore, Walter J: Physical Chemistry, 3rd ed., Prentice Hall, Inc., Englewood Cliffs, N. J., 1962, p. 52.

2. Turro, Nicholas J.; Dalton, J. Christopher; and Weiss, David S.: Photosensitization by Energy Transfer. Org. Photochem, Vol. 2, 1969, p. 1-62.

3. The triplet energy of *trans*-styrylpyridine is 50 kcal/mole and that of benzil is about 52 kcal/mole, Turro, Nicholas J.: Molecular Photochemistry. W. A. Benjamin, Inc., New York, 1965.

4. This term is defined in: Wrighton, Mark: The Photochemistry of Metal Carbonyls. Chem. Rev., Vol. 74, no. 4, August 1974, p. 401-430.

5. Wrighton, Mark S., Morse, David L.; and Pdungsap, Laddawan: Intraligand Lowest Excited States in Tricarbonyl-halo-bis-(styrylpyridine)rhenium(I) Complexes. J. Amer. Chem. Soc., Vol. 97, no. 8, 16 Apr. 1975, p. 2073-2079.

6. Balzani, V.; and Carassiti, V., Editors: Photochemistry of Coordination Compounds. Academic Press, New York, 1970.

7. Heidt, Lawrence J.; and McMillan, Alan F.: Conversion of Sunlight into Chemical Energy Available in Storage for Man's Use. Science, Vol. 117, 23 Jan. 1953, p. 75-76.

8. Wrighton, M.: unpublished observations.

9. Bock, C. R.; Meyer, T. J.; and Whitten, D. G.: Electron Transfer Quenching of the Luminescent Excited State of Tris(2,2'-bipyridine)ruthenium(II). A Flash Photolysis Relaxation Technique for Measuring the Rates of Very Rapid Electron Transfer Reactions. J. Amer. Chem. Soc., Vol. 96, no. 14, 10 July 1974, p. 4710-4712.

10. Navon, Gil; and Sutin, Norman: Mechanism of the Quenching of the Phosphorescence of Tris(2,2'-bipyridine)ruthernium(II) by Some Cobalt(III) and Ruthenium(III) Complexes. Inorganic Chemistry, Vol. 13, no. 9, Sept. 1974, p. 2159-2164.

11. Laurence, Gerald S.; and Balzani, Vincenzo: Reduction by the Triplet Charge-Transfer State of Tris(bipyridyl)ruthenium(II). Photochemical Reaction between Tris(bipyridyl)ruthenium(II) and Thallium(III). ibid, Vol. 13, no. 12, Dec. 1974, p. 2976-2982.

12. Fujishima, Akira; and Honda, Kenichi: Electrochemical Evidence for the Mechanism of the Primary Stage of Photosynthesis. Bull. Chemical Society of Japan. Vol. 44, no. 4, April 1971, p. 1148-1150.

13. Fujishima, Akira; and Honda, Kenichi: Electrochemical Photolysis of Water at a Semiconductor Electrode, Nature, Vol. 23, 7 July 1972, p. 37-38.

14. Becquerel, Edmond: Hebdomadaire des Sciences de L'Academie des Sciences. Compt. Rend., Vol. 9, no. 19, 4 Nov. 1838, p. 561-567. Memoire sur les Effects Electriques Produits Sous L'Influence des Rayons Solaines.

15. Cronemeyer, D. C.: Electrical and Optical Properties of Rutile Single Crystals. Physical Review, Vol. 87, no. 5, 1 Sept. 1952, p. 876-886.

TABLE 1. – TEST FOR DISAPPEARANCE OF TiO_2 UPON IRRADIATION

TiO_2		Initial TiO_2, moles	O_2[b] evolved, moles	Crystal
Initial weight, ±0.001, g	Final weight,[a] ±0.002, g			
0.1210	0.1206	1.51×10^{-3}	2.4×10^{-4}	A
0.0187	0.0191	2.38×10^{-4}	2.2×10^{-4}	B
Not measured	0.2427[c]	Not measured	9.2×10^{-4}	C
0.0658	0.0640	8.24×10^{-4}	1.7×10^{-4}	D
0.0041	0.0039	5.13×10^{-5}	1.1×10^{-4}	E

[a]The error is larger than initial weight because the TiO_2 crystal must be removed from the electrode and epoxy and metallic backing must be cleaned off.

[b]Moles of O_2 evolved by irradiation of the TiO_2 electrode in a cell as in figure 1(a) or 1(b). If used in the one compartment cell (fig. 1(b)) the applied voltage was 2.0 V or less.

[c]No obvious deterioration of the crystal during its use. The value of the data rests in the fact that a large absolute amount of O_2 was evolved from this crystal.

TABLE 2. – PHOTOASSISTED ELECTROLYSIS OF H_2O IN A TWO COMPARTMENT CELL[a]

Electrolyte at TiO_2	Electrolyte at Pt	Irradiation time, min	H_2, moles	O_2, moles	Electrons, moles	Φ[b] for H_2 production
1 M NaOH[c]	1 N H_2SO_4	426	1.6×10^{-4}	8.0×10^{-5}	4.10×10^{-4}	0.04_7
1 M $NaClO_4$[c] + 0.1 M NaOH	1 M $NaClO_4$ + 0.1 N H_2SO_4	572	1.5×10^{-4}	7.6×10^{-5}	4.2×10^{-4}	0.03_7
1 M NaOH[d]	1 N H_2SO_4	1280	4.8×10^{-4}	2.4×10^{-4}	8.4×10^{-4}	0.04_7

[a]Cell assembly as in figure 1(a).
[b]Light intensity striking electrode is 8×10^{-6} ein/min.
[c]TiO_2 electrode from first synthesis of n-type TiO_2 crystal C in table 1.
[d]TiO_2 electrode from a second synthesis of n-type TiO_2 crystal.

TABLE 3. – PHOTOASSISTED ELECTROLYSIS OF H_2O IN A ONE COMPARTMENT CELL[a]

Electrolyte	Applied voltage, V	Irradiation time, min	H_2, moles	O_2, moles	Electrons, moles	Φ for H_2[b] production
1 M NaOH[c]	2.0	207	1.8×10^{-4}	8.5×10^{-5}	3.9×10^{-4}	0.11
1 M $NaClO_4$[c]	2.0	507	2.2×10^{-4}	1.1×10^{-4}	5.7×10^{-4}	0.05_4
1 M $NaClO_4$[c]	2.0	180	1.3×10^{-4}	6.3×10^{-5}	2.7×10^{-4}	0.09_0
0.1 M NaOH[c]	2.0	252	2.2×10^{-4}	9.2×10^{-5}	4.2×10^{-4}	0.11
0.1 M NaOH[c]	2.0	777	2.9×10^{-4}	1.2×10^{-4}	7.6×10^{-4}	0.04_7
0.1 M Na OH[c] + 4 M $NaClO_4$	2.0	96	1.0×10^{-4}	5.4×10^{-5}	1.9×10^{-4}	0.13
1 N H_2SO_4[c]	2.0	471	2.9×10^{-4}	8.9×10^{-5}	6.5×10^{-4}	0.07_7
1 N H_2SO_4[d]	2.0	3579	5.0×10^{-4}	1.6×10^{-4}	1.2×10^{-3}	0.01_7
0.1 N H_2SO_4[c]	2.0	1001	3.5×10^{-4}	1.2×10^{-4}	7.6×10^{-4}	0.04_4
0.1 M NaOH[c]	0.5	1266	1.7×10^{-4}	8.9×10^{-5}	5.2×10^{-4}	0.01_7
1.0 M NaOH[c]	0.5	666	1.2×10^{-4}	5.8×10^{-5}	3.4×10^{-4}	0.02_3
1.0 M NaOH[e]	0.5	1514	3.1×10^{-4}	1.0×10^{-4}	5.9×10^{-4}	0.02_6
1.0 M $NaClO_4$[e]	2.0	413	1.7×10^{-4}	7.4×10^{-5}	3.4×10^{-4}	0.05_1
2.0 M NaOH[c]	0.25	990	7.6×10^{-5}	3.6×10^{-5}	1.6×10^{-4}	0.01_0
2.0 M NaOH[f]	2.0	801	2.5×10^{-4}	1.1×10^{-4}	4.8×10^{-4}	0.03_9

[a]Cell as in figure 1(b); no current flows without light.
[b]Light intensity striking electrode is 8×10^{-6} ein/min.
[c]Electrode C in table 1.
[d]Electrode A in table 1.
[e]Electrode D in table 1.
[f]Electrode E in table 1.

TABLE 4. – EFFICIENCY OF STORAGE OF OPTICAL ENERGY AS HYDROGEN[a]

Applied potential, V	Irradiation time, sec	Average current, ma	H_2, moles	Energy stored[b] as H_2, cal	Energy in from[c] power supply, cal	Energy in from[d] laser, cal	Optical energy[e] storage efficiency %
0.5	7.6×10^4	0.66	1.7×10^{-4}	12.0	6.0	810	0.74
0.5	4.0×10^4	0.82	1.2×10^{-4}	8.2	3.9	430	1.0_0
0.5	9.1×10^4	0.63	3.1×10^{-4}	21.0	6.8	980	1.4_5
0.25	5.9×10^4	0.26	7.6×10^{-5}	5.2	0.9	640	0.6_7

[a]From data given in table 3.
[b]Assuming H_2 can be recovered at 68 kcal/mole which is the standard heat of formation of H_2O, reaction (1).
[c]Energy from power supply = (applied potential)(average current)(irradiation time)(0.239 cal/J).
[d]8×10^{-6} ein/min at 351, 364 nm is equivalent to ~0.011 cal/sec.

[e]*Optical energy storage efficiency* $= \dfrac{\text{(energy stored as } H_2\text{)} - \text{(energy in from power supply)}}{\text{(energy in from laser)}} \times 100.$

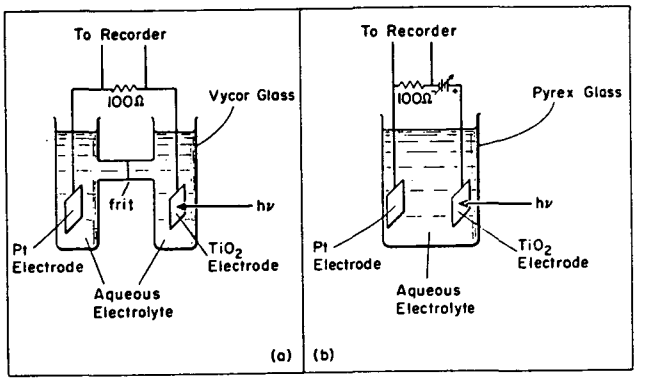

(a) The two electrode compartments are separated by a fine glass frit to prevent diffusion of the 1 N H_2SO_4 on the Pt side and the 1 M NaOH on the TiO_2 side.

(b) The external power supply indicated is a Hewlett-Packard Model 6241A with variable applied potential (0-12 V). The "hν" and heavy arrow indicate the laser beam.

Figure 1.– Photochemical cells used for the photo-assisted electrolysis of H_2O.

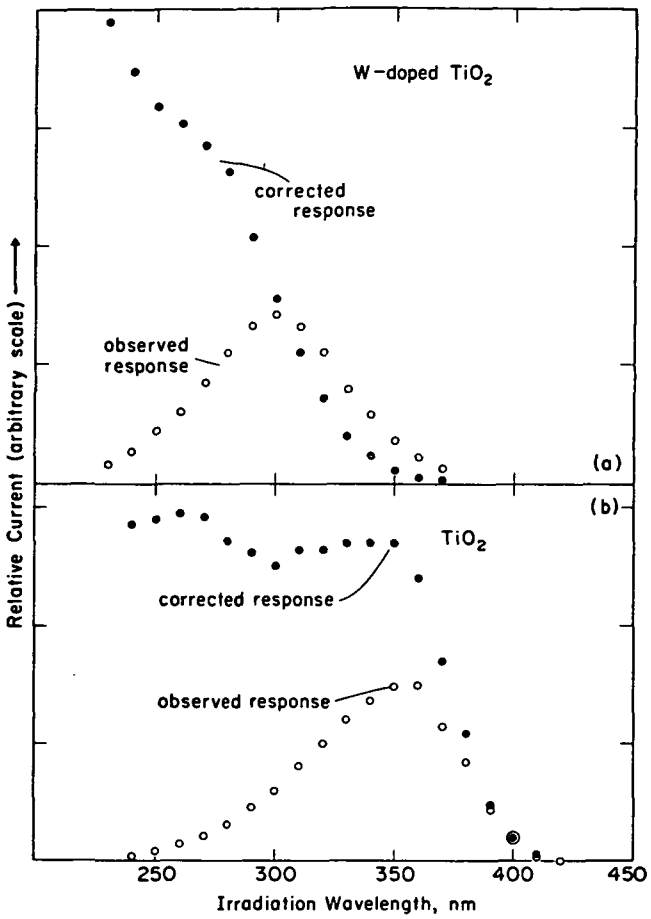

(a) Tungsten doped n-TiO_2.
(b) n-TiO_2 electrode when used in a cell.

Figure 2.– Relative current vs. excitation wavelength. The open circles (O) show the uncorrected, observed response and the filled circles (●) show the actual, corrected response after correction for variation of the excitation light intensity as a function wavelength. The observed response is given to show the magnitude of the correction factors. Note, however, that even without application of the correction one can see a difference in response of the two crystals.

DISCUSSION

Dick Miles, Princeton University – Did you find that you had to replace the base or the acidic solutions?

Answer: We never reacted enough water that the concentration changed. When you think about what a mole of photons is – it's really a long time at fifty milliwatts. Some of the irradiation times are like a day and to make a mole of photons would take 10,000 days with our laser.

Bill Bottoms, Princeton University – Just to pursue the same question-over the long term just what is going to happen to the pH of those electrolytic solutions? How will you deal with that problem?

Answer: I think the way to go in this system is not to use the two-compartment system. Clearly, we've demonstrated that in a homogenous solution the electrode system serves as a photo-assistance reagent for the reaction and, under those conditons, the only thing that ever needs to be added to that system is water.

Bob Hess, Langley Research Center – Didn't you look at some systems to reduce the applied voltage by using a single cell?

Answer: Well it turns out the current-voltage curves, of course, depend on the electrode reactions which are taking place. Most of our effort has clearly been in trying to make hydrogen at platinum and oxygen at titanium dioxide, but there is no reason why one cannot couple this excitation energy to other electrode processes. For example, if you just toss in iron three at the platinum electrode you can obtain current densities which are as high as in any experiment with iron three going to iron two. So electricity can be the direct result of these systems as well as chemical energy.

Bill Bottoms, Princeton University – It seems to me you are dealing with a wide band gap semiconductor and you could, by doping, shift the inner potential by the one half volt you are applying with a battery. Have you explored the possibility of just using a PN junction in a wide bandgap semiconductor which is effectively what you are doing electrically anyway?

Answer: In fact we are collaborating with some people in Electrical Engineering at M.I.T. and have suggested that they give us some materials which we can put on there which will bias it in a way that is appropriate.

Bill Bottoms, Princeton University: There are some fairly straight-forward ways to establish a one-half volt drop in a wide bandgap semiconductor which will give you a highly reducing surface on one side and highly oxidizing on the other. You will gain back the energy thrown away in the power supply.

Max Garbuny, Westinghouse – You mentioned your laser limitations. Couldn't you use a high pressure mercury arc to obtain higher fluxes? In fact you could obtain an einstein or mole of photons in a relatively short time.

Answer: Yes, in fact with the tin oxide, the band gap is sufficiently high that we really can't get very much out of our system with the argon ion laser. So we've been using a super high pressure mercury arc lamp and under those conditions we can get sustained currents over 0.01 amps and under those conditions you can make quite a bit of hydrogen and oxygen. We have the pleasant problem of not having sufficient volumetric glassware which is large enough to handle the gases!

Katsonori Shimada, J. P. L. – Can you make a comment on the work that is going on at UCLA using rutile? For example, are they getting about the same results as you?

Answer: I guess I don't know about the work at UCLA. Maybe you can tell me about it.

Shimada: As I understand it, JPL has a contract with UCLA to supply the crystal TiO_2.

Wrighton: I don't know what those results are, but the results that we have show that TiO_2 is inert and all the oxygen which is liberated is coming from the solution. This is determined both by the labeling experiments with O^{18} and by the fact that the crystal doesn't disappear when its illuminated.

Dick Pantell, Stanford University – If the purpose of the light is to generate minority carriers, wouldn't the PN junction then eliminate the necessity of the laser light at all?

Bill Bottoms: Perhaps I can answer that since I'm one of those people from an electrical engineering department such as you mentioned. The difficulty is that you have to put in energy from somewhere. You can do it with a battery and then have copious numbers of minority carriers. You can also do it with light. Its a question of which is preferable.

Mark Wrighton: That is just it. If you just toss something into the water and let it sit there, unless it is a battery itself, it is not going to evolve any high energy products. People talk about photo-catalysis and they really mean they are trying to accelerate thermodynamically favorable reactions. Thats the important problem with respect to energy conversion.

Bill Bottoms, Princeton University –You mentioned the low absorption of laser light. This indicates another reason for going to heavily doped PN junctions since you would enhance this absorption on both sides.

Answer: Yes, some are transparent to visible light. Perhaps I should say the following: Reduced TiO_2 is a black material which is totally opaque to visible light. But even if it were transparent to visible light that doesn't mean that it wouldn't absorb one-hundred percent in the region where its active. For example, the tin oxide is a clear material which looks like a chip of glass but it does absorb quite substantially in the ultraviolet, the relative response at 250 nm and 350 nm being four orders of magnitude.

PHOTOCATALYTIC GENERATION OF HYDROGEN FROM WATER

W.R. Bottoms and R.B. Miles

Princeton University

N76-21508

INTRODUCTION

The dissociation of simple molecules provides a potentially efficient method of storing energy in a transportable form. Among the numerous chemical systems that have been proposed for energy conversion are the following:

$$2NOCl \xrightarrow{h\nu} Cl_2 + 2NO$$

$$2H_2O \xrightarrow{h\nu} 2H_2 + O_2$$

$$2CO_2 \xrightarrow{h\nu} 2CO + O_2$$

Hydrogen offers the advantages of being a clean burning fuel, easily stored in gas, liquid, or hydride form, and efficiently transferable. It may be used as a fuel for a variety of energy conversion processes including fuel cells and rocket engines as well as conventional heat engines. In conjunction with a water dissociation process, it holds forth the promise of providing a closed cycle, photon powered, energy system where photon energy may be efficiently stored for future use and converted to thermal or electrical energy on demand. In this paper we will discuss a new concept which is designed to overcome the problems encountered when using photodissociation for the generation of hydrogen.

Two fundamental problems limiting the efficiency of photodissociation of water are the separation of the photolysis products and the high energy photons necessary for the reaction. Although there has not been a great deal of work with metal-water systems, it has been shown that the dissociation energy of a large number of molecules is catalytically reduced when these molecules are in intimate contact with a surface of certain metals (ref. 1). The spontaneous dissociation of water has been demonstrated for Cu (ref. 2), Fe (ref. 3), and Ni (ref. 4) at room temperature in the dark. We suggest the possibility of engineering a surface which will take advantage of this catalytic shift in dissociation energies to reduce the photon energy required to produce hydrogen. This same catalytic surface can be used to separate the reaction products if it is made so that one of the dissociations products is soluble in the metal and others are not. This condition is met by many metal systems such as platinum group metals which have been used commercially (ref. 5) to separate hydrogen from other gases and liquids.

The generation of hydrogen by unassisted photolysis of water is an inefficient process. This inefficiency arises from the high photon energies required for direct photodissociation, the energy lost in secondary reactions, and rapid recombination of the products into water. The maximum quantum efficiency measured by Chen and Taylor (ref. 6) was 30 percent; however, that required photons in the 1650 Å range, intense illumination, and flowing water vapor. In a static system, the quantum yield was about 1 percent. Since the energy stored in each hydrogen molecule is equivalent to about 4000 Å, Chen and Taylor's overall efficiencies ranged from 0.4 percent to 12 percent. It is well to remember that there is no solar flux in the 1650 Å region, so such a system is not suitable for solar conversion.

The photodissociation of water to produce hydrogen and oxygen proceeds in the ultraviolet around 1650 Å mostly by the reactions

$$H_2O \rightarrow OH + H \tag{1}$$

$$OH + OH \rightarrow O_2 + H_2 \tag{2}$$

$$H + H \rightarrow H_2 \tag{3}$$

The energy required for the first step is equivalent to 180 kcal/mole if a single photon is absorbed or approximately 117 kcal/mole thermally. The difference is due to the Frank-Condon principle which requires that a photon be absorbed to a high energy state, followed by exothermic dissociation. The overall reaction

$$H_2O \rightarrow \frac{1}{2}O_2 + H_2 \tag{4}$$

on the other hand, requires 68 kcal/mole because the recombination of the H and OH radicals is exothermic. If reaction (4) could be done in a single step with a photon, the photon wavelength would have to be 4000 Å or less. Water is not absorbing at this frequency, thus some intermediate reactions are necessary for efficient generation of hydrogen from water using visible light.

Numerous photocatalytic paths have been suggested including salt compounds, semiconductors, and dyes (ref. 4) to improve the efficiency of photolysis of water. Molecules adsorbed in surface complexes on metals are capable of multistep processes not possible in gas or liquid phase. The presence of the surface alters the molecular bonds, and the proximity of the molecules to each other and to the surface provides the possibility of intermediate reactions and lower activation energies for direct reactions.

Depending on the chemisorptive activity, the dissociation process on a metal surface may be photoassisted in one of or a combination of the following ways. [(MH) denotes a metal hydride.]

1. Strongly Chemisorptive Case

$$H_2O + M \rightarrow (MH) + MOH \quad (5)$$

$$\rightarrow 2\,(MH) + MO \quad (6)$$

{ Chemisorption and absorption

$$MOH + h\nu \rightarrow M + OH \quad (7)$$

$$2MO + h\nu \rightarrow 2M + O_2 \quad (8)$$

{ Photodesorption

Contact with the water molecules causes the breakdown of the H_2O into absorbed hydrogen and strongly adsorbed OH or oxygen complexes. This behavior proceeds at room temperature and in the absence of illumination. The photoassisted step is therefore directed toward breaking the OH or oxygen complex bond with the surface, thus opening additional sites for continuation of the dissociative process.

2. Mildly Chemisorptive Case

$$H_2O + M \rightarrow H_2OM \quad (9)$$

{ adsorption

$$H_2OM + h\nu \rightarrow (MH) + MOH \quad (10)$$

{ photolysis & absorption

$$MOH \rightarrow M + OH \quad (11)$$

or

$$2MOH \rightarrow 2(MH) + O_2 \quad (12)$$

{ desorption

The H_2O molecule is adsorbed onto the surface nondissociatively. Surfaces become saturated with adsorbed H_2O, and subsequent illumination breaks the H_2O molecule allowing the hydrogen to be absorbed into the metal or metal alloy and releasing the remaining dissociation products into the solution.

3. Strongly Hydrogen Absorptive Case

$$H_2O + M \rightarrow (MH) + OH \quad (13)$$

$$\rightarrow 2(MH) + O_2 \quad (14)$$

{ dissociation and absorption

$$2(MH) + \text{heat} \rightarrow M + H_2 \quad (15)$$

{ hydrogen recovery

H_2O on the surface is dissociated; the hydrogen atom is strongly absorbed into the metal or metal alloy, and the oxygen and OH radicals either evolve into the solution or are weakly held onto the metal surface.

Final separation of the hydrogen from the hydride form may involve a physical separation of the metal hydride from the reaction region or diffusion through a film of metal and evolution from

the other side. Energy is added to remove the hydrogen from the metal or metal alloy. Since this is a bulk rather than surface effect, energy must be added as heat, rather than light, although the light may be converted to heat on the particle surface.

A more detailed look at the adsorption process in transition metals indicates that water molecules are adsorbed with the oxygen atom close to the surface (ref. 8). Probably one of the hydrogen atoms is also close to the surface and the other is free to move about. Adsorption energies are about 11 kcal/mole for copper and will probably be similar for other transition metals (ref. 9). A metal that forms a hydride will attract the hydrogen atoms into inner lattice bonds, and if the hydride is to be useful, the metal hydride bond must be of approximately the same strength as the H_2 bond. Thus the reaction

$$H_2 + 2M \rightarrow (MH) + (MH) \tag{16}$$

is in equilibrium or slightly exothermic.

A possible compound is $LaNi_5$, recently found to be a candidate for storage of hydrogen in hydride form (ref. 10). If we assume the surface behaves like Ni, then we may write

$$(MH) \cong 53 \text{ kcal/mole}$$

$$M\text{–}O \cong 58 \text{ kcal/mole}$$

$$H_2O\text{–}M \cong 7 \text{ kcal/mole (to liquid state)}$$

$$H_2O \rightarrow OH + H - 75 \text{ kcal/mole (including evolution from the surface)}$$

These estimates arise from

1. The slightly exothermic nature of hydrogen absorbing in the metal.
2. The binding energy of NiO.
3. The adsorption energy of water vapor to copper, which is similar to that on nickel.

The reactions will be a combination of all three processes discussed previously.

$$H_2O + M \rightarrow H_2OM \qquad -5 \text{ kcal/mole} \tag{17}$$

$$H_2OM \rightarrow (MH) + MOH \qquad x \text{ kcal/mole (photo activated)} \tag{18}$$

$$MOH \rightarrow (MH) + MO \qquad 75\text{–}x \text{ kcal/mole (photo activated)} \tag{19}$$

$$MO + MO \rightarrow 2M + O_2 \qquad -2 \text{ kcal/mole} \tag{20}$$

$$(MH) + (MH) \rightarrow 2M + H_2 \qquad +2 \text{ kcal/mole (thermally activated)} \tag{21}$$

The metal hydride to hydrogen evolution step is performed after the physical separation of the particles from the fluid or on the back side of a thin film. If x = 50 kcal/mole, reaction (18) requires radiation at 5600 Å and the 25 kcal/mole, remaining for reaction (19) correspond to about 0.9μ. Assuming light of these colors can be delivered to the appropriate bonds, the catalytic decomposition of H_2O into free hydrogen and oxygen may be achieved. The strength of the M-OH bond will determine the relative endothermicity of the reactions 18 and 19. An increase in the bond strength, however, will most likely mean an increase in the metal oxide bond strength and a subsequent energy requirement for cleaning the oxygen off the surface (reaction 20).

OPTICAL PROCESSES

As mentioned previously, the separation of water into hydrogen plus oxygen would require photons of 4000 Å or less if it could be accomplished in a single step. The absorption spectrum of water vapor (fig. 1), however, shows that there is virtually no absorption at wavelengths longer than about 1800 Å (ref. 11). Thus any energy efficient process will require that water be broken down into hydrogen plus oxygen via one or more intermediate states. These intermediate reactions, then, may be selected so they are affected by visible radiation.

If one assumes that the reactions 18 and 19 can indeed be photoactivated, then the possibility of high conversion efficiency is conceivable. Two particular cases are important: the first is the conversion of laser energy to hydrogen, and the second is the conversion of solar energy. Since the bandwidth of a laser is very narrow, optimization of a surface for laser conversion is quite different from the optimization for solar conversion.

Theoretically, laser light may be converted with 100 percent efficiency into hydrogen gas; obviously such an efficiency will never be achieved. The value of x in equations 18 and 19 will probably be determined by the absorption spectra of the adsorbed surface compound. This will be somewhat determined by surface engineering and selection of metals, but may well be somewhere in the near infrared where water vapor absorption bands are known to lie. Such a level would require either two different lasers, or one laser driving a multiple photon process, to achieve enough energy to favor the water to hydrogen reaction.

As can be seen from figure 2, the amount of solar radiation with wavelengths shorter than 4000 Å is small: hence the need for a two-step process for efficient solar conversion. One hydrogen molecule would then be formed for each pair of photons whose energy sums to the equivalent of 4000 Å. In that manner a large portion of spectrum of the solar radiation may be used. Even the far infrared might contribute by heating the catalyst, thus aiding with desorption of surface compounds, the diffusion of hydrogen or, if concentrated at another location, with desorption of absorbed hydrogen from metal particles.

A calculation of the efficiency for such a device cannot be made until the surface properties of the catalyst are known. The optical absorption bands associated with the surface compounds, and the way in which these will react when optically excited, must be studied. It is clear, however, that a particle slurry or very porous surface can be made to appear black. Thus most of the visible and infrared light is absorbed. Any light absorbed that does not produce a hydrogen atom will heat the catalyst or surrounding medium. Thus the catalytic activity may also change with exposure to light.

Since the molecules will be complexed with the metal surface, absorption bonds are broadened and shifted. Energy may be transferred by direct photon absorption into a surface complex, or by absorption by the bulk of the particle. Most metal particles tend to be reflective: thus photons not absorbed by a surface compound are likely to be reflected and may be absorbed by some other surface molecule. A rough metal film surface (ref. 12) or a large number of suspended particles will allow multiple reflections until absorption occurs. Photons absorbed by the particles or the solution, or by both, will heat the surfaces and aid with oxygen/OH desorption.

An optimum situation will exist if one photon with somewhat greater energy than 0.8μ first interacts with the water-catalyst to create an absorbed hydrogen atom and a surface compound. A second photon, with lower energy, then reduces the surface compound, freeing the remaining oxygen and leaving the hydrogen in the catalyst. Subsequent heat (perhaps also derived from electromagnetic radiation) then releases the hydrogen.

Referring again to equations 17 through 21, we can estimate the efficiency as a function of x. The energy regained by combustion of H_2 is 68 kcal/mole assuming the water is condensed from vapor phase. Assuming optimistically that any photon with energy higher than x for reaction 18 and 75-x for reaction 19 will be absorbed and cause the reactions to proceed, the energy efficiency may first be calculated.

$$\eta = \left(\frac{68 \text{ kcal/mole}}{\text{sum of average energy of both photons}}\right) \cdot$$

(percent of solar radiation with energy $\geqslant$ x) $\cdot$ (percent of solar radiation with energy $\geqslant$ 75-x).

One extreme of course is reached if x = 75; that is, only light with wavelength shorter than $\sim 0.4\mu$ is useful. Then $\eta \cong \left(\frac{68}{80}\right) \cdot (0.05)\ (100) \cong 4$ percent. If x = 0 the same efficiency is found. Optimum conversion occurs if x = 95/2, or $\eta \cong \frac{68}{100} \cdot 0.6 \times 0.6 \cong 24$ percent. Figure 3 is a plot of η vs x assuming the thermal photons do not contribute.

If the photons are reflected around until they are absorbed and the heat of condensation is recovered

$$\eta = \left(\frac{68 \text{ kcal/mole}}{\text{sum of average energy of both photons}}\right) \cdot \text{(percent of solar radiation with energy} \geqslant \text{x)}$$

$\cdot$ (percent of solar energy with rad. $\geqslant$ 75-x + percent of solar energy between x and 75-x)

The percentage of energy between 75-x and x varies from $\sim$95 percent if x = 0 to 0 if x = 75/2. This treatment introduces a quadratic factor into the efficiency as shown in figure 4. Thus x $\cong$ 50 will provide a peak of approximately 30 percent conversion efficiency.

SEPARATION PROCESSES

Thin Films

Thin films of palladium and palladium alloys are used for industrial purification of hydrogen. The diffusion of hydrogen through palladium has been known for over a century (ref. 13) although the particulars of the diffusion mechanism have not yet been determined. At low temperatures palladium absorbs hydrogen up to about 60 percent H/Pd atom ratio as is shown in figure 5, then the material alters structure from what is termed the α phase to the β phase. As figure 5 indicates, the β phase may also be achieved at higher temperatures and lower concentrations, and above 295°C no α phase exists at all.

Diffusion is observed in both phases. Diffusion rates approximately $10 cc/cm^2/sec$ for films about 1μ thick are easily achieved. Very thin films remain in the α phase even at high temperatures and can be efficiently used as separators.

Two major problems must be overcome if films are to be used. Even if photo induced dissociation of H_2O can be achieved on the surface, the small absorption cross section of the surface region will not allow many photons to be absorbed. Most photons will pass through and reflect off into space. The second difficulty is to promote hydrogen evolution from the back surface and not the front. Otherwise a vacuum must be maintained on the back and the hydrogen subsequently repressurized resulting in a decreased energy efficiency.

Some headway has already been made toward the solution of both these problems. The surface roughness can be controlled by thin film fabrication techniques and extremely rough surfaces have been made (ref. 14). Such a surface may be treated to form a palladium black layer thereby increasing the optical cross section and enhancing hydrogen uptake (ref. 15). Work on inhibiting the evolution of hydrogen from palladium points toward the creation of an alloy or coating on the front surface, thus forcing evolution from the rear surface only. Copper alloys of palladium have been shown to inhibit hydrogen evolution (ref. 16). Figure 6 shows schematically an arrangement for separation of hydrogen using a thin film diffusion barrier.

Particle Suspension

A suspension of finely ground particles in water or air is an alternative configuration for separation. Particles have the advantage of large surface to volume ratios, thus a suspension would expose more surface area to the incident radiation and water molecules than would a thin film. Figure 7 shows in diagramatic form a conceivable arrangement for activating and separating the particles.

The optical scattering cross section of small particles is very dependent on size and wavelength. Generally speaking, particles on the order of the wavelength of the light are strong scatterers. Sizes on the order of 1μ or so in diameter can easily be seen (e.g. cigarette smoke). Even in the atmosphere, particles of this size have a coat of water surrounding them.

A concentration of particles of some easily hydrated metal such as Pd, $LaNi_5$, would ideally act as light scatterers unless one of the adsorbed water molecules or surface compounds was to

absorb the radiation. Thus, photons arriving would be scattered numerous times before being absorbed. This multiple scattering alleviates the problem of mono-molecular layers of water molecules not being capable of absorbing the light.

An absorbed photon would either heat the particle or release a hydrogen atom into the particle. Typical solar fluxes unconcentrated range about 10^{19} photons/cm^2/sec. Thus each 1-μ diameter particle would see on the order of 10^{11} photons/sec, assuming low absorption. The water solution is, of course, virtually transparent to photons with energies greater than about 2.5 μ, thus most of the photons in the frequency range of interest would be seen by the particles.

The surface area of a 1-μ particle is about 10^{-7} cm^2. Generally speaking, surface densities range around 10^{15} molecules/cm^2, so a typical particle would attract 10^8 water molecules around it. The volume of the 1-μ particle is about 4×10^{-12} cm^3 and the atom density $\sim 10^{13}$/cc; thus there are on the order of 4×10^{11} atoms of metal. Since saturation occurs at about 50-60 percent hydrogen-to-metal ratio, each particle is capable of holding 2×10^{11} hydrogen atoms or the equivalent of 10^{11} hydrogen molecules. At STP this hydrogen would occupy 3×10^{-9} cc or about 1000 times the volume of the particle.

If the absorption cross section of adsorbed water in the region of interest is low, $\sigma \cong 10^{-20}$ cm^2, then the water around each particle will absorb 10^{-4} of the 10^{11} photons/sec seen by the particle. If 50 percent of the solar flux is in the region of interest, 2×10^{-7} sec of exposure per particle will be necessary for the creation of one hydrogen atom. Saturation of each particle, therefore will take on the order of 40000 sec, or a couple of weeks. This approximation is mitigated by several factors.

1. Unabsorbed photons are scattered, thus the number of photons/cm^2/sec seen by each particle is increased by the number of times a particle is scattered before being absorbed. Reference to Figure 1 indicates that each photon may be scattered four to five times before there is a 90 percent chance of absorption.

2. Absorption of a photon by the metal rather than the adsorbed water might also couple to the water since the photon still must be absorbed on the surface. This effect will be important for achievement of high efficiencies unless the absorption cross section of the adsorbed water molecule can be made greater than 10^{-18} cm^2 or so.

The addition of other metals (Cu, Ag, Au) has been shown to increase the heat of solution for hydrogen. The explanation proposed for this is that the interstitial sites are enlarged by increasing the percent of alloying metal thereby making the hydrogen interstitials more stable (ref. 17). Assuming this model is correct, we can expect to adjust the heat of solution for hydrogen and and control the heat required to release hydrogen from the metal hydride.

Summary

A system involving separation of hydrogen from water will most likely proceed on a mildly chemisorptive surface, using a transition metal or transition metal alloy whose activation energy for hydrogen absorption is several kilocalories per mole thus providing stable storage of hydrogen in the hydride form at room temperature. Such a metal may be palladium, an alloy of palladium and silver

or copper, or $LaNi_5$. The adsorption of water molecules on the surface will produce light absorbing bands in the infrared, visible, and ultraviolet portions of the spectrum. Although the optical cross sections of some of the bands may be small, the depth of the suspension and particle concentration or the surface roughness can be made large to totally absorb the incident light energy. The absorbed energy will promote dissociation of adsorbed species by the direct excitation of electrons out of their bonding orbitals. Additional energy absorbed by the particles will produce localized heating and will further facilitate dissociation and desorption.

Separation by diffusion will involve a thin film of palladium or palladium alloy through which the hydrogen will diffuse and evolve on the back side. The diffusion of hydrogen through palladium is a well known phenomenon currently used for hydrogen purification. The flow rate through such a film is determined by the partial pressure on either side, the thickness of the film, and the temperature. Flow rates on the order of 10 $cc/sec/cm^2$ are easily achievable. Thus the flow limiting step will be the hydrogen uptake at the active surface. A simple calculation shows that the diffusion limit for a 51-μ film at 500°C would be the energy equivalent of approximately 100 kW/m^2.

Separation by particles from the suspension may proceed by numerous techniques. Settling tanks or filtration probably are the least expensive, but for magnetic alloys, magnetic separation may be attractive. In either case, the adsorbed hydrogen may be reclaimed by heating or lowering the pressure below equilibrium. Particles may then be recirculated in the system.

The process described here is in many ways similar to the observed behavior of palladium. Palladium, or the other platinum group catalysts, are used to enhance the probability of specific reactions occurring by breaking selective bonds, thereby allowing certain molecules to rearrange their structure. This process frequently involves the removal of hydrogen from a particular functional group and placement in another. Because of the solubility of hydrogen, palladium is preferred for hydrogen-transfer type reactions (ref. 18). Typically, hydrogenation-dehydrogenation reactions use nickel or palladium alloys suspended on carbon, alumina, or any of a variety of substrates. An alternatively used method, however, is a slurry of particles which are mixed with the solution and subsequently filtered out. (See, for example, ref. 19.) This separation process is operational on an industrial scale and could probably be adapted to the separation problem discussed here.

It appears to be possible to produce a system for the generation of hydrogen by the photolysis of water. The information available in the current scientific literature supports the essential principles underlying the concept including the reduction of the dissociation energy and the separation of the reaction products using a metal alloy system. The efficiency of such a scheme will depend on the optical cross sections and the relative reaction rates for the various processes involved. There remains, at this point, a serious question about the ultimate efficiency of such a scheme. Although we can make both optimistic and pessimistic assessments of the outlook, the answer will be known only after an experimental program has been carried out.

REFERENCES

1. Glasstone, S.: Textbook of Physical Chemistry: Chapter XIII, Chemical Kinetics; D. Van Nostrand Co., New York, 1956, p. 1146.

2. Suhrmann, R.; Heras, J. M.; de Heras, L. Viscidio; and Wedler, G.: Chemisorption und Zerfall der Wassermolekel an reinen Eisen-und Kupferoberflachen bei niedrigen Temperaturen. Berichte der Bunsengesellshaft fur Physikalische Chemie, Vol. 72, no. 7, 1968, p. 854-863.

3. Lazarov, D.; and Bliznakov, G.: Einfluss der Adsorption von Sauerstoff und Wasserdampf auf die elektrische Leitfahigkeit dunner Eisenschichten. Zeitschrift fur Physikalische Chemie, Vol. 233, no. 3/4, 1966, p. 255-265.

4. Suhrmann, R.; Heras, J. M.; de Heras, L. Viscido; and Wedler, G.: Chemisorption und Zerfall der Wassermolekel an reinen Nickeloberflachen bei niedrigen Temperaturen. Berichte der Bunsengesellshaft fur Physikalische Chemie, Vol. 68, no. 5, 1964, p. 511-516.

5. Cohn, J. G. E.: Hydrogen Diffusion Process. U. S. Patent #3,238,700. 8 March 1966.

6. Chen, Mei C.; and Taylor, H. Austin: Photolysis of Water Vapor. J. Chem. Phys., Vol. 27, Oct. 1957, p. 857-863.

7. Paleocrassas, S. N.: Photocatalytic Hydrogen Production: A Solar Energy Conversion Alternative? Solar Energy, Vol. 16, no. 1, Aug. 1974, p. 45-51.

8. Trasatti, Sergio: Work Function, Electronegativity, and Electrochemical Behaviour of Metals. 1971, p. 351-351. La Chimica et Inoustria, Vol. 53, no. 4, Apr. 1971, p. 364-365.

9. Lazarov, Dobri; Manev, St.; and Rangelov, B.: The Structure of Metal Films and the Changes in Their Conductivity During Adsorption. I. Adsorption of Water Vapor on Copper. J. of Catalysis, Vol. 21, no. 1, 1971, p. 12-19.

10. Phillips Research Labs: The Eindhoven Giant. Phys. Today, Vol. 27, no. 6, June 1974, p. 61-62, 64.

11. Watanabe, K.; and Zelikoff, Murray: Absorption Coefficients of Water Vapor in the Vacuum Ultraviolet. J. Opt. Soc. America, Vol. 43, no. 9, Sept. 1953, p. 753-755.

12. Wehour, G. K.; and Hajicek, D. J.: Cone Formation on Metal Targets during Sputtering. J. Appl. Phys., Vol. 42, no. 3, 1 Mar. 1971, p. 1145-1149.

13. Graham, Thomas: On the Occlusion of Hydrogen Gas by Metals. Proc. Roy. Soc. (London), Vol. 16, 11 June 1868, p. 422-427.

14. Vossen, J. L.: Control of Film Properties by rf-Sputtering Techniques. J. Vacuum Science and Technology, Vol. 8, no. 5, Sept./Oct. 1971, p. S12-S30.

15. Brodowsky, H.; and Wicke, E.: Solubility and Diffusion of Hydrogen and Deuterium in Palladium and Palladium Alloys. Engelhard Industries Technical Bulletin, Vol. 7, no. 1-2, 1966, p. 41-50.

16. Pfeferle, W.: Engelhard Industries, private communication.

17. Maestas, S.; and Flanagan, Ted B.: Diffusion of Hydrogen in Gold-Palladium Alloys. J. of Physics and Chemistry, Vol. 77, no. 6, 15 March 1973, p. 850-854.

18. Wise, Edmund J.: Palladium Recovery, Properties and Uses. Academic Press, New York, 1968, p. 160.

19. Rylander, Paul N.: Catalytic Hydrogenation over Platinum Metals. Academic Press, New York, 1967.

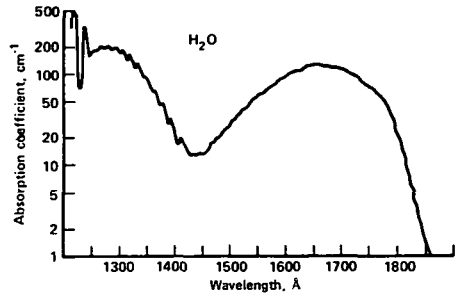

Figure 1.– Absorption spectrum of water vapor.

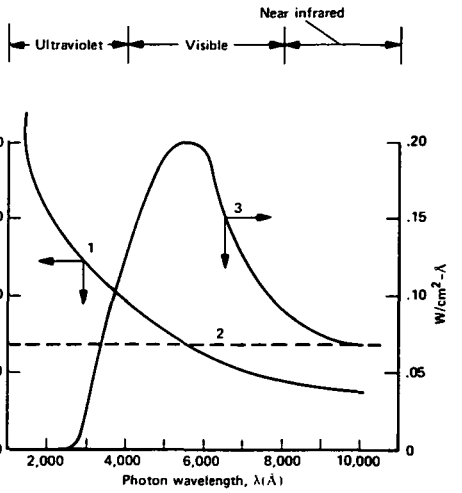

Figure 2.– Photon energy (1), water dissociation (2), and solar irradiance (3) versus photon wavelength.

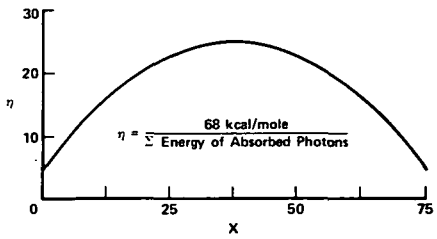

Figure 3.– Potential process efficiency.

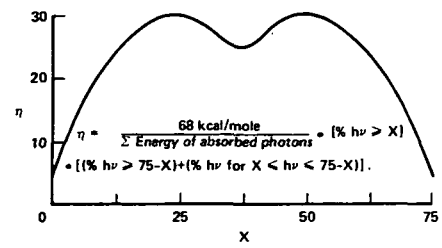

Figure 4.– Potential efficiency, including solar irradiance effects.

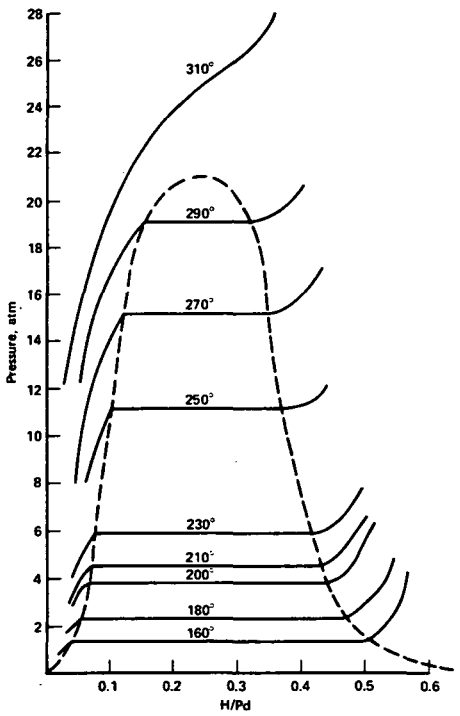

Figure 5.– Plots of p C relationships.

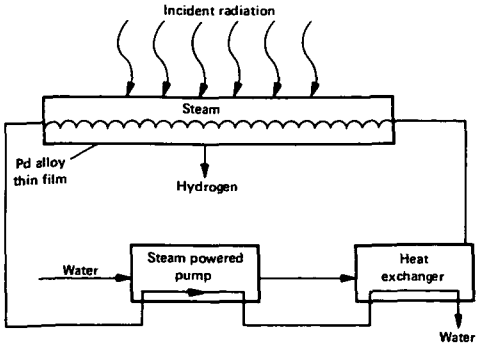

Figure 6.– Hydrogen generator using thin film separator.

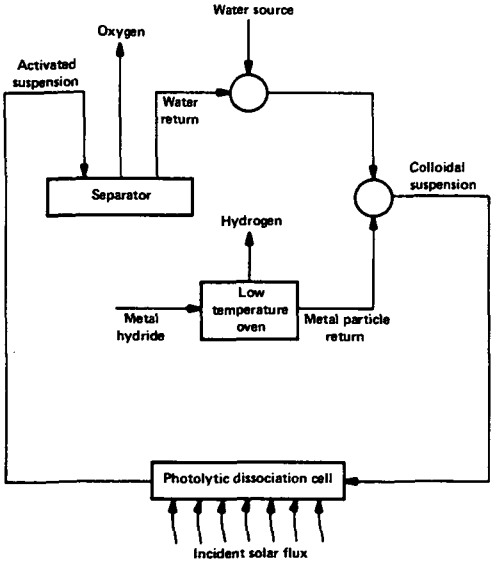

Figure 7.– Catalytic separation of hydrogen from water.

DISCUSSION

Dick Miles, Princeton University – I have a comment. I just want to say that there are two problems – which was not entirely clear. The first one is the use of the laser. It appears that if we can reduce the activation energy such that one can use 4000 Å or so and create hydrogen in either a hydride form or evolving to the surface, then we have a very high laser conversion efficiency. Solar conversion is a very different question – requiring two photons since the solar spectrum doesn't have very many 4000 Å photons. Thus it will be necessary to use a two step process which of course will require an intermediate state which would be either the breaking of an OH band off the surface or getting one hydrogen into a metal hydride and the other into the OH. That's why there are two considerations here. However, from the point of view of laser conversion, it doesn't have to be a double step process.

Dick Pantell, Stanford – Is there a deterioration of the palladium catalyst, do you have to replace it periodically?

Answer: No. First of all let me say we are speaking about a system that has not yet been built. But the deterioration of hydrogenation catalysts in the petroleum industry is only associated with the available carbon. We shouldn't have that problem. So the question is will we remove the catalysis products, will we oxidize them. We suspect the answer is no, unless we have contamination of the feed stream.

Mark Wrighton, M. I. T. – You are essentially separating hydrogen and oxygen on a catalyst and the stability comes in because of the complex which is formed.

Answer: It's very stable.

Mark Wrighton, M. I. T. – But if you ever wish to make large amounts of hydrogen and oxygen in that system, you will decompose back to water since platinum is an extremely good catalyst for that.

Answer: That's just the point. You see, we are removing the reaction products as the reaction takes place. In the thin film situation we are keeping the concentration of the reaction products down by, on the front surface, continually replenishing with fresh water and, on the back surface, by removing the hydrogen. In the case of the collodial particle we are talking about the same situation. When the particle comes reasonably near the saturation point where you have to worry about back reactions, its gone since another particle takes its place.

Mark Wrighton: Another question. If you have this material in there, all that's going to happen is that its going to heat up. I don't see the advantage over using a piece of black paper and letting the laser heat it.

Answer: That's not true at all. In fact if it were, *you* would have problems also.

Mark Wrighton: Yes, but in my system there are discrete photochemical reactions which correspond to electronic transitions – optical transitions. In this case, I don't know of any examples of photochemical reactions on surfaces.

Answer: Well, photochemical reactions that Greg has done in solution are exactly the same thing.

Dick Miles: Let me comment. This is something we are going to be studying. Obviously what we do will depend upon the absorption band of the surface complex. We hope to be able to couple to the vibrational absorption bands and increase the probability of this reaction going over the thermal probability. That is what the apparatus we just showed is set up to demonstrate.

Bill Bottoms: The question is basically, if we are just absorbing the energy directly into the palladium its just going to heat up and you are right, its just going to get hot. If, however, we are absorbing the energy into the surface complex, then we have the same kinds of transitions available that anyone else does that is irradiating a complex of metal and water.

Karlheinz Thom, NASA Headquarters – In both talks we've heard that the speakers have avoided considering the use of uv photons because they are too expensive. But photochemists feel that they will make progress in their fields and they should allow, therefore, that the laser people will make progress in their field also. Being an optimist, I predict that we will have cheap uv photons in the not too distant future and we shouldn't neglect this possibility.

Bill Bottoms: These uv photons are expensive, not because its expensive to buy a laser, but because the energy you can get back is less than the energy you have invested with the uv photon. So its expensive in terms of chemistry. When you burn water you don't get as much energy back as you put in with one uv photon, so you want to bring down the photon energy to as low a value as possible.

Max Garbuny: Because of the great interest in isotope separation it is quite likely that work of this type will be investigated thoroughly in the near future.

Bill Bottoms: Thank you for the interesting comment. However, I must point out that the literature has data on the diffusion through palladium of both hydrogen and deuterium and, unfortunately, they are disturbingly similar! The rates are not as far apart as one would like.

PHOTOVOLTAIC CONVERSION OF LASER ENERGY*

Richard J. Stirn

Jet Propulsion Laboratory

INTRODUCTION

One obvious technique for converting laser to electrical energy is by the use of photovoltaic devices because of our experience with them as solar cells. The efficiency of such devices is dependent on the wavelength and even on the energy density of the laser beam because of temperature effects. In general, though, one would expect useful operation in the range of a few tenths microns to several microns in wavelength, but *not* at 5 or 10μ. The energy density range is estimated to be from any lower level up to about 15 to 20 kW/m^2. With the addition of active cooling, the upper value could be increased considerably.

Photovoltaic devices are attractive for laser conversion for the following reasons: (1) relative ruggedness, (2) efficient light absorption, (3) built-in redundancy leading to high reliability, (4) absence of hazardous materials, (5) present conversion efficiencies of 30 percent with 40 percent feasible, (6) high flexibility in the system design and in transportation and assembly in space because of the small physical size of the devices, and (7) in the case of Schottky barrier devices, ability to match the laser wavelength (within the range mentioned above).

At the first conference held 2 years ago, Professor Martin Wolf presented an excellent tutorial talk on the basics of photovoltaics. The talk was oriented toward silicon technology, and particularly toward p/n homojunction devices, since that technology is presently used in space for solar cells. However, this technology is very limited for laser conversion in that practical maximum efficiencies for silicon (about 40 percent) occur only for a wavelength around 0.9μ. There is presently no high energy laser being developed that will operate in the 0.9-μ range. Operation at shorter wavelengths, and hence, at higher photon energies, will only provide excess heat as explained by Professor Wolf. Only an energy of 1.12 eV, the band gap of silicon at room temperature, corresponding to a wavelength of 1.1μ, is required to generate the electron-hole pairs that will contribute to the output current. However, photons of wavelengths between 0.9 and 1.1μ will not be efficiently utilized either because of the low light absorption in silicon – typical in indirect band gap semiconductors.

If efficient conversion is required at wavelengths shorter than about 1μ, wider band gap semiconductors are required. Indeed, the band gap energy should nearly equal the laser photon energy for maximum efficiency. Since most such semiconductors with a reasonable history of materials technology development are direct gap materials (III-V compounds), light absorption is very high, and the operating wavelength can be very near the absorption edge; that is, the photon

*This paper presents the results of one phase of research carried out at the Jet Propulsion Laboratory, California Institute of Technology, under Contract NAS 7-100 sponsored by the National Aeronautics and Space Administration.

energy can be just slightly higher than the band gap energy. However, the technology of good p/n junction photovoltaic devices is virtually non-existent for such materials. Another alternative is clearly needed.

An alternative that has been under investigation at JPL is the Schottky barrier (SB) photovoltaic converter. As will be shown, efficiencies to 30 percent at any wavelength in the visible and near infrared region are now attainable with potential for even higher efficiency. Furthermore, the devices can be made in solar cell sizes, such as 4 cm^2 or 9 cm^2, and the semiconductors used (GaAs and $GaAs_{1-X}P_X$) are readily available, as they are commercially grown by vapor epitaxy in very large quantities for the present light-emitting diode market.

PHOTOVOLTAIC CONCEPTS FOR SCHOTTKY BARRIERS

Structure

The structure of the SB converter is shown on the right hand side of figure 2. Physically it is very similar to a conventional solar cell except that the p/n junction is replaced by a simple metal-semiconductor interface. (The oxide layer will be discussed below.) The semiconductor can be nearly any semiconductor depending on the photon energy of the laser; however, the ternary compounds of GaAs containing phosphorous have been chosen because of their relatively high state of development, commercial availability, crystal sizes of 6-10 cm^2, and large scale production potential. The compounds under investigation ($GaAs_{1-X}P_X$, $0 \leqslant X \leqslant 0.5$) are epitaxially grown from the vapor phase on highly doped substrates of GaAs. The latter provide for lower bulk series resistance and for good ohmic back contacts. The photo-active layer need only be several microns thick because of the high light absorption.

The semi-transparent metal film currently being used is an evaporated 60Å-thick gold film. The grid contact has been a thicker film of gold – soon to be changed to another metal for soldering ease. The antireflection coating is presently Ta_2O_5. All fabrication steps can be done sequentially in one vacuum evaporation station without breaking vacuum. Neither the AR coating nor grid contact have been optimized to date.

A number of advantages of the SB approach as compared to p/n junctions are given in figure 2. As we shall see, the current output of SB devices is substantially better than a junction solar cell for a given wavelength and intensity, but the voltage output is inherently lower. Two approaches to improve the voltage will be discussed later.

Current Output

The basic mechanism of all photovoltaic devices is the absorption of photons of sufficient energy to generate electron-hole pairs – usually one pair per photon. Professor Wolf's talk at the last conference described some of the loss mechanisms in the collection efficiency (η_c) which prevent the current generated from being equal to the maximum possible current ($q N_{ph}$), where q is the electronic charge and N_{ph} the photon density. Figure 3 shows the generation of the hole-electron pair for a direct-gap semiconductor such as GaAs. For photon energies above the band

gap, the excess energy is converted to heat by lattice interactions. The amount of light generated current (J_L) for a given power input (P_{in}) is given by

$$\frac{J_L}{P_{in}} = \frac{q}{hc} \lambda \eta_c , \tag{1a}$$

$$\frac{J_L}{P_{in}} \left(\frac{\text{amps}}{\text{Watt}}\right) = 0.80 \ \lambda \ (\text{microns}) \ \eta_c \left(\frac{\text{electrons}}{\text{photon}}\right), \tag{1b}$$

where h is Planck's constant, and c the velocity of light. Figure 4 shows the relationship between P_{in} and J_L for various collection efficiencies. Typical values of η_c, the number of electrons collected per photon absorbed, are from 0.7 to 0.9 in an SB device. For example, with a wavelength of 0.5 μ and a power of 10 kW/m^2, the output current density would be about 300 to 350 mA/cm^2 with no reflection losses.

The simplest model for current generation (ref. 1) leads to the expression for J_L given in figure 5, where $\phi \equiv N_{ph}$ (absorbed), α is the absorption coefficient, W is the space charge region width (see figure 1), and L_p the hole (minority carrier) diffusion length. The last term in the expression for J_L is negligible. Experimental measurements of the spectral response do not agree well with this expression, particularly at short wavelengths, probably due to recombination in the inversion layer (in figure 1, $0 < X < \lambda$). This effect should decrease with increasing doping concentration since both λ and W decrease in width. Devices are now being made to verify this. In any case, such expressions for current density or collection efficiency are only valid for photons absorbed in the semiconductor. The wavelength dependence for the transmission of light through the metal film for the thicknesses utilized is not that well known to be able to calculate exactly the density of photons transmitted into the semiconductor.

On the basis of some computer calculations, it is believed that the amount of absorption in the 60-Å gold film is about 10 percent, with another 5-10 percent lost because of the grid structure. Despite these losses, the output current of the SB cells is generally better than that in junction devices, particularly at short wavelengths. Figure 6 shows some results of the calculated optical characteristics, which have primarily been used to determine the antireflection coating requirements.

In summary, the expected current densities from SB cells are those obtained from equations (1a and 1b) or from figure 4 using a value of ~ 0.8 for η_c. These current densities are satisfactory, especially for GaAs which has good values of minority carrier diffusion length (L_p). Little improvement can be expected except by decreasing the metal film thickness or grid area, neither of which is compatible with higher laser intensities.

Voltage Output

Improvements in conversion efficiency can only come from increases in the voltage output. This parameter, in particular the open-circuit voltage V_{oc}, is determined by the magnitude of the dark diode current density J_D. Referring to figure 5, the expression for J_D is for an ideal or near-ideal metal-semiconductor contact. For doping densities below about 5×10^{16} cm^{-3}, field

emission or tunneling are negligible, and J_D is determined by the barrier height ϕ_B since the current is by thermionic emission over the barrier. The constant A* is the modified Richardson's constant, $A^* = m^*/m_o \times A_o$, where $A_o = 120\ A/^oK^2/cm^2$, and m^*/m_o is the ratio of effective-to-free electron mass; R_s is the series resistance and k the Boltzmann constant. The empirical factor n describes non-ideal behavior due to image forces, field-tunneling, and interfacial layers.

Upon setting the current J equal to zero, the expression for V_{oc} in figure 5 follows. We see that for a fixed light intensity, and hence, fixed J_L, V_{oc} is linearly dependent on n and logarithmically on J_D. An obvious means of increasing V_{oc} is by raising ϕ_B. Since the barrier height is approximately two-thirds of the band gap for many n – type semiconductors, this increase in V_{oc} can, and indeed is, raised by using higher band gap materials. Figure 7 shows this effect assuming a modest value for n of 1.1. Unfortunately for laser energy conversion, the wavelength must be decreased correspondingly so as to assure absorption in the semiconductor. But for a given power density, the total number of photons decreases as the wavelength decreases according to

$$N_{ph} = \frac{\lambda}{hc} P_{in} \tag{2}$$

Consequently, the amount of current generated drops, even as the voltage rises, and we find that the conversion efficiency remains approximately the same. The means of varying the band gap, and hence, the barrier height, is simply done by adding phosphorous or aluminum to GaAs (figure 8). Since Schottky barriers can be made with equal ease on any of these ternary compounds, the increase in band gap to "tailor" the converter to any specific laser with about the *same* efficiency is one of the major features of the SB cell. Figure 9 gives the spectral response, or actually η_c, measured for three ternary compounds. We see that the peak of response, as expected, does shift to shorter wavelengths as the phosphorous content is increased. Thus, for example, the ideal converter material for matching the copper vapor laser under development at JPL ($\lambda = 5106$Å) is $GaAs_{1-X}P_X$ with X about 0.4.

In summary, increasing the voltage output by raising the semiconductor band gap does not increase the efficiency due to the drop in current (assuming that the laser wavelength is kept near the equivalent band-gap wavelength). To further increase the efficiency, which is about 20 percent for the "ideal" SB cell (n = 1.0), other concepts must be utilized.

ADVANCED CONCEPTS

Multilayer Schottky Barrier Cell

We have seen that raising the semiconductor band gap, and hence, the barrier height, increases the voltage output. However, for monochromatic light, we are limited by the fact that the energy of the band gap can not exceed the photon energy. For polychromatic light, such as sunlight, the increase in band gap will decrease the current because of reduced light absorption.

A concept such as that shown in figure 10 is currently under development on another program to obtain the higher voltage without a major drop in current. The top layer upon which the Schottky barrier is made has a band gap of about 2 eV and is epitaxially grown on GaAs which has a

band gap of 1.42 eV. Photons which are not absorbed in the top layer are absorbed in the GaAs. Because of the difference in band gaps, there will be a 0.5-eV barrier for the minority carriers (holes) to surmount or penetrate if they are to be collected at the surface. For this reason, the top layer thickness should ideally be not larger than the width of the space charge region W, in which case, the built-in electric field should improve the hole transport by thermionic-field emission. Since GaAsP compounds require a region of graded composition to minimize the effect of dissimilar lattice constants with GaAs, the top layer semiconductor was chosen to be $Al_XGa_{1-X}As$ which has a much better lattice match with GaAs. Unfortunately, AlGaAs is presently grown only by liquid epitaxy. This process does not give as smooth a surface as vapor phase epitaxy, and does not allow for large areas or large quantity production. Suitable devices with the required physical characteristics have not been grown to date. In any case, the major interest in such a device, if successfully grown, will be for broad-band light, that is, sunlight energy conversion, since these would be only limited improvements for laser energy conversion.

AMOS Solar Cell

A major advance in increasing the efficiency of both laser and solar energy Schottky barrier converters has recently been made at JPL. With an addition of a controlled amount of oxide layer between the semi-transparent metal film and the semiconductor, as shown in figure 1, the open-circuit voltage was found to increase by as much as 50 percent. Figure 11 shows a comparison between two cells under water-filtered tungsten lighting – one without the oxide and the other with (called AMOS – *A*ntireflection coated *M*etal-*O*xide-*S*emiconductor). The oxide process also works on GaAsP compounds and figure 12 shows a light I-V characteristic for laser illumination at 5154Å. This cell has an efficiency of 30 percent when AR-coated. The enhanced effect occurs at all light intensities investigated, and cells have been operated at current densities of nearly 0.4 A/cm^2, or over 10 times the current density of a silicon solar cell in space.

The oxide layers reported on here were thermally grown in air at temperatures between 100° and 200°C. The oxide films are apparently patchy and nonuniform, thus the ultimate enhancement in efficiency has not been obtained. Increasing the oxide thickness increases the value of the empirical factor n, through at the same time it increases the value of the pre-exponential part of J_D. The diode current departs from purely thermionic emission as the thickness increases, thus tending to lower the increase in voltage. The *net* effect though, is to substantially raise the voltage to some unknown limit, before which the series resistance of the oxide film degrades the curve factor of the light I-V curve. This occurs at about 50-Å thickness depending on the light intensity level being used.

An explanation for such a marked effect is not completely understood at this time, but undoubtedly is related to the density of surface states at the oxide-semiconductor interface. The presence of an interfacial layer modifies the transmission coefficient of the barrier, and hence, the value of J_D at a given bias. Since there will be a bias dependent voltage drop across the insulating layer, there will also be a reduced dependence of the semiconductor surface potential on bias leading to an increased value of n in the expression for J_D. The degree of the effect on the value of n depends on whether the interface states are in better communication with the metal or with the semiconductor. The analysis of the interfacial effect on n for dark current-voltage curves was first reported by Card and Rhoderick (ref. 2), who showed that increasing the oxide thickness (on silicon) increases the communication between the interface states and the semiconductor, and in

turn, increases the value of n. We have been able to double the value of n, although the aforementioned increase in the pre-exponential term limits the corresponding increase in voltage to some degree.

Our current effort is to improve and optimize the oxidation process and to better understand the underlying physics of the enhanced effect, with a goal of 40 percent efficiency at any wavelength in the visible.

REFERENCES

1. Gartner, W. W.: Depletion-Layer Photoeffects in Semiconductors. Physical Review, Vol. 116, no. 1, 1 Oct. 1959, p. 84-87.

2. Card, A. C.; and Rhoderick E. H.: Studies of Tunnel MOS Diodes I. Interface Effects in Silicon Schottky Diodes, J. Phys. D: Appl. Phys., Vol. 4, no. 10, 1 Oct. 1971, p. 1589-1601.

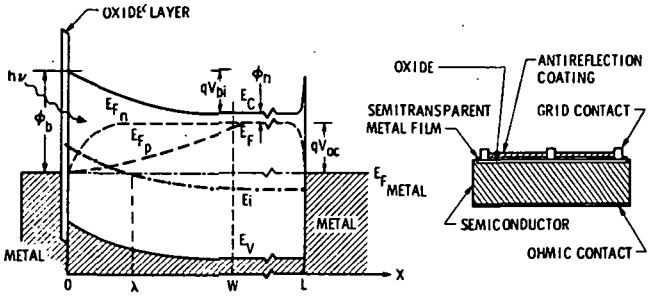

Figure 1.– AMOS solar cell.

- ADVANTAGES OF BARRIER CELLS
  - LOW TEMPERATURE FABRICATION
  - HIGH CONTROL OF CHARACTERISTICS
  - LOW COST BARRIER FABRICATION
  - CARRIERS GENERATED IN SPACE-CHARGE REGION
  - ELIMINATES PROBLEM OF SHALLOW JUNCTIONS
  - ELIMINATES PROBLEM OF SURFACE RECOMBINATION
  - COMPATIBLE WITH POLYCRYSTALLINE FILMS
- REQUIREMENTS OF METAL FILM
  - HIGH LIGHT TRANSMISSION
  - LOW SHEET RESISTANCE
  - STABLE
  - HIGH BARRIER HEIGHT
  - COMPATIBILITY WITH A-R COATING

Figure 2.– Schottky barrier cells.

$$\frac{J_l}{P_{in}}\left(\frac{\text{amps}}{\text{watt}}\right) = 0.8\ \eta_c\left(\frac{\text{electrons}}{\text{photon}}\right)\lambda\ (\mu)$$

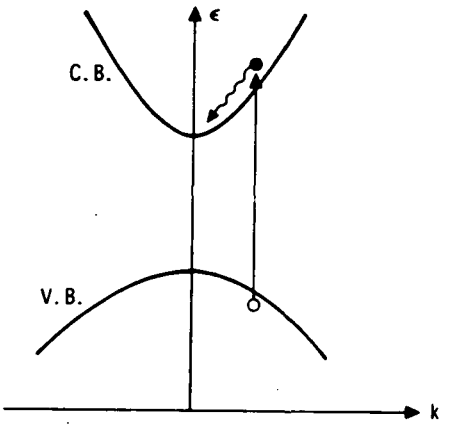

Figure 3.– Current generation.

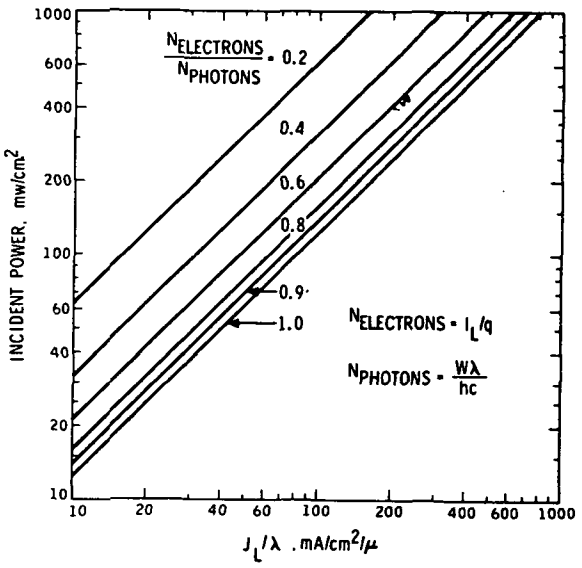

Figure 4.– Determination of collection efficiency.

$$J = J_D - J_L$$

$$J_L = -q\phi\left\{1 - \exp\left[-\alpha W(V)\right]/1+\alpha L_p\right\} - \frac{qD_p}{L_p} p_o \left[\exp(-qV/kT)-1\right]$$

$$J_D = A^* T^2 \exp(-\phi_B/kT) \exp\left[q(V-IR_s)/nkT - 1\right]$$

$$V_{oc} = nkT/q\left[\ell n (J_L/J_D) + 1\right]$$

Figure 5.– Solar cell equations.

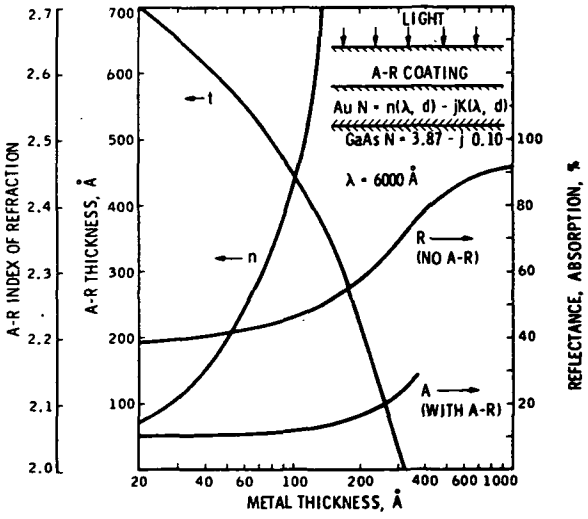

Figure 6.– Optical characteristics.

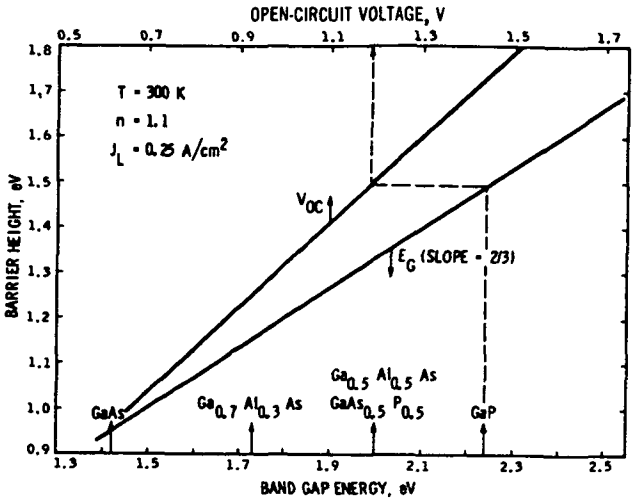

Figure 7.– Effect of higher band gaps.

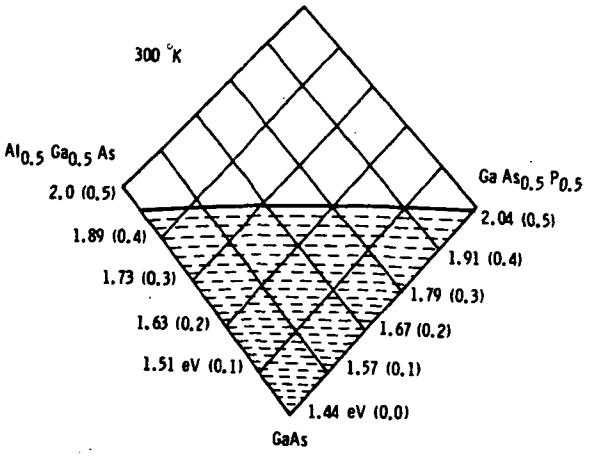

Figure 8.– Ternary compounds of Ga As.

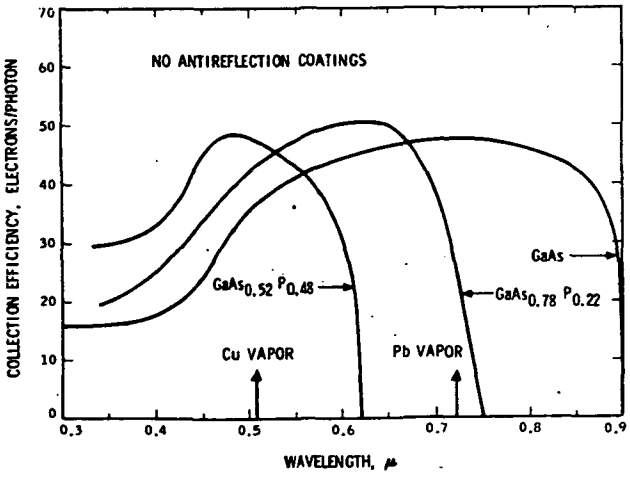

Figure 9.– Absolute spectral response.

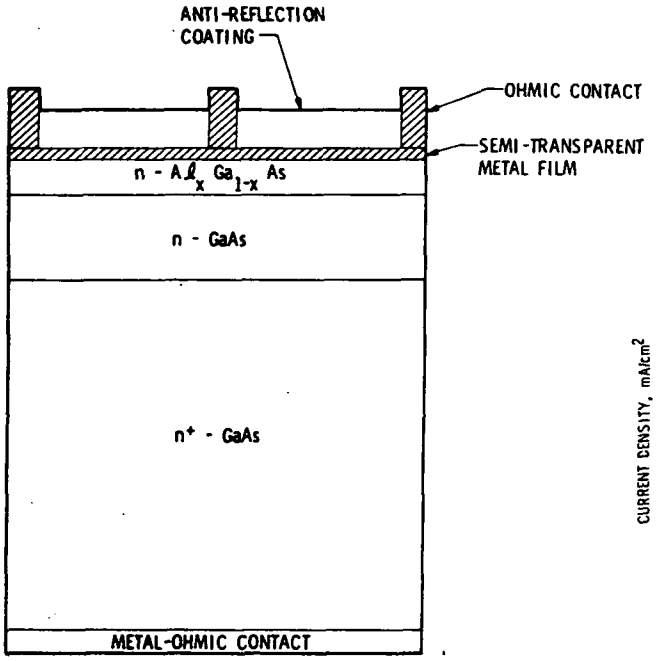

Figure 10.– Multilayer Schottky barrier solar cell.

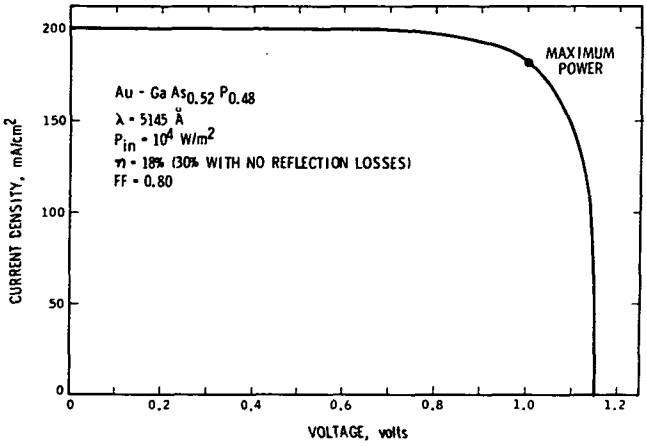

Figure 12.– Light 1-V characteristic.

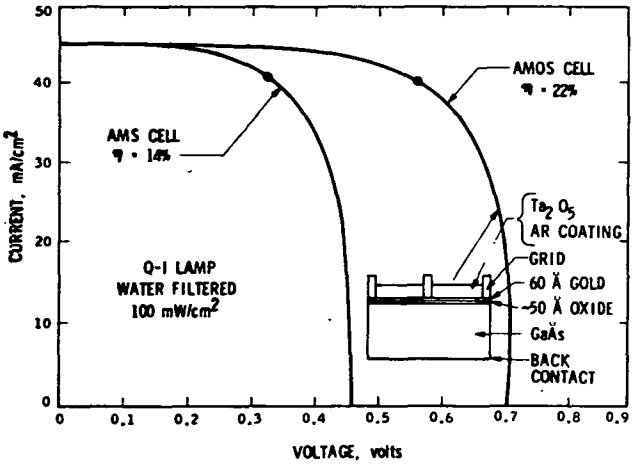

Figure 11.– AMOS solar cell.

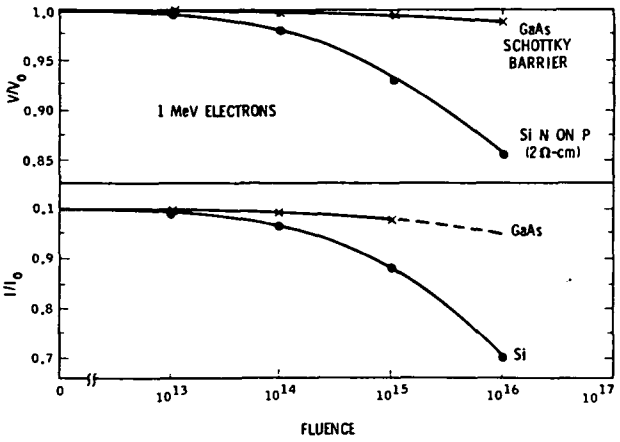

Figure 13.– Radiation resistance.

DISCUSSION

Ned Rasor, Rasor Associates – I assume all these results were recorded at room temperature?

Dick Stirn: Yes.

Ned Rasor: I wonder if you could mention how high you could go and not get well out of this performance range.

Dick Stirn: That's a very pertinent question, of course, and I did mean to mention that at the beginning but overlooked it. All photovoltaic devices, of course, have this problem. It comes in the reverse saturation current since there is a temperature dependence. As one increases temperature, the output drops. In silicon its like 2 mV/°C and that corresponds in sunlight to about 2 mW/°C. Normally with PN junction devices as you go up in band gap this improves, the source of this reverse saturation current in a junction is related to the diffusion current and that's related to the band gap, But, unfortunately, for a Schottky barrier device it's thermionic current and who knows what with the oxide layer AMOS cell. We don't know for sure since we haven't yet investigated its temperature dependence. But for the thermionic emission, of course, that has different temperature characteristics and in practice its turning out to be comparable to that of silicon. So even though we are working with a higher band gap, the temperature characteristics are similar to silicon and we would expect to see that kind of decrease. So we predict that its going to be about 2 mV/°C loss and you can carry that as far as you like. The big question is how high these will be operated at, of course. That's hard to say – it depends on the system we are finally going to talk about. Certainly, even if we could shield the cells from the sun by orientation or with a narrow band filter, this would help a lot. A solar panel stabilizes at about 60°C. How well heat sinked these are and radiate to outer space will determine their temperature.

Mark Wrighton, M. I. T. – What is the highest absolute current you have been able to achieve?

Dick Stirn: We haven't particularly shot for that; we haven't even ran the laser at full power. We are just putting on AR coatings which will remove a 40 percent loss. Dr. Lundholm was there the other day. What was it – gallium arsenide that we stuck on which did have an AR coat? I remember that we were running about 0.5 A/cm^2 I think with the laser we have now, we can run up to 1 A/cm^2.

Joe Horwath, Lockheed – It is well known that the quantum efficiency for light generation from gallium arsenide can be dramatically improved by lowering the temperature to, for example, 77°K. Have you, in fact, lowered your temperatures to see what the efficiencies become?

Dick Stirn: I don't think the collection efficiencies will change much with temperature; of course you are referring to the inverse processes. But for electrical output, the inverse process – conversion – the current is relatively insensitive to temperature. What will happen is the voltage will go up. Thus the inverse of what Ned Rasor mentioned will happen – the voltage will increase by 2 mV/°C down until other processes take over. Thus the efficiency goes up even higher.

Joe Horwath, Lockheed – But there is no, abrupt nonlinear type effect?

Dick Stirn: Not that I am aware of; physically I can't see of any.

Dick Pantell, Stanford – The use of AR coatings means that you have to be concerned about orientation.

Dick Stirn: That's true – we always assume normal incidence. In the system they would be on panels which you assume will be oriented for the beam so the cosine of the angle, even for 20°, will be small.

Dick Pantell, Stanford – But with interference multilayer films this will be quite sensitive – much more sensitive than a cosine law.

Dick Stirn: No, we will use a very simple layer AR coating, and this should not be very orientation-sensitive.

Joe She, Colorado State University – I guess these Schottky barrier devices are only applicable to wavelengths shorter than 0.9 μ? Could you comment on the possibility of extension to longer wavelengths?

Dick Stirn: They are not very attractive. The same is true with PN junctions. The problem is that the voltage is dropping. As you go to lower and lower band gaps the reverse saturation current keeps increasing just as if you were going up in temperature. For larger than 1 μ of course, you would have to leave silicon. And the band gap and Schottky Barrier will be small, so that the voltage output will be small. This oxide might help, but you still will only have about one-half volt output.

Joe Horwath, Lockheed – Except for gallium arsenide phosphide, I really don't see that the economics of the system are ever going to be in favor of Schottky barrier devices of the type you mentioned as opposed to the silicon devices.

Dick Stirn: Are you talking about terrestrial use or space use where in the latter case you can tolerate a high cost for performance? The present Schottky substrates are about five times that of silicon; with mass production they tell me this can be lowered to two and one-half times. As long as you brought that up – let me mention that one of the reasons for working on Schottky barriers is that the approach should lend itself to polycrystalline thin films, unlike other photovoltaic devices. We are going to look into this for the terrestrial solar energy program in the very near future. Because the Schottky is made by a low temperature process, without too much loss in efficiency this could be adapted to a polycrystalline thin film which will cut down the cost tremendously.

HIGH PHOTOVOLTAGES IN FERROELECTRIC CERAMICS

Philip S. Brody

Harry Diamond Laboratories

INTRODUCTION

Photovoltaic effects which seem specifically connected with ferroelectricity have only a brief history. Weak steady photocurrents in flux-grown single crystals were observed by Chynoweth (ref. 1) in the middle 1950s. These were seen in connection with studies of pyroelectricity and polarization of surface layers in single crystals. A similar effect, observed by Brody and Michael Vrabel in 1968 (ref. 2), originated in pyroelectric surface regions of disordered ferroelectric ceramic barium titanate. The photo-emf's were clearly related to a remanent polarization within these layers exhibiting the same temperature dependence as this polarization. The emf's were considerably less than 1V.

A high-voltage effect was observed by Brody in polarized barium titanate ceramic in 1971 (ref. 3), and soon afterward in other polarized ferroelectric ceramics (ref. 4). The high emf was proportional to the sample length. Such a phenomenon is usually called a high voltage – bulk photovoltaic effect. High-voltage effects have been previously observed in ZnS single crystals by Merz (ref. 5). A length dependent photo-emf also appears in evaporated polycrystalline films of semiconductors in which the evaporation source was at an angle to the substrate. These are fairly well known from the work of Pensak (ref. 6) and others.

The photovoltaic effect in ferroelectric ceramics is characterized by a high photo-emf parallel to remanent polarization and proportional to its magnitude. The emf is proportional to sample length in the direction of polarization, and generally to the number of grains per unit length. A rectangular slab with electrodes on opposing edges, such as that shown in figure 1, uniformly and steadily illuminated on its unobscured face, appears as a source comprised of an intensity-saturable emf in series with a photoresistance. For saturation intensities there appears a steady short-circuit current depending linearly on intensity. The current also depends strongly on the wavelength peaking sharply for light with energy in the vicinity of the band-gap energy. Typically in these materials, this is the near ultraviolet or violet. The emf is also, but less strongly, dependent on wavelength.

We have measured the short-circuit current and photo-emf for various ceramics including barium titanate, lead metaniobate, and lead titanate – lead zirconate solid solutions, these latter with niobium, strontium and lanthanum additives. Results include emf's of 1500 V/cm in centimeter-size samples of small-grain-size $Pb(Zr_{.65},Ti_{.35})O_3$ with 7 percent lead substituted for by lanthanum – a hot pressed ceramic known as PLZT 7/65/35. In the ceramic $Pb(Zr_{.53},Ti_{.47})O_3$ plus 1 wt% nb_2O_5 the saturation photo-emf is about 500 V/cm and the short-circuit current, for the wavelength producing the peak current, is about 1 $\mu A/cm/W/cm^2$. This last material is the best material that we have measured thus far in terms of energy conversion. A short-circuited sample converts 0.06 percent of incident light to electrical energy.

From the view point for energy conversion, such a number is discouraging. However, up to the present we have done no material research and have used materials that are commercially produced for their piezoelectric or electro-optical properties. There are undoubtedly ways to increase efficiency. In this light it should be remembered that the efficiency of the first photocells using cuprous oxide did not exceed 0.1 percent (ref. 7).

The experimental results will be described in greater detail, and completing this, a mechanism for the effect will be proposed.

PHENOMENA

The steady voltage produced is proportional to the length, ℓ, between the electrodes in an arrangement such as that shown in figure 1. Dividing the sample in two equal segments along a line perpendicular to the direction of remanent polarization and placing new electrodes on the cut edges results in new samples producing photo-emf's which are one-half the original photo-emf.

An arrangement such as that shown in figure 1 can be described roughly by an equivalent circuit shown in figure 2. This circuit has a saturation photo-emf in series with the photoresistance of the illuminated sample. The sample capacitance C is across the electrodes. Figure 3 is the current-voltage characteristic of a typical illuminated ferroelectric slab. It has the form expected from the equivalent circuit in figure 2, except for the slight tendency to saturation in the lower-left quadrant. The photo-emf saturates as a function of intensity at relatively low levels of illumination. The short-circuit photocurrent is, however, linear with light intensity. Typical results showing the intensity dependence are shown in figure 4. The implication of these results and of the equivalent circuit in figure 2 is that the photoresistance is inversely proportional to intensity.

Photo-emf's and short-circuit currents for a number of ferroelectric materials are shown in table 1. The photo-emf is also a function of grain size. Results showing this are given in table 2.

The wavelength dependences of the photo-emf and photocurrent for $Pb(Zr_{.53}Ti_{.47})O_3 + 1$ wt% Nb_2O_5 shown in figure 5, are typical of these materials. The current (ordinate) is that produced by illumination contained in a small band, of about ±10 nm, about the wavelength indicated on the abscissa. A mercury source and notch-type dichroic filters were used. The total intensity within each band was only roughly constant. Therefore, the current that has been plotted has been normalized to constant intensity – assuming that the relation between current and intensity is linear.

The photo-emf is less strongly dependent on wavelength. Results for a particular material, using notch-type dichroic filters are shown also in figure 5. These values are saturation values, independent of intensity.

Similar results for the same material using dichroic, short wavelength cutoff filters are shown in figure 6. Here it is seen that high emf's continue to be produced at wavelengths shorter and also considerably longer than the 373-nm wavelength at which the short circuit current peaks.

In the arrangement shown in figure 1 the direction of polarization, and consequently the direction of the photo-emf, is perpendicular to the direction of incidence of the light, which is also the direction in which the light is strongly absorbed. The light only enters into a region near the surface of the material. The rapidity of the absorption depends strongly on the wavelength of the light, the light becoming fully absorbed in a region closer and closer to the surface as the wavelength of the light approaches the band-gap wavelength. For shorter wavelengths, the light no longer enters the material, and light-induced emf vanishes.

Polishing the surfaces of these materials increases the transparency by decreasing the amount of diffuse reflection. Then, as expected, the magnitudes of the photocurrent and the photovoltaic conversion efficiency increase.

An emf will also be produced by the arrangement shown in figure 7, in which the front surface electrode is transparent. The emf now appears across the thickness of the material in the direction of the remanent polarization. The currents, however, are limited by the high dark-resistance of the unilluminated region of the sample.

MECHANISM

We now propose that the photo-emf results from the action of internal fields within individual ceramic grains on non-equilibrium carriers generated by illumination. These carriers move to screen the internal field. This is a change in charge distribution upon illumination, which changes the voltage across a grain from an initial value of zero to the photovoltages that are observed.

The photo-emf's appear across individual ceramic grains. What is observed as a length-dependent high photovoltage is the series sum of the photo-emf's appearing across grains, each of which is characterized by a saturation remanent polarization. The situation is shown schematically in figure 8. Individual grains are small, typically of the order of 10 μ in diameter. To produce a high photovoltage-per-unit-length in the ceramic, the voltage across an individual grain need not be large. For example, the results in table 2 for $Pb(_{.65}Zr,_{.35}Ti)0_3$ (7% La) can be explained by individual grain photovoltage of only about 0.5 V per grain. The implication of the experimental results (table 2 and figure 5) is that for the range of grain sizes investigated, the photo-emf across a grain is more or less independent of the size of the grain.

ORIGIN OF INTERNAL FIELDS

Ferroelectric ceramics are characterized by a large remanent polarization that would be expected to produce a large emf even in the dark. Such an emf is not observed even across highly insulating materials. This absence of an emf must be the result of space charge within the volume or on the surface of the individual ceramic grains. The space charge produces a potential across a grain cancelling the potential produced by the net polarization. It seems obvious that as long as there are, within a grain, charges that are free to move, any potential produced by an internal polarization will eventually vanish.

In our argument this dark zero-potential state produced by the presence of space charge is assumed to be the initial state of a ceramic grain. The absence of a net potential in the dark does not however necessarily mean the absence of internal fields. Internal fields can be expected to exist as a consequence of an extended but not uniform spatial distribution of the charges which bring the net potentials across grains to zero. These spatial distributions cannot be arbitrarily assigned but are subjected to constraints of a basic physical nature.

Were there no space charge producing a field negating the bound polarization charge, there would be a potential across a grain. The electric field within this grain would, however, be well above the dielectric breakdown strength of a real dielectric. For example, in a single-domain ferroelectric crystal of barium titanate, the spontaneous polarization is $P_s = 26 \times 10^{-2} C/m$, and the relative dielectric constant ϵ_r in the direction of polarization is 137. The maximum field in the materials would not exist for long but be reduced to some value below the dielectric strength of the material. The strong field would break down the material and a charge flow would produce a space charge distribution, resulting in a new lower value for the internal fields within the bulk of such a crystal. The fields within the space charge layers themselves do not produce an additional breakdown within the layers. The mean free path of the charges involved have now become larger than the layer thickness itself, resulting in the elimination of the breakdown phenomena, an avalanche process.

We assume that such a space-charge distribution exists within each grain. The space charge serves to reduce the potential across each grain to zero. Such charges are assumed to have limited mobility and the materials behave as insulators for ordinary-strength applied fields.

The space charge must occupy a finite volume. If these charges are localized near the surface of the crystal, then an internal field E_b exists within the bulk of the material, and additional fields E_s exist in the space charge regions near the surface.

Reasons for hypothesizing that these space-charge regions are near the surface of real crystals with the charge distributed within a surface layer of small thickness ℓ are the following. (First, the surface regions ferroelectric crystals are characterized by regions whose dielectric, ferroelectric, and thermodynamic properties differ markedly from that of the bulk and these differences are best explained by the existence of strong fields in this region that would be produced by the space charge. There is a considerable body of information in the literature supporting the existence and delineating the properties of these layers (see, for example, ref. 8). Second, the interplay of space charge and the very nonlinear dielectric constant of ferroelectrics would be expected to localize space charge in a low dielectric-constant layer near the surface. In ferroelectrics unusually high, low-field relative dielectric constants (of the order of 1000) can be expected to be reduced in value with increasing field strength. Thus, charge in a region reduces the region's dielectric constant *of that region*, and increasing its field strength. This feedback mechanism can be shown to localize charge within a layer (ref. 9).

A schematic description of a hypothetical grain, with space charge regions of thickness s, and a bulk region of thickness ℓ, is shown in figure 9. The grain has within the bulk region a dielectric constant ϵ_b and uniform remanent polarization P_o. Within the surface layers the dielectric constant, ϵ_s, is considerably less than that of the bulk. There are also remanent polarizations in the surface regions $P_s(x)$. These will generally be parallel to the bulk polarization at one end and anti-parallel at the other end. It is the space charge that produces the high fields which reduce the highly nonlinear

dielectric constant of the bulk to the lesser value E_s in the surface layers, and also produce a remanent polarization by ordering domains within the surface. The fields within the grain can be easily calculated using the two-dimensional model shown in figure 10.

The remanent polarizations within the various regions are assumed to be uniform within these regions. This is done to simplify the calculations. Again, only for simplicity, the polarizations in the surface layers and the bulk are assumed equal in magnitude (that is, $P_s(x) = P_o$). The space-charge densities $\pm n_o e$ are also assumed uniform and equal in magnitude. The polarizations are equivalent to four bound-surface charge densities,

$$\sigma_1 = P_o, \quad \sigma_2 = -2P_o \quad \sigma_3 = O \quad \sigma_4 = P_o$$

From Gauss's law, the electric fields are

$$E_1 = \frac{1}{\epsilon_s}(P_o + n_o ex), \tag{1}$$

$$E_2 = \frac{1}{\epsilon_b}(-P_o + n_o es), \tag{2}$$

$$E_3 = \frac{1}{\epsilon_s}[-P_o + n_o e(L-x)] \tag{3}$$

We have assumed that the voltage across the crystal vanishes

$$\int_o^{\ell+2s} E(\alpha)\, d\alpha = 0 \tag{4}$$

The variables n_o and s, from this and the three preceding equations, must be related by the expression

$$n_o es = \frac{P_o}{1 + \frac{\epsilon_b}{\epsilon_s}\frac{s}{\ell}} \tag{5}$$

and the bulk field must be

$$E_2 = -\frac{P_o}{\epsilon_b}\left(\frac{\frac{s}{\ell}\frac{\epsilon_b}{\epsilon_b}}{1 + \frac{s}{\ell}\frac{\epsilon_b}{\epsilon_s}}\right) \tag{6}$$

To obtain a photo-emf of the correct sign it is now assumed that illumination has the effect of producing charges that screen only the internal field, E_2, causing it to vanish. The negative voltage vanishes and a positive potential appears across the sample. The light makes the sample look more positive. This is exactly what happens using the conventions of figure 10, as the result of a thermally produced decrease in polarization of the bulk. The pyroelectric voltage is in the same direction as the photovoltage. This is what is actually observed.

Thus, light-generated free electrons, produced only within the bulk, set up a counter-field that tends to cancel the bulk field, E_2, producing a voltage drop across the bulk that is less than would occur in a completely insulating medium; this is what is meant by the term screening. At sufficiently high intensities the counter-field approaches the bulk-field. Assuming the shielding occurs only in the bulk, the total voltage across the grain is now the sum of the voltage across the surface layers, which are equal but opposite in sign to that initially across the bulk.

Surface layers in barium titanate ceramic grains have been estimated at 10^{-6} cm (ref. 8). The remanent polarization typical of the ceramic material is about 8×10^{-2} C/m^2; the relative dielectric constant of the poled ceramic is about 1300. We will estimate that the high-field dielectric constant is roughly one half the bulk dielectric constant. From equation (6) the bulk-field, for a typical 10^{-3} cm grain is,

$$E_2 = -0.35 \text{ V}$$

The saturation photo-emf would thus be 350 V/cm, or at least of that order of magnitude.

The potential across the surface layer is

$$\int_0^s E_1 \, dx + \int_0^s E_2 \, dx = (n_o e s)\, s$$

The saturation photo-emf and the polarization are therefore related linearly in the model, as is experimentally observed.

It should be noted that, as the temperature increases, not only is P_o decreasing, but the dielectric constant, ϵ_s, is undoubtedly increasing. The saturation photo-emf might therefore be expected to decrease with temperature more rapidly than the remanent polarization. Such a behavior has been observed in $BaTiO_3$ + 5wt% $CaTiO_3$ ceramic (ref. 4).

CONCLUDING REMARKS

Summarized, our suggestion is that the emf's (and currents) arise from the presence of photoconductor-insulator sandwiches in the presence of space-charge-produced internal fields. The experimental results are in general agreement with the theory. Nevertheless, the model remains so

over-simplified that the possibility of the agreement being fortuitous is a reasonable one. Quite different explanations for high photo-emf's in ferroelectrics have been propounded by Johnson (ref. 10) and others in connection with studies of light-induced refractive index changes in lithium-niobate single crystals.

The experimental results are significant, however, when taken alone. They suggest a general phenomenon in ferroelectric ceramics, significant in magnitude and with unique characteristics. We not only have a consistent producer of high-voltage photoelectricity but a photo-battery, the polarity and magnitude of which can be switched by application of an electrical signal. It is also a phenomenon involving cheap polycrystalline materials. Certainly it warrants further investigation, especially from a materials point of view.

Acknowledgements – I would like to thank Frank Crowne and Harold Watkins of the Harry Diamond Laboratories who contributed in essential ways to this paper.

REFERENCES

1. Chynoweth, A. G.: Surface Space Charge Layers in Barium Titanate. Phys., Vol. 102, no. 3, 1 May 1956, p. 705-714.

2. Brody, Phillip S. and Vrabel, Michael J.: Pyroelectric Surface Layers and Photovoltaic Effect in Ceramic $BaTiO_3$ and Single Crystal $SrTiO_3$. Bull American Phys. Soc., Vol. 13, no. 4, April 1968, p. 617.

3. Brody Phillip S.: Large Polarization-Dependent Photovoltages in Ceramic $BaTiO_3$ + 5 wt. % $CaTiO_3$. Solid State Communications, Vol. 12, no. 7, 1 April 1973, p. 673-676.

4. Brody, Phillip S.: High Voltage Photovoltaic Effect in Barium Titinate and Lead Titanate – Lead Zirconate Ceramics, J. of Solid State Chemistry, Vol. 12, no. 314, 15 Jan. 1975, p. 193-200.

5. Merz, Walter J: The Photovoltaic Effect in Striated ZnS Crystals. Helv. Phys. Act., Vol. 31, no. 6 1958, p. 625-635.

6. Pensak, L.: High Voltage Photovoltaic Effect. Phys. Rev., Vol. 109, no. 9, 15 Jan. 1958, p. 601.

7. Ioffe, Abram F.: The Physics of Semiconductors, Translation Edited and Indexed by A. J. Goldssmid. Info search Ltd., London, 1960, p. 220.

8. See for example, Jona, Franco; and Shirane, G.: Ferroelectric Crystals. The MacMillan Co., New York, 1962, p. 181-186.

9. Bloomfield, Phillip E.; Lefkowitz, I.; and Aronoff, A. D.: Electric Field Distribution in Dielectrics, with special Emphasis on Near-Surface Regions in Ferroelectric. Phys. Rev. B, Vol. 4, no. 3, 1 Aug. 1971, p. 974-987.

10. Johnston, W. D. Jr.: Optical Image Damage in $LiNbO_3$ and Other Pyroelectric Insulators. Journal of Applied Physics, Vol. 41, no. 8, July 1970, p. 3279-3285.

TABLE 1. – PHOTOVOLTAIC OUTPUTS AT WAVELENGTHS PRODUCING MAXIMUM SHORT CIRCUIT CURRENTS

Material	Illumination wavelength, nm	Photo-emf, V/cm	Photocurrent, $\mu A/cm/W/cm^2$
$BaTiO_3$ + 5wt% $CaTiO_3$	403	360	0.020
PLZT 7/65/35, polished	382	1500	0.030
PLZT 8/65/35, polished	382	750	0.015
$Pb(Zr_{.53}Ti_{.47})$ + 1wt% Nb_2O_5, unpolished	373	420	0.63
$Pb(Zr_{.53}Ti_{.47})$ + 1wt% Nb_2O_5, polished	373	510	1.0

TABLE 2. PHOTO-emf FOR DIFFERENT GRAIN SIZE (The material is PLZT 8/65/35.)

Grain size, μ	Photo-emf, V
2-4	750
3-5	510
4-6	330
greater than 6	250

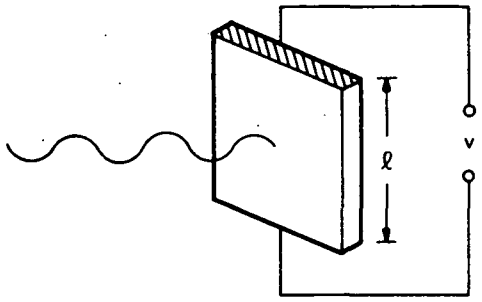

Figure 1.– Schematic of an illuminated sample.

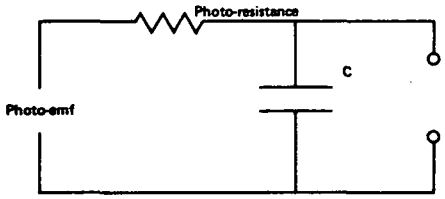

Figure 2.– The equivalent circuit of an illuminated sample. C is the sample capacitance.

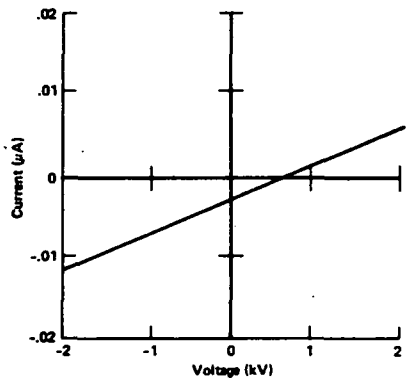

Figure 3.– Current vs applied voltage for an illuminated sample.

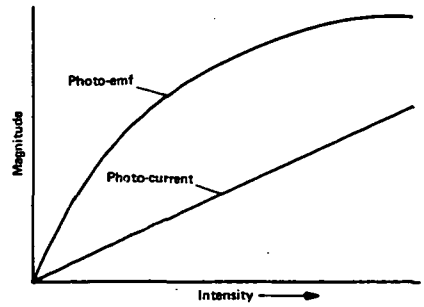

Figure 4.– Intensity dependence of photo-emf and photocurrent for a typical material.

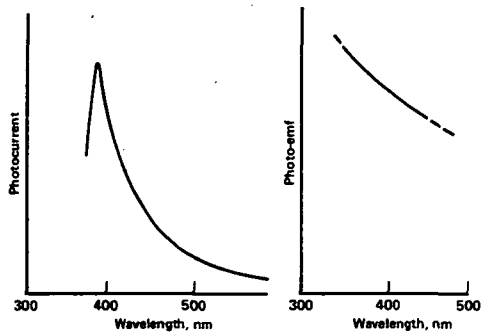

Figure 5.– Spectral behavior of photocurrent and photo-emf for $Pb(Zr_{.53}Ti_{.47})O_3$ + 1wt% Nb_2O_5.

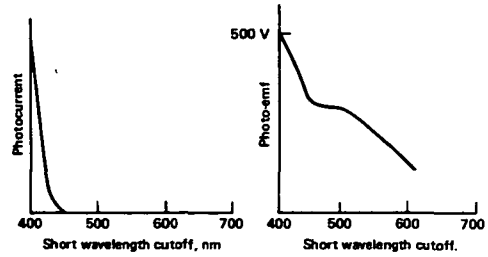

Figure 6.– Spectral dependence of photocurrent and photo-emf for $Pb(Zr_{.53}Ti_{.47})O_3$ + 1wt% Nb_2O_5.

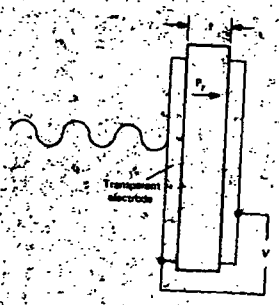

Figure 7.– Light incident through transparent electrode. P_r is the remanent polarization.

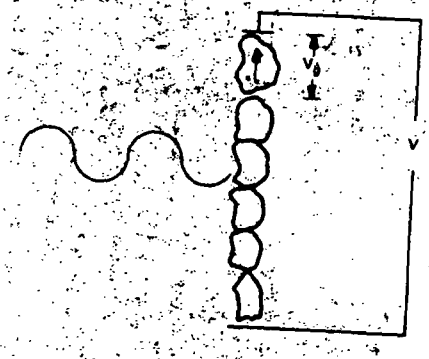

Figure 8.– Emf's across grains adding to produce a length dependent effect in a ceramic.

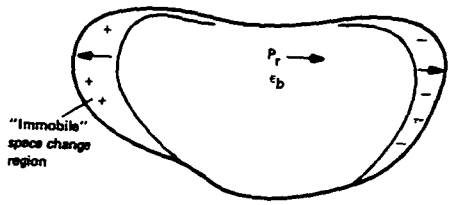

Figure 9.– Structure of a grain.

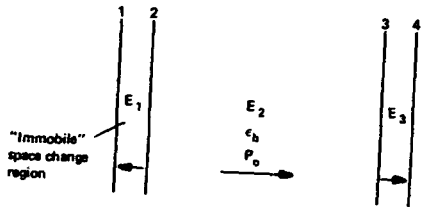

Figure 10.– 2-D model of a grain.

DISCUSSION

Joe She, Colorado State University – Is there a phase transition temperature in these materials?

Philip Brody: Yes, the phase transition in barium titanate is at 120°. You have to operate below the phase transition which is at 465°C for the material which has the highest efficiency that I have examined so far. It drops linearly with the temperature, but the current goes up. With the PZT materials I've gone up to 120°C and the power is not dropping. That is, the current is going up with temperature while the voltage is going down.

Dick Stirn, J. P. L. – From the last slide, are you interpreting the high voltage as from one grain of material rather than a series effect?

Philip Brody: Well, the voltage appears across a grain but the high voltage is a series effect. Each grain only has about one-half volt across it. I've also looked at single crystal barium titanate and seen the order of one volt. However, I've just gotten some recent measurements in lead niobate which are producing about forty volts per centimeter in a true bulk effect.

Dick Stirn, J. P. L. – You recognize, of course, that the large series resistance of these materials will limit their usefulness for power conversion; even one tenth of an ohm will be a problem.

Philip Brody: Right, although it has not yet been examined at high laser intensities. Perhaps it will blow up before high currents are achieved. However, this is a new phenomena and it needs investigation. It seems that it would find its greatest use in production of high voltages at somewhat reduced powers.

Ned Rasor, Rasor Associates – I assume that you haven't made any estimates or projections of the energy conversion efficiency.

Philip Brody: I did the simplest thing you could do. I said what is the photon energy and how many volts is the electron dropping and it comes to 20 to 30 percent.

Ned Rasor, Rasor Associates – The problem comes, of course, whether you can deliver that at one volt and with a reasonable current density. My thought is that perhaps this device could operate in a periodic discharge mode. Since the capacitance is too great, what you are looking at is merely the sort of leakage, whereas if you charged and discharged on a periodic basis you could perhaps get around the impedance problem.

Philip Brody: Yes, that's true. We operate in the static or dc mode to separate this effect from pryolytic effects, however you could go in a charge-discharge mode to achieve large currents. The efficiency would not increase, however.

Max Garbuny, Westinghouse – Have you tried a Q-switched laser pulse on these materials?

Philip Brody: No, we have been so short of money that even the cost of $2000 to replace a laser tube right now is holding up the research. In the future we hope to be able to.

OPTICAL ELECTRONICS

A. Javan

Physics Department, Massachusetts Institute of Technology

In the radio and microwave frequency region, the science of electronic devices operating on the principles of alternating currents flowing through the device elements, is broadly known as radio and microwave-electronics. Its vast discipline encompasses the whole technology of classical electronic devices made up of vacuum tubes and solid state elements along with lumped circuits or distributed components; oscillators, amplifiers, converters, counters, etc., are just a few examples.

Quantum electronics, on the other hand, is based on entirely different principles. In this case, instead of electric current flow through individual device elements, electrons resonating in atoms or molecules determine the device properties. These devices are, accordingly, based on quantum mechanical concepts rather than classical; maser oscillators and amplifiers, quantum counters, etc., are examples of these in the radio and microwave frequency regions.

In order for an element to allow an alternating current at a high frequency to flow through it, its time constant, τ, must be less than or comparable to the period, T, of the alternating frequency current. An element's time constant is determined by its own inherent speed and the RC time constant of the lumped circuit to which it is coupled. In addition to this time domain requirement, a vast majority of radio or microwave electronic applications demand that the overall size of an element and its associated lumped circuit components be less than the wavelength corresponding to the alternating current frequency. This latter condition obviates problems due to phase shifts which can occur over distances larger than one wavelength and results in cancellation whenever the current through an element runs out of phase with respect to the voltage wave.

In the low radio frequency region, the dimensions of the component elements (that is, the vacuum tubes, transistors, tank-circuits, etc.) are generally considerably less than a wavelength. At higher frequencies, however, it is possible to distribute these components over distances exceeding several wavelengths; in these, the phases of currents in the various elements are kept in step with the voltage wave to prevent the cancellation.

In quantum electronics, one usually does not think in these terms; however, analogies exist – for one, an atom or a molecule's time constant is sufficiently short, allowing it to respond to frequencies where its resonances lie. And as for the phase consideration, we note that here inherently we deal with a distributed system with atoms or molecules filling volumes of dimensions exceeding a wavelength. The atoms' keeping up with the spatial phase of the electromagnetic wave follows from the laws of stimulated emission of radiation or the phase-matching criterion of the parametric processes. As a result, neither the time constant nor the phase requirements were at any time in the past a problem in our efforts to extend quantum-electronic devices into the optical regions; this became a reality with the advent of lasers early in the 1960s.

Extensions of radio and microwave electronics into optics, however, have required devising a high-speed element of microscopic size with a time constant less than an optical period and dimension less than one light wavelength. Starting in the mid-1960s, in a continuing series of

research efforts (refs. 1 and 2), we succeeded in making a two-terminal high-speed junction element capable of responding at very high frequencies. And with it we have shown that it should be possible to extend the whole science of radio and microwave electronics into the far-infrared, infrared, and eventually the visible regions. While this is still in its infancy, these experiments, (which include some recent and as yet unpublished MIT works), show the future possibilities in this whole new set of technology, which we now identify as Optical Electronics.

Naturally, as in quantum electronics, optical electronic devices will be expected to fulfill substantially different types of need, compared to their counterpart devices in the radio or microwave regions. Similarly, optical electronic applications will lie in enormously different areas than existing laser applications. And the two fields in combination promise to play major parts in such diverse uses as advanced computer memory and holographic imaging schemes in real-time. Much further work, however, is needed to reduce these far-reaching possibilities (which are in large part as yet theoretical) to practice.

In these, the research workhorse will have to be highly-specialized microelectronic methods; examples include photolithography, electron-lithography, X-ray lithography, etc. Inspection shows that, with thin-film microelectronics, it should be possible to form on a substrate, for instance, an L-C tank-circuit of micro-size dimensions with a resonance frequency in the far-infrared or infrared. Such a tank-circuit can be integrated to a microscopic two-terminal high-speed deposited junction with nonlinear I–V characteristics. Such a unit can be used, e.g., as a phase bi-stable subharmonic parametric oscillator, driven with an external laser beam. Or, for a similar junction with a negative differential conductivity, the unit can be made to self-oscillate.

A useful tank-circuit will not necessarily be required to have a high-Q. For this, we need to be reminded that a radio-frequency oscillator can be made with an L-C circuit consisting of a coil and a capacitance with a Q of five or ten (occupying volumes with dimensions much less than a wavelength). An analogous situation can be envisaged for a deposited circuit forming the L-C tank of an oscillator, designed to oscillate, e.g., at a submillimeter frequency (see figure 1). Such an oscillator would not be a power oscillator, and, in fact, it might be used as an active unit internal to a device, (say in the form of a local oscillator), and with little or no energy coupled out of it.

Other embodiments can be envisaged in which a high-speed junction with negative differential conductivity is used as a bi-stable element, forming a high-speed flip-flop. This, along with a host of other possibilities, has far-reaching high-speed computer memory applications. For instance, an integrated system consisting of a large number of unit-cells can be envisaged in which all signal leads to the individual unit-cells are eliminated and, instead, each cell is communicated by light pulses (or with electron beams). (In the existing computer memory systems, the stray lead-capacitance limits the speed.)

One can also envisage a system in which the necessary bias-field for an active element is provided by integrating it to a deposited power supply consisting, e.g., of small rectifiers powered by an external radiation field. All these can, in principle, be done by focused laser beams or via integrated optics.

A summary of some early experiments and their immediate implications is as follows. The various developments followed the advent of a high-speed two-terminal junction element of microscopic dimension with a nonlinear I-V characteristic, and capable of supporting alternating

currents at infrared frequencies (refs. 3 through 5). The element is used at these high frequencies as a diode, in much the same way as an ordinary rectifier frequency-mixer diode is used at radio frequencies. The optical diode consists of a metal-dielectric-metal junction in which the high-speed electric conduction process occurs due to quantum mechanical electron tunneling across the dielectric barrier. In a series of experiments, we have shown that, when subjected to an infrared radiation, alternating frequency current at the frequency of the applied radiation can flow through the junction. This takes place following the nonlinear I-V characteristics, which results in a sizable distortion of the infrared frequency current waveform. In fact, it is possible to clip the waveform and produce a square-wave at the corresponding frequency. Further, the current rectification results in conversion of the applied sine-wave to a dc voltage appearing across the diode. Two different frequencies can be mixed in the diode, with the result that detectable infrared radiation is emitted from the diode at new synthesized frequencies (ref. 6). In addition, it has been possible to mix in the diode two infrared frequencies differing by more than several octaves, and thus compare the two precisely (ref. 7). This has enabled constructing a frequency multiplier chain to compare a laser frequency with a microwave clock. By now, the method has been used at MIT and a number of centers internationally, to determine precisely the frequency of laser radiation in highly accurate spectroscopic observation, and in precise measurements of the speed of light; major contributions have been made to this field by K. Evenson (ref. 8), J. Hall (ref. 9), and their colleagues at NBS. The MIT activities have now shifted to the exploitation of the high-speed junction elements in optical electronic devices outlined in this report.

The early models of the diode consisted of a mechanically-contacted unit. In a recent major advance, a new version of the diode element is developed in which the element is printed on a substrate (ref. 10). This is done by thin-film vacuum deposition and the application of photolithography and micro-electronics. The junction is integrated to a small infrared-frequency antenna for coupling to the radiation field. With this method, instead of one diode element, it is now possible to deposit simultaneously a large number of them and, when desired, distribute them in the form of a phased-array configuration at infrared wavelengths. Among several new applications, a two-dimensional array of these high-speed diodes can make possible superheterodyne imaging in infrared; the holographic application mentioned above is based on this principle.

In a series of as yet unpublished MIT works, we are able to show that, in our high-speed metal-dielectric-metal junction, it should be possible to control the growth of the dielectric layer (which is required to have a thickness under 10 Å) and, in fact, reproduce tunneling barriers whose properties are known from previous experiments on large-area tunneling junctions. (The latter junctions are low-speed, with cutoffs in the MHz region.) The large body of the existing theoretical and experimental information in quantum mechanical electron tunneling in large area metal-dielectric-metal junctions (refs. 11 and 12) can now be extended to our case. We now know that it should be possible to construct high-speed junctions with I-V characteristic curves resembling the previously known low-speed junctions. For instance, it is known that, in a multi-barrier tunneling junction, or in a Josephon tunneling junction between two dissimilar superconductors, I-V characteristics with negative differential conductivity can be obtained; we can now expect to manufacture high-speed versions of these same junctions for use as bi-stable elements and other computer application. Furthermore, there are cases in which the nonlinearities of the I-V curves are known to be very large (ref. 13). Estimates show that if these are reproduced in the form of high-speed junctions, conversion of an applied radiation to dc voltages by rectification in such junctions can be obtained with nearly unity efficiency. Beyond these, it is to be noted, multi-terminal high-speed elements of microscopic dimensions can also be envisaged. A high-speed

triode, for instance, would make possible new classes of high-frequency amplifiers with dimensions of tens of micron or less.

Far from implying that the above are all within an immediate reach, it is to be emphasized that a great deal of high technology research is required to establish all these various possibilities.

REFERENCES

1. For a review, see: Javan, A.: Modern methods in precision spectroscopy; a decade of development. Fundamental and Applied Laser Physics, Proceedings of the Esfahan Symposium, edited by Feld, Javan and Kurnit, John Wiley Interscience, 1973, p. 295. This article gives references to early works in frequency mixing including the works of K. Evenson and colleagues at NBS.

2. For a review discussion of physical processes and some future applications, see: Javan, A.; and Sanchez, A.: Extension of Microwave Detection and Frequency Measuring Technologies into the Optical Region. Laser Spectroscopy, edited by Brewer and Mooradian, Plenum Press, 1975, p. 11. For other works, see: Twu, Bor-Long; Schwarz, S. E.: Mechanism and Properties of Point-Contact Metal-Insulator-Metal Diode Detectors at 10.6μ. Appl. Phys. Letters Vol. 25, 1974. p. 595. Schwarz, S. E.: Triode Amplifiers for the Infrared. IEEE J. of Quantum Electronics, Vol. Q. E. 10, 62, 1974. Wang, S. Y.: Favis, S. M.; Siu, D. P.; Jain, R. K.; and Gustafson, T. K.: Enhanced Optical Frequency Detection with Negative Differential Resistance in Metal-Barrier-Metal Point-Contact Diodes, Appl. Phys. Letters Vol. 25, 1974, p. 493.

3. Hocker, L. O. et al: Frequency Mixing in the Infrared and Far-Infrared Using a Metal-to-Metal Point Contact Diode. Appl. Phys. Letters Vol. 12, 1968, p. 401.

4. Daneu, V.; Sokoloff, D. R.; Sanchez, A.; and Javan, A.: Extension of Laser Harmonic-Frequency Mixing Techniques into the 9μ Region with an Infrared Metal-Metal Point-Contact Diode; Appl. Phys. Letters Vol. 15, 1969, p. 398.

5. Sokoloff, D. R.; Sanchez, A.; Osgood, R. M.; and Javan, A.: Extension of Laser Harmonic-Frequency Mixing into the 5μ Regions, Appl. Phys. Letters Vol. 17, 1970, p. 257.

6. Sanchez, A.; Singh, S. K.; and Javan, A.: Generation of Infrared Radiation in a Metal-to-Metal Point-Contact Diode at Synthesized Frequencies of Incident Fields: A High-Speed Broad-Band Light Modulator. Appl. Phys. Letters Vol. 21, 1972, p. 240.

7. Javan, A.; and Sanchez, A.: loc cit, ref. 2.

8. Evenson, K. M.; Wells, J. S.; and Matarrese, L. M.: Absolute Frequency Measurements of the CO_2 CW laser at 28 THz (10.6μ). Appl. Phys. Letters Vol. 16, 1970, p. 251. See also: Evenson, K. M. et al.: Speed of Light from Direct Laser Frequency and Wavelength: Emergency of a Laser Standard of Length. Laser Spectroscopy, edited by R. G. Brewer and A. Mooradian, Plenum Press, 1975.

9. Hall, J.: Saturated Absorption Lineshape. Fundamental and Applied Laser Physics, Proceedings of the Esfahan Symposium, edited by Kurnit, Javan, and Feld, John Wiley Interscience, 1973, p. 463.

10. Small, J. G. et al.: A. C. Electron Tunneling at Infrared Frequencies. Appl. Phys. Letters Vol. 24, 1974, p. 275.

11. Giaver, Ivan: Electron Tunneling and Superconductivity. Science, Vol. 183, 1974, p. 1253.

12. Tsu, R.; and Esaki, L.: Tunneling in a Finite Superlattice. Appl. Phys. Letters Vol. 22, 1973, p. 562.

13. Shen, L. Y. L.; and Rowell, J. U.: Zero-bias Anomalies-Temperature, Voltage and Magnetic Field Dependence. Phys. Rev. Vol. 165, 1968, p. 566.

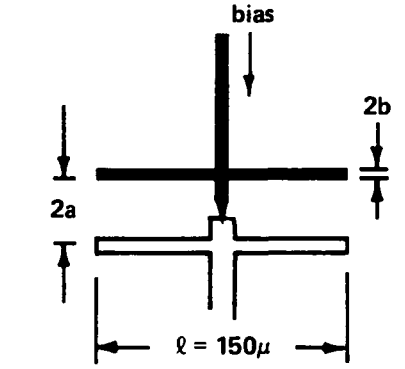

$$\frac{L}{\ell} = \frac{\mu_0}{\pi} \ln\left(\frac{a + \sqrt{a^2 - b^2}}{b}\right)$$

$L = 2.5 \times 10^{-11}$ H

$C_j = 10^{-15}$ (for $A = .1\mu^2$)

$$\omega_0 = \frac{2\pi c}{\lambda_0} = \frac{1}{\sqrt{LC}} \qquad \lambda_0 \simeq 300\mu$$

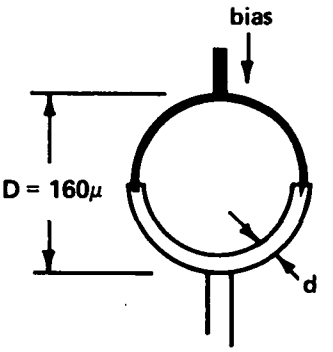

$$L = \mu_0 \frac{D}{2}\left(\ln\frac{8D}{d} - \frac{7}{4}\right) = 2.5 \times 10^{-11} \text{ H}$$

$C_j = 10^{-15}$

$$\omega_0 = \frac{1}{\sqrt{LC}} \qquad \lambda_0 \approx 300$$

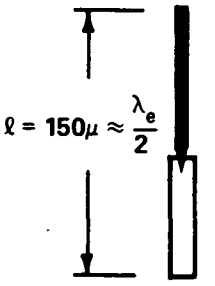

$C = 10^{-14}A$ A in μ^2

$\tau = R_A C \approx 10^{-12}A$

$$\omega_0 = \frac{2\pi c}{\lambda_e} \approx \frac{\pi c}{\ell}$$

Figure 1.– Tank circuits resonating in the far infrared. Capacitance in the lumped circuits are dominated by the junction capacitance.

DISCUSSION

Ernest Brock, Los Alamos Scientific Laboratory – Professor Javan, I believe all of us, in the spirit of your talk, are feeling stimulated response! I wanted to raise the issue of fabrication. The materials you are working with, for example, nickel and chromium, are evaporated and come down as polycrystalline materials, do they not?

Ali Javan: Yes, although we haven't studied the epitaxy, they probably do. I must mention that a major problem we have with the evaporated junctions, although we can print one or one hundred of them, the yield is very poor. Sometimes the yield is only 1 or 2 percent, at other times we can get to 40 to 50 percent. But there are holes and we have reason to believe they are polycrystalline.

Ernest Brock, LASL – With regard to polycrystalline aspects, we all know that in tunneling phenomena, not only the Fermi level but also the work function are important in establishing the contact potential difference. With a polycrystalline material you have some sort of average work function. If you could work with single crystal surfaces in contact with one another, then one would not have a spectrum, even with nickel and chromium, of the order of a volt of contact potential difference.

Ali Javan: Yes. Could I say that we have seen effects with a few junctions which we could explain as two junctions, one about 6 Å thick, the other about 7 Å thick, but in parallel. Sometimes the average is not random. By all means we have to go into the epitaxy.

Ernest Brock, LASL – One other aspect – with nickel you're working with a face-centered cubic material. Cadmium, perhaps, comes down hexagonal close packed, perhaps in a cubic modification. So far as going to cool temperatures, the detailed lattice structure would be quite important, you know the k vector, and so I'm wondering if you should be considering the phonon bath in which you are doing this, especially as your techniques become more sophisticated.

Ali Javan: Absolutely. Frankly, there is a whole field ahead and we are just beginning. So much will depend upon what we can do in the areas of microelectronics and thin films. There are only a few sophisticated microelectronics laboratories – we are attempting to duplicate a poor man's version of one, but much remains to be done. For example, we are looking forward to the possible use of electron microscope techniques for laying down 1000 Å x 1000 Å junctions. Also we wish to control oxide thickness carefully – quite possibly interesting photo emission effects can be seen. I am looking forward to hearing Dr. Gustafson's talk since he has been working in the interesting visible range of wavelengths which is a marvelous area to study barrier heights i.e. where the wavelength exceeds the barrier height.

Ned Rasor, Rasor Associates – Just a comment relative to the previous question. That is, you do not have to have single crystals to have single work function surfaces. You have a polycrystalline surface and then etch it just to expose a single crystal plane.

Ali Javan: May I also say that another thing enters here and that is that for cross sections like 1000 Å, the current densities in these junctions are extremely high. Thus we shouldn't think of a one-electron picture where the tunneling electron sees its image charge. We have to consider cooperative phenomena here.

OPTICAL DIODES*

T. K. Gustafson

University of California, Berkeley

Since the previous laser energy conversion conference, significant progress has been made in understanding the rather detailed phenomena which have characterized optical diode work (See, for example, ref. 1.) Of particular interest to us has been the fact that such structures can couple and rectify infrared and optical radiation in complete analogy to similar structures operating at microwave or radio frequencies. A recent achievement has been a direct demonstration of antenna coupling and rectification characteristics with high resistance evaporated structures at a wavelength of 10 μ. Earlier, optically induced signals had been demonstrated at 6328 A. We feel that as a result of the 10-μ work that high frequency arrays are inevitable.

The present summary contains a descriptive review of some of the aspects of our own work on metal-barrier-metal structures. Coherent conversion of laser radiation and infrared and optical circuit elements are seen as among the potentially exciting applications of such devices. Figure 1 shows the two basic types of structures which we, as well as others, have utilized for these investigations. Although many of the results have been achieved with the point-contact type of diode structure, recent rapid development of the more stable photo-lithographic structures has also occurred. Some of the particular advantages and disadvantages of each are quite apparent:

Diode structure	Advantages	Disadvantages
Point-Contact	Low bulk loss Small area Clean antenna structure	Mechanical instability Etching problems
Evaporated (Photolithographic or electron beam)	Stability Ease of design Amenable to arrays and complex configurations	Large area Thermal problems Difficult to obtain low junction resistances

*Contributors: D. P. Siu, S. Y. Want, S. M. Faris, Tatzuo Izawa, R. Jain, and B. Fan, University of California, Berkeley.

In both the point contact and evaporated structures it is apparent that the primary mechanism involved is electronic tunneling. The appropriate band diagram is shown on the left-hand side of figure 2. The difference between the Fermi levels of the two metals is the applied voltage eV which upsets the dynamical equilibrium of electron exchange across the barrier. Simmons (ref. 2) has deduced the basic semi-classical expression given in figure 2. This is seen to depend exponentially upon the voltage. The characteristic thus displays curvature which can of course be used to rectify and therefore to convert electromagnetic energy to electrical energy.

S. M. Faris has performed extensive rectification experiments at 1.06 μ and 0.6328 μ, the results of which have been well explained by the rectification theory (ref. 3); that is, that the voltage difference eV between the Fermi levels is in fact the sum of the bias voltage plus an optically induced voltage whose frequency is that of the incident optical radiation. Since these results are published, it is sufficient for the present purposes to provide an outline of the theory and point out the important characteristics which are supported by the experimental observations. Figure 3 contains a summary of the steps in the derivation of the rectification signal in terms of the Bessel functions of an imaginary argument and figure 4 displays the comparison between experiment and theory for the rectification of the He-Ne 6328 Å radiation. Experimentally rectified voltage V_ω is obtained using phase sensitive detection (direct detection arrangement at a chopping frequency of 1 kHz) and is plotted as a function of a dc bias potential V_B. Comparing the experimental results with the theoretically predicted behavior, one notes the agreement in curvature and intersection with the $V_\omega = 0$ axis. This behavior depends upon the behavior of the Bessel functions of an imaginary argument and, because the parameter z is directly proportional to the barrier thickness, upon the impedance of the junction as well as the optical voltage.

By fitting the theoretical curves with those measured experimentally one is able to obtain an estimate of the optical voltage and coupling characteristics. One finds that the optical voltage is of the order of 100 mV. Assuming this to be induced across the junction through the whisker acting as an antenna, the effective area of the antenna must of the order of 4×10^{-8} cm^2. The coupling efficiency is found to be of the order of 10^{-5}, indicating the expected very poor mismatch.

The success of the rectification experiments has prompted further work in several important directions:

1. Basic experiments in which high frequency antenna coupling could be clearly demonstrated (ref. 4).

2. Basic experiments which would confirm tunneling predictions at high frequencies and the presence of negative differential resistance at high frequencies (ref. 5).

3. Design and demonstration of evaporated (photolithographically fabricated) junctions which would behave similarly to the point contact structure.

4. High frequency arrays which would couple more efficiently to a given laser mode.

Several experimental and theoretical considerations have already demonstrated the principles involved in several of these directions. At this point it is worthwhile considering these and indicating directions in which future effort is most likely to be concentrated.

Generalizing from the particular case of rectification, higher order mixing characteristics of the diode junctions can become considerably more complicated. Relating to the excitation and coupling, the nonlinear mixing can be current controlled rather than voltage controlled, the case considered thus far. In addition, since the quasi-static equations of Simmons describe the nonlinearity it is important to check the validity of theoretical predictions relating higher order mixing processes. Finally, with respect to potential conversion, one should ask whether rectification is the most appropriate process to exploit.

Experimental evidence thus far strongly suggests that the coupling and nonlinear mixing processes can be either voltage or current controlled depending upon the antenna and junction impedance, antenna loss, etc. (ref. 6). In the submillimeter and far-infrared portion of the spectrum current control appears to be almost exclusive.

Figure 5 shows a schematic of a general (n+1)th order mixing process involving two incident frequencies. This is the most common process involved and has been discussed earlier by several authors. For current excitation the RMS voltage at the i.f. frequency $V_n(\omega_1 - n\omega_2)$ is proportional to the (n+1)th derivative of the voltage with respect to the current as indicated in figure 5.

The theoretical results are shown for n = 1 to 6. The minima and maxima, which occur for finite bias voltages and which number n for (n+1)th order mixing are the most striking characteristic. These can be used to definitively distinguish current from voltage excitation. No such minima would occur for voltage controlled excitation.

These characteristics have been observed experimentally by Sakuma and Evensen (ref. 7). We have included one of their experimental results corresponding to n = 5 in figure 5 to illustrate the striking agreement. In addition to their experimental results, Javan has discussed oscillations in the detected signal and Faris has obtained experimental results at 1.15 μ for n = 1 (rectification) which indicate current controlled rectification. The latter is shown in figure 6.

We are presently investigating more general aspects of the mixing theory. In particular we are attempting to employ two diode structures, one as a transmitter and the other as a receiver, to investigate the characteristics directly at 10.6 μ. This would represent a generalization of the transmission-reception experiments carried out by Javan and others and has been discussed previously. The transmission diode is to be situated on one focus of a half-ellipsoidal cavity configuration and the receiving diode at the other focus. Heterdyne detection at this receiving diode is anticipated.

This experiment has provided a significant guide to the development of better diode structures and consideration of the coupling characteristics. Point contact structures are being replaced by more carefully designed, single junction, photolithographically fabricated structures; eventually arrays will be used. The successful achievement of such an experiment will require fairly sensitive structures whose coupling and junction characteristics are quite well known and designed.

With respect to the development of the photolithographically fabricated structures, significant progress has been made. Recent results are particularly encouraging and warrant optimism. Figure 7 displays the two dimensional single junction structures which are presently being utilized. On a germanium substrate, a nickel base plate is first fabricated. This is then oxidized to obtain an oxide layer $\simeq$ 15-Å thick. A gold antenna is then evaporated, the overlap with the nickel base forming the

metal-barrier-metal junction device. The current-voltage characteristic shown indicates that it is a tunneling junction of high quality with a zero bias resistance in the hundreds of kΩ range.

Figure 8 displays the detection characteristics of such a structure at 10.6 μ for a radiation intensity equal to 10 W/cm^2. The angle is measured between the normal to the substrate surface and the propagation vector of the incident laser beam. Parallel (") polarization represents the electric field polarized along the gold antenna and perpendicular, electric field polarization across the antenna.

For the high impedance structure " and $^{\perp}$'r polarization give very different results. The peak polarization ratio is $\simeq$ 20, parallel coupling being much larger at an angle of $\simeq$ 10° with respect to the substrate. Verification of the antenna coupling was accomplished by shortening the diode junction thereby preventing rectification. The "signal then behaves similarly to the $^{\perp}$'r signal both being characteristic of a cos θ thermally induced signal.

For such an antenna structure we have estimated the optical voltage to be 10^{-5} to 10^{-6} V for the 10 W/cm^2 incident intensity. The angular dependence of the detected signal for " polarization agrees well with that expected from antenna calculations.

We are presently extending these results to obtain resolution of the antenna lobes. We expect to work toward the ultraviolet portion of the spectrum where absorption becomes large and antenna coupling should fail. Figure 9 indicates several possible directions that are being considered. It is quite apparent that the micro-structures will become important as infrared and optical components, particularly in the light of the rapid development which has already occurred.

REFERENCES

1. Faris, S. M.; Gustafson, T. Kenneth; and Wiesner, John C.: Detection of Optical and Infrared Radiation with DC-Biased Electron-Tunneling Metal-Barrier-Metal Diodes. IEEE J. Q. E. Vol. QE-9, no. 7, July 1973, p. 737-745. Also see the preceding presentation by Ali Javan.

2. Simmons, John G.: Generalized Formula for the Electric Tunnel Effect Between Similar Electrodes Separated by a Thin Insulating Film. J. Appl. Phys. 34, no. 6, June 1963, 1793-1803. He has several other publications which appeared at this time in J. Appl. Phys; (for dissimilar electrodes see "Electric Tunnel Effect between Dissimilar Electrodes Separated by a "Thin Insulating Film." J. Appl. Phys. Vol. 34, no. 9 Sept. 1963, p. 2581-2590.

3. Does, J. W. "Detection and harmonic generation in the sub-millimeter wavelength region. Microwave J., Vol. 9, Sept. 1966, p. 48-55.

4. Previous mixing and detection experiments with clear indications of antenna coupling include: Matarrese, L. M.; and Evenson, K. M. "Improved Coupling to Infrared Whisker Diodes by Use of Antenna Theory." Appl. Phys. Lett. 17, no. 1, 1 July 1970, p. 8-10; Sanchez; A, Singh; S. K.; and Javan, A. Generation of Infrared Radiation in a Metal-to-Metal Point-Contact Diode at Synthesized Frequencies of Incident Fields: A High-speed Broadband Light Modulator. Appl. Phys. Lett. Vol. 21, no. 5, 1 Sept. 1972, p. 240-243; Radiation of Difference Frequencies Produced by Mixing in Metal-Barrier-Metal Diodes, p. 240-243 Gustafson, T. K; and Bridges, T. J.: Appl. Phys. Lett. Vol. 25, no. 1, 1 July 1974; p. 56-59; Recent Antenna Coupling Investigations of Point Diodes at 10.6 μm by Twu and Schwarz (private communication); and Small, J. G.; Elchinger, G. M.; Javan, A.; Sanchez, Antonio; Bachner, F. J.; and Symthe, D L.: AC Electron Tunneling at Infrared Frequencies: Thin-film M-O-M Diode Structure With Broad-band Characteristics. Appl. Phys. Lett. Vol. 24, no. 6, 15 March 1974, p. 275-279.

5. Negative differential resistance at low frequencies has been reported by Wang, S. Y.; Faris, S. M.; Siu, D. P.; Jain, R. K.; and Gustafson, T. K.: Enhanced Optical Frequency detection with Negative Differential Resistance in Metal-Barrier-Metal Point-Contact Diodes. Appl. Phys. Lett. Vol. 25, no. 9, 1 Nov. 1974, p. 493-495.

6. Farris, S. M.; and Gustafson, T. K.: Harmonic Mixing Characteristics of Metal-Barrier-Metal Junctions as Predicted by Electron Tunneling. Appl. Phys. Lett., Vol. 25, no. 10, 15 Nov. 1974, p. 544-549.

7. Sakuma, Eiichi; and Evenson, Kenneth M.: Characteristics of Tungsten-Nickel Point Contact Diodes Used as Laser Harmonic-Generator Mixers. IEEE J.Q.E., Vol. QE-10, no. 8, Aug. 1974, p. 599-603.

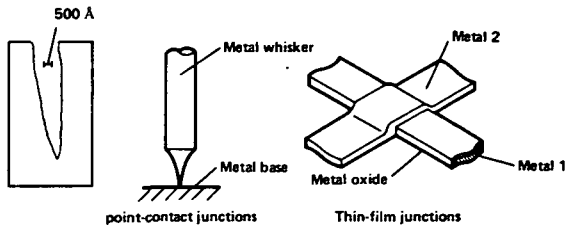

Figure 1.– Metal-barrier-metal structures. At the left is shown an electron microscope scan of an etched tungsten wire; point-contact geometry is shown in the center; and the early evaporated two-dimensional structure is at the right.

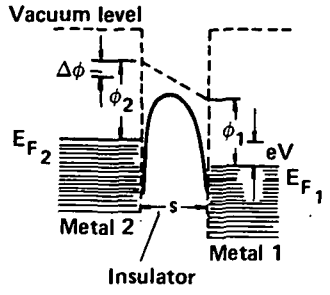

Potential barrier of M-B-M junction

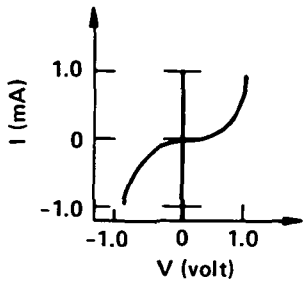

I-V characteristic of M-B-M junction

$$I(V) = \frac{e}{2\pi h(\Delta s)^2}\left\{ \bar{\phi}_f e^{-A_f\bar{\phi}_f^{1/2}} - (\bar{\phi}_f + eV)e^{-A_f(\bar{\phi}_f + eV)^{1/2}} \right\}, \quad V > 0$$

$$\bar{\phi}_f = \int_{s_1}^{s_2} \left[\phi_2 - (\Delta\phi + eV)\frac{x}{s} - \frac{\lambda s^2}{x(s-x)} \right] dx/\Delta s, \quad A_f \cong 1.025\,\Delta s$$

$\Delta s = s_2 - s_1$, s_1 , s_2 classical turning points

Figure 2.– Simplified band diagram and current-voltage characteristic of the metal-barrier-metal structure. The expression for I(V) is that deduced by Simmons. Parameter definitions are:

E_{F_1}, E_{F_2} Fermi energies of metals 1 and 2, respectively.

ϕ_1, ϕ_2 work functions of the two metals

$\Delta\phi = \phi_1 - \phi_2$

s barrier thickness

s_1, s_2 W.K.B. turning points for electrons with energy: E_{F_2}

$\Delta s = s_1 - s_2$

$eV = eV_B + ev(t)\cos\omega t$, where V_B is the voltage bias

f forward for which metal 2 is positive with respect to metal one. For opposite bias a similar expression is obtained as shown in figure 3.

v(t) the induced optical voltage and ω the optical frequency

λ parameter defining strength of surface charge ($\cong$ 5 Å(eV))

$$\left.\begin{aligned} I_f(V) &= J_f\left\{\bar{\phi}_f \exp(-A_f\bar{\phi}_f^{1/2}) - (\bar{\phi}_f + eV)\exp[-A_f(\bar{\phi}_f + eV)^{1/2}]\right\}; \quad V > 0 \\ I_r(V) &= J_r\left\{(\bar{\phi}_r - eV)\exp[-A_r(\bar{\phi}_r - eV)^{1/2}] - \bar{\phi}_r \exp(-A_r\bar{\phi}_r^{1/2})\right\}; \quad V < 0 \end{aligned}\right\} \tag{1}$$

$$V(t) = V_b + v(t)\cos \omega t \tag{2}$$

$$I_{rect}(t) = \int_{-\pi}^{\pi} I[V_b + v(t)\cos \theta]d\theta/2\pi \tag{3}$$

$$\begin{aligned} I_{rect}(t) \cong\ & J_i \exp(-A_{ib}\bar{\phi}_{ib}^{1/2})\left\{\bar{\phi}_{ib}[I_o(z_i v) - 1] - \beta_{ib} v I_1(z_i v)\right\} \\ & -J_i \exp(-A_{ib}\bar{\phi}'^{1/2}_{ib})\left\{\bar{\phi}'_{ib}[I_o(z'_i v) - 1] - \beta_{ib} v I_1(z'_i v)\right\} \end{aligned} \tag{4}$$

$$z_i = \beta_{ib} A_{ib} (4\bar{\phi}_{ib})^{-1/2}$$

Figure 3.– Outline of the derivation of the rectified current I_{rect}. $\bar{\phi}_r$ is analogous to $\bar{\phi}_f$ but with the 1 and 2 interchanged. Similarly with $A_r \cdot J_r = -J_f \cdot s_1$ and s_2 are the turning points for an electron of energy E_{F_1} and x is measured from metal 1 for the reverse (r) biased case ($V < 0$).

In the expression for $I_{rect}(t)$, i is chosen as either f or r for $V > 0$ or $V < 0$, respectively. The subscript b refers to parameters evaluated at the bias voltage V_B. z_i' is the same as z_i with β_{ib} replaced by $1 - \beta_{ib}$. Similarly for $\bar{\phi}_{i'b}$.

I_0 and I_1 are the zero and first order Bessel functions which describe the curvature characteristics of the rectified signal.

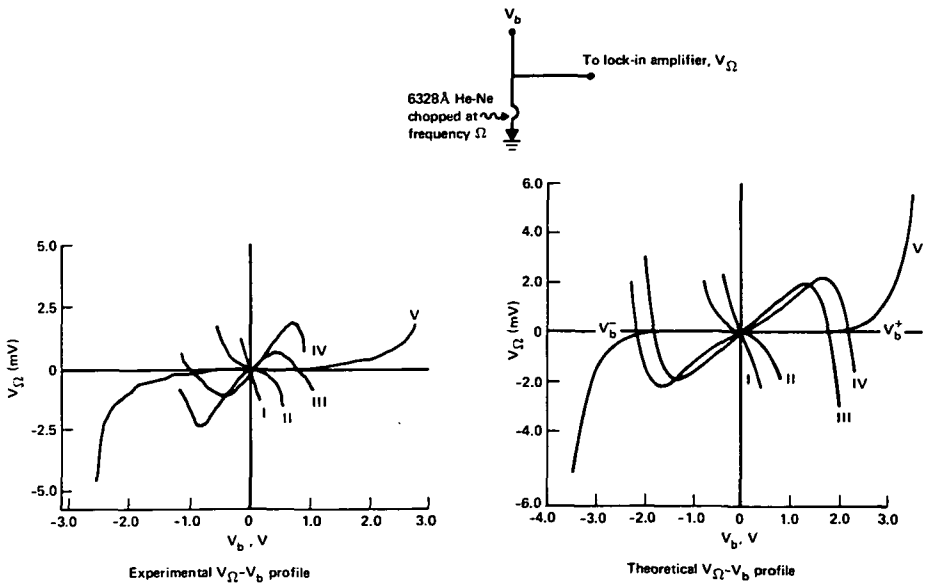

Figure 4.– Rectification experiments with He-Ne 6328 Å radiation. Experimental results are shown on the left-hand side; the theoretical comparison on the right-hand side. V_Ω is the phase sensitively detected signal at the chopping frequency of 1 kHz. V_B is the voltage bias.

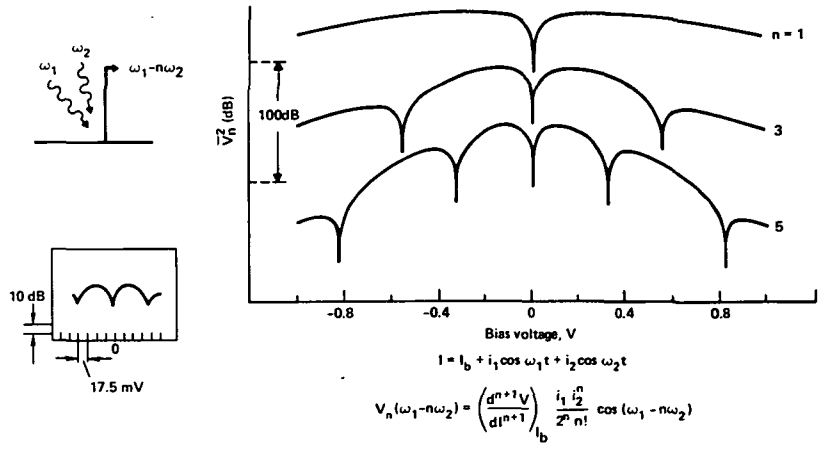

Figure 5.– Current dependent nonlinear mixing processes in metal-metal-barrier-metal structures. I_b is the current bias; $i_1 \cos \omega_1 t$ and $i_2 \cos \omega_2 t$; currents induced by two incident laser signals at frequency ω_1 and ω_2 respectively. $\overline{V_n^2}$ is the mean square i.f. signal at frequency $\omega_1 - n\omega_2$. The insert shows an experimental curve obtained by Evensen and Sakuma in the sub-millimeter range for $n = 5$. Figure 5 shows curves for $n = 1, 3, 5$.

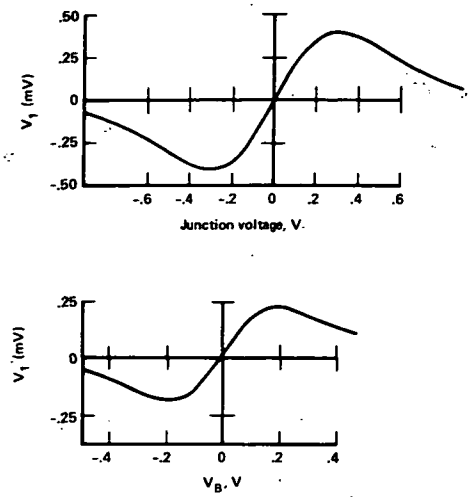

Figure 6.– Current rectification at 1.15 μ. The top curve shows V_1 (V_n for n = 1) and the bottom curve the theoretical comparison for suitably chosen parameters (ref. 1).

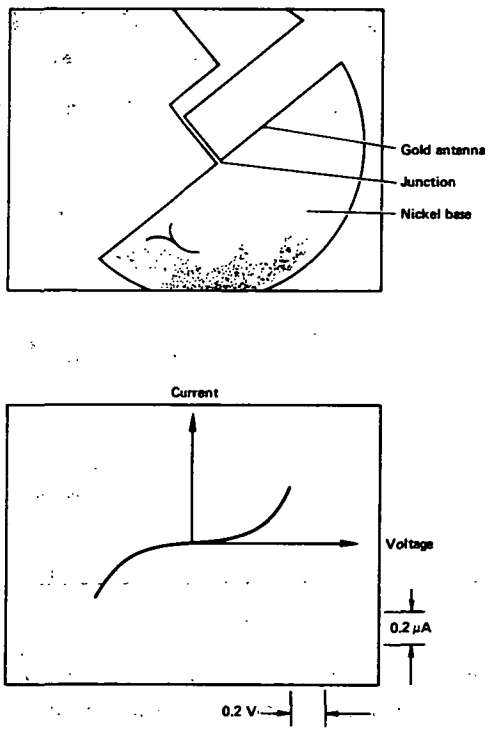

Figure 7.– Photolithographically fabricated metal-barrier-metal structure and associated antenna coupler. The lower curve displays the experimentally measured current-voltage characteristic. The structure is planar, the black background being the nonabsorbing silicon substrate.

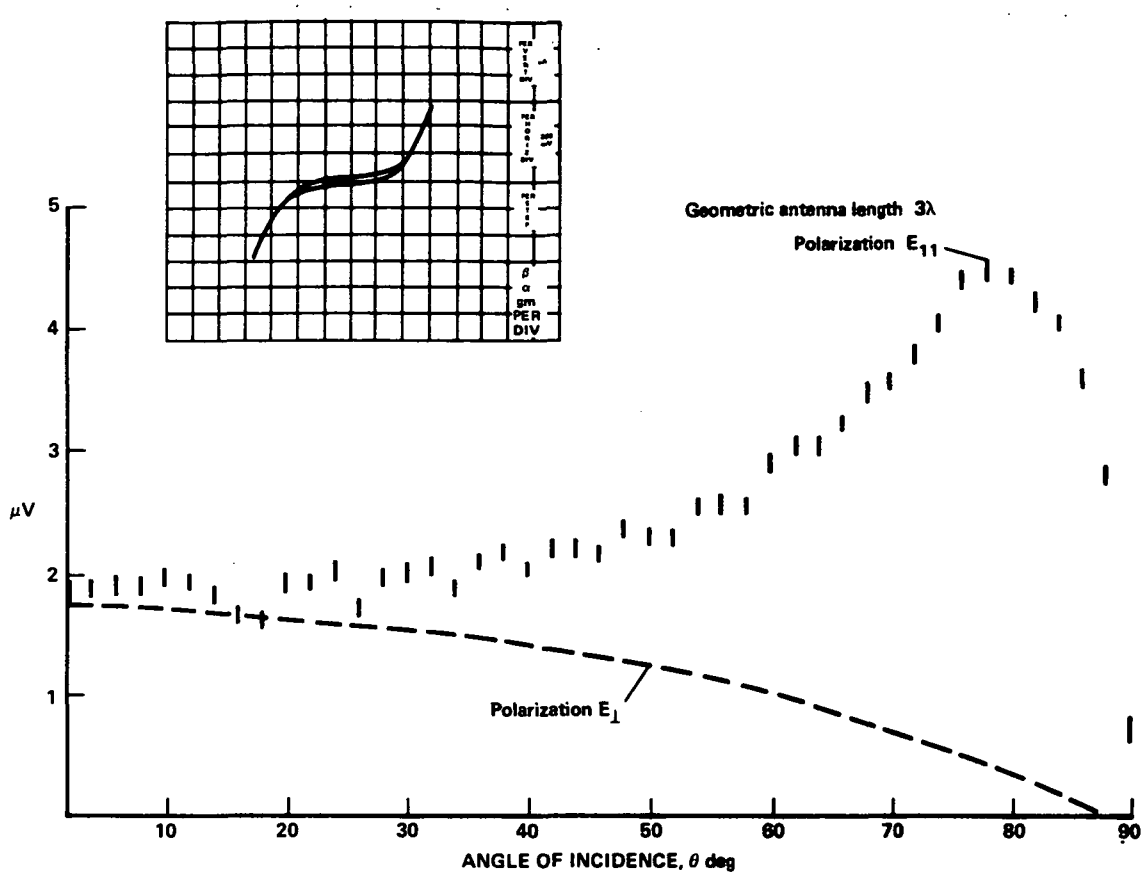

(a) The E_{11} signal displays antenna coupling, the $E_{\perp}$ signal a thermally induced signal.

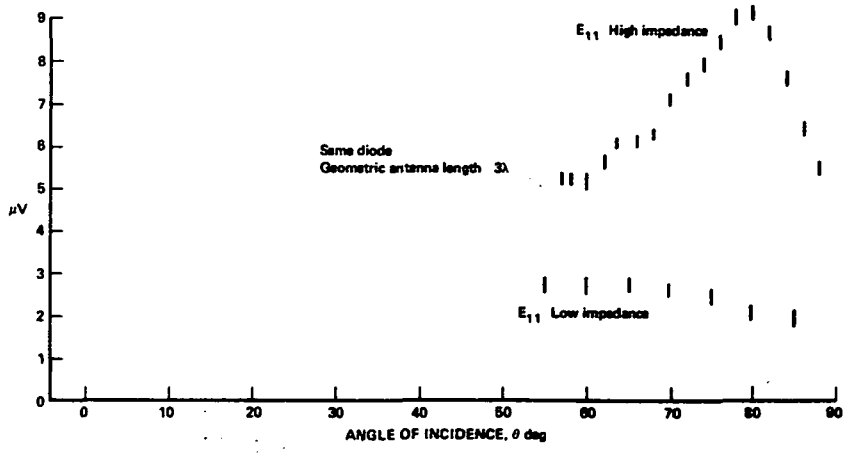

(b) High impedance junction (same one as for fig. (8a)) for E_{11} induced signal displays antenna coupling. A short circuit junction (lower curve) shows only the thermal response for E_{11} as well as for $E_{\perp}$.

Figure 8.– Antenna coupling and rectification with the evaporated structure of figure 7. The induced rectified voltages are due to 10.6 μm, 10 W/cm^2 of CO_2 laser beam intensity. The beam is directed in the plane containing the diode and normal to the substrate surface and θ is the angle of the propagation vector with respect to the normal. E_{11} represents the electric field polarized along the gold wire and $E_{\perp}$, polarized perpendicularly.

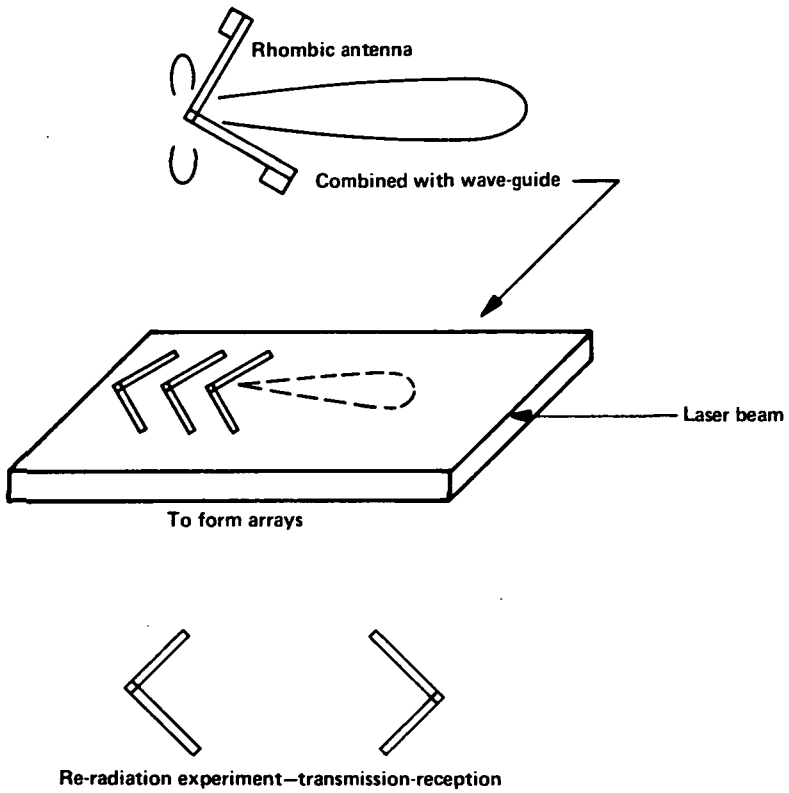

Figure 9.– Proposed work using evaporated antenna structures.

DISCUSSION

Max Garbuny, Westinghouse – The cross section of an antenna or atom is of the order of $\lambda^2/2\pi$. Do these junctions exhibit this same cross section?

Ken Gustafson: The $\lambda^2/2\pi$ is appropriate for a dipole antenna. Since our diodes exhibit many lobes, they are no simple dipoles. So the antenna area will depend upon this lobe structure.

Ali Javan: We find that one can characterize the area by something like λ^2; it turns out that for a 10-μ junction it is approximately $(20\,\mu)^2$.

Katasonori Shimada, J. P. L. – The volt-ampere characteristics you show always have a symmetric shape. If you use different metals for example, gold and nickel, could you get a true diode characteristic?

Ken Gustafson: We are looking at that whole question of whether its possible to obtain an asymmetric VI characteristic. It's too early to tell. The problem is that as you examine the theory, the odd order or rectification coefficients come in as the difference between the work functions of the metals. The other coefficients come in as the sum. So to get the characteristic you ask for, we need to use metals with large work function difference. An interesting question is: could this converter be as good as a thermoelectric converter, because the thermionic converter suffers from precisely the same fault – that is, the thermoelectric voltage is proportional to the difference between the two work functions.

Ali Javan, M. I. T.: A comment. If you keep making and breaking a point contact diode, looking for its characteristics with various pressures, or oxide thicknesses, you are able to get occasional asymmetric characteristics. But with our evaporated junctions, they are always symmetrical.

Ken Gustafson: Yes, we have found the same.

IR PUMPED THIRD-HARMONIC GENERATION AND SUM-FREQUENCY GENERATION IN DIATOMIC MOLECULES

C. Y. She
Colorado State University

and

Kenneth W. Billman
NASA-Ames Research Center

It is well known that the efficient lasers we have, approximately 20 percent for CO_2 around 10.6 μ and 60 percent for CO around 5 μ, have inherent disadvantages for certain types of power transmission. First, since beam divergence scales as λ/D, we are confronted with either limited range or excessively large optics (e.g., 30-m diameter collection mirror at geostationary orbit for Earth-to-space transmission of 10.6-μ wavelength) for reasonable transmission efficiency. Secondly, the use of solid state converters is limited to 2μ and, for maximum efficiency, wavelengths below 1 μ are desirable. Even if the laser-driven engine is used for conversion, the need for high temperature strength and transmission of the beam entrance window dictates the use of sapphire which has a long wavelength cutoff at about 5.5 μ. Thus the CO_2 laser wavelength would certainly need up-conversion.

For these reasons, we began a study recently to assess the possibility and potential efficiency of using nonlinear up-conversion techniques for the high efficiency type lasers (CO, CO_2 and chemical). This paper is a preliminary report on what we believe are some encouraging results. Although the conversion efficiencies are not extremely high, it should be borne in mind that this may be improved as we examine other candidate molecular gases. Also, especially for ground-based laser type missions, one might be more tolerant of overall laser and up-converter efficiency, especially if it reduces the need for many large onboard collection optics systems by area factors of nine, say, or if this overall efficiency exceeds that of the best direct (no up-converter) laser operating at the same wavelength.

Efficient up-conversion of visible laser radiation by third-harmonic and sum-frequency techniques, using metallic vapors with added atomic vapor for phase-matching, has recently been an active and successful area of research (refs. 1 through 4). Very high conversion efficiencies (ref. 5) are attributable to the use of resonance enhancements, particularly a resonance at twice the pump frequency (refs. 4 and 5). In principle, such conversion processes should also be possible for longer wavelength laser radiation. However, the smaller pump photon energy necessitates the use of molecular media for conversion if resonance enhancement is to be used. Molecular systems present certain difficulties: their levels are complex and transition probabilities often unknown. Also, the oscillator strengths among vibrational levels in the ground electronic state of a molecule are either zero or much smaller than those among electronic states of an atom, thus limiting the magnitude of nonlinear interactions. However, as we will show here, this potential problem in the up-conversion process can be eliminated by making use of virtual vibronic (vibration-electronic) transitions which, being primarily electronic transitions have much larger matrix elements and efficient conversion *can* be achieved with molecular systems.

The energy diagram of a typical molecule is shown in figure 1. Both the ground and excited electronic states are split into rotation-vibrational levels with each denoted by electronic, vibrational, and rotational quantum numbers (e, v, and J). The incident infrared laser frequencies are ω_1 and ω_2 and the converted (or generated) frequency is ω_3. For many molecules, the rotation-vibrational levels in the ground electronic state are well separated in comparison with their linewidths; thus only one pair of such levels, with energy separation $\hbar\omega_o$, may be assumed to satisfy the condition of two photon resonance, namely, $\omega_o \simeq 2\omega_1$. Only this pair of levels, denoted by $|g>$ and $|a>$ in figure 1, will make a significant contribution to the nonlinear interaction in question.

Because there is no resonance requirement of the rotation-vibrational levels in the excited electronic state, all those levels which are electric-dipole-allowed will participate in the nonlinear process. The energy of all these levels in the excited electronic state may be approximated by their average value $\hbar\Omega$ because $\Omega >> \omega_2$ and ω_3. We therefore lump all these excited vibronic levels into a single upper state $|b>$, and the molecule depicted in figure 1 may be represented by a three-level system with energies $\hbar\Omega$ for $|b>$, $\hbar\omega_o$ for $|a>$, and zero for $|g>$.

The basic difference between the molecular system considered here and the atomic system considered by previous investigators (refs. 1 through 5) is that Ω is much greater than ω_3. Hence, the only possible resonance enhancement effect which may be used is the two-photon resonance namely, $\omega_o = 2\omega_1$. Because there is no resonance enhancement at ω_3 the system considered here would have relatively lower conversion efficiency but, as will be seen, much wider bandwidth than those considered by Harris and Bloom (ref. 6). The simplified expression for the relevant third-order susceptibility for the three level system depicted in figure 1 can be found by standard methods (ref. 7) to be

$$\chi^{(3)}(\omega_3 = 2\omega_1 + \omega_2) = \frac{1}{4\hbar^3} \frac{\mu_{gb}\mu_{ba}\mu_{ab}\mu_{bg}}{(\omega_o - 2\omega_1) + i(\delta\omega_o/2)} \frac{2\Omega - \omega_3 + \omega_2}{(\Omega-\omega_1)(\Omega+\omega_2)(\Omega-\omega_3)} \quad (1)$$

where μ_{ab} is the electronic dipole matrix element between $|a>$ and $|b>$, $\delta\omega_o$ is the linewidth of level $|a>$, and all frequencies are expressed in circular measure. Since $\Omega >> \omega_1$, ω_2, and ω_3, the susceptibility of equation (1) is insensitive to ω_2 (and ω_3), and the conversion efficiencies for third harmonic and sum-frequency generation would be comparable. We therefore consider the third harmonic generation only. By setting $\omega_2 = \omega_1$ and $\omega_3 = 3\omega_1$, the expression needed for $|\chi^{(3)}(3\omega_1)|^2$ may be easily obtained from equation (1).

The general expression for the ratio of third harmonic output to pump input, or conversion efficiency, can be written as (refs. 7 through 9)

$$\epsilon = \alpha\eta^4 N^2 \left|\chi^{(3)}(3\omega_1)\right|^2 \quad (2)$$

where the wave impedance is $\eta = \sqrt{\mu/\epsilon}$, N is the effective molecular concentration (to be explained later), and the value of α is dependent upon whether the pump beam is unfocussed (plane wave) or is a focussed Gaussian beam in the medium. For the former case, the cross-sectional areas for both the fundamental and third harmonic are the same and hence $\epsilon_I = I(\omega_3)/I(\omega_1)$, the intensity ratio, and $\alpha = \alpha_I = 9\omega_1{}^2 I^2(\omega_1) F^2 L^2$. The coherence factor is $F = \sin(\Delta kL/2)/(\Delta kL/2)$,

$\Delta k = 6\pi(n_3 - n_1)/\lambda_1$, where $(n_3 - n_1)$ is the refractive index difference for ω_3 and ω_1, and L is the interaction length. For the focussed Gaussian case, the effective cross section of the fundamental is three times that of the third harmonic because the pertinent induced nonlinear polarization is cubic in the electric field (refs. 7 through 9). Then the conversion efficiency, written in terms of powers, $\epsilon_p = P(\omega_3)/P(\omega_1)$ is found using $\alpha = \alpha_p = (3/4)\,(\omega_1/\lambda_1)^2\,P^2\,(\omega_1)\,|\,F'\,|^2$, where F' is the phase mismatch integral $I(\Delta k, \xi, \zeta)$ given by Ward and New (ref. 9).

In order to evaluate these efficiencies for a given molecular gas, the matrix elements of individual rotation-vibrational levels between different electric states must be known to calculate $|\,\chi^{(3)}(3\omega_1)\,|^2$. These transition probabilities have been reported (ref. 10) for the $B^1\Sigma_u^+ - X^1\Sigma_g^+$ band system of molecular hydrogen. A slight complication arises because of the difference in statistical weight of para (J = 1) and ortho (J = 0) states: at 300°K the ground state population density of the J = 1 level is 65 percent while that of J = 0 is only 13 percent of the total molecular density N_o. For this reason, we calculate the para-hydrogen conversion, that is, setting $|g> = |X^1\Sigma_g^+,\ 0, 1>, |a> = |X^1\Sigma_g^+,\ 1, 1>, N = 0.65\ N_o$. To evaluate the product of the four matrix elements in equation (1), a sum over all the rotation-vibrational levels in the excited state must be made. Standard application of the Born-Oppenheimer approximation $|\,e, v, J> = |\,e, v> |\,> J$, the rotation sum-rule, and algebraic simplification gives the desired matrix product

$$M = (2J_a + 1)\left[\sum_{v'} <e'', v_g\,|\,\mu\,|\,e', v'><e'\,v'\,|\,\mu\,|\,e'', v_a>\right]^2 \qquad (3)$$

where, for the case considered here, $J_a = 1$, $v_g = 0$, and $v_a = 1$. With the reported band oscillator strengths $f_{v'v''}$ for $B^1\Sigma_u^+ - X^1\Sigma_g^+$ of H_2 (table 4 of ref. 10), the linearly polarized dipole matrix elements of equation (3) may be calculated through the relationship, $f_{v'v''} = 2\Omega m\,|<e'', v''\,|\,\mu\,|\,e', v'>|^2/\hbar e^2$, where m is the mass and e the charge of the electron. Using the averaged value of the electronic state energy, $\Omega = 103710\ cm^{-1}$, we finally obtain $M = 1.14 \times 10^{-117}\ (C\text{-}m)^4$.

The value of the linewidth, $\delta\omega_o$ to use in equation (1) is complicated to a certain extent by a pressure dependent quadrupole interaction in hydrogen which produces collision-narrowing (refs. 11 and 12). The full width at 300°K is calculated to be narrowed to less than $16 \times 10^{-3}\ cm^{-1}$ for pressures between 1-4 atm with a minimum of $12 \times 10^{-3}\ cm^{-1}$ at 2 atm. For simplicity, we will ignore this factor in calculated efficiency and use the Doppler full width of $36.5 \times 10^{-3}\ cm^{-1}$, together with an assumed pump frequency of $\omega_1 = \omega_o/2 = 2077.6\ cm^{-1}$ (at resonance) to obtain $|\,\chi^{(3)}\,(3\omega_1)\,|^2 = 1.52 \times 10^{-115}\ m^5V^{-2}$.

The conversion efficiencies may now be calculated. Without using special provisions for phase matching, the maximum interaction length is just the coherence length $L_c = \lambda_1/6(n_3 - n_1)$. Using the standard equation (ref. 13) to calculate the index difference in hydrogen at 300°K, one obtains $L_c = 240$ cm at 1 atm and $L_c = 60$ cm at 4 atm. For the pressure range of 1-4 atm, $NL_c = 3.83 \times 10^{25}\ m^{-2}$, approximately pressure independent. Since the intensity conversion efficiency $\epsilon_I \propto (NL_c)^2$, no enhancement is obtained by increasing the pressure. On the other hand, the power conversion efficiency for the focussed Gaussian beam $\epsilon_p \propto N^2$, and there is a definite advantage in using higher pressures. Of course, both cases must be more closely examined to include the pressure narrowing effect, which cannot be done in this brief note. Using $F = 2/\pi$ and $L = L_c$, the calculated ϵ_I is 10 percent for $I(\omega_1) = 19.9\ MW/cm^2$ and 30 percent for $I(\omega_1) = 34\ MW/cm^2$. For the focussed case, we choose the confocal parameter b to be three times the interaction length, that is, $(b/L) = 3$ and use the maximum $|\,F'\,|^2$ which, according to Miles and Harris (ref. 8), is about 0.5.

The calculated ϵ_p is then 10 percent for $P(\omega_1) = 1.80$ MW at 4 atm. Should the pressure narrowing be included, only 780 kW is necessary to achieve the same efficiency. It should be noted that, for the pressures and laser pulses of interest here, competing processes, such as two-photon absorption (ref. 6) and gas breakdown (ref. 14) occur at intensities around 10^3 MW/cm^2 and therefore should not present a problem.

It has been pointed out by Harris (ref. 15) that the microscopic processes for third harmonic generation with two-photon resonance enhancement and stimulated Stokes-Raman scattering are similar, and that the calculated third harmonic conversion efficiency may be checked independently by existing Raman gain data. We have derived the relationship between the intensity (plane wave) conversion efficiency, ϵ_I, with $L = L_c$, and the normalized stimulated Raman gain coefficient g as

$$\epsilon_I = \left[\frac{3\omega_1}{\pi\omega_s} \left| \frac{\chi^{(3)}(3\omega_1)}{\chi''_R(\omega_s)} \right| L_c I(\omega_1) g \right]^2 \tag{4}$$

where $\omega_s = \omega_\ell - \omega_o$ is the Stokes frequency stimulated by a laser at frequency ω_ℓ, and $\chi''_R(\omega_s)$ is the associated Raman tensor. Using the measured gain (ref. 16) for H_2 at 300°K and 1 atm, $L_c = 240$ cm, and the calculated ratio $|\chi^{(3)}/\chi''_R| = 1.107$, we find from equation (4) the pump intensity necessary for 10 percent conversion efficiency to be 39.2 MW/cm^2, a value in favorable agreement with the value of 19.9 MW/cm^2 calculated above.

The question of phase-matching is of interest. If the conversion medium is positively dispersive, like H_2, this can be accomplished by adding the appropriate mole fraction of a selected negatively dispersive diatomic molecule. If heteronuclear molecules are selected as the interation medium, and the v = 2 level is used for the two-photon level $|a>$, the medium could have negative dispersion if the pump frequency ω_1 is smaller than, but very close to, the v = 1 level. For such a negatively dispersive conversion medium, phase matching can be achieved by adding positively dispersive diatomic molecules to the system. However, since neither oscillator strengths nor refractive indices at infrared frequencies are known for most molecules, phase-matching may have to be determined by experiment rather than *a-priori* quantitative calculation.

In summary, we have suggested a mechanism with which efficient third-harmonic and sum-frequency generation, pumped by infrared lasers, should be practically achievable. We have outlined the method for calculating the third-harmonic conversion efficiencies for unfocussed and focussed Gaussian pump beams. A single relation for estimating the intensity conversion efficiency, when the appropriate Stokes-Raman gain coefficient is known, has been given. Our major reason for using H_2 as our model molecular converter was the availability of the oscillator strengths needed for the calculation. However, the required resonance pump radiation at $\omega_1 = 2077.6$ cm^{-1} for hydrogen molecules, falls between the strong lines of the CO and chemical lasers, the nearest line being a $v' = 2 \rightarrow v'' = 1$, $J' = 9 \rightarrow J'' = 10$ transition in CO at 2077.1 cm^{-1}. Other molecular systems, which have either Rydberg transitions (ref. 17) or smaller Ω, should yield similar conversion efficiencies. The purpose of this paper was to demonstrate that indeed efficient conversion in molecules is possible and to motivate thereby the further study of other common molecules such as HCl, N_2, CO, and CN, which would undoubtedly result in suitable systems for experimentation. For example, both CO and CH_3F molecules (ref. 18) would be candidates for up-converting CO_2 laser radiation. Other possibilities, rather than such chance laser-molecule wavelength matches, are available, however. With the recent advance in the development of high pressure infrared lasers, it should be possible to tune the laser to achieve resonance. It must be noted, however, that if the

C. 2

laser linewidth is larger than $\delta\omega_o$, the required power to achieve a given conversion efficiency is proportionately increased. Alternately, the molecule can be brought to resonance with a nearby laser line by Stark tuning with an external electric field (ref. 18).

Acknowledgements – Stimulating discussions with Professor S. E. Harris, who suggested the use of virtual electronic transitions, and with Professor Y. R. Shen are gratefully acknowledged. Discussions with C. Chackerian, J. O. Arnold, S. Bowen, and R. L. McKenzie have also been very helpful.

REFERENCES

1. Young, J. F.; Bjorklund, G. C.; King, A. H.; Miles, R. B.; and Harris, S. E.: Third-Harmonic Generation in Phase-Matched Rb Vapor. Phys. Rev. Lett. Vol. 27, no. 23, 6 Dec. 1971, p. 1551-1553.

2. Harris, S. E.; and Miles, R. B.: Proposed Third-Harmonic Generation in Phase Matched Metal Vapors. Appl. Phys. Lett., Vol. 19, no. 10, 15 Nov. 1971, p. 385-387.

3. Kung, A. H.; Young, J. F.; Bjorklund, G. C.; and Harris S. E.: Generation of Vacuum Ultraviolet Radiation in Phase-Matched Cd Vapor. Phys. Rev. Lett. Vol. 29, no. 15, 9 Oct. 1972, p. 985-988.

4. Hodgson, R. T.; Sorokin, P. P.; and Wynne, J. J.: Tunable Coherent Vacuum-Ultraviolet Generation in Atomic Vapors. Phys. Rev. Lett. Vol. 32, no. 7, 18 Feb. 1974, p. 343-346.

5. Bloom, D. M.; Yardley, James T.; Young, J. F.; and Harris, S. E.: Infrared Up-Conversion with Resonantly Two-Photon Pumped Metal Vapors. Appl. Phys. Lett. Vol. 24, no. 9, 1 May 1974, p. 427-428.

6. Harris, S. E.; and Bloom, D. M.: Resonantly Two-Photon Pumped Frequency Converter. Appl. Phys. Lett., Vol. 24, no. 15, 1 Mar. 1974, p. 229-230.

7. Armstrong, J. A.; Bloembergen, N.; Ducuing, J.; and Pershan, P. S.: Interactions Between Light Waves in a Nonlinear Dielectric. Phys. Rev., Vol. 127, no. 6, 15 Sept. 1962, p. 1918-1939.

8. Miles, Richard B.; and Harris, Stephen E.: Optical Third-Harmonic Generation in Alkali Metal Vapors. IEEE J. Quant. Elect., Vol. QE-9, no. 4, April 1973, p. 470-484.

9. Ward, J. F.; and New, G. H. C.: Optical Third Harmonic Generation in Gases by a Focused Laser Beam. Phys. Rev. Vol. 185, no. 1, 5 Sept. 1969, p. 57-72.

10. Allison, A. C.; and Dalgarno, A.: Transition Probabilities for the $B^1\Sigma^+_u - X^1\Sigma^+_g$ Band System of H_2 J. Quant. Spec. Radiat. Transfer Vol. 9, no. 11, No. 1969, p. 1543-1551.

11. Lallemand, P.; Simova, P.; and Bret, G.: Pressure-Induced Line Shift and Collisional Narrowing in Hydrogen Gas Determined by Stimulated Raman Emission. Phys. Rev. Lett., Vol. 17, no. 25. 19 Dec. 1966, p. 1239-1241.

12. James, Thomas C.: Calculation of Collision Narrowing of the Quadrupole Lines in Molecular Hydrogen. J. Opt. Soc. Am., Vol. 59, no. 12, Dec. 1969, p. 1602-1606.

13. Born Max; and Wolf, Emil: Principles of Optics; Electromagnetic Theory of Propagation, Interference and Diffraction of Light. Pergamon Press, New York, 1959, p. 93.

14. Rockwood, Stephen D.: A Comparison of Laser Induced Gas Breakdown in Various Gases. IEEE J. Quan. Elec., Vol. QE-10, no. 9, Sept. 1974, p. 732.

15. Harris, S. E.: private communications.

16. Hagenlocker, E. E.; and Rado, W. G.: Stimulated Brillouin and Raman Scattering in Gases. Appl. Phys. Lett., Vol. 7, no. 9, 1 Nov. 1965, p. 236-238.

17. Herzberg, G.: Spectra of Diatomic Molecules. van Nostrand Reinhold New York, 1950, p. 383.

18. Bischel, William K.; Kelly, Patrick J.; and Rhodes, Charles K.: Observation of Doppler-Free Two-Photon Absorption in the ν_3 bands of CH_3F. Phys. Rev. Lett. Vol. 34, no. 6, 10 Feb. 1975, p. 300-303.

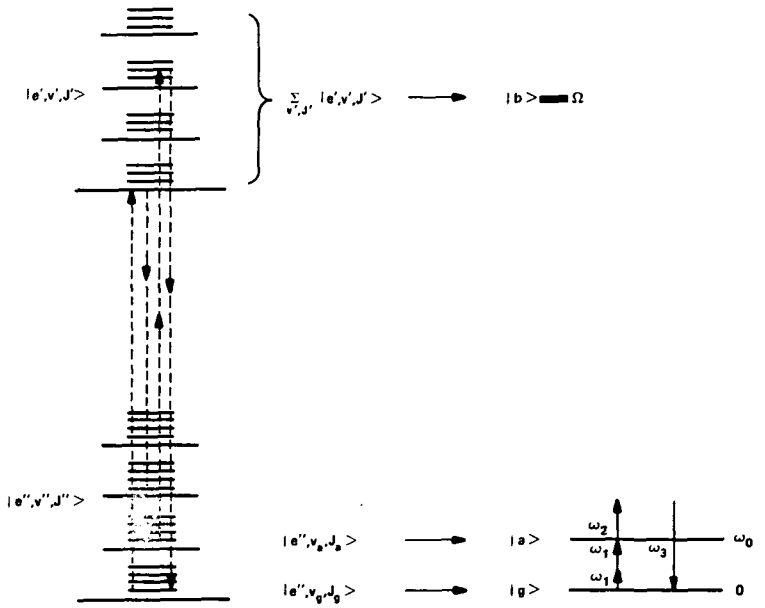

Figure 1.– Energy levels of a typical diatomic molecule. Each electronic state is split into a series of rotation-vibrational levels, with short horizontal lines indicating rotation sublevels. One possible path of virtual vibronic transitions contributing to the product of four matrix elements in equation (1) is shown by the four vertical dashed lines. For the up-conversion process of interest, the molecule may be represented by a three-level system with the upper-state $|b>$ forming a band containing all sub-levels in the excited electronic state. For the interaction considered (using the $B^1\Sigma_u^+ - X^1\Sigma_g^+$ band system of H_2), $|e', v', J'> = |B^1\Sigma_u^+, v', J'>$, $|a> = |e'', v_a, J_a> = |X^1\Sigma_g^+, 1, 1>$ and $|g> = |e'', v_g, J_g> = |X^1\Sigma_g^+, 0, 1>$.

DISCUSSION

Ernest Brock, Los Alamos Scientific Laboratory – With respect to the dispersion in the infrared in the hydrogen molecule, there has been a recent report in JETP Letters, September-October, where some Soviet scientists use a Raman pumping technique to pump hydrogen from v = 1 to v = 2, ground state. They observed a fringe shift which they were able to interpret as an index change. Their experimental data is supported by a German calculation, which they reference.

Joe She: Thank you for calling it to our attention.

Dick Miles, Princeton University – You might consider focusing as a means of phase matching.

Joe She: Yes, for other molecules this may work, but you need an actively dispersive medium which is not the case for hydrogen.

LASER-ELECTRON BEAM INTERACTION APPLIED TO OPTICAL AMPLIFIERS AND OSCILLATORS

R. H. Pantell and M. A. Piestrup

Stanford University

Coherent energy exchange between a laser and a free electron beam has potential applications for particle acceleration and for optical signal amplification and oscillation. A laser electron accelerator can provide high acceleration gradients and short duration electron pulses, and the optical electron beam amplifier can be broadly tunable with high gain and high average power.

There are several ways to achieve this energy exchange. If the interaction extends over many wavelengths then momentum matching is required, either by having a slow wave circuit to retard the electromagnetic wave or by using a medium for which the phase velocity of the wave is less than or equal to the electron velocity. For short interaction lengths there is uncertainty in the final state electron momentum so that momentum conservation is not necessary. Short lengths may be obtained either by focusing the light or by using a light guide.

Recently, we have observed momentum modulation of a relativistic electron beam by a Nd:YAG laser. The electrons, at 100 MeV energy, interacted with the laser light in helium gas at standard temperature and pressure. At an angle of 6.55 mrad between the two wavevectors, corresponding to the Cerenkov angle, a given electron remained in a field of constant phase as it passed through the light beam.

Figure 1 is a drawing of the experimental arrangement, showing the trajectories of the electrons and light. The particle momentum was measured by a mass spectrometer, and the angle between the wavevectors was controlled by a rotatable mirror. Figure 2 is a photograph of the experimental arrangement with the helium gas bag removed. Electrons entered the interaction region through a 1/4-mil mylar window, shown at the lower left corner of the photograph, and passed into the mass spectrometer at the upper center.

Parameters for the experiment were as follows:

1. Electron beam parameters
   - 100 MeV
   - Measured divergence (half-angle) = 0.54 mrad
   - 0.6-mm diameter beam
   - ΔE = 63 keV (FWHM)
   - 13 nsec duration

2. Laser Parameters
   - Nd:YAG
   - $\lambda = 1.06\ \mu$
   - Power = 2.0 MW
   - < 0.1 mrad divergence in the interaction region

20 nsec duration
0.65 mm spot size
0.3 cm^{-1} line width

3. Medium Parameters
Helium at standard temperature and pressure (STP)
Cerenkov angle = 6.55 mrad at 100 MeV

Figure 3 illustrates the experimental results. Since electrons are equally likely to be accelerated as decelerated, the primary effect of the interaction is to change the linewidth of the electron energy spectrum. The ordinate in figure 3 is the full-width, half-maximum of the spectrum, and the abscissa is the separation between the axes of the electron and laser beams in mils. Each beam has a diameter of approximately 25 mils. The theoretical curve, obtained from a Monte Carlo simulation that included electron scattering and laser multimoding is shown as the solid line in figure 3. It is seen that the 2 MW, TEM mode laser changes the energy spectrum linewidth by approximately 40 keV for a single pass through the electron beam.

Momentum modulation of an electron beam, as demonstrated by the experimental results, may be used for amplification of radiation. An optical klystron amplifier would be similar in appearance to a microwave klystron, with a bunching section, a drift space, and an output coupler. At relativistic velocities the electromagnetic field produces primarily momentum modulation rather than velocity modulation. However, this does not preclude klystron bunching at optical wavelengths, because very little velocity modulation is required to shift the electron position by a fraction of an optical wavelength.

Figure 4 illustrates a possible configuration for an optical klystron, where a vapor (e.g., benzene or pentane) is used for index matching. Electrons pass through a membrane or thin foil into the interaction region, where an optical interferometer is used to resonate the electromagnetic radiation. The angle between the interferometer axis and the electron beam direction is the Cerenkov angle. After passing through the buncher section, the velocity modulation of the particles is converted to current modulation, where the amplitude of the current, I_1, at the bunching frequency is given by

$$I_1 = 2I_0 J_1(X) \tag{1}$$

where

I_0 ~ dc electron beam current

$X \sim \frac{\Delta v}{v} \frac{\omega}{\omega_p} \sin \frac{\omega_p z}{v}$

J_1 ~ the Bessel function of first kind and order

$\Delta v/v$ ~ fractional velocity modulation for an electron seeing maximum field strength.

ω_p ~ plasma frequency for the electron beam

z ~ distance down the drift region measured from the buncher

v ~ electron velocity

To obtain maximum bunching at the fundamental frequency, the drift distance z should be such that $X = 1.84$, so that $J_1(X)$ is maximized. For relativistic electrons,

$$\frac{\Delta_v}{v} \cong \left(\frac{E_0}{E}\right)^2 \frac{\Delta_E}{E} \tag{2}$$

where

E_0 ~ rest energy = 0.511 MeV

E ~ electron kinetic energy

$\frac{\Delta_E}{E}$ ~ fractional energy change of the electron seeing the maximum field.

From equations (1) and (2) the optimum bunching distance may be determined.

At the output coupler the electron beam current, modulated at the frequency applied to the buncher, excites an electromagnetic field in another interferometer. The extracted power may be an appreciable fraction of the dc power in the electron beam, whereas the input power is only that amount required to establish a field in the presence of resonator losses. Therefore, high power gain is possible. In contrast to the quantum amplifier, there is no feedback path to provide self-sustained oscillations. Frequency may be tuned by adjusting the interferometers, and, if an oscillator is desired, this may be obtained by providing a feedback loop from the output interferometer to the buncher.

Some of the problems associated with the optical klystron are:

1. As the electrons pass through the membrane and index matching medium, an energy spread occurs resulting from ionization and bremsstrahlung. The coherent energy from the laser must exceed this random spread.

2. There is an energy spread for the incident electrons, and this must also be small compared to the coherent modulation.

3. Electrons are scattered in different directions because of the nuclear coulomb forces in the various media. If Cerenkov synchronism is satisfied along one direction, phase mismatch will occur along the other directions. This effect must be small.

4. There is a loss of mean energy for the electrons, and this also introduces some phase mismatch.

To overcome these problems it is necessary that the field in the buncher introduce an energy modulation in excess of the random energy, and that the phase mismatch effects be sufficiently small so that most electrons remain in a field of constant phase in transit through the buncher.

As an example, consider an optical klystron to amplify 10-μ radiation, with an electron beam at 6 MeV energy and an energy spread $\Delta E/E = 10^{-3}$. Current density is 3 A/cm^2, and the beam area is 1 cm^2. The index matching medium is a vapor (e.g., benzene or pentane) at several atmospheres pressure to provide an index of refraction equal to $(1 + 8.5 \times 10^{-3})$. A 1/4-mil mylar membrane separates the vacuum from the vapor (differential pumping might be preferable), and it is assumed that the loss in both interferometers is 0.4 percent per round trip pass. Each electron pulse is 1 μsec long with a repetition rate of 60 pps.

For these parameters the Cerenkov angle is 6°, and with an input power of 12 kW the optimum bunching distance is 9.1 cm. Most electrons remain in a field of constant phase and the energy introduced by the laser is well in excess of the random energy spread. Output power is 0.54 MW (0.54 J per pulse, 60 pps), corresponding to a 3 percent efficiency, where efficiency is defined as the ratio of the output power to the dc electron beam power. Power gain, that is, the ratio of output to input power, is 45. Harmonic bunching distances and power are as follows:

Harmonic	Optimum bunching distance, cm	Harmonic power, MW
1	9.1	0.54
2	7.4	0.38
3	6.9	0.30

Since the input is 12 kW, harmonic generation is achieved with power gain.

With a high power linear accelerator as the electron source, extremely large peak and average power tunable optical radiation may be obtained. For example, the 140 MeV Linac at Oak Ridge has a peak current of 15 A and an average current of 0.8 A. With 5 percent conversion efficiency a tunable optical source could be developed at a peak power of 10^8 W and an average power of 5.6 MW.

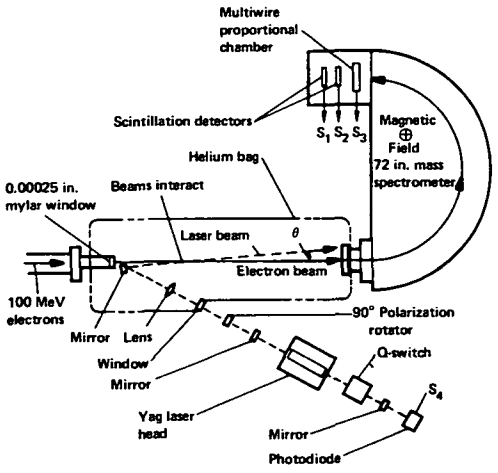

Figure 1.– Experimental setup showing trajectories of electrons and light.

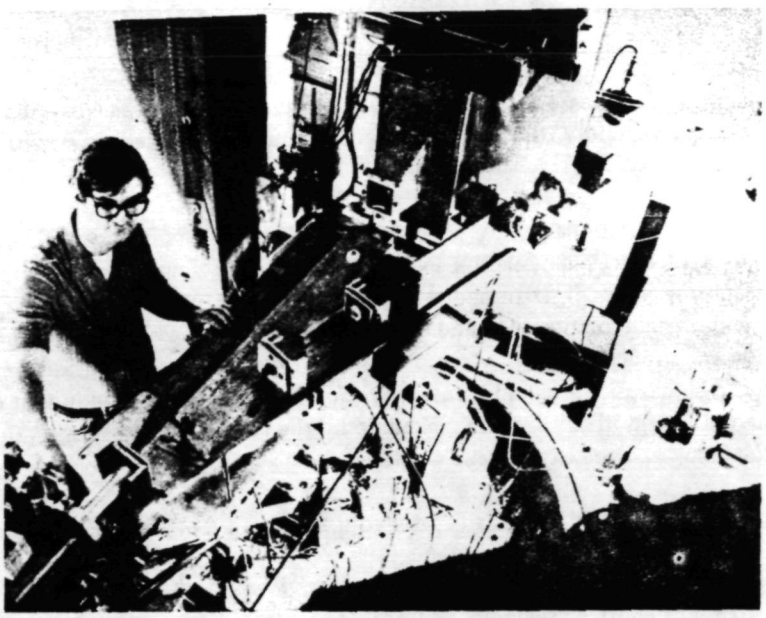

Figure 2.– Experimental setup with the helium bag removed.

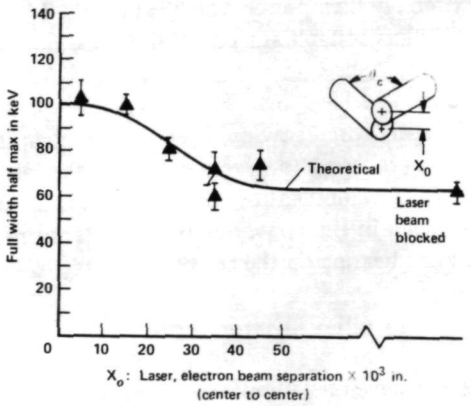

Figure 3.– Experimental results; full-width, half-maximum of the spectrum *vs* separation between axes of the electron and laser beams.

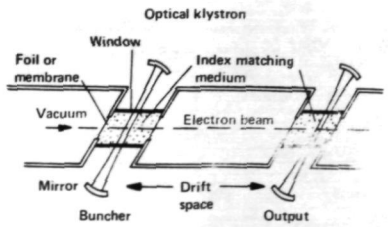

Figure 4.– Optical klystron configuration.

DISCUSSION

Max Garbuny, Westinghouse – Two questions occur. Why not use a liquid or solid rather than the gas? Would this not give higher conversion efficiency? Secondly, the Klystron effect reminds one of the Schwarz-Hora effect which, of course, remains in doubt.

Dick Pantell: Yes, I shall answer both questions. I have gone through an analysis with regard to liquids and solids and the problem is to have a coherent energy modulation in excess of the straggling or the random energy spread that you pick up in going through the material. It turned out that the gas was optimum in this regard. The other point you mentioned was the experiment of Schwarz and Hora where it was suggested that there was a possible modulation of the wavefunction of an electron. Other people have not been able to duplicate this experiment. I made a calculation of the straggling, that is, the random energy spread they would have had in that experiment and it was far in excess of the coherent energy that could be picked up by the laser. So, at least using the principle that I've considered, I don't think the Schwarz-Hora experiment would work.

Karlheinz, Thom, NASA Headquarters – Could you clarify how your work applies to laser energy conversion?

Dick Pantell: Yes, as was stated this morning by Dr. Lundholm, the entire system you're considering has elements of generation of high power, perhaps short wavelength and even tunable radiation, transmission-reception and conversion. What I have discussed is the generation of optical or infrared power. For example, with the Klystron configuration which I used, if one puts in a feedback loop from the output coupler to the buncher (this only takes a small fraction of the output since you have a gain of 45 in the power) then one has an oscillator. Depending on the electron beam you use, one has an oscillator of extremely high power which is tunable. I believe these concepts fit in the category of very high power oscillators and amplifiers suitable for power transmission.

Ken Billman, NASA Ames Research Center – Dick you have answered Karlheinz's question, but I would like to add a small comment since there will be similar papers tomorrow on lasers, rather than laser energy converters. I decided to devote a small fraction of our time in this meeting to developments in the laser area which, to my best judgement, are new and potentially important to the development of convertors. This development in the laser area is entangled with the necessary developments we need in the converter field. So tomorrow you will hear a lot of short summaries of laser developments that may have a bearing on the converter problem.

Ned Rasor, Rasor Associates – Have you considered the reflex klystron for this?

Dick Pantell: No, it's an interesting suggestion, but I haven't. I think you want to use a magnetic field to bend the electrons back, and it probably should work.

Ernest Brock, LASL – You might also consider using a multicavity klystron.

Dick Pantell: Yes, the high efficiency microwave oscillators and amplifiers do use multicavity configurations. That would be something to do eventually.

Ken Billman, Ames Research Center – Everyone wants you to "run before you walk", Dick!

Dick Pantell: Yes!

APPLICATION OF HIGH POWER LASERS TO SPACE POWER AND PROPULSION

Donald L. Nored

Lewis Research Center, NASA

INTRODUCTION

The National Aeronautics and Space Administration (NASA) is engaged in a high-power laser research program. The objective of this effort is to define the potential of high-power lasers for space missions of the future. The Lewis Research Center is responsible for the systems portion of the overall effort. Of necessity, the areas of investigation for system evaluations cover a broad range of technologies. Key areas in the Lewis effort are indicated in table 1.

Of particular interest to NASA is the transmission of power over long distances for applications such as direct conversion to propulsive thrust or electrical power. A key area of work pertains to problems inherent in transmitting, propagating, and receiving the laser beam over long ranges. The space-oriented applications of interest to NASA suggest that long duration and closed-cycle operation, with high efficiencies and reliabilities, are important technical goals for the laser. In addition, continuous wave (CW) operation is deemed of primary importance, at least for space operation, since such operation requires no high voltage switching components and reduces the peak intensities placed on the mirrors. Currently, only CO_2 lasers satisfy these criteria.

Accordingly, a major area of investigation is to advance CO_2 laser technology relative to these goals. However, wavelengths shorter than that of CO_2 (10.6 μ) are desirable (e.g., providing smaller transmitter and receiver mirrors); hence, efforts are also underway to explore other possible lasing media. Particular emphasis is being placed on visible portions of the spectrum due to possibly better compatibility with photovoltaic power conversion devices and possibly better atmospheric propagation. Here again, the goals are high efficiency, closed-cycle, CW operation. In this paper, the laser application to electrical power conversion and propulsion, and the associated problems of transmission of the laser beam, will be summarized.

POWER CONVERSION

The electrical power requirements of current Earth orbital satellites are typically less than 10 kW, and quite often in the 1-2 kW range. Solar cells are the primary power conversion source for these requirements. In the future, larger amounts of power may be required for applications such as direct broadcast satellites or manned space stations. Power conversion systems, other than solar cells, that may be considered include nuclear heated Brayton-cycle or Rankine-cycle systems, or solar-heated Brayton systems. A concept of a solar-Brayton system (ref. 1) is shown in figure 1. The large mirror at the bottom concentrates the solar energy into a receiver/heat exchanger system located at the top. The large ring surrounding the receiver is the radiator.

With the advent of the laser, and the possibility of transmission of high power beams over long ranges to a receiver of relatively small diameter, the solar-Brayton system of figure 1 can also be envisioned as a laser-Brayton system. The mirror concentrator, for a laser beam, would then no longer be a variable with power output. Instead, its size would only be a function of distance from the laser beam transmitter and size of the transmitter. Figure 2 is an example of a low-Earth requirement. The mass of solar cells, solar-Brayton, and laser-Brayton systems (based on weight assumptions for the solar-Brayton, ref. 2) are compared for a range of power outputs. In all cases, energy storage is included to account for night power or power required when out of sight of the laser transmitter. As can be seen, the laser-Brayton is competitive with the other two systems because of the small mirror required for a low-Earth orbit. In this example, the laser beam generator is assumed to be on the Earth, hence, the mirror is only 2 m in diameter for the 185-km range with a CO_2 laser having a 2 meter transmitter mirror. The receiver mirror mass is estimated to be about 7-9 kg.

Figure 3 is a similar comparison for the geostationary orbit case. Here the laser-Brayton system is at a decided disadvantage at less than 100 kW due to the very large (30-m diameter) and heavy (1725 kg) mirror required for a CO_2 laser beam. Obviously, this case could be improved by using a shorter wavelength laser, thus permitting use of a smaller mirror size.

The above two examples are for laser-Brayton engine systems of about 25-30 percent efficiency, systems that are compatible with state-of-the-art CO_2 laser (or, for that matter, with a laser of almost any wavelength) because the beam is only used as a heat source. Photovoltaic cells, similar to solar cells, are predicted to be capable of about 40 percent efficiency when illuminated by laser radiation in the visible wavelengths (ref. 3). Use of such cells would improve the comparisons. (Currently however, high-power visible wavelength lasers, capable of closed-cycle CW operation, are only in the conceptual feasibility stage.) Indeed, the mirror weight line on figure 3 would potentially become the power conversion system mass, if a photovoltaic cell system or similar such device became available and if the cell could withstand the higher laser beam flux levels (that is, watts per square centimeter as contrasted to solar cell technology of tenths of watts per square centimeter). For low-Earth orbit (fig. 2), the comparison would then be even more favorable to the laser system.

Other types of laser energy conversion devices are now only in the conceptual and discovery stages. It appears, however, that any system for conversion of laser beam energy to electrical power must not only have the general desired attributes of high efficiency, low mass, and low cost, but also must have the capability to operate at high laser beam flux levels. Of course, the required wavelength for conversion must be compatible with efficient laser beam generators. Other factors, such as altitude, total power, total mass, launch vehicle constraints, location or locations of the laser beam generator, and total cost, also will enter into the final power system selection process.

LASER PROPULSION

Another use of laser energy is for propulsion. The concept involves transmission of power from a remote laser station to a rocket vehicle where the laser radiation is used to heat a propellant, thus providing thrust. The laser could be located on the ground, in an airplane, or on a space station.

This concept is unique compared with other forms of propulsion in that it separates the energy source from the vehicle and also permits independent control of specific impulse, thrust, and choice of propellant. A schematic drawing of the concept showing the laser, in this case on the ground, and the rocket vehicle is illustrated in figure 4.

A number of technical areas must be considered in evaluating this concept. The major areas are:

1. Mission (trajectory constraints)
2. Laser power (scale-up to high power levels)
3. Transmitter (pointing stability, adaptive phased array design)
4. Atmospheric propagation (if operating within the atmosphere)
5. Receiver (vehicle constraints; lightweight design)
6. Engine (heat transfer; laser beam coupling)

Missions envisioned for this concept include orbit-to-orbit transfer, interplanetary injection, orbit drag make-up, and vehicle launch.

For a laser powered launch vehicle, perhaps 10^9 W of laser power would be required on target over a period of a few minutes, and even then the payload would only be about 1000 kg or less (ref. 4). At the present, launch vehicles using laser power appear to be quite remote. One mission of importance with lower power requirements, and therefore a more feasible application of the laser, is the one of delivering a payload from low-Earth orbit to geostationary orbit.

Figure 5 is a plot of payload mass delivered to geostationary orbit from low-Earth orbit as a function of trip time for an initial vehicle, propellant, and payload mass of 28,200 kg (the payload capability of the Space Shuttle). In this case, the trip time is the total round trip time required for the vehicle to go to geostationary orbit, drop off its payload, and return empty to low-Earth orbit. Parametrically presented are calculated values of specific impulse and laser power. Values of specific impulse of 1000 sec or greater offer significant improvements over a chemical rocket vehicle and require laser power levels possibly achievable in the near future. For instance, delivery of a 15,450 kg payload to geostationary orbit in less than 10 days would require a laser input of only 4 MW. This represents a fourfold improvement in payload capability over a chemical tug, which is currently under study for use with the Space Shuttle. For this example, the laser powered rocket engine operates continuously. This requires that the vehicle receiver be in continuous view of a laser transmitter. One way of accomplishing this would be to place laser beam generators on two or more space stations.

Other mission profiles for delivery of a payload from one orbit to a higher orbit are also possible. A concept for one such trajectory, which requires only one laser station located on the ground, is shown in figure 6. This concept is called perigee propulsion (ref. 5). Starting with the vehicle in low-Earth orbit, power is beamed to the vehicle via a ground-based laser for only a brief period of time as the vehicle passes overhead. This point corresponds to the perigee of the

trajectory. The orbit is increased as a result of the rocket thrust, but thrust time is controlled so that upon completion of each orbit, the vehicle trajectory returns to the same perigee, which in all cases is directly over the laser station. Upon reaching the desired altitude, the orbit is circularized either by the laser rocket engine or by use of an auxiliary chemical rocket engine. The primary advantages of this concept are that only one laser is required for the mission, and, because the vehicle always returns to the same location relative to the laser station, pointing and tracking requirements are simplified compared to other techniques where continuous power is required. This concept, however, because of atmospheric propagation losses and trajectory constraints, does require higher laser power than the space-based laser concept shown previously in figure 5.

Other techniques for using the laser to supply power to a rocket vehicle, in addition to the two discussed, are also possible. Multiple laser stations on the ground, or airborne lasers having greater maneuverability and operating above a large portion of the Earth's atmosphere, are other approaches of interest.

LASER-POWERED ROCKET ENGINE

Relatively high values of specific impulse, hence high temperatures, are required to achieve the high levels of performance shown on figure 5. Figure 7 shows the specific impulse in space for hydrogen propellant as a function of temperature. Two curves are presented, one in which the thermodynamic state of the hydrogen is assumed to be frozen throughout the expansion process, and one in which the thermodynamic state is in local equilibrium during expansion.

This figure shows the temperature requirements likely to be imposed upon the rocket engine. For example, specific impulse values of 1000 and 2000 sec, for frozen expansion, require average chamber temperatures of about 3200° K and 10,000° K, respectively. It can be seen that at 3200° K the specific impulse of hydrogen greatly exceeds the deliverable specific impulse of the high-energy chemical bipropellant combination of hydrogen and oxygen operating at this temperature. For laser rocket engines at the lower specific impulse level, energy from the laser could conceivably be transferred to the hydrogen propellant by conduction from a laser heated plug. Such development would probably not require significant advances in technology. The engine with a specific impulse of 2000 sec, however, would be well beyond current technology.

A possible schematic for such an engine is shown in figure 8. In concept, laser energy would be beamed through a window and absorbed directly in the propellant, creating a sustained plasma. Either the heated plasma would exhaust directly through the nozzle, or coolant gas would be heated from the stable plasma core and act as the propellant (similar to the nuclear gas-core rocket concept). Some of the research areas associated with this laser rocket engine concept are:

1. Plasma initiation – This entails techniques for absorbing the radiation by the cold gas, causing it to ionize sufficiently so that inverse bremsstrahlung absorption can be initiated. Cesium particles, carbon particles, molecular gases, or starting arcs have been proposed as possible techniques.

2. Plasma stability – After initiation, subsequent changes in absorption may occur; these would result in an instability which might be detrimental to performance and operating life.

3. Energy transfer – Techniques for transfer of plasma radiation to the propellant are required. Seeding the propellant gas with micron-sized tungsten or carbon particles might be a possible approach. These would also protect the chamber walls.

4. Window technology – The window must pass a high-power laser beam for long periods of time. And, in addition, it may receive radiation from the very hot plasma. Cooling problems may be severe and require further evaluation.

Figure 9 shows an experimental test device to be used at Lewis for preliminary laser-heated flow visualization studies. These studies should help us to better understand the phenomena and problems associated with a laser beam interacting with a flowing seeded gas. Contracted efforts are also underway to evaluate both analytically and experimentally laser-plasma phenomena in rocket-type devices.

LASER TRANSMISSION

Most of the laser power and propulsion applications of interest to NASA will involve transmission of the laser beam over long distances. Such transmission may be in space (vacuum) or through the atmosphere. Current lasers provide different intensity distributions at the output aperture, depending on the type of optical resonator used for the cavity. Uniform illumination, Gaussian-type profiles with varying degrees of truncation, and annular modes are some more common profiles. From a systems point of view, it is important to know the propagation characteristics of the various beam shapes and, more importantly, to know the optimum intensity profile to place at the transmitting aperture to achieve a desired result at the receiver. (In some cases, maximum intensity might be desired; in other cases, maximum power in a given receiver diameter might be the desired result.) An analysis is underway at Lewis to evaluate these characteristics in a vacuum (that is, space).

Figure 10 shows some of the types of transmitter profiles we have considered to date. These profiles, emanating from a circular aperture (comprised of a single mirror or multiple segments) all have the same total integrated transmitting power. The scale at the left of the figure provides an indication of the relative intensities. The distribution with the lowest intensity is the uniformly illuminated case. Intermediate in intensity is a Gaussian beam truncated at its $1/e^2$ radius. To achieve the same total power on the transmitting aperture as the uniform distribution, the truncated Gaussian central intensity must be larger by a factor of 2.3. The third profile shown is that of a Gaussian with only a very slight truncation, in this instance at twice its $1/e^2$ radius. Here the central intensity is eight times as large as for the uniformly illuminated case to achieve the same total transmitter power. One can also see that the thermal gradient and thermal loading on the transmitting optics will be much more severe for the Gaussian-type beams.

Figure 11 shows the shape of the same beams when they reach the receiver in the far field. In this figure, relative intensity is plotted against receiver radius, which is expressed in terms of $\lambda L/D_T$, where λ is laser wavelength, L is range to the receiver from the transmitter, and D_T is diameter of the transmitter. For all beams, diffraction limited propagation (e.g., in a vacuum) is assumed. Notice that the beam from the uniformly illuminated aperture now has the highest central intensity, the one leaving as a $1/e^2$ truncated Gaussian becomes about 92 percent as great, and the Gaussian with

only a slight truncation at the transmitting aperture becomes only 48 percent as great. For applications requiring maximum intensity, the uniformly illuminated beam would be the best choice of the three considered. These results are only valid, of course, for the case considered, that of equal power beams at the transmitter.

For those applications involving optimization or maximization of delivered power within the smallest spot, the uniformly illuminated beam may not be the most desirable. This is illustrated in figure 12. Power is shown as a percentage of transmitted power versus the receiver radius, again in terms of $\lambda L/D_T$. The uniformly illuminated beam, at the "classic" value of $1.22\,\lambda L/D_T$ (that is, radius of the Airy disk), is seen to give 84 percent of the total transmitted power. The $1/e^2$ truncated Gaussian beam provides the same amount of power in a smaller radius, or, at the same radius, will give an increase to 94 percent transmitted power. It appears that the $1/e^2$ truncated Gaussian is the most efficient for the cases considered. Obviously, trade-offs are required for each specific application depending on weight of receiver, cost of receiver relative to the transmitter, and intensity limits of the receiver and transmitter.

Using the truncated Gaussian profile on the transmitter, receiver diameter is plotted versus transmitter diameter in figure 13, for transmission distances of 160 km (low-Earth orbit) and 36,000 km (corresponding to geostationary orbit altitude) and for the case of 86 percent transmitted power. Again, diffraction limited propagation is assumed, as would be the case for laser beam transmission from a space station to another satellite or space vehicle. Also, the wavelength is assumed to be $10.6\,\mu$, as from a CO_2 laser. For the general case of equal diameter receiver and transmitter, it can be seen that the diameter would correspond to only 1.7 m for the 160 km range, a value well within the state of the art. For 36,000 km, however, the diameter is 25.7 m, a size well beyond the current capabilities of fabrication for the precise transmitter mirror that would be required.

For the receiver, however, large diameter, lightweight structures are most likely feasible. Figure 14 is a picture of a prototype solar mirror for the solar-Brayton power system (ref. 1). This mirror is fabricated from sections machined from magnesium and then formed to shape. The mass of this prototype is 4.9 kg/m^2. Figure 15 shows a more recent solar mirror fabricated at Lewis. This mirror is made of thin aluminum sheet material, including the supporting rib structure. The mass of this mirror is 1.5 kg/m^2. Based on this technology, laser receivers of quite large size appear feasible.

Since large transmitters appear necessary for most space applications, we have initiated efforts to evaluate techniques for fabrication of such mirrors. A current contracted effort is investigating the feasibility of several concepts for a 30-m diameter space-based laser transmitter. One of the concepts is schematically shown in figure 16. A composite base structure is used to provide stiffness and low mass. The mirror itself is segmented, with each segment (which could be either circular or hexagonal in shape) being limited to a diameter such that the mirror is within current state-of-the-art fabrication capability. To control the figure, or shape, of the mirror, each segment is individually controlled by precision actuators. In operation, a separate detection scheme would sense the figure (surface contour) and signal the appropriate actuators if corrections were required. In another concept, not shown, the segmented mirrors would be replaced with a thin deformable membrane surface.

The use of either thin membranes of uncooled segments appears feasible since only 0.6 W/cm^2 would be incident on the 30-m diameter mirror surface for a 4000 kW laser beam. And, of this

amount, only 6 mW/cm^2 would be absorbed. The large size of a transmitter, as required for the CO_2 laser wavelength, thus might become an advantage under certain circumstances due to heat transfer considerations.

Another approach to active control is the use of coherent optical adaptive techniques (COAT) (ref. 6) with a multiple mirror system. The advantage of such phased array control is shown in figure 17. As indicated by the sketch on the left, diffraction-limited focusing is possible in a vacuum. In the atmosphere, however, turbulence cells cause defocusing, as shown in the center schematic, due to phase changes in the waves as they pass through the cells. In the adaptive phased array, a return wave is detected at the transmitter.

The detection system provides a means to obtain an error signal resulting from atmospheric aberrations, transmitter jitter, and optical misalignment. Active control of the high power transmitter mirror system can then be accomplished to tailor the phase of the wavefront, thus providing maximum power on target. COAT systems are highly versatile and applicable to either high power, master oscillator-power amplifier (MOPA) configuration lasers or to high power, unstable oscillator lasers. Indeed, with the MOPA configuration, adaptive control can be applied to the low-power master oscillator prior to amplification, thus correcting for perturbations in the amplifier gain medium. Another advantage to a COAT system is that it allows automatic acquisition and tracking of the target, thus easing the pointing and tracking requirements for the mirror mount system. Overall, it now appears that adaptive phased arrays may be the only feasible technique for near-diffraction limited transmission of power over long distances, and we have initiated contract effort in this area.

SUMMARY

The general objective of defining the potential of high power lasers for future space missions, forces our research program into consideration of all elements of the total system. The laser beam generator, its associated power supply, and the transmitter optical system will generally comprise a complete unit, which will be remote to the end use application. Such a unit may be located on the ground or in space. Limitations in beam propagation must be considered if the beam passes through the atmosphere. Typically, the receiver will be located in the space environment and will have unique characteristics, depending on whether electrical power is desired or whether beam energy is used to heat propellants for rocket thrust. Perhaps the greatest unknown area is that of highly efficient conversion of laser beam energy into electricity. In all cases, detailed trade-offs between the various components, their efficiencies, and their characteristics will be required to optimize the system.

Technology is not available today to undertake many of the applications discussed in this paper. On-going efforts in this area give promise, however, that such technology will become available in the future, thus providing an advancement in space capabilities and offering a choice among future mission options.

REFERENCES

1. Stewart, Warner L.; Anderson, William J.; Bernatowicz, Daniel T.; Guentert, Donald C.; Packe, Donald R.; Rohlik, Harold E.: Brayton Cycle Technology. Paper presented at the Space Power Systems Advanced Technology Conference, NASA, Lewis Research Center, Cleveland, Ohio, 23-24 August 1966. NASA SP-131, p. 95-145.

2. Lubarsky, Bernard; and Shure, Lloyd I.: Applications of Power Systems to Specific Missions. Paper presented at the Space Power Systems Advanced Technology Conference, NASA, Lewis Research Center, Cleveland, Ohio, 23-24 August 1966. NASA SP-131.

3. Wolf, M.: Photovoltaic Conversion of Laser Energy, Proceedings of Laser-Energy Conversion Symposium, NASA, Ames Research Center, Moffett Field, California, 18-19 January 1973, NASA TM-X-62269, p. 6-18.

4. Rom, Frank E.; and Putre, Henry A.: Laser Propulsion NASA TM-X-2510, April 1972.

5. Minovitch, M. A.: Reactorless Nuclear Propulsion – The Laser Rocket. Paper presented at the AIAA/SAE 8th Joint Propulsion Specialists Conference, New Orleans, Louisiana, 29 November – 1 December 1972, AIAA Paper No. 72-1095.

6. Bridges, W. B.; Brunner, P. T.; Lazzara, S. P.; Nussmeier, T. A.; O'Meara, T. R.; Sanguinet, J. A.; Brown, W. P., Jr.: Coherent Optical Adaptive Techniques. Applied Optics, Vol. 13, No. 2, February 1974, p. 291-300.

TABLE 1.– NASA/LEWIS RESEARCH CENTER HIGH-POWER LASER SYSTEMS RESEARCH PROGRAM

Key areas	Potential requirements
Application concepts	Power; propulsion
Transmission	Long ranges; high beam quality
CO_2 lasers	High reliability; closed cycle operation
New lasing media	Short wavelengths; high efficiency; closed cycle operation

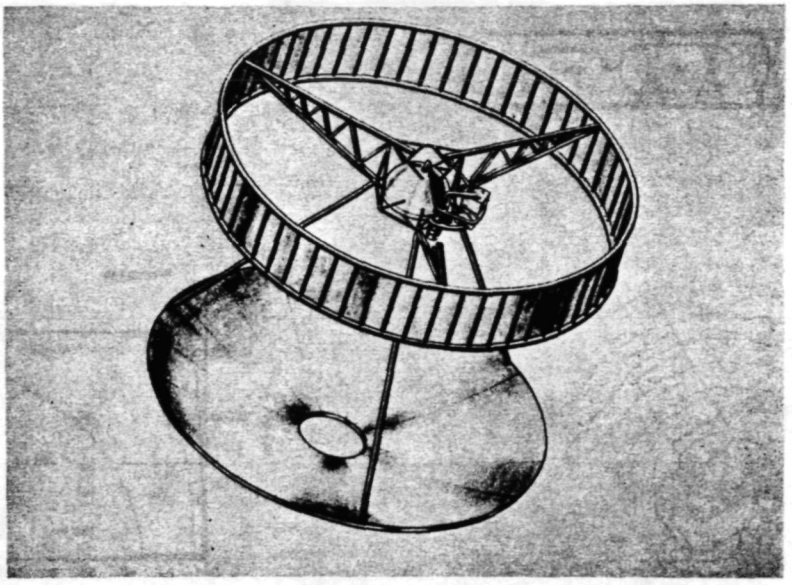

Figure 1.– Solar Brayton cycle space power system.

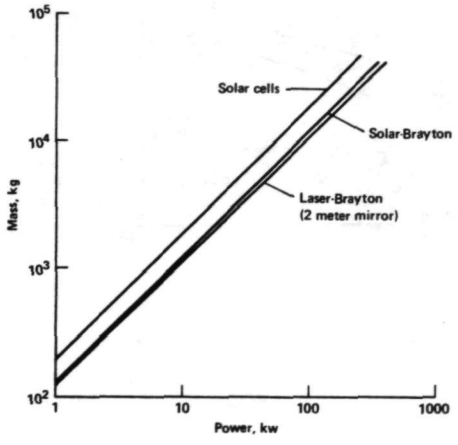

Figure 2.– Weight comparison – low orbit.

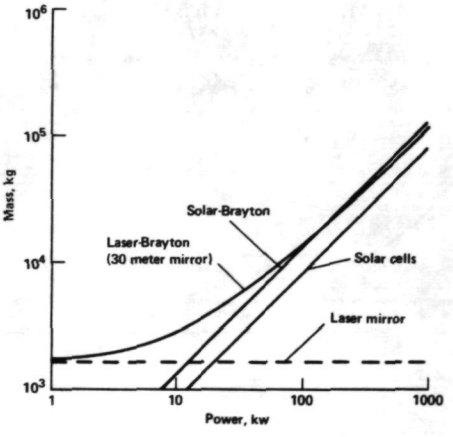

Figure 3.– Weight comparison – synchronous orbit.

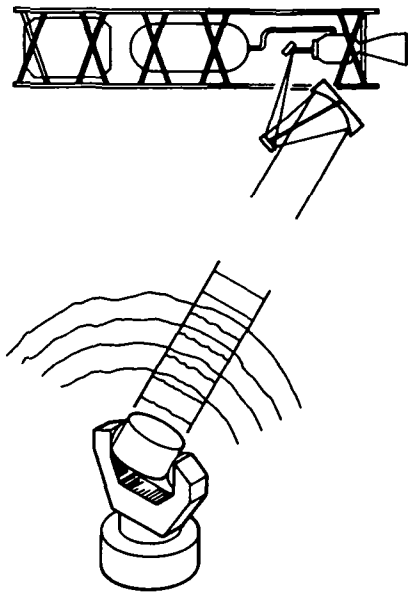

Figure 4.– Laser rocket space vehicle employing a ground-based adaptive transmitter.

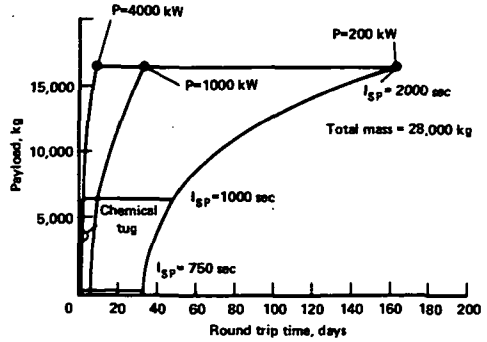

Figure 5.– Laser propulsion potential – payload to geostationary orbit.

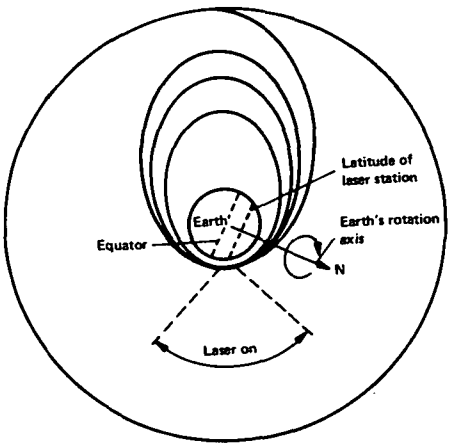

Figure 6.– Orbit raising with single Earth-based laser.

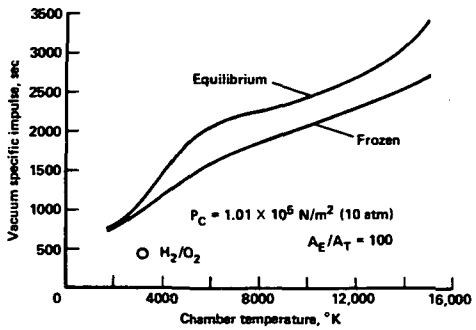

Figure 7.– Propulsion performance of hydrogen.

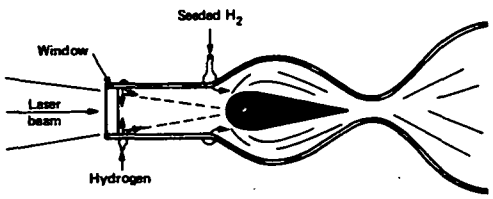

Figure 8.– Laser rocket thruster concept.

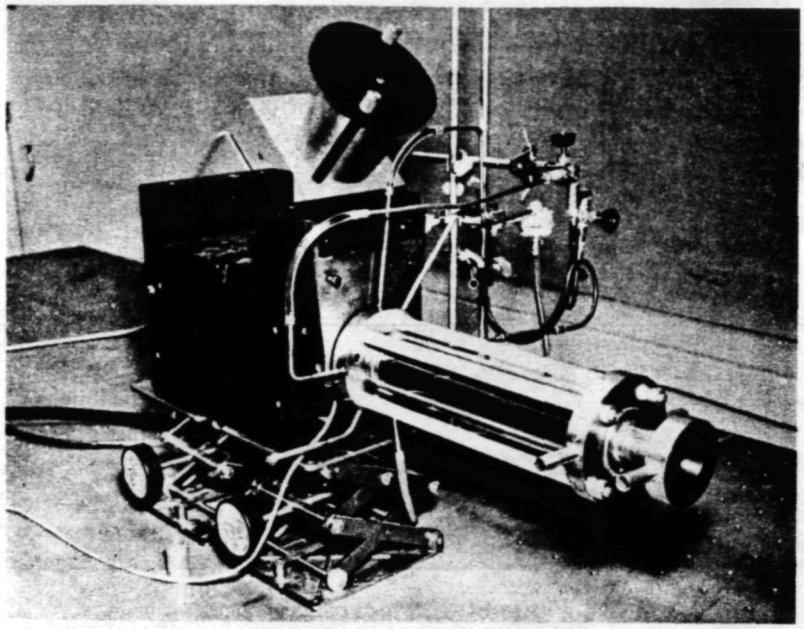

Figure 9.– Laser plasma flow visualization device.

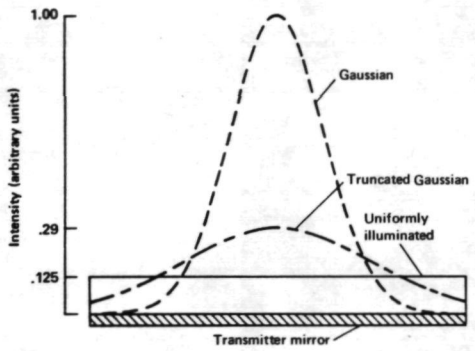

Figure 10.– Transmitter intensity profiles for equal total power.

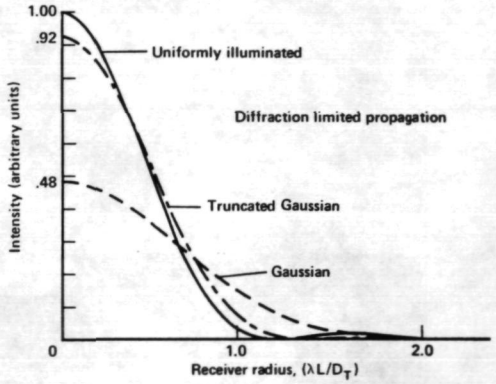

Figure 11.– Receiver intensity profile for equal power beams at transmitter.

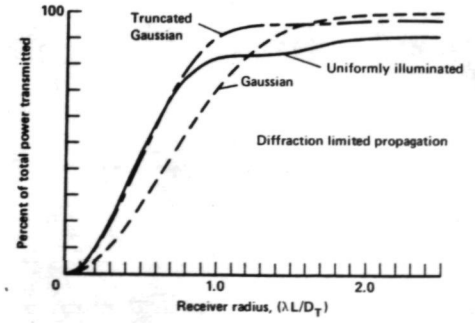

Figure 12.– Receiver power for equal power beams at transmitter.

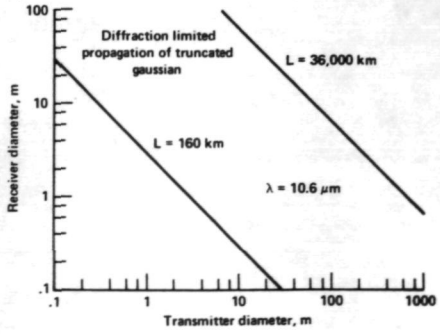

Figure 13.– Laser transmitter/receiver sizes.

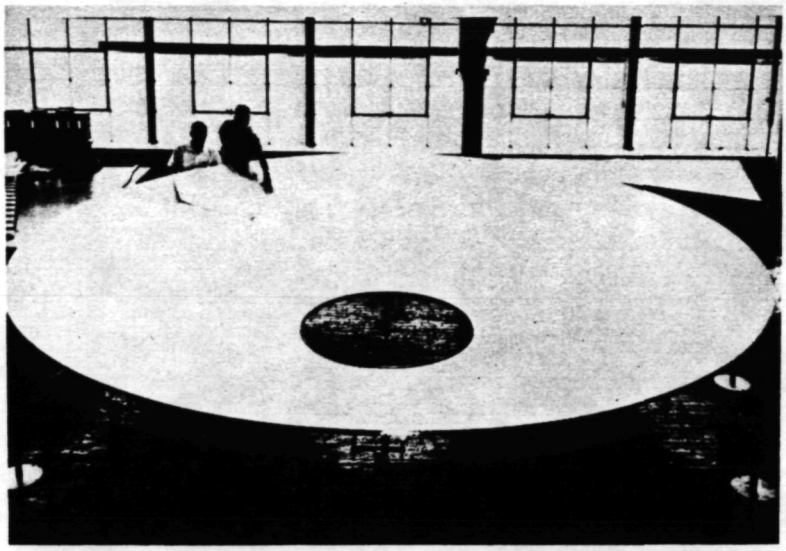

Figure 14.– 20-foot concentrator.

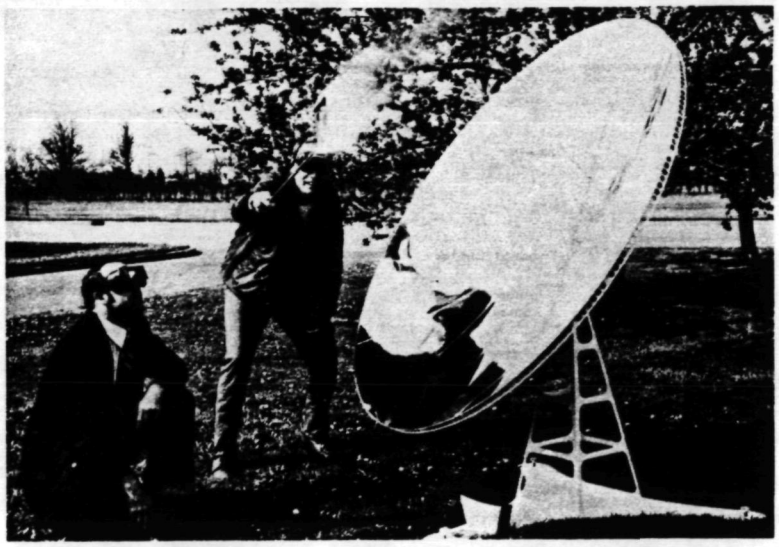

Figure 15.– Lightweight solar mirror.

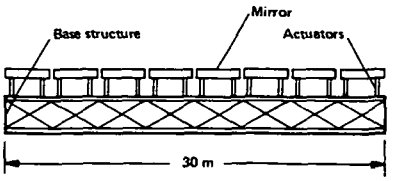

Figure 16.– Transmitter mirror with active segments.

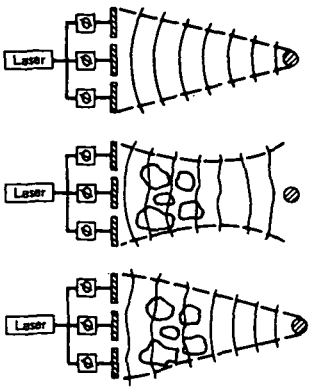

Figure 17.– Adaptive optics for atmospheric propatation.

DISCUSSION

George Sutton, AVCO Everett Research Laboratory – I have three comments. First, I think it is misleading to discuss truncated Gaussian beams from high power lasers. You must run saturated if you want high efficiency. If you run saturated then the beam possibly will not come out Gaussian. In fact, for all high power lasers built in the United States, none have even near-Gaussian profile. So the attributes of the Gaussian should not be incorporated into your systematic thinking about this application. Secondly, in your view of the atmosphere you omitted two very important propagation problems. One, for ground transmission, is thermal blooming and the other one is propagation through clouds. In the case of blooming, Hughes Labs. has reported, in December, on experiments and theory of the use of adaptive optics and the results of those are, for either uniform or Gaussian illuminated apertures, the adaptive optics provides no correction for thermal blooming for a CW focused beam. Their results indicate that if you go pulsed, however, you can get back almost to diffraction limited operation. So these results look a little dismal for the CW case. I should mention that at the same meeting, however, others discussed a possible way to beat this and that is by apodization or beam intensity shaping.

Don Nored: The phased array technique allows a way to shape the beam. I am aware that, from current lasers, you don't get a truncated Gaussian beam profile. But we have looked at a phased array, putting a uniform illumination on each of the phasor mirrors and then we could simulate the truncated Gaussian.

George Sutton, AVCO – But are you suggesting building a separate laser for each of the phasors?

Don Nored: Yes, that's one proposition. There are a number of ways of doing this. We are looking at them. Similarly, we are aware of thermal blooming and it would seem that high power CW beams have a problem. But we can break them up in to smaller beams. It may be that we will be forced, with CO_2, to ultimately go pulsed. Now on the pulsed copper vapor laser, that *is* quasi-CW, and the relaxation time in air may be all right.

Walter Schafer, Schafer Associates – You of course realize you are talking about pointing and tracking accuracies of about 0.3 μrad and therefore have to have this in your system.

Don Nored: Yes, one of the things we are trying to do is let the adaptive system help us because we can expand the beam, lock on it, contract it, and do it electronically to alleviate a lot of the requirements back on the transmitter base structure.

OUTLOOK FOR METAL LASERS*

Gary R. Russell

Jet Propulsion Laboratory

Pasadena, California

Lasers using atomic metallic vapors have drawn considerable attention since their invention in 1965 because of their potential for producing high power in the visible spectrum. Because, as yet, none of these lasers can be operated continuous wave (CW), the potential of high average laser power is tied to the attainment of both high laser energy density per pulse and the achievement of large pulsing rates.

Early attempts to attain lasing in metallic vapors utilized single pulsing in heated discharge tubes (refs. 1 and 2). Although lasing was demonstrated in a number of different metals, copper vapor was found to have the largest energy output per pulse and the best efficiency. Following the earlier work in heated discharge tubes, flowing laser devices were constructed to achieve multiple pulsing where the pulsing rate would not be limited by the laser kinetics, but only by the lasant flow velocity through the optical cavity (refs. 3 and 4).

Many of the early attempts to demonstrate lasing in both static and flowing laser systems were successful. However, the potential of this class of cyclic laser remained in doubt because of the high operating temperatures they required and the attendant and serious materials problems and heat transfer losses associated with vaporizing the metals. As an example, static copper vapor lasers generally operate at about 1500°C, and the stagnation temperature of supersonic copper vapor lasers can exceed 2000°C.

It has been apparent for some time to the workers in this field that, if metallic compounds having lower melting points than pure metals and correspondingly high vapor pressures at a given temperature could be utilized, the high operating temperatures could be lowered appreciably. Attempts at JPL and other laboratories to use metallic halides and organic metallic compounds with single discharges have heretofore failed to produce any power output from a laser cavity. Recent work carried out at JPL (ref. 5) using copper chloride and other metallic halides has indicated that this failure occurs because it is not possible to obtain simultaneous dissociation and lasing in a single electrical discharge. The dissociated metal from a single discharge contains an appreciable population of the lower metastable lasing levels which prevents lasing.

A double-discharge technique developed at JPL has proven to be a way of circumventing this problem. The metallic compound is heated and vaporized in a laser cavity and then is dissociated by an electrical discharge. A population inversion is attained in a subsequent second discharge applied at an appropriate time delay after the first discharge. There is an optimum time interval between the two discharges and an optimum lasant temperature for maximum laser power output per laser pulse.

---

*This work is supported by the National Aeronautics and Space Administration (NASA) and the Defense Advanced Research Projects Agency (DARPA).

To date, lasing has been attained utilizing the double-discharge technique in manganese chloride, lead chloride, copper chloride, copper iodide, and copper formate (refs. 6 through 7).

Characteristics of these lasers are summarized in table 1. Although lasing can be attained in copper formate in several sequential double discharges, decomposition of the copper formate subsequently causes carbon plating on the laser windows terminating the laser power output. Therefore, no reliable energy or power density data could be obtained using this compound. Because copper chloride appears to be the best lasant investigated thus far, a comprehensive parametric and spectroscopic absorption study has been initiated at JPL to determine the most dominant features of the laser kinetics and to optimize the efficiency and power output of both static and flowing copper chloride laser devices.

In heated copper chloride laser discharge tubes the power output is a function of the time delay between electrical discharges, the lasant temperature, the tube length and diameter, buffer gas composition and density, the optical cavity characteristics, and the power supply and laser electrical circuit characteristics.

Typical data for a copper chloride lasant, demonstrating the effect of time delay after the first electrical discharge and the effect of lasant temperature, are shown in figure 1. For times shorter than the optimum delay time the lower metastable levels of the copper are not depleted enough to establish a large inversion. For times larger than the optimum, chemical recombination of the copper and chlorine causes a decrease in the excitation of the upper lasing levels because of a diminishing of the copper ground state population. A diagnostic study utilizing absorption techniques is being conducted to measure the temporal variation of the copper lower metastable states and the ground state. The copper ground state density is determined by the absorption of radiation from a pulsed xenon flashtube at 3247 Å, the wavelength of one of the copper resonance lines. One of the metastable levels, the lower level of the lasing transition at 5106 Å, is determined by absorption at 5106 Å. The results obtained thus far confirm the original hypothesis that the copper metastable population is large following the first electrical discharge, and that these metastable levels must decay appreciably before lasing can be achieved in a second pulse.

Figure 2 shows the results of some absorption measurements utilizing a 13 mm diameter laser tube. Three types of measurements are indicated in the figures. The three upper curves are obtained from absorption measurements at the resonance wavelength of 3247 Å at three different lasant temperatures. The lowest of these three curves was obtained at a temperature just lower than the lasing threshold. A single curve at the lower left resulted from absorption of the 5106 Å line. For these measurements, only the dissociation pulse was activated and the abscissa represents the time delay between the dissociation pulse and the peak of the xenon flash.

The remaining two curves, representing the laser energy, were obtained at the same conditions as the absorption measurements but with the laser mirrors in place and the laser pumping pulse operating. For the purpose of displaying the laser energy on a basis that is directly comparable with the absorption measurements, the measured radiation at 5106 Å was converted to the number of copper atoms necessary to produce the measured radiation at 5106 Å. Since a mirror having a transmission of 16 percent was used as the output mirror, the number density indicated represents the minimum number of atoms, in the $^2P_{3/2}$ state, that must be stimulated to produce the measured energy. The chief conclusion one can draw from figure 2, which is representative of most of the data taken thus far, is that the onset of lasing is definitely dependent on the rate of decay of

the copper lower metastable levels, and that this rate of decay is much faster than the chemical recombination rate.

In figure 1, a plot of laser power output as a function of lasant temperature at a fixed time delay exhibits an optimum operating temperature of about 400°C. This optimum temperature is also applicable to other laser tube geometries and laser operating conditions. It is understandable that at low temperatures the copper chloride density is too low to provide enough copper atoms for lasing. However, the reason for the decrease in the laser power beyond the optimum temperature at increasing copper chloride densities is not clear at this time. It is this facet of the operation of the copper chloride laser that is currently being intensively studied; particularly to determine if the limitation in increases in the lasant density is of a fundamental nature or whether it is associated with the particular laser system that is currently under study.

Because of the relatively slow chemical recombination relaxation time compared to the time required for the evolution of the laser kinetics, it was decided to pulse continuously a copper chloride-helium mixture where the laser waste heat would be used to vaporize the copper chloride as was demonstrated in pure metal vapors in reference 8. Multiple pulsing was carried out in discharge tube diameters using frequencies corresponding to data taken in double-discharge heated laser tube experiments (fig. 3). Note that the optimum delay time decreases as the discharge tube diameter decreases, indicating that diffusion as well as electronic deexcitation is acting to deplete the lower lasing levels between current pulses.

Multiple lasing is observed when a train of single identical current pulses are spaced according to the data shown in figure 3. The initial current pulse acts as a pure dissociation pulse; successive current pulses serve both as laser pumping and dissociation pulses. Similar results have been obtained recently with copper iodide used as the lasant (ref. 9).

Data have been obtained utilizing multiple pulsing for discharge diameters varying from 1 to 4 cm (ref. 10). Although insufficient data have been obtained to determine the limits on laser efficiency at small pulsing rates, the data obtained thus far show that the efficiency increases as the pulsing rate increases. As the pulsing rate is increased beyond the corresponding optimum rates obtained in the double-discharge experiments, one would expect this trend to reverse because of an insufficient time between pulses required to deplete the lower lasing levels. However, this point has not been reached yet in the current experimental work.

To date, the best data have been obtained at 5106 Å using a 30-cm length and a 1-cm-diameter discharge tube with a pulsing rate of 2×10^4 sec^{-1}. At an average efficiency of 1 percent, the energy and power density per pulse are 35 $\mu J\ cm^{-3}$ and 1.7 $kW\ cm^{-3}$ respectively; the laser pulse width is 20 nsec and total average power output is 16.5 W at an average power density of 0.7 $W\ cm^{-3}$. The efficiency is defined as the ratio of the laser energy output and the energy stored in the capacitor. Thus far, only a helium buffer gas has been used with the copper chloride lasant in the multiply-pulsed experiments. The best laser performance is obtained at 10 torr. The effect of pressure and buffer gas composition will be the subject for future study.

In the multiply-pulsed experiments, although the lasant temperature is initially maintained with a laser heater as in the double-discharge experiments, the heater is turned off when the data are obtained. Without exterior cooling, multiply-pulsed operation can only be continued for a few minutes before the laser waste heat raises the lasant temperature and the performance decreases in a

manner similar to that observed in the double-pulsed experiments. The average laser power measured with a thermopile agrees, within experimental error, with the power calculated from the time-averaged values of the pulse power obtained with a photodiode. The laser output is very continuous with no missing laser pulses; a laser pulse is obtained with every current pulse. This feature of a one-to-one correspondence between laser and current pulses is shown in figure 4.

An average laser efficiency of 1 percent can probably be improved with further optimization of the discharge tube geometry and power supply characteristics, but our best estimate is that the improvement will not exceed 10 percent and more probably be of the order of 1 to 3 percent. In order to increase the average power from a copper chloride laser beyond that which can be attained from a static system, which appears to be about 100 W, one is faced with two problems. The first is removal of the waste heat deposited in the optical cavity with each electrical discharge, and the second is the upper limit in the pulse repetition rate imposed by the rate of relaxation of the copper lower lasing levels.

One possible solution to both problems is the technique of flowing the copper vapor through the optical cavity at high velocities. This technique removes the waste heat by forced convection and, at the same time, by replenishing the copper vapor charge in the optical cavity between pulses, allows higher pulse repetition rates and therefore higher average powers. To date, repetition rates of approximately 10^4 Hz have been achieved, for short periods, in static systems. To increase this rate one needs velocities greater than 10^4 cm/sec for a 1-cm-diameter cavity. A velocity of 10^5 cm/sec would increase the average power tenfold.

A system designed to study this technique is shown schematically in figure 5. The essential features of the system are an electrically heated graphite container that is used to continuously vaporize the copper chloride, a plenum chamber into which preheated helium is injected and mixes with the copper chloride vapor, a subsonic electrical discharge channel, and a supersonic nozzle to expand the halium-copper chloride mixture into a supersonic jet. The dissociation pulse is applied in the subsonic flow prior to the supersonic expansion. The second lasing pulse is positioned in the supersonic flow at a distance downstream from the dissociation pulse such that the flow time between the two discharges corresponds to the optimum delay time in a static double-pulsed discharge tube. Studies conducted with this supersonic laser facility have been partially completed. Parameters such as the location and electrical characteristics of the dissociation and pumping current pulses, optical cavity characteristics, copper chloride vapor density, and control of boundary layers have been investigated. Results obtained to date show that the copper chloride vapor remains supersaturated in the supersonic expansion, confirming the theoretical predictions made using non-stationary nucleation theory (ref. 11). Laser power extraction in the supersonic flow has been attained at 5106 Å with laser energy densities of about 2.5 $\mu J\ cm^{-3}$ at flow velocities exceeding 10^5 cm/sec, thus demonstrating that a supersonic copper chloride laser can be pulsed at rates of 10^5 Hz.

Work is continuing to determine what problems would be encountered in a much larger supersonic laser. At this time, there do not appear to be any fundamental problems associated with scaling up this laser device to produce average laser powers in the multi-kilowatt regime. In addition, larger supersonic jets will allow the number of lasing pulses to be large compared to the single initial dissociation pulse, so that the flowing laser has the potential of attaining a 1 percent or better efficiency, equal to the efficiencies currently being attained in multiply-pulsed laser discharge tubes, but with laser pulsing rates an order of magnitude faster.

REFERENCES

1. Piltch, M.; Walter, W. T.; Solimene, N.; Gould, G.; and Bennett, W. R. Jr.: Pulsed Laser Transitions in Manganese Vapor. Appl. Phys. Lett. Vol. 7, no. 11, 1 Dec. 1965, p. 309-310.

2. Walter, W. T.; Solimene, N.; Piltch, M.; and Gould, G.: Efficient Pulsed Gas Discharge Lasers, IEEE J. of Quant. Elect. Vol. QE-2, no. 9, Sept. 1966, p. 474-479.

3. Ferrar, C. M.; Copper Vapor Laser with Closed Cycle Transverse Vapor Flow, IEEE J. Quant. Elect., Vol. QE-9, Aug. 1973, p. 856-857.

4. Russell, G. R.; Nerheim, N. M.; and Pivirotto, T. J.: Supersonic Electrical-Discharge Copper Vapor Laser. Appl. Phys. Lett., Vol. 21, no. 12, 15 Dec. 1972, p. 565-567.

5. Chen, C. J.; Nerheim, N. M.; and Russell, G. R.: Double-Discharge Copper Vapor Laser with Copper Chloride as a Lasant. Appl. Phys. Lett., Vol. 23, no. 9, 1 Nov. 1973, p. 514-515.

6. Chen, C. J.: Manganese Laser Using Manganese Chloride as a Lasant. Appl. Phys. Lett., Vol. 24, no. 10, 15 May 1974, p. 499-500.

7. Chen, C. J.: Lead Laser using Lead Chloride as a Lasant. J. Appl. Phys., Vol. 45, no. 10, Oct. 1974, p. 4663-4664.

8. Isaev, A. A.; Kazaryan, M. A.; and Petrash, G. G.: Effective Pulsed Copper-Vapor Laser with High Average Generation Power. Soviet Physics JETP Lett., Vol. 16, no. 1, July 1972, p. 27-29.

9. Liberman, I.; Babcock, R. V.; Liu, C. S.; George, T. V.; and Weaver, L. A.: High-Repetition-Rate Copper Iodide Laser. Appl. Phys. Lett., Vol. 25, no. 6, 15 Sept. 1974, p. 334-335.

10. Chen, C. J.; and Russell, G. R.: High-Efficiency Multiply Pulsed Copper Vapor Laser Utilizing Copper Chloride as a Lasant. Appl. Phys. Lett., Vol. 26, no. 9, May 1975, p. 504-505.

11. Harstad, K. G.: Nonstationary Homogeneous Nucleation. J. Heat Trans., Vol. 97, no. 1, Feb. 1975, p 142-144.

TABLE 1. – OPERATING CHARACTERISTICS OF DOUBLE PULSED METALLIC VAPOR LASERS

Operating parameters	Lasant				
	Manganese chloride	Lead chloride	Copper chloride	Copper iodide	Copper formate
Time delay[a], μsec	150	150	100	100	100
Temperature, °C	680	500	400	575	135
Buffer gas, torr	He at 1-2	He at 1-2	He and Ar at 1-20	He at 1-2	He at 1-2
Laser energy density, $\mu J/cm^3$	1.3	4	35	11	–
Laser peak power density, W/cm^3	33	160	1700	500	–
Wavelength, Å	5341	7229	5107	5107	5107

[a]1-in. - diameter tubes

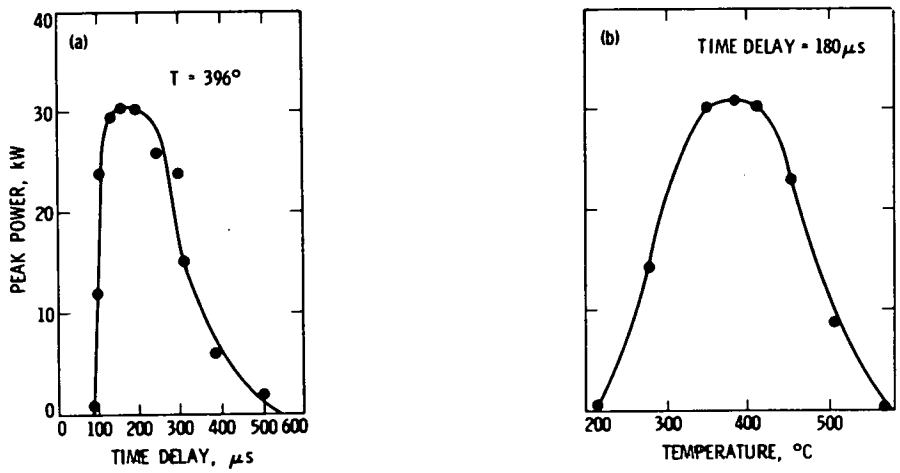

(a) Time delay between pulses.

(b) Temperature.

Figure 1.– Dependence of laser peak power.

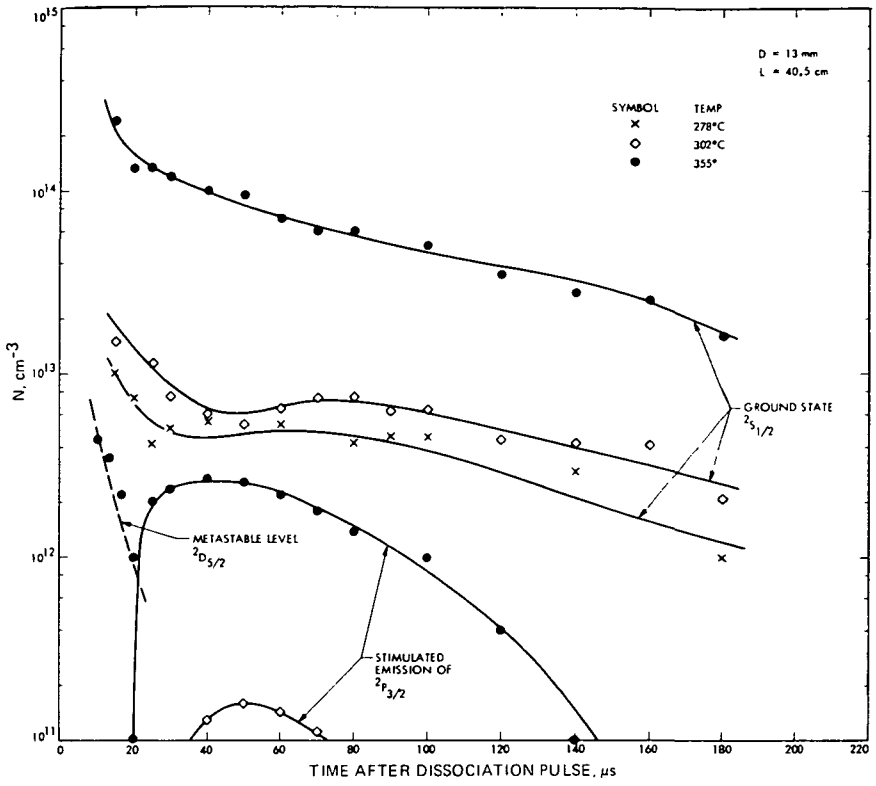

Figure 2.– Measured densities of copper ground state and metastable levels as a function of time after the dissociation pulse. Laser energy at the same lasant conditions is also shown as the minimum number of stimulated emissions needed to produce the measured laser energy.

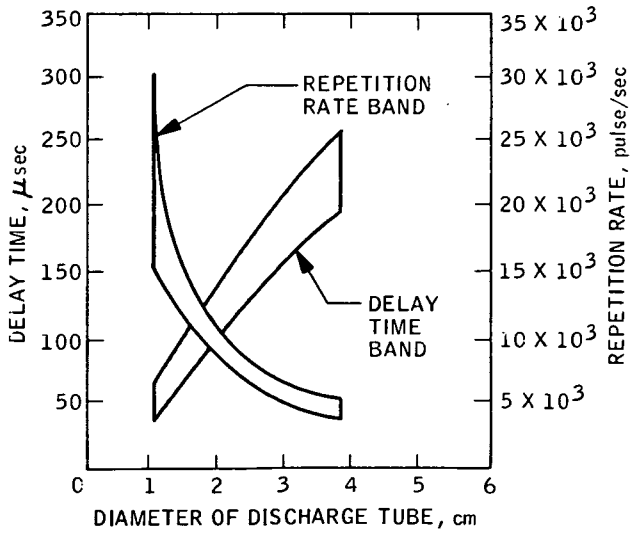

Figure 3.– Delay time and repetition rate as a function of laser tube diameter.

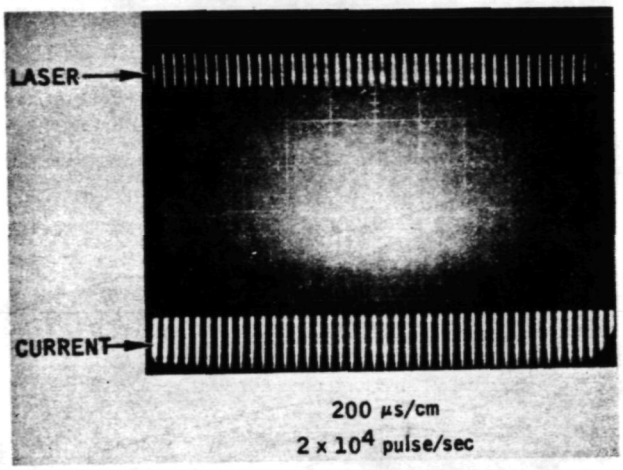

Figure 4.– Oscillogram of current and laser pulses.

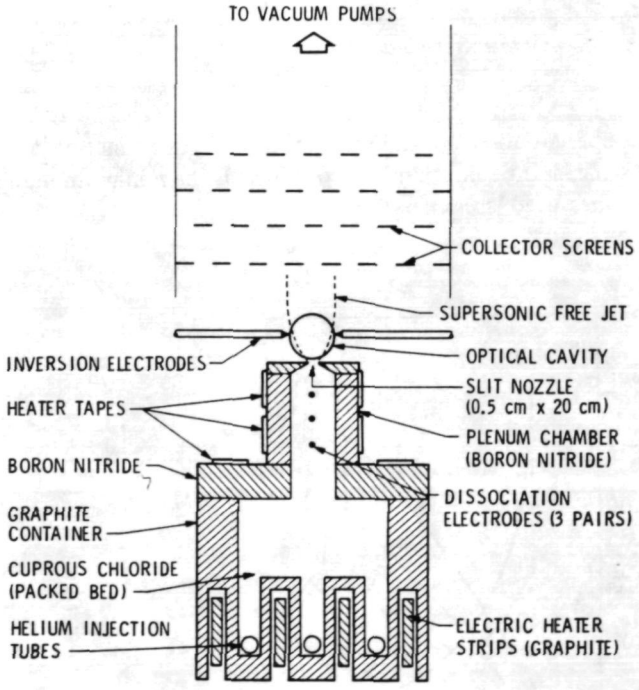

Figure 5.– Schematic of supersonic copper chloride laser.

DISCUSSION

Tom Karras, General Electric Co. – You mentioned an average power of 0.7 W. Was that per unit volume?

Gary Russell: Yes 0.7 W/cm^3.

Tom Karras: Thus the 30 W comes from a 40 cc system?

Gary Russell: Right.

Ned Rasor, Rasor Associates: – Would a pure copper vapor laser be more efficient, that is, does dissociation take much of your power?

Gary Russell: In the double-pulsed experiments we were surprised that, under certain conditions, the dissociation pulse could take up to ten times the laser pulse energy. But when you continuously pulse it, as we are doing here, the chemical recombination time is so much slower that you don't have to start over every time. So you have a very small amount of energy being used for dissociation in each pulse, that is, just enough to make up for the small amount of recombination between pulses.

Tom Karras, General Electric Co. – Just a comment. For our stationary copper vapor system our numbers are very comparable.

Gary Russell: Yes. I should also mention that the chlorine just acts like a buffer gas. Our theory indicates that it influences the discharge a little, but it doesn't enter kinetically in any way.

Ernest Brock, Los Alamos Scientific Lab. – Not to detract from your 1 percent efficiency here, but what do you have in mind for pulsing to higher efficiencies?

Gary Russell: I would say an upper bound in a static system is 10 percent. We are shooting for somewhere between 1 and 3 percent. In the flowing systems, the small systems are going to be inefficient because you can't pulse many times in flow. If you go to a large enough system, however, say a 100 kW system, 1 J per pulse, then the volume would be large enough so that you can discharge many, many times in the flow in addition to the one dissociation pulse. You are then back in the same kinetic situation as you are in the static tubes where the dissociation losses are small compared with the lasing losses. So with the flowing system, when it's made large, and if the aerodynamic problems are not severe, I would say we should approach 1 percent efficiency.

Mark Wrighton, M.I.T. – Have you considered using volatile metal compounds such as tetraethyl lead which can photalyze at room temperatures to give metal atoms?

Gary Russell: No we haven't since the copper chloride and lead chloride work so well. One thing we must keep in mind in the static systems is that you don't necessarily want to go to too low temperatures since you want to conduct waste energy out of the tube.

Abe Hertzberg, University of Washington – Gary, I want to compliment you on a fine piece of work. When I see people struggling with improving the efficiency of their argon ion lasers to the levels you are starting from, it only indicates how much of an accomplishment it is.

TUNABLE HIGH PRESSURE LASERS

R. V. Hess

Langley Research Center, NASA

SUMMARY

Atmospheric transmission of high energy $C^{12}O_2{}^{16}$ lasers can be considerably improved by high pressure operation which, due to pressure broadening, permits tuning the laser lines off atmospheric $C^{12}O_2{}^{16}$ absorption lines. Pronounced improvement is shown for horizontal transmission at altitudes above several kilometers and for vertical transmission through the entire atmosphere. NASA missions for laser energy transmission through the atmosphere have important spin-offs to closely related missions in remote atmospheric sensing. Initial efforts in tuning high pressure CO_2 lasers are discussed and future research is outlined which is vital to NASA missions and national goals such as isotope separation.

INTRODUCTION

Within the last 5 years, new types of high energy gas lasers were developed which, because of operation at high pressures, have the potential of producing tunable laser radiation by tuning across pressure broadened lines. The initial efforts of these so-called Transversely Excited Atmospheric, or TEA lasers, concentrated mostly on their importance as high energy density devices, but recently efforts have been initiated at several laboratories to explore their tunability. These efforts are of great importance to diverse applications (fig. 1) such as atmospheric energy transmission, with subsequent energy conversion, as well as remote atmospheric sensing, optical radar, isotope separation, and photochemistry.

Rather than giving a broad survey of the field, I will first discuss in-house theoretical feasibility studies for applications of tunable high pressure CO_2 lasers to energy transmission and, briefly, to remote sensing; the latter is discussed in more detail in an NASA publication by Hess and Seals (ref. 1). It will be shown that for these important NASA missions, the requirements for high pressure and tunability are not severe. Subsequently, I will give a brief review of the tuning characteristics and design requirements of high pressure lasers which form, respectively, part of a broad NASA basic research grant with Prof. Javan and a Langley contract with Plasma Physics Corp.

ATMOSPHERIC TRANSMISSION OF TUNABLE HIGH PRESSURE $C^{12}O_2{}^{16}$ LASERS

The importance of tunable $C^{12}O_2{}^{16}$ lasers for increasing atmospheric laser transmission is shown in figure 2 for the P(20) laser line centered at 10.5911 μ. As indicated by the reduction in calculated absorption coefficient, the advantage in tuning off the line center increases with altitude. Since the absorption coefficient k in km^{-1} is related to the transmittance τ through

$$\tau = e^{-\int_0^L k d\ell}$$

it is representative of horizontal transmittance without having to specify the length L over which the transmittance occurs. As indicated by the reduction in calculated absorption coefficient, the advantage in tuning off the line center increases with altitude due to reduction in pressure broadening with altitude.

All the calculations presented here have been performed using our line-by-line absorption and transmission computer program, including gases such as H_2O, CO_2, O_3, N_2O, CO, CH_4, SO_2, NH_3, NO, HCℓ and continuum absorption for H_2O and N_2 from studies by McClatchey, *et al.*

For NASA missions of energy transmission to or from space it is of special interest to plot the vertical transmittance of the tunable high pressure $C^{12}O_2{}^{16}$ laser from an altitude h through the entire atmosphere vs frequency $\nu-\nu_o$ from line center. Figure 3 indicates that the transmittance from h = 0 (ground) and h = 2.5 km or 6.5 km (mountains or aircraft) can be considerably increased by tuning 5 GHz off the line center. However, by positioning the laser at moderately high altitudes of h = 2.5 and 6.5 km, even half this tuning range yields large vertical transmittance which should be useful for various applications of laser energy transmission. The reason is that at these moderate altitudes the absorption by H_2O vapor is sufficiently reduced so that great benefits are derived by tuning off the center of atmospheric CO_2 lines.

The pressures required to accomplish this tuning are not very high as seen from the following. In order to tune 5 GHz off the line center, a CO_2 laser line $\geqslant$ 10 GHz is required since the centers of the laser line and the atmospheric CO_2 absorption line coincide. Since the line broadening per atmosphere pressure is $\simeq$ 3 GHz, a laser pressure $\geqslant$ 3 atm would be needed; however, even half this pressure would be sufficient for a large improvement in transmittance. It is further shown in reference 1 that for vertical transmission and for transmission at moderately high altitudes, tuned $C^{12}O_2{}^{16}$ lasers compare favorably with $C^{12}O_2{}^{18}$ –, CO–, DF–, and HF–lasers.

Since, only moderately high pressures are required to provide sufficient tuning for considerably improved transmission, the possibility of operating continuous wave (CW) CO_2 lasers at pressures of $\simeq$ 2 atm needs to be investigated. The feasibility of operating CW CO_2 lasers at atmospheric pressures without the use of preionization is indicated in references 2 and 3. Recent discussions with Dr. George Sutton indicate that AVCO Everett has operated an E-Beam preionized CW CO_2 laser at pressure of $\simeq$ 1 atm and that CW operation at higher pressures may be possible.

Possible advantages of pulsed operation for control of nonlinear effects have been discussed with Dr. Gebhardt from United Aircraft and Dr. Sutton from AVCO Everett. Dr. Gebhardt indicates that thermal blooming can be reduced by multi-pulse operation instead of CW operation, using for experimental studies a TEA laser with photo-preionization. Dr. Sutton suggests improvement of vertical atmospheric transmission through bleaching of atmospheric CO_2 requiring very high pulsed laser fluxes. This involves positioning the CO_2 laser at moderately high altitudes, for reduction of H_2O vapor effects, as also indicated for the tuned high pressure laser transmission, discussed here in some detail.

It is concluded (fig. 4) that the development of pulsed and CW high pressure CO_2 lasers could be vital to NASA energy conversion missions and, of course, also to non-NASA missions requiring atmospheric transmission. It should be further pointed out that presently strong efforts are being made to resolve the comparative advantages of CW and pulsed transmission. Tuned pulsed lasers, because of low average power requirements, may also offer promise for near term evaluation of atmospheric transmission experiments into space or from space between Earth and aircraft, balloons, satellites, or shuttle. A possible cost reduction may be achieved by combining transmission experiments with related experiments in remote sensing, optical radar tracking, and communications, which may also benefit from tunable high pressure pulsed lasers. A strongly related remote sensing experiment is discussed next.

SOME APPLICATIONS TO REMOTE SENSING

In reference 4, a variety of tunable laser applications to remote atmospheric sensing are studied. An especially strong relation exists between transmission problems of tunable $C^{12}O_2^{16}$ lasers and a certain remote sensing technique which has been theoretically evaluated by LaRC (ref. 5) and JPL (ref. 6). This technique, shown in figure 5, is remote sensing by laser differential absorption using diffuse reflection from the Earth. The term differential implies a reference laser "on" the constituent or pollutant absorption line as well as one "off" the line, as in the transmission problem; the difference in atmospheric transmittance is a measure of the pollutant. In its simplest form this technique yields an average concentration over the entire path. Information about the vertical constituent or pollutant distribution can be obtained by tuning across the corresponding absorption lines whose collision broadened widths vary with altitude. The actual vertical distribution is obtained through a mathematical inversion technique. The differential absorption technique can also be used for ranging whereby the signal is backscattered by particulates or molecules in the atmosphere as shown, e.g., by Byer and Garbuny (ref. 7).

Four laser types are being used or proposed (fig. 6) for the IR remote atmospheric sensing techniques used in references 1, 5, and 6: (1) select frequency CW lasers operating at comparatively low pressures whose wavelength range is extended through use of various isotopes; (2) tunable CW diode lasers, that have the advantage of tunability over a wide wavelength range but operate at comparatively low power of the order of several mW; (3) tunable CW waveguide lasers, that are tuned across pressure broadened lines, but with restricted tuning range because higher pressures require increasingly narrow waveguide tubes (the CW powers of these lasers approach several watts); and (4) the high pressure tunable lasers which have the potential of overcoming these limitations. Since they can be operated at very high pressures their tuning range can be considerable for any particular lasing gas. In order to increase the tuning range over the entire infrared the alternative exists of using different lasing gases, frequency multiplication (as discussed by Dr. Billman), or nonlinear optical mixing techniques using crystals or gases. Extensive research in these areas is performed by Drs. Byer and Harris at Stanford University, Dr. Garbuny at Westinghouse Research Laboratory, and others. Another promising technique involves laser pumped lasers. The use of high energy pulses increases the signal-to-noise ratio of differential absorption techniques and also permits the use of ranging in remote sensing. These techniques for increasing the tuning range are also vital for isotope separation and photochemistry.

RECENT PROGRESS IN TUNING OF HIGH PRESSURE TUNABLE LASERS

The key requirement for tuning of high pressure/energy pulsed lasers is the production of a uniform lasing medium. For this purpose, electron beams or uv photons from flashlamps or open arc discharges have been used for preionization. Several references to researchers pursuing these techniques are given in reference 1. The use of laser pumped lasers also shows great promise for producing a uniform lasing medium aside from its value in increasing the tuning range.

Tuning high pressure/energy pulsed CO_2 lasers have recently been reported by Alcock (ref. 8), Harris (ref. 9), and Bagratashvili (ref. 10). The lasers in references 8 and 9 are operated at high pressures of 15 atm (fig. 7) where line broadening is sufficient to provide overlapping (ref. 11) and continuous tuning over a wide spectral range; the lasers in reference 10 operate at $\simeq 5$ atm. Alcock performs tuning with a grating (with maximum resolution increased by beam expansion) having spectral resolution $\geqslant 0.2\ cm^{-1}$ and Harris uses an etalon for tuning; personal discussions with O'Neil and Harris indicate a resolution of $\leqslant 0.2\ cm^{-1}$ for the etalon. (Note: $0.2\ cm^{-1}$ corresponds to 6 GHz.) It must be emphasized, though it is now generally recognized, that this resolution does not refer to the actual linewidth of the laser output. The reason is that, for the homogeneously broadened lines of the high pressure laser mode, competition occurs. As a result, the oscillation of one mode depletes the population and channels the energy into this single mode; thus oscillations of other modes, as shown by Goldhar (ref. 12) and Nurmikko (ref. 13), are prevented. Measurements by Nishihara (ref. 14) of line structure in a pulsed atmospheric CO_2 TEA laser, with a high resolution Fabry Perot interferometer, suggests single mode operation with linewidth of the order of 20 MHz. It must be emphasized that for pulsed operation the uncertainty principle, $\Delta\nu\Delta\tau \geqslant 1$, sets a lower limit for the bandwidth; for example, for the 300 nsec pulse duration in reference 14 the bandwidth $\Delta\nu \geqslant 10^7/3 \simeq 3$ MHz. As shown by Stiehl (ref. 15) chirping (frequency sweeping) in a pulsed laser may also influence the true time scale of the pulse and thus influence the bandwidth; however, it may also help in smearing out deviations from homogeneous broadening, thereby encouraging single mode operation. The importance of Stiehl's work lies partly in the fact that he uses laser heterodyning which is needed for high resolution measurements.

Our research plan with Prof. Javan and Plasma Physics Corp. is as follows. A 5-atm pulsed CO_2 laser is being built (fig. 8) which uses uv photo-preionization of seed material, such as propylamine (ref. 16), to produce a uniform lasing medium. Gross tuning will first be performed with a grating; however, much more extensive efforts than heretofore will be made to obtain the mode structure with heterodyning, using Prof. Javan's contact diode at M. I. T. and tunable diode lasers at Langley. Subsequently, finer tuning techniques will be used. This effort should be of great importance for improved atmospheric transmission as well as for remote sensing, optical radar, isotope separation, and photochemistry.

REFERENCES

1. Hess, R. V.; and Seals, R. K.: Application of Tunable High Energy/Pressure Pulsed Lasers to Atmospheric Transmission and Remote Sensing. NASA TMX-72010, Sep. 1974.

2. McLeary, Ross; and Gibbs, W. E. K.: CW CO_2 Laser at Atmospheric Pressure. IEEE J. of Quantum Electronics, Vol. QE-9, no. 8, Aug. 1973, p. 828-833.

3. Nighan, W. L.; and Wiegand, W. J.: Causes of Arcing in CW CO_2 Convection Laser Discharges. Appl. Phys. Lett., Vol. 25, no. 11, 1 Dec. 1974, p. 633-636.

4. Allario, F.; Seals, R. K.; Brockman, P.; and Hess, R. V.: Tunable Semiconductor Lasers and Their Application to Environmental Sensing. The 10th Anniversary Meeting of the Society of Engineering Science. Raleigh, North Carolina, 5-7 Nov. 1973.

5. Seals, R. K.; and Bair, C. H.: Analysis of Laser Differential Absorption Remote Sensing Using Diffuse Reflection from the Earth. Second Joint Conference on the Sensing of Environmental Pollutants, Washington, D. C., 10-12 Dec. 1972. Instrument Society of America, Pittsburgh, 1973. p. 131-137.

6. Menzies, R. T.; and Chahine, M. T.: Remote Atmospheric Sensing with an Airborne Laser Spectrometer. Applied Optics, Vol. 13, Dec. 1974, p. 2840-2849.

7. Byer, Robert L.; and Garbuny, Max: Pollutant Detection by Absorption Using Mie Scattering and Topographic Targets as Retroreflectors. Applied Optics, Vol. 12, no. 7, July 1973, p. 1496-1505.

8. Alcock, A. J.; Leopold, K.; and Richardson, M. C.: Continuously Tunable High-Pressure CO_2 Laser with UV Photopreionization. Appl. Phys. Lett., Vol. 23, no. 10, 15 Nov. 1973, p. 562-564.

9. Harris, N. W.; O'Neil, F.; and Whitney, W. T.: Operation of a 15-atm Electron-Beam-Controlled CO_2 Laser. Appl. Phys. Lett., Vol. 25, no. 3, 1 Aug. 1974. p. 148-151. Plus personal communication.

10. Bagratashvili, V. N.; Knyazev, I. N.; Kudryavtsev, Yu. A.; and Letokhov, V. S.: Frequency Tuning of an e-Beam Preionized High-Pressure CO_2 Laser. Optics Communications, Vol. 9, no. 2, Oct. 1973, p. 135-138.

11. Christiansen, W. H.; Mullaney, G. J.; and Hertzberg, A.: Absorption in CO_2 at 10.6 μ with Rotational Line Overlap. Appl. Phys. Lett., Vol. 18, no. 9, May 1971, p. 385-387.

12. Goldhar, J.; Osgood, R. M. Jr.; and Javan, A.: Observation of Intense Superradiant Emission in the High-Gain Infrared Transmitions of HF and DF Molecules. Appl. Phys. Lett., Vol. 18, no. 5, 1 Mar. 1971, p. 167-169.

13. Nurmikko, A.; DeTemple, T. A.; and Schwarz, S. E.: Single-Mode Operation and Mode Locking of High-Pressure CO_2 Lasers by Means of Saturable Absorbers. Appl. Phys. Lett., Vol. 18, no. 4, 15 Feb. 1971, p. 130-132.

14. Nishihara, H.; and Kronast, B.: An Investigation of the Line Structure of a Helical TEA-CO_2- LASER. Optics Communications, Vol. 5, no. 1, Apr. 1972, p. 65-67.

15. Stiehl, W. A.; and Hoff, P. W.: Measurement of the Spectrum of a Helical TEA CO_2 Laser. Appl. Phys. Lett., Vol. 22, no. 12, 15 June 1973, p. 680-682.

16. Levine, J. S.; and Javan, A.: Observation of Laser Oscillation in a 1-Atm CO_2-N_2-He Laser Pumped by an Electrically Heated Plasma Generated Via Photoionization. Appl. Phys. Lett., Vol. 22, no. 2, 15 Jan. 1973, p. 55-57.

- Atmospheric energy transmission and remote sensing
  - In-house theoretical feasibility studies
  - Tuning and design of high pressure CO_2 laser, Prof. Javan and Plasma Physics Corp.
- Optical radar
- Isotope separation, photochemistry

Figure 1.– Application of high pressure tunable lasers.

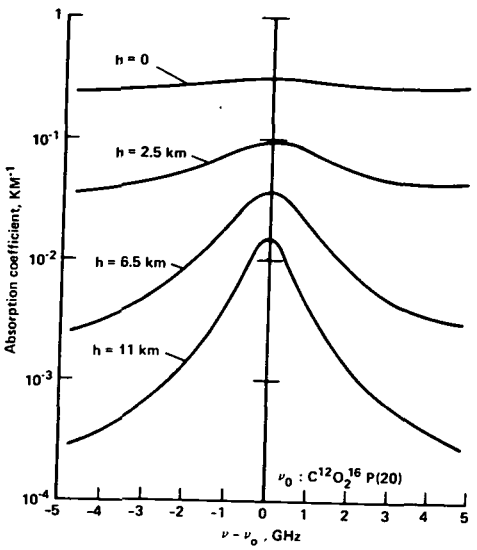

Figure 2.– Calculated frequency variation of absorption coefficient with altitude.

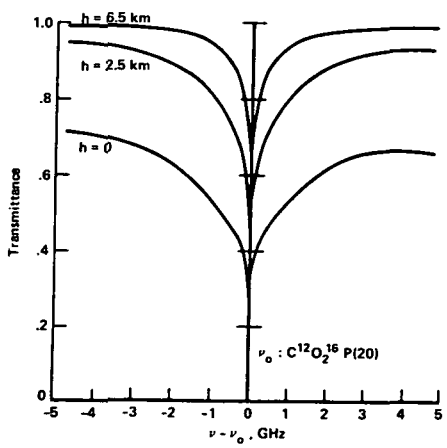

Figure 3.– Calculated frequency variation for tunable $C^{12}O_2{}^{16}$ laser for vertical transmittance from various altitudes.

- Could be vital to NASA – and other agencies
- Offer promise for near term evaluation of transmission experiments between Earth/aircraft, balloons, shuttle
- Possible cost reduction by combining with related experiments
  - Remote sensing, optical radar tracking, communications

Figure 4.– High pressure/energy tunable CO_2 lasers for atmospheric transmission.

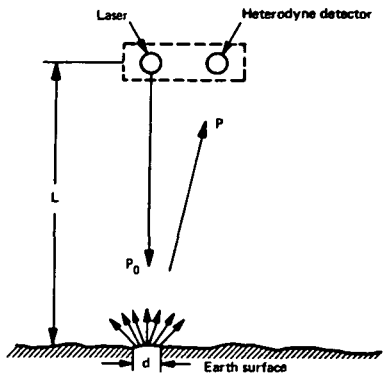

Figure 5.– Laser differential absorption with diffuse reflection from earth.

- Select frequency lasers, wavelengths extended through isotopes
- CW tunable diode lasers, wide tuning range, low mW powers
- Tunable CW waveguide lasers, tuning restricted by pressures in narrow tubes, power approach several watts
- High pressure tunable lasers, wide tuning range due to high pressures and nonlinear optical mixing

Figure 6.– Four laser types proposed for IR remote sensing.

- Experiments at ~15 atm, line overlapping
  - Tuning with grating and etalon, resolution ~0.2 cm^{-1} = 6 GHz
- Resolution does not refer to laser linewidth
  - Homogeneous broadening channels power into single mode
  - High resolution Fabry Perot suggests single mode, linewidth ~20 MHz
- Pulsed operation bandwidth ⩾ 1/pulse duration from uncertainty principle
- Heterodyning needed for high resolution

Figure 7.– Tuning of high pressure/energy pulsed laser.

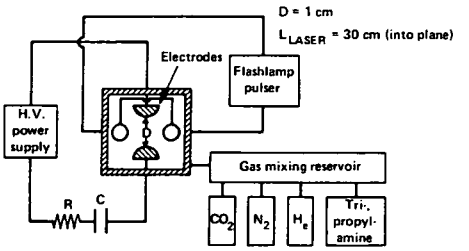

Figure 8.– High energy/pressure pulsed CO_2 laser with photo-preionization.

DISCUSSION

Charles Chackerian, NASA Ames Research Center – If you are concerned with atmospheric transmission, why isn't it better to use an O^{18}–CO_2 laser?

Answer: We have compared this but $CO_2{}^{18}$ is more expensive, especially in military use.

Max Garbuny, Westinghouse – What total tuning range could you obtain with CO_2?

Answer: If you use overlapping, which occurs at about 10 atmospheres, you can tune essentially from 9 to 11 μ. With doubling, tripling, and harmonic mixing with CO and HF frequencies, you can span the entire infrared range. For example, people at Los Alamos are attempting to get to 15 or 16 μ.

Dick Pantell, Stanford University – I don't understand why the homogeneity of the line broadening is going to discourage other modes. For example, in ruby or glass, which are essentially inhomogeneously broadened at room temperature, oscillation in one mode doesn't deplete oscillation in other modes because they occupy different spatial regions. Do you think the same thing would happen here?

Answer: There is some of this spatial hole burning. But that occurs when a crest of the oscillation of the laser meets with a node. By proper positioning of the laser, and proper phasing, you can reduce that. CO_2 lasers have been known to work very well on a single mode. In addition, some tricks can be performed by proper positioning of the laser. Some moderate amount of chirping, for example, can smooth this out also. We are looking into all of these things. With a heterodyning detector we are going to look to see exactly what we have.

Abe Hertzberg, University of Wahington – I would like to comment on chirping. I believe we are just beginning to understand that you cannot have a short pulse laser, with any bandwidth, without chirping. In fact, no mode-locked laser operates unchirpped.

NUCLEAR PUMPED GAS LASER RESEARCH

K. Thom

NASA Headquarters

A nuclear-pumped gas laser is excited by the interactions of energetic particles from nuclear reactions with a laser gas. Such nuclear reactions can be of various natures, such as fission in a nuclear chain reaction, or radioactive decay resulting in fast particles, for example, from polonium 210. For practical reasons, I confine my discussion to the nuclear pumping of lasers by fission-fragments from nuclear chain reactions, because this mechanism promises to result in the highest laser power level. The NASA work on the nuclear pumped laser has evolved as a sideline of plasma core nuclear reactor research, in the course of which it was realized that a fissioning gaseous medium should emit em radiation in a nonequilibrium spectral power distribution and, hence, provide the basic conditions for lasing.

In principle, the conversion of fission-fragment kinetic energy into laser light is the direct conversion of nuclear energy into work in a controlled fashion. It is a breakthrough in the usage of nuclear energy, avoiding thermalization and the employment of a thermodynamic cycle with all its limitation of efficiency and temperature tolerances.

Nuclear pumped lasers are only a few months old. On 2 October 1974, NASA announced a nuclear pumped helium-xenon laser (ref. 1) and the Sandia Corporation announced a nuclear pumped carbon monoxide laser on 11 October 1974 (ref. 2). The efficiency in both of these experiments is quite low, if one relates the laser power with the power of the nuclear reactor that provides the neutron fluxes needed to induce the nuclear pumping. However, when one envisions nuclear power stations in space, that beam their power via laser beams to customers at various locations – to other spacecraft for propulsion or onboard power, to lunar bases for industrial processing, and, perhaps, back to Earth for utilization of power without pollution and hazards – a direct-pumped nuclear laser system need not be very efficient to be competitive with laser systems that involve more conventional pumping methods, and whose power is derived from the conventional conversion of nuclear heat into electricity. One can easily see that an efficiency of a few percent would already establish a quite attractive system, in addition to the potential of significant savings of mass and cost.

A schematic of the NASA experiment (ref. 3) is shown in figure 1. The Sandia experiment is somewhat different in the geometrical configuration, but very similar in its functional components.

In figure 1, one sees basically an arrangement in which fission fragments are produced and are made to interact with a gas for studying optical radiation. Fission reactions occur in a foil of enriched uranium by neutron capture and a good part of the fission fragments can escape from the foil and penetrate into the gas inside a laser tube. In the NASA experiment, a mixture of 1 part xenon in 20 parts of helium at 300 torr pressure lased at a wavelength of 3.5 μ, during a pulse of about 0.1 msec. The integrated energy at these first experiments was about 10 mJ, measured by means of a gold-doped germanium detector, 10 m away from the laser. The laser beam was bent three times by 90° in order to locate the detector behind heavy shielding against nuclear radiation from the reactor.

Left in the figure is the Los Alamos "Godiva" fast burst reactor, the origin of the neutrons that cause the fissions in the uranium coating in the laser tube. In this device, two half-critical masses of enriched uranium 235 are pneumatically shot into each other, whereupon the machine becomes supercritical and starts a chain reaction, running up to 10,000 MW of power. The system expands immediately by heat, thus slightly increasing its surface. In that moment, enough neutrons can escape to interrupt the chain reaction and shut down the reactor. Only a very small fraction of the nuclear fuel is burned, but nevertheless about a megajoule of energy is released – which makes the fraction of a joule of laser light that comes out of the laser tube, indeed, appear to be a very poor effect.

Figure 2 shows the Godiva reactor as a handsome little research machine, which it is, as long as one stays far away from it at operation. Also seen is a little laser tube, wrapped in a polyethelene moderator.

Looking back at figure 1, one recognizes immediately the reason for the very low efficiency of this arrangement. Only the neutrons of the reactor are used for the nuclear pumped laser experiment, and those neutrons, particularly when moderated, carry practically no power. What is needed, apparently, is to combine the laser tube and the reactor into one unit, that is, to make the laser tube nuclear critical, or, in other words, to make a gaseous core reactor that lases.

If everyone would be entirely biased and perfectly objective, and if he thus could see things as I do, he would immediately join us in the research on nuclear-pumped lasers and the related gaseous fueled reactors!

Gaseous core reactor research is well underway under a NASA interagency agreement with the Los Alamos Scientific Laboratory.

As mentioned before, the nuclear-pumped laser research is closely connected with this gaseous core reactor work. In the following, only our experimental program on nuclear lasers will be discussed. We plan to test a high pressure xenon laser for nuclear pumping with the Godiva. Before we achieved lasing with the helium-xenon mixture, numerous luminosity measurements were conducted which indicated that the generation of light by fission-fragment, gas-atom interactions increases with shorter wavelength. Because of insufficient instrumentation, we could not yet make measurements in the uv spectrum. However, we suspect that most of the conversion of fission-fragment energies into light occurs in the ultraviolet. Colleagues of the JPL will hopefully soon be ready to join our friends at the LASL in conducting nuclear-pumped, high pressure xenon experiments.

When increasing the pressure, the fission-fragment stopping distance will eventually become smaller than the diameter of the laser tube diameter. In that case, the technique of using an uranium foil inside the laser tube becomes less effective. Instead of a surface source of energetic nuclear particles, a volume source must be used (ref. 5). One possibility is an admixture to the laser gas of He^3, which upon the capture of a neutron undergoes the reaction He^3 (n T)p, where the triton and proton carry about 700 keV energy. From other laser systems it is known that helium will not quench lasing in certain systems. Another option for a volume source of energetic nuclear particles would be enriched uranium hexafluoride that undergoes fission in a neutron bath.

UF_6 may quench laser action, because of its many degrees of internal freedom; perhaps it does not do so, however, and instead may offer many lasing opportunities. This is a subject of forthcoming research.

For the research involving enriched UF_6 and He^3, we have shipped our ballistic piston compressor from the University of Florida to Los Alamos. This compressor and the Godiva reactor seem to be an ideal match to produce, for a fraction of a millisecond, all conditions that one possibly could desire for nuclear-pumped laser research: the cannon will compress gas mixtures to almost any degree of needed density and temperature. A schematic of this cannon is shown in figure 3. Very fortunately the free flying piston in this device, an old 50 mm Navy gun barrel, is driven by compressed air and not by gun-powder; had the latter been the case, the reactor people of LASL would have let the gun not come near the Godiva! Sometime in the near future we will compress enriched UF_6 or He^3 in the cannon and expose it to the high neutron flux from the Godiva reactor. The high neutron fluence combined with the large uranium particle density should give us an estimated 1000 joules of fission energy generated in the gun!

A good faction of this energy could be converted into laser light. Or that part of this energy could be used to recharge the air compressor – such that the machine would run like a Nuclear Otto Engine!

REFERENCES

1. NASA RELEASE NO. 74-269, Sanchez, Gerald; Nuclear Source Converts Directly into Laser Light. 2 Oct. 1974.

2. Sandia Laboratories News Release, 11 Oct. 1974.

3. Helmick, H. H.; Fuller, J. L.; and Schneider, R. T.: Direct Nuclear Pumping of a Helium-Xenon Laser. Appl. Phys. Lett., Vol. 26, no. 6, 15 Mar. 1975, p. 327-328.

4. Schwenk, Francis C.; and Thom, Karl H.: Gaseous Fuel Nuclear Reactor Research. Frontiers of Power Technology, 9-10 Oct. 1974. Energy Environment and Engineering, Oklahoma State University Extension, College of Engineering.

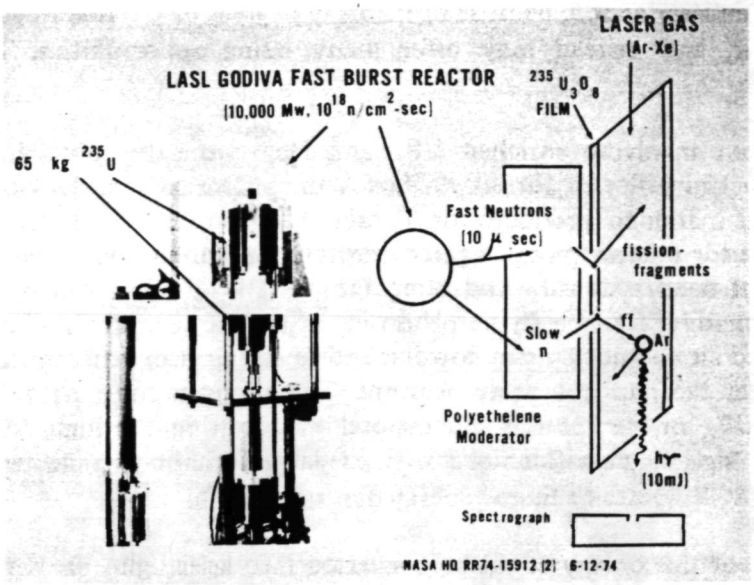

Figure 1.– Nuclear pumped laser research.

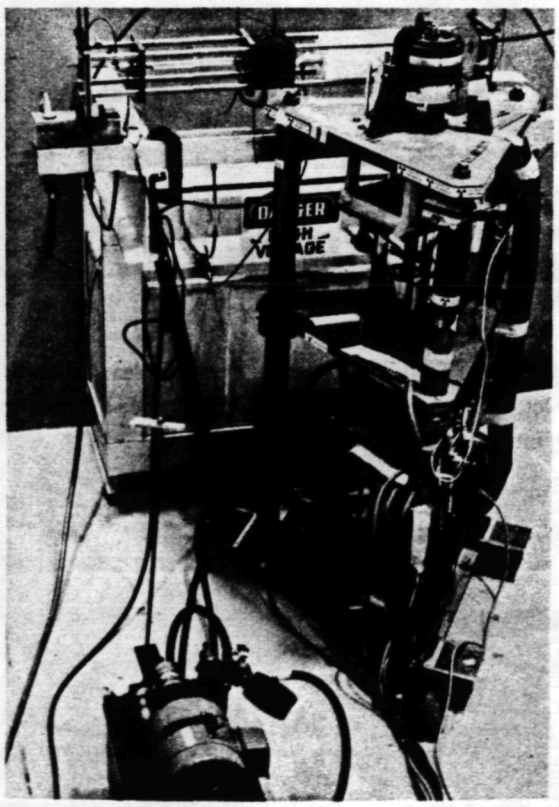

Figure 2.– The "Godiva" reactor.

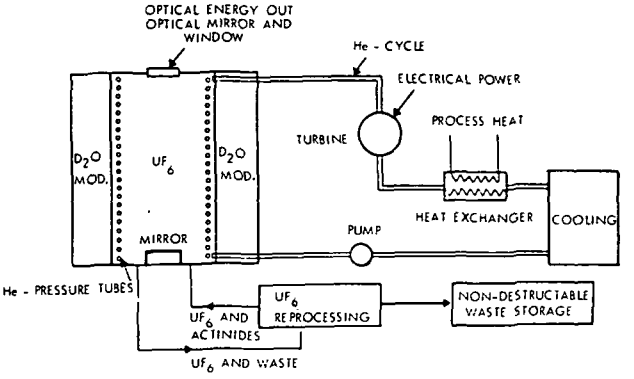

Figure 3.– Nonequilibrium nuclear reactor system.

DISCUSSION

Abe Hertzberg, University of Washington – Karl, even though I'm very impressed with the success of these experiments, all those nuclear radiation signs on the apparatus tend to keep me at arms length!

Stuart Bowen, Stanford University – Are the pumping requirements of this device in any way compatible with the usage of reactor nuclear waste material? That is, can the waste actinides, etc., be used for this?

Answer: No, we wouldn't pump with it – we would hope to put it back into the reactor and burn it. The trans-uranium actinides, of course, are fissionable.

Abe Hertzberg, University of Washington – But that's not really connected with your laser. What you're indicating, of course, is that if you could build a UF_6 gas core reactor, you could recycle some of these wastes?

Answer: Yes.

Dick Stirn, J. P. L. – What is your feeling about the materials problems of mirrors, etc., at these high radiation levels?

Answer: It may be a big problem. Of course we might use aerodynamic windows and there are other ways of promoting self-anealing of materials. Such work at United Aircraft showed that some radiation damage can be self-anealed by heat. There are various possibilities.

Abe Hertzberg, University of Washington – What mixture did the group at Sandia use?

Answer: They used carbon monoxide. We believe we have to go to high pressure xenon to get better efficiency and shorter wavelength.

Abe Hertzberg, University of Washington – Have you made any calculations of what are the possible efficiencies of such a system?

Answer: Many attempts have been made. However, the problem is that the real cross sections involved are not known. Our approach will be to measure some of these and then use them to assist the theory.

THERMO ELECTRONIC LASER ENERGY CONVERSION*

Lorin K. Hansen and Ned S. Rasor

Rasor Associates

INTRODUCTION

At the first symposium on laser energy conversion it was suggested (ref. 1) that an energy converter introduced more than a decade ago by Waymouth (ref. 2) might be used for the conversion of laser energy to electrical power. The present paper reports a preliminary study undertaken to determine the expected performance of such a device, and to better define inherent problems.

The Waymouth converter is closely related to the cesium vapor thermionic converter. For the laser converter, it is helpful to keep both devices in mind for comparison. The basic operation of the thermionic converter is described first. The potential distribution and essential geometry of the conventional thermionic converter are shown in figure 1a. The electrodes have about equal areas. Heat supplied to one electrode is absorbed by thermionic emission of a high current of electrons at the emitter temperature. The electron gas in the interelectrode plasma is then heated to a higher temperature through bombardment by the electrons from the emitter which have been accelerated across the plasma sheath V_E at the emitter.

Part of this investment of energy in the plasma is then extracted as the electron gas is cooled when it surmounts the sheath barrier V_C and reaches the collector. The remaining thermionic energy is dissipated in the arc drop V_d required to produce the positive ions which sustain the plasma. The asymmetry required to obtain a net electron flow through the plasma arises because of the thermionic emission at the emitter and because the higher sheath barrier at the emitter blocks the electron gas from returning to the emitter. The total output current is limited primarily by the saturation emission current from the emitter. Output voltage is limited by the arc voltage drop V_d needed to sustain the plasma and by the contact potential difference ($\phi_E - \phi_C$) between the converter electrodes.

Cesium vapor is used in the conventional thermionic converter since its low ionization potential minimizes the arc drop V_d, and its adsorption on the electrode surfaces gives sufficiently low values of the electrode work functions ϕ_E and ϕ_C. About 25 percent of the original energy delivered to the electrons is delivered as electrical power to the external circuit. The remainder is dissipated in the arc drop (~15 percent) and in the collector (~60 percent).

Figure 1b shows the essential geometry and potential distribution for the originally-described Waymouth converter. This device is similar to the thermionic converter except that the primary energy input is directly into the plasma instead of through the emitter. As in the thermionic converter, the hot electron gas in the plasma (heated by rf in Waymouth's demonstration) is cooled

*Supported by NASA-Ames Research Center, Moffett Field, California

by collection across a large collector sheath V_C. The asymmetric flow of the electron gas into the collector is obtained by having the emitter area much smaller than the collector area. The collected electrons are replaced by thermionic emission from the emitter. Waymouth experimentally demonstrated an overall energy conversion efficiency of 36 percent with a plasma electron temperature T_e corresponding to an average electron energy $kT_e \simeq 2$ eV. He estimated this would approach 55 percent at higher electron temperatures.

The thermo electronic laser energy converter (TELEC) considered here is essentially a Waymouth converter with the input energy supplied by a high energy laser beam. It is shown that the constraints of this application cause the operating conditions for the TELEC to be substantially different from those envisioned by Waymouth and, in fact, that these conditions more closely approach those for the thermionic converter. The geometry for this initial examination is concentric cylindrical electrodes with the laser energy introduced axially as shown in figure 2.

The calculations and results of this study are only outlined here. Further details are described in a technical summary report (ref. 3).

RADIATION BALANCE

The description of a TELEC device requires a detailed examination of the processes of laser absorption in the interelectrode plasma and of the processes of subsequent re-radiation of this energy. The only radiation considered here is the 10.6-μ line of the CO_2 laser. The dominant laser absorption processes are electron-ion and electron-neutral inverse bremsstrahlung. The latter process dominates when there is a significant presence of neutrals. Radiation from the plasma is a very complicated process involving line radiation from specific transitions, continuum radiation from radiative recombination, and finally bremsstrahlung radiation. Both hydrogen and cesium are considered as candidate gases to determine the dependence of the results on ionization potential.

The calculation of laser absorption in hydrogen is based on the extensive work of Stallcop (ref. 4). The analytical results for hydrogen plasma excitation and radiation processes obtained by Bates, Kingston and McWhirter (ref. 5) and by McWhirter and Hearn (ref. 6) are also used here.

Approximate formulas of Stallcop (ref. 7) are used to calculate laser absorption in cesium. The results of Norcross and Stone (ref. 8) are used for the radiation properties of the cesium plasma.

Some results for the absorption and radiation characteristics for hydrogen plasmas (without electron cooling or heating) are shown in tables 1 and 2, and corresponding results for cesium plasmas are shown in tables 3 and 4. In the tables, the following quantities are shown as functions of plasma density n_e (cm^{-3}) and electron temperature $\hat{T}_e$ (°K):

f ~ degree of ionization

P ~ total pressure (torr)

R_A ~ atomic (line, recombination) radiation intensity, W/cm^3

B_B ~ bremsstrahlung radiation intensity, W/cm^3

R_t ~ total radiation intensity, W/cm^3

K_{en} ~ absorption coefficient due to neutral atoms, cm^{-1}

K_{ei} ~ absorption coefficien due to ions, cm^{-1}

K_t ~ total absorption coefficient, cm^{-1}

Q_m ~ input radiation intensity required to maintain an isolated plasma, W/cm^2

From the calculations of radiation balance it is evident that high plasma densities ($n_e > 10^{15}$ cm^{-3}) are required to obtain reasonable stopping lengths ($1/K_t < 10$ m). It is also evident that the laser flux required to achieve this plasma density is very high for cesium ($\gtrsim 10^4$ W/cm^2) and is generally one to two orders of magnitude higher for hydrogen. For this reason, a detailed TELEC performance analysis is made only for cesium. These results show that for a significant presence of neutrals, electron-neutral inverse bremsstrahlung is the dominant absorption process, and line radiation is the dominant radiation from the plasma. For essentially fully ionized plasmas, electron-ion inverse bremsstralung is the dominant absorption process and recombination is the dominant plasma radiation process.

An important consequence of the high plasma density needed for stopping the laser beam in the TELEC is the possibility of significant effects arising from loss of ions to the electrodes. The energy required to produce these ions is potentially a serious energy loss in the TELEC. The maximum currents possible (twice the random ion current) are shown in figure 3. Actually, the ion losses will be substantially less than indicated in figure 3. The ion-atom scattering cross section is very large in cesium due to resonance charge exchange. The diffusion of ions to the electrodes therefore will be greatly impeded in the presence of neutral atoms. This is true even for fully ionized plasmas since ions which leave the plasma return as atoms, causing large ion density gradients and reduced ion currents near the electrodes. If necessary, ion currents can be reduced still further by the use of a background gas, such as argon, that has a large ion scattering cross section but a low electron scattering cross section. Since a detailed calculation of ion losses is quite complex, and since it is estimated that the resulting effects can be neglected for a first approximation, these effects are not included in the following TELEC performance estimates.

DESCRIPTION OF TELEC OPERATION

In order to calculate the performance characteristics of the TELEC it is necessary to develop analytical expressions for the various converter phenomena. These expressions, given in detail in reference 3, involve the following processes:

1. Plasma particle transport phenomena involving both electron-neutral and electron-ion interactions.

2. Sheath phenomena at the plasma boundary based on particle flux conservation.

3. Emission and work function effects for surfaces with absorbed cesium.

4. Emitter thermal balance involving black-body radiation, plasma radiation and electron cooling.

5. Plasma ionization and multiple component ideal gas behavior.

6. Overall energy balance

To these must be coupled the plasma radiation and absorption effects discussed above. This large system of simultaneous, nonlinear, analytical expressions is solved simultaneously to obtain solutions for all descriptive parameters of the device at various operating points.

Figures 4 through 8 show the electrical output characteristics and efficiency η of TELEC operation calculated for a variety of design variables. because of the very large number of variables, the complexity of the calculations, and the absence as yet of clearly-defined engineering and system constraints, it has not been possible to establish an optimum region of operation. The set of operating conditions for figure 4 are therefore chosen somewhat arbitrarily as a specific reference case for illustration of approximate magnitude of the variables, and for illustration of the effect of changing each design variable in figures 5 through 8.

DISCUSSION OF RESULTS

Laser-Maintained Plasmas

Figure 9 shows that the laser power required to maintain a constant-pressure plasma at first increases with increasing electron temperature and then decreases as complete ionization is approached. This occurs because the plasma density and atomic radiation increase rapidly as the laser radiation initially heats and progressively ionizes the plasma; but as full ionization approaches, the plasma density becomes constant and the atom-electron inverse bremsstrahlung absorption and atomic radiation rapidly disappear with the disappearance of the atoms. This region near full ionization is the typical plasma condition for practical TELEC operation since it results in minimum converter length and radiation losses for a given energy conversion power density requirement.

Another potentially important aspect of laser-maintained plasmas is that above the maximum in figure 9 the dissipation of laser energy in a constant-pressure, isolated plasma tends to increase faster than the plasma can re-radiate this energy; that is, a fluctuation of the electron temperature upward tends to increase the absorption and thus further increase the electron temperature, and vice versa. This suggests that the absorption process may be unstable and that ionization waves may occur.

Although investigation of this complex phenomenon is beyond the scope of this study, it deserves further attention for the following reasons. First, it could profoundly increase or decrease the absorption length, and therefore could critically affect the feasibility of the TELEC. Second, if

laser radiation can directly drive strong, coherent density waves in a plasma, this could lead to a plasma-laser rf generator which might be superior to the TELEC.

Feasibility of TELEC

Efficiency – Inspection of figures 4 through 8 shows that maximum efficiencies in the region of 30 to 45 percent are computed for a TELEC operating in the vicinity of the arbitrary and therefore probably off-optimum, reference case (fig. 4). In general, it is likely that the operating point of a practical device would be chosen to be at a voltage somewhat less than that for maximum efficiency (~ 2.0 V in fig. 4) since absorption length $L = K_T^{-1}$ (and also device length) is significantly smaller at lower voltages. In fact, if system weight is more important than efficiency, optimum operation would tend toward the point of maximum output power density (12 W/cm^2 at 1.0 V in figure 4, where efficiency is 26 percent).

It is likely that the optimum operating condition occurs at a higher cesium pressure than the 2 torr reference value. As shown in figure 5, doubling the pressure significantly increases the efficiency and power density and about halves the absorption length. Higher efficiencies also are obtained at larger device diameter D_C and higher laser power density Q but, as seen in figures 6 and 7, these changes alone cause a significant increase in absorption length. The shorter abosprtion length can be mostly recovered by increasing the cesium pressure, however.

Electrode materials – The materials parameters used in the analysis represent the present state of practical electrode development in thermionic converters. The value, $\phi_o = 5.0$ eV for the vacuum work function of the emitter, can be readily achieved by available materials (e.g. oriented rhenium, and oxygenated tungsten). Preliminary exploration indicates that this value is near optimum for the reference case. The required emitter temperatures indicated in figures 4 through 8 (that is, 1600 – 1900° K) coincide with the temperature range of thermionic converter operation where similar electrodes have been operated in a substantial number of devices continuously for several years without degradation.

The value $\phi_C = 1.5$ eV is the collector work function which is obtained spontaneously when most structural metals (e.g. nickel, stainless steel, copper, molybdenum, niobium, etc.) are operated in cesium vapor under typical collector conditions. The effect of collector back-emission in the TELEC is not known. However, if the criterion for thermionic converter collector operation applies in this case, the optimum collector operating temperature for $\phi_C = 1.5$ eV would be near 900°K. This is an important consideration for space-power applications because this is near the optimum temperature for small, lightweight radiators constructed of ordinary structural metals.

A substantial program is presently under way to develop lower work function surfaces for thermionic converter collectors. Values of $\phi_C \simeq 1.3$ eV have been observed for several potentially useful materials, and it is hoped that surfaces similar to the 1.0 eV, S-1 commercial photocathode can be developed also for this application. As can be seen in figure 8, the use of a 1.0 eV collector would significantly increase the efficiency of TELEC operation. It should be recognized, however, that this would probably require a significantly low collector (heat rejection) temperature, probably near 650°K.

Absorption length – The absorption lengths occuring in the reference case, that is, of the order of 10 m for 10.6-μ laser radiation, at first seem to be excessive for a practical device. Specifically, this would mean that only about 60 percent of the laser radiation energy would be absorbed in a 10-m long TELEC, with a corresponding reduction in efficiency. Furthermore, a 10-m long TELEC array may be undesirable from structural and weight considerations. However, a reflector at the exit end of the TELEC cylinder (fig. 2), which allowed a second pass through the device, would permit capture of up to about 85 percent of the incident beam energy, or would allow the length of the TELEC to be halved. Further increases in capture efficiency or decreases in length, or both, could be obtained by constructing the TELEC collector as a cavity with mirrors at both ends; the mirrors result in multiple passes of the laser beam through the device.

Laser beam intensities – The incident radiation intensities required for typical TELEC operation at 10.6 μ that is, 10^4 to 10^6 W/cm^2, also may be excessive by present standards. The ability to achieve such intensities is crucially dependent on collector optics, and on the ability to achieve multiple passes of the beam through the device.

It should be recognized that the absorption length and required laser beam intensity are essentially inversely proportional to the square of the wavelength of the incident radiation. Therefore efficient TELEC operation probably is not feasible at wavelengths much shorter than 10.6 μ, and it becomes much more attractive at longer wavelengths.

Alternate sets of design parameters to those in the reference case can be chosen that result in absorption lengths and laser beam intensities an order of magnitude less than those for the reference case, but with significant reductions in conversion efficiency and output power density. It is clear that a system design study is required to evaluate these trade-offs.

Comparison with the Waymouth and Thermionic Converters

It is instructive at this point to examine briefly how operation under TELEC conditions differs from the operation of the Waymouth converter, since the TELEC is more of an "electron superheat" version of a thermionic converter than a Waymouth converter. Figure 10 is a potential diagram illustrating the operating conditions at Point A of figure 4. It can be seen that most of the energy of the hot electrons from the plasma is first delivered to the emitter, rather than to the collector as in the Waymouth converter. The electron energy flow therefore is as follows.

The energy abosrbed from the laser beam by the plasma is mostly transferred to the emitter. The electrons in the emitter absorb $\phi_E + 2\,kT_E$ as they are emitted (evaporate) at temperature T_E. They are then "superheated" to an electron temperature T_e in the plasma by the laser radiation, and absorb an energy $V_C + 2\,kT_e$ from the plasma as they reach the collector. The electrons dissipate $\phi_C + 2\,kT_e$ as reject heat in the collector, and deliver their remaining energy V_o to the external circuit as they are returned to the emitter.

The primary effect of the superheat portion of the cycle is to allow the plasma electrons to surmount a much larger barrier at the collector, and thereby to deliver a correspondingly larger output energy for each unit of heat rejected; that is, at a higher efficiency. From a thermodynamic viewpoint, this extends the Carnot temperature interval from the emitter temperature T_E to the

much higher plasma electron temperature T_e. Since the efficiency of the thermionic energy conversion process is ideally about 60 to 70 percent of Carnot efficiency, the efficiency of such a "superheated" thermionic converter is inherently much greater than that obtainable in the conventional thermionic converter at feasible emitter temperatures.

A design variable which may have a profound effect on TELEC performance is the fraction of incident laser radiation that is captured directly by the emitter, that is, without first being absorbed by the plasma. For the reference case, allowing 15 percent of the laser beam to be directly captured by the emitter causes the overall maximum efficiency to increase from 35 percent to over 42 percent. The basic and engineering implications of operation with the laser energy input divided between the emitter and plasma have not been adequately explored as yet. However, it may be advantageous to supply only the heat to the plasma necessary for the superheat energy and for sustaining the required plasma density to intercept this energy, and to deliver the remainder directly to the emitter.

SUMMARY

Preliminary evaluation suggests that the TELEC concept can potentially convert 25 to 50 percent of incident laser radiation into electric power at high power densities and high waste heat rejection temperatures. Relatively high laser beam intensities (10^4 to 10^6 W/cm^2) and long absorption lengths (1 – 100 m) appear to characterize typical operation with 10.6 μ incident radiation. Detailed system studies, including consideration of collector optics for concentration and multiple passes of the laser beam through the device, and the possibility of longer wavelength laser radiation, are required for assessment of feasibility.

Two important basic aspects of device operation deserve further analysis and experimental evaluation. The possible instability of laser radiation absorption in plasmas under TELEC conditions would profoundly affect the feasibility of the concept, and could possibly lead to direct rf generation by laser radiation in such plasmas. Also, it is possible that interception of most of the laser beam by the emitter, and use of only a small portion to maintain and "superheat" the plasma, may be preferred mode of operation that could result in a substantially higher efficiency than for the reference case studied. Operation in this mode also may significantly relieve some of the design constraints imposed by full beam absorption in the plasma.

Acknowledgement – The authors would like to express appreciation to K. W. Billman for his interest and encouragement and to J. R. Stallcop for helpful discussions on radiation absorption.

REFERENCES

1. Rasor, Ned S.: Thermionic, Plasma, and Photoemission Energy Conversion. Laser-Energy Conversion Symposium, NASA Ames Research Center, Jan. 1973, NASA TM X-62, 269, p. 51-62.

2. Waymouth, J. F.: Electrical Energy from High-Temperature Plasmas. J. Inst. of Electrical Engrs., Vol. 8, no. 92, Aug. 1962, p. 380-383.

3. Hansen, L. K.; and Rasor, N. S.: Thermoelectronic Laser Energy Conversion. Final Summary Technical Report for Contract MAS2-8155, Jan. 1975.

4. Stallcop, James R.: Absorption Coefficients of a Hydrogen Plasma for Laser Radiation. J. Plasma Phys., Vol. 11, Part 1, Feb. 1973, p. 111-129.

5. Bates, D. R.; Kingston, A. E.; and McWhirter, R. W. P.: Recombination Between Electrons and Atomic Ions: I. Optically Thin Plasmas. Proc. Roy. Soc., Vol. A267, no. 1330, 22 May 1962, p. 297-312.

6. McWhirter, R. W. P.; and Hearn, A. G.: A Calculation of the Instantaneous Population Densities of the Excited Levels of Hydrogen-like Ions in a Plasma. Proc. Phys. Soc., Vol. 82, pt. 5, 1 Nov. 1963, p. 641-654.

7. Stallcop, James R.: Absorption of Infrared Radiation by Electrons in the Field of a Neutral Hydrogen Atom. Astrophys. J., Vol. 187, no. 1, pt. 1, 1 Jan. 1974, p. 179-183.

8. Norcross, D. W.; and Stone, P. M.: Recombination, Radiative Energy Loss and Level Populations in Nonequilibrium Cesium Discharges. J. Quant. Spectrosc. Radiat. Transfer, Vol. 8, Feb. 1968, p. 655-684.

TABLE 1. – HYDROGEN LOG $N_E = 15$[a]

Quantity	T_e, °K					
	4000	8000	16000	32000	64000	128000
f	6.04×10^{-13}	4.1×10^{-4}	.938	.9997	1.00	1.00
P	6.86×10^{11}	2.0×10^{3}	3.42	6.63	13.25	26.5
R_A	7.75×10^{4}	2.40×10^{2}	9.28	1.35	.460	2.31×10^{-1}
R_B	8.98×10^{-3}	1.27×10^{-2}	1.80×10^{-2}	2.54×10^{-2}	3.59×10^{-2}	5.08×10^{-2}
R_T	7.75×10^{4}	2.40×10^{2}	9.30	1.38	4.96×10^{-1}	.282
R_A/R_B	8.63×10^{6}	1.89×10^{4}	517	53.3	12.8	4.55
K_{en}	7.70×10^{5}	1.18×10^{-3}	3.05×10^{-8}	9.54×10^{-11}	2.96×10^{-12}	2.74×10^{-13}
K_{ei}	1.2×10^{-4}	4.50×10^{-5}	1.79×10^{-5}	7.34×10^{-6}	3.04×10^{-6}	1.26×10^{-6}
K_T	7.70×10^{5}	1.23×10^{-3}	1.80×10^{-5}	7.34×10^{-6}	3.04×10^{-6}	1.26×10^{-6}
Q_m	1.01×10^{-1}	1.96×10^{5}	5.16×10^{5}	1.84×10^{5}	1.51×10^{5}	1.84×10^{5}

[a]Plasma density

TABLE 2. – HYDROGEN LOG $N_E = 16$[a]

Quantity	T_e, °K					
	4000	8000	16000	32000	64000	128000
f	3.29×10^{-13}	2.44×10^{-4}	.91	.9997	1.00	1.00
P	1.26×10^{13}	3.39×10^{4}	34.7	66.25	132.5	265
R_A	7.28×10^{6}	2.50×10^{4}	8.83×10^{2}	1.25×10^{2}	$4.08 \times 10'$	$2.04 \times 10'$
R_B	8.98×10^{-1}	1.27	1.80	2.54	3.59	5.08
R_T	7.28×10^{6}	2.50×10^{4}	8.86×10^{2}	1.27×10^{2}	$4.44 \times 10'$	25.49
R_A/R_B	8.11×10^{6}	1.97×10^{4}	4.92×10^{2}	4.91 x 10	$1.14 \times 10'$	4.02
K_{en}	1.41×10^{8}	2.0×10^{-1}	4.40×10^{-6}	1.17×10^{-8}	3.27×10^{-10}	2.69×10^{-11}
K_{ei}	1.20×10^{-2}	4.51×10^{-3}	1.79×10^{-3}	7.34×10^{-4}	3.04×10^{-4}	1.26×10^{-4}
K_T	1.41×10^{8}	2.05×10^{-1}	1.80×10^{-3}	7.34×10^{-4}	3.04×10^{-4}	1.26×10^{-4}
Q_m	5.15×10^{-2}	1.22×10^{5}	4.91×10^{5}	1.70×10^{5}	1.34×10^{5}	1.62×10^{5}

[a]Plasma density

TABLE 3. – CESIUM LOG $N_E = 15$[a]

Quantity	T_e, °K				
	2000	4000	6000	8000	10000
f	3.2×10^{-5}	.89	.9986	.9999	1.000
P	6.4×10^{-3}	.88	1.24	1.66	2.07
R_A	4.34×10^{2}	2.626	.572	.244	.138
R_B	6.35×10^{-3}	8.98×10^{-3}	1.10×10^{-2}	1.27×10^{-2}	1.42×10^{-2}
R_T	4.34×10^{2}	2.64	.583	.257	.152
R_A/R_B	6.8×10^{4}	2.92×10^{2}	52.0	19.2	9.72
K_{en}	.120	6.67×10^{-7}	8.92×10^{-9}	9.32×10^{-10}	2.29×10^{-10}
K_{ei}	3.61×10^{-4}	1.20×10^{-4}	6.70×10^{-5}	4.51×10^{-5}	3.34×10^{-5}
K_T	.120	1.21×10^{-4}	6.70×10^{-5}	4.51×10^{-5}	3.34×10^{-5}
Q_m	3.61×10^{3}	2.18×10^{4}	8.71×10^{3}	5.70×10^{3}	4.56×10^{3}

[a]Plasma density

TABLE 4. – CESIUM LOG $N_E = 16$[a]

Quantity	T_e, °K				
	2000	4000	6000	8000	10000
f	3.39×10^{-6}	.43	.98	.998	.9996
P	6.1×10^{5}	13.7	12.5	16.6	20.7
R_A	4.34×10^{4}	2.49×10^{2}	52.0	21.6	12.0
R_B	6.35×10^{-1}	8.98×10^{-1}	1.10	1.27	1.42
R_T	4.34×10^{4}	2.50×10^{2}	53.1	22.9	13.4
R_A/R_B	6.8×10^{4}	2.77×10^{2}	47.3	17.0	8.46
K_{en}	1.135×10^{2}	7.01×10^{-4}	1.08×10^{-5}	1.24×10^{-6}	3.20×10^{-7}
K_{ei}	3.61×10^{-2}	1.20×10^{-2}	6.70×10^{-3}	4.51×10^{-3}	3.34×10^{-3}
K_T	1.136×10^{2}	1.27×10^{-2}	6.71×10^{-3}	4.51×10^{-3}	3.34×10^{-3}
Q_m	3.82×10^{2}	1.97×10^{4}	7.91×10^{3}	5.08×10^{3}	4.03×10^{3}

[a]Plasma density

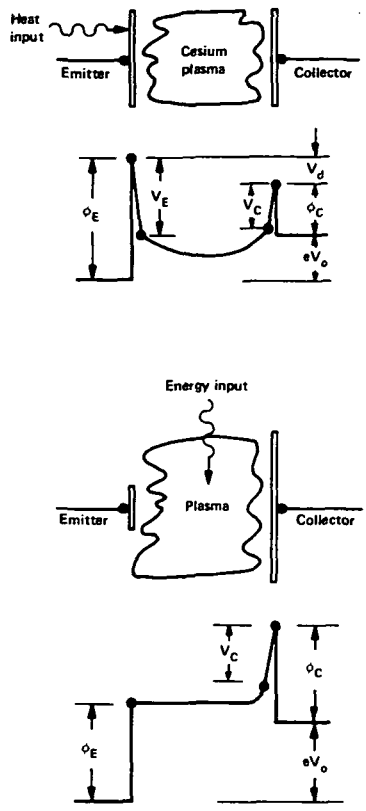

Figure 1.– Geometry and potential distribution.

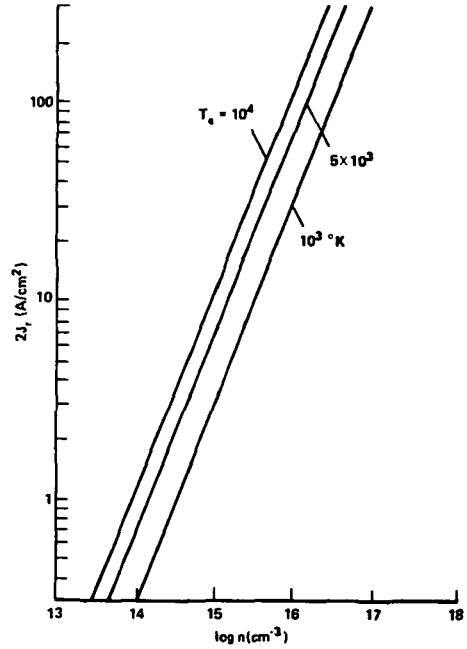

Figure 3.– Twice random ion current.

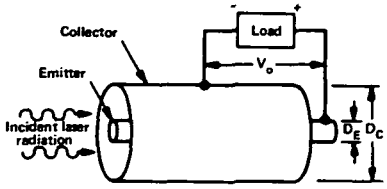

Figure 2.– Elementary TELEC configuration.

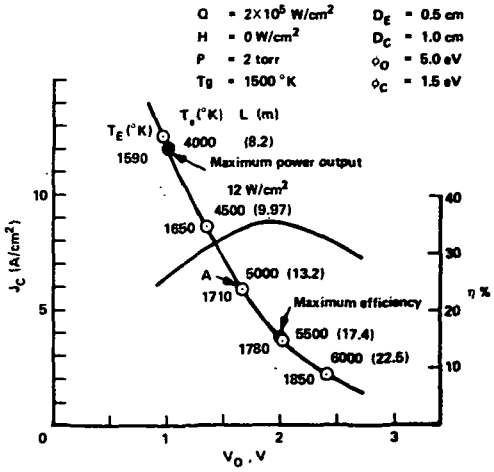

Figure 4.– Electrical output characteristics and efficiency η of TELEC.

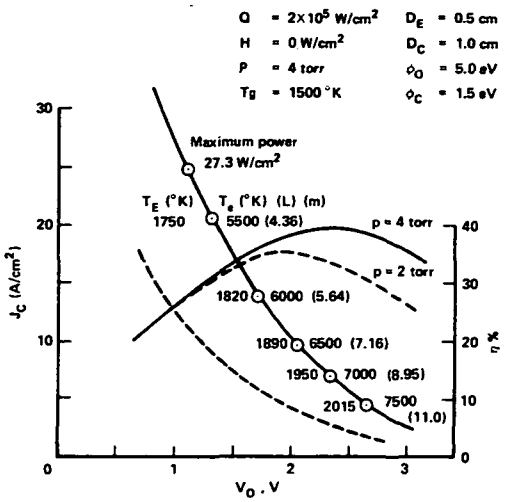

Figure 5.– Electrical output characteristics and efficiency η of TELEC; p = 2 torr.

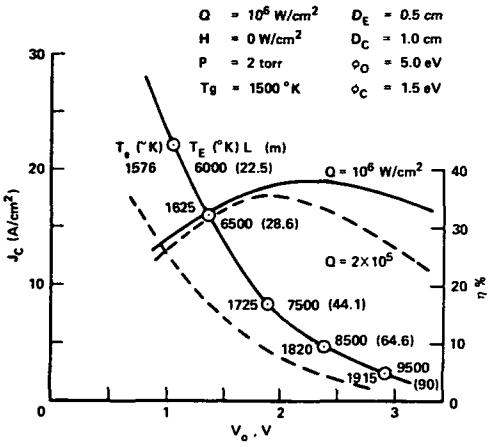

Figure 7.– Electrical output characteristics and efficiency η of TELEC; Q = 10^6 W/cm^2.

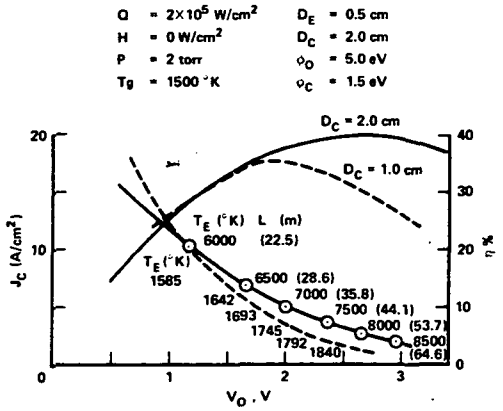

Figure 6.– Electrical output characteristics and efficiency η of TELEC; D_C = 2 cm.

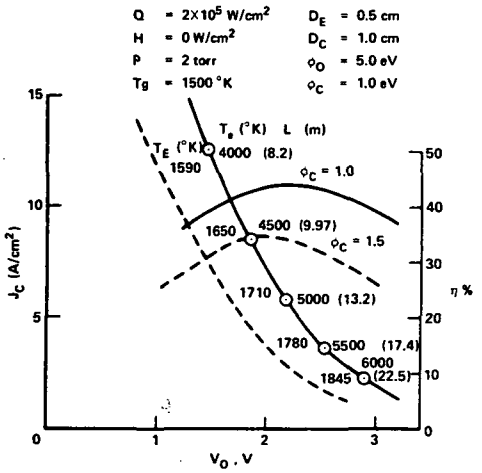

Figure 8.– Electrical output characteristics and efficiency η of TELEC; Q_C = 1.5 eV.

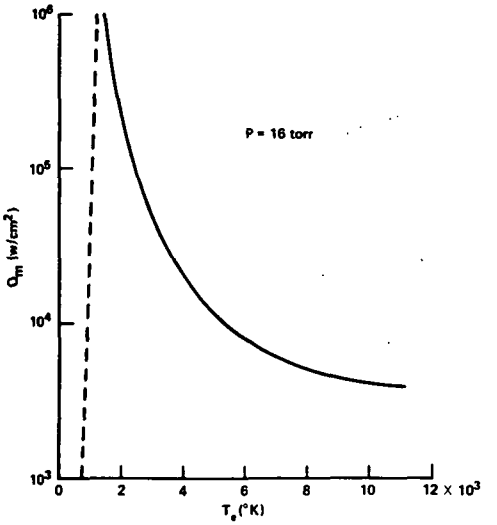

Figure 9.– Laser maintenance flux for cesium.

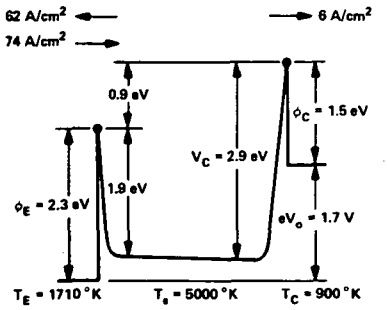

Figure 10.– Conditions at point A in figure 5.

DISCUSSION

Dick Stirn, J. P. L. – Could you go over again how you calculate your efficiencies?

Answer: Yes. First of all we take a unit length of the device. The laser radiation is decreasing with length. It's the ratio of the electrical power out to the total input laser power absorbed in that unit length. So, for example, if you have a 10-cm-diameter device, that's about 30 cm around so you would have 10 W/cm^2 times 30 cm or 300 W per centimeter of device length.

Tom Karras, General Electric – I'm a little confused on the effects of increasing the pressure. At one point you mentioned that you would increase the efficiency, but later on you said the reverse.

Answer: That was the one exception to that statement and I didn't want to go back and correct it! The pressure, in the couple of cases we have done – Lorin, why didn't you run another case? – was increasing the efficiency as we raised it. But we did not run high enough to see where it is optimum – it must turn over somewhere, however. Our results, 30 percent, are not, therefore, optimum. We don't know how high it will go. When you increase the pressure two good things happen – the efficiency goes up and you shorten the device.

Abe Hertzberg, University of Washington – I thought this was a very interesting paper, but I don't know why you are worrying so much about the intensity problem. Is it because you do not want to add a collector?

Answer: No. For one thing, the emitter is sitting there in the middle of the device. If it's a long device, you are going to have to aim the beam along this long path.

Abe Hertzberg, University of Washington – I think that, compared with some of the other problems, is not a big concern.

Don Nored, NASA Lewis Research Center – Just one comment on your stability work. This is very similar to some work we have been sponsoring at Physical Sciences, Inc. We should intercompare the studies.

LASER PLASMADYNAMIC ENERGY CONVERSION*

K. Shimada

Jet Propulsion Laboratory

INTRODUCTION

For efficient conversion of laser energy to electrical energy, which is required for realizing the transmission of energy via laser beam, various methods are being investigated at several laboratories under NASA sponsorship. One such method, described in this paper, utilizes the generation of electrons and ions by interacting an intense laser beam with cesium vapor. Theoretical calculation shows that the conversion efficiency is as high as 40 percent if the entire photon energy is utilized in ionizing the cesium vapor that is generated initially by the incoming laser beam. An output voltage is expected to be generated across two electrodes, one of which is the liquid cesium, by keeping the other electrode at a different work function. Evaluation of the laser plasmadynamic (LPD) converter has been performed using pulsed ruby and Nd-glass lasers. Although the results obtained to date indicate an efficiency two orders or magnitude smaller than that of theoretical predictions, an unoptimized LPD converter did demonstrate the capability of converting laser energy at large power levels. The limitations in the performance may be due to converter geometry, the type of lasers used, and other limitations inherent to the cesium plasma.

DESCRIPTION OF THE LPD CONVERTER

The LPD converter is a diode having one electrode holding approximately 1 g of liquid cesium and one electrode made of stainless steel having a semi-spherical surface (fig. 1). The cesium electrode is designated as an emitter and the other electrode as a collector. The radius of the sphere is 8 mm. An incoming laser beam is introduced through a hole in the collector with a lens so that the beam strikes the cesium surface at its focal point. For an estimated focal spot area of 1 mm^2, the peak power density at the focal point is approximately 1.6×10^3 W/cm^2 with a 1-J pulse with a duration of 600 μsec – the value which was used during the experiments. Steps involved in the operation of the LPD converter are: (1) evaporation of a small amount of cesium at the focal spot; (2) generation of cesium ions and electrons by interacting the laser beam with evaporated cesium atoms having a large particle density (obtained immediately following the evaporation) and (3) separation of ions and electrons by means of built-in potential energy difference between two electrodes having two different work functions. To achieve higher work functions at the collector, it is provided with a sheathed heater which is capable of raising the collector temperature up to 800°C. At this temperature the collector work function will be approximately 3 eV, and therefore,

*This paper presents the results of one phase of research carried out at the Jet Propulsion Laboratory, California Institute of Technology, under Contract NAS 7-100 sponsored by the National Aeronautics and Space Administration.

the contact potential will be 1.2 eV between the collector and the cesium electrode (work function equaling 1.8 eV). Therefore, the ideal open-circuit voltage will be 1.2 V with its (conventional) polarity being positive at the collector electrode.

Other features of the converter include: (1) one sapphire window for introduction of the laser beam, (2) another window for visual observation of the interior of the converter, (3) cesium liquid held in a cup-shaped portion of a copper rod whose temperature is controlled by means of an external heater and a water-cooled heat sink, and (4) an evacuated stainless steel cross envelope, 1-1/2" in diameter. During the experiments, the temperature of this envelope was kept at least 50°C higher than the cesium reservoir temperature, by means of heater tapes and a thermal blanket, to avoid formation of any parasitic reservoir.

EXPERIMENTAL SETUP

An optically-pumped laser, which could operate either with a ruby or a Nd-glass rod, and the LPD converter were mounted on an optical bench. The laser beam was reflected by a mirror and focused by a lens before entering the converter through a sapphire window. To measure the laser power incident on the cesium liquid, a known amount of laser power was sampled by a mirror having a calibrated reflectivity. Transmittances of lenses and a window were calibrated to obtain the laser energy incident on the cesium liquid target. The measuring circuit is shown schematically in figure 2. The LPD converter was connected to an external circuit having a resistor and a power supply, the latter of which was short circuited during the operation of the converter as an energy conversion device. However, the power supply was left connected during the measurements requiring acquisition of volt-coulomb characteristics.

Volt-coulomb characteristics were preferred over the volt-ampere characteristics because of the pulsed operation of the LPD converter. The total charge output per laser pulse was obtained by integrating the current output with an analogue integrator, with respect to time, for a duration of 600 μsec, a period that equalled the laser pulse duration. At the same time, the sampled laser pulse and the resultant LPD output were displayed on an oscilloscope to determine their wave forms and temporal relationships. For measurements of output energy, the time integral of the joule heat loss was obtained by integrating the square of the voltage across the load resistor. During all of the above measurements, the cesium temperature was maintained slightly above its melting point, and the collector temperature was varied and maintained higher than any other parts of the converter.

EXPERIMENTAL RESULTS

Figure 3 shows four oscillograms each showing the laser (top trace) and electrical outputs (bottom trace). The left figure on the top shows the characteristic of electric current (negative) and the right figure shows the characteristic of the ion current (positive) collected by the collector electrode. These curves were obtained by irradiating the biased LPD converter with a laser pulse at approximately 0.5 J of energy at the target cesium. The bias of +0.5 V means that the collector electrode is positive with respect to the cesium electrode so that the current is dominated by electrons. The time scales are 100 μsec/cm except the figure for applied voltage of −2.0 V which is

200 μsec/cm. The current scales are 0.2A/cm for the electron current and 0.5A/cm for the ion current.

These results show that: (1) charge separations are achieved with voltages of the order of 1 V; (2) electron current closely follows individual laser pulses, thus showing comparatively jagged wave forms; and (3) the current at an applied voltage of −2.0 V indicates that the current wave form is smooth (likely a characteristic of heavy particle flow such as caused by ions). The largest current observed reached as high as 3 A, which corresponded to a current density of 300 A/cm^2 from the area of 1 mm^2 where the laser beam was focused. The bottom left figure shows the open-circuit voltage observed with an elevated collector temperature. The largest peak value observed was +1.5 V. The polarity as well as the magnitude depends on the temperature of the collector; the polarity is negative at the collector when its temperature is low and the polarity becomes positive when the collector temperature is raised to drive off condensing cesium. An open circuit voltage of 1.5 V is considered reasonable since the LPD converter was operated under pulsed conditions, although it was a few tenths of a volt higher than expected with a CW laser.

Figures 4 and 5 show the volt-coulomb curves obtained with the ruby laser. The major difference between two figures is the difference in the current I_{CH} through the collector heater. The estimated collector temperature at I_{CH} = 2.6 A is 200°C and 450°C at I_{CH} = 7.5 A. Curves in the second quadrant indicate that the net charge collected is positive when the collector bias is negative while the curves in the fourth quadrant show the opposite. In figure 4, a trend for the collected charge to saturate is observed when the magnitude of bias voltage is of the order of 1 V. The open-circuit voltage, (which occurs when the collected charge is zero), is approximately −0.5 V.

It should be pointed out that the power-generating quadrants are the first and the third quadrant. At a low collector temperature (I_{CH} = 2.6A), the power is generated mainly by electrons. On the other hand, it is seen that the power is generated in the first quadrant by net positive charges when the collector temperature is raised (I_{CH} = 7.5A in fig. 5).

Although the temperature dependence of the output was qualitatively in agreement with expectations, the magnitude of the output was far less than what was expected. Possible explanations for this lack of output and an extrapolated performance will be discussed in Section V. In figure 5, a large increase of the collected charge in the second quadrant is evident in contrast to no change in the net charge in the fourth quadrant of the figure. Considering the fact that: (1) the increase in positive charge to the collector was only observed when the laser pulse was applied, and (2) the calculated thermionic electron emission from the collector, which would have contributed to the net increase, was far too small to account for the increase, the observed increase of positive charge may be due to more effective neutralization of positive space charge by thermionically emitted electrons.

Figure 6 shows similar results using a Nd-glass laser instead of a ruby laser. The shapes of the curves are similar to the previous curves with the exception of the reduced amount of charge collection. If the charges were solely generated by multi-photon ionization process, one would expect a much larger reduction with a Nd-glass laser (λ = 1.06 μ) than with a ruby laser (λ = 0.69 μ). (Further discussion of this matter is also given in Section V.)

Other experiments were performed to determine: (1) the functional relationship between the laser input and the charge output; (2) the dependence of charge output on cesium reservoir

temperature; and (3) the effect of the duration of the laser input on the output charge. The results of the first two experiments are shown in figures 7 and 8, respectively.

These curves were generated by measuring the output charge with a constant bias voltage of 4.0 V. A linear dependence of the output charge on the light input, up to an input of 1.4 J is shown in figure 7. The output is seen to fall off above this input level due to the depletion of cesium liquid in the reservoir caused by a rapid vaporization. Figure 8 also supports the above reasoning. At an increased reservoir temperature, the gaseous cesium increases relative to the liquid cesium. Figure 8 also indicates that the gaseous cesium is not contributing significantly to the ionization at a density of 10^{14}/cc ($T_{CS} \simeq 150°C$). Instead, the laser-cesium interaction must be occurring immediately following the application of laser the pulse (within a few hundred μsec). During this time the evaporated cesium does not expand significantly or maintain high gas density sufficient enough to result in a significant net ionization cross section.

An additional experiment (results are not included in this report) indicated that the duration of the laser pulse can be cut down to 100 μsec from the original 600 μsec without affecting the charge output. The results also indicated that a subsequent pulse, which followed 100 μsec after the first, did not produce a noticeable amount of charge. Though it is not conclusive at this point, the result may be explained by the existence of a threshold laser energy level, a level that was not exceeded with the subsequent pulse nor with an increased duration of the first laser pulse.

DISCUSSION OF RESULTS

To gain some insight into the mechanism of cesium ionization in an LPD converter, an order of magnitude estimation of charge output was made using a theory (ref. 1) based upon a simultaneous multiple photon process. For the wavelength of a ruby laser (0.69 μ), each ion produced requires three ruby photons since the photon and ionization energies are 1.79 eV and 3.89 eV, respectively. The total number of generated ions calculated from this theory was much too small in comparison with the observed charge output, of the order of 500 μC (3.13×10^{15} electrons). On the other hand, if each ion is produced by a simultaneous two-photon collision with an excited cesium atom (excitation energy of cesium = 1.47eV) which could be generated efficiently by a single photon collision, experimental results are in better agreement with the calculation. It leads us to believe that very efficient ionization could be obtained with a laser whose photon energy is slightly above that of the cesium ionization energy as long as the cesium gas density is larger than 10^{18}/cc at which an interaction length will be less than a few millimeters. Such a density would occur at the focal point on the cesium surface.

As an alternate explanation to account for the net charge output, cesium gas breakdown conditions were calculated (ref. 2) by considering the laser beam as an electromagnetic wave. As shown in figure 9, the electrostatic field intensity required for a breakdown is 872 V/cm at its minimum point on the curve. This value, as well as the cesium gas pressure, which would occur locally at the focal point of the laser, are both in a correct order of magnitude being used in the LPD experiments. However, there is another important mechanism which could contribute to the cesium ionization, that is, the inverse bremsstrahlung absorption of laser energy by the preionized cesium gas. A comparison of results obtained from the ruby and the Nd-glass lasers tends to support this idea since the inverse bremsstrahlung absorption will occur more efficiently at longer

wavelength, whereas the direct photon-cesium process drops off very rapidly as the photon energy decreases. This absorption mechanism merits further investigation.

The output voltage behaved qualitatively as expected. For example, the output voltage became positive when the collector was heated to 450°C (723°K) so that its work function was increased to approximately 2.2 eV. At this point, the output voltage would have been 0.4 eV (that is, 2.2 – 1.8). To achieve a higher output voltage the collector temperature should have been much higher. Unfortunately, the experiments were not possible since a cesium gas breakdown occurred without an application of laser pulse as occurs in a thermionic diode.

Lastely, the relative insensitivity of the output charge on the output voltage was considered. Although it is not conclusive, a space charge limitation or the charge recombination, or both, may account for the observed charge transport.

In summary, the LPD converter did demonstrate the feasibility of converting laser energy to electrical energy by producing electric charges of the order of 1000 μC. The measured conversion efficiency was 0.01 percent (10 μJ output at 100 mJ input). If the output was not impeded by the transport process and if the collector temperature was made high enough to produce an output voltage of 2.0 V, the efficiency could have been 2 percent (1000 μC output at 2.0 V).

A modification of the converter geometry and of the electrode material is being planned to increase efficiency and to verify the laser energy absorption theory.

REFERENCES

1. Tozer, B. A.: Theory of the Ionization of Gases by Laser Beams. Phys. Rev., Vol. 137, no. 6A, 15 Mar. 1965, p. 1665-1667.

2. Brown, S. C.: Basic Data of Plasma Physics. John Wiley and Sons, Inc., N. Y., 1959, p. 142-150.

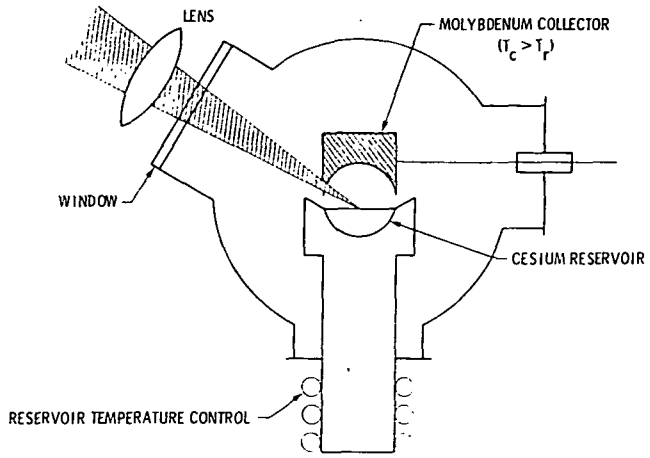

Figure 1.– Schematic drawing of an LPD converter (collector electrode was made of stainless steel for this experiment instead of molybdenum as shown).

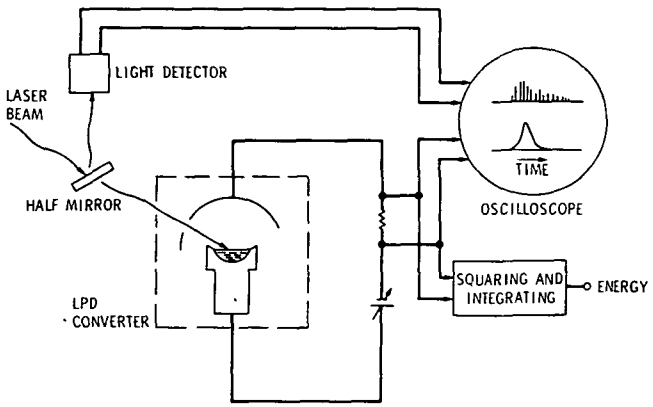

Figure 2.– Measuring circuit.

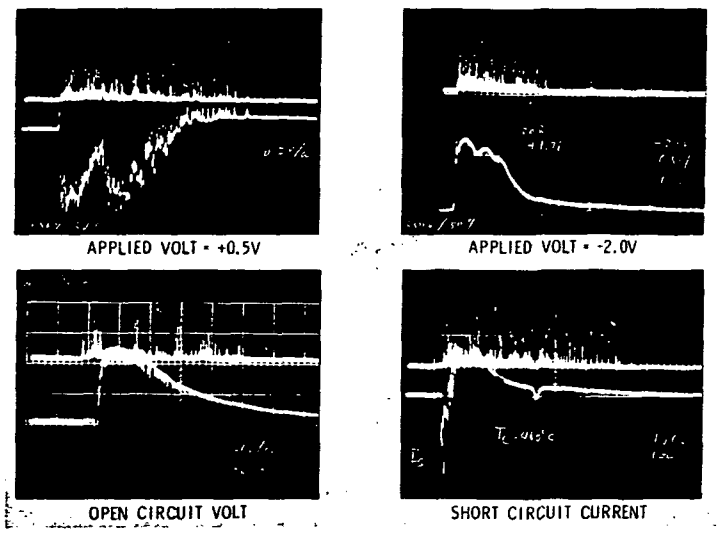

Figure 3.– Oscillogram of LPD outputs.

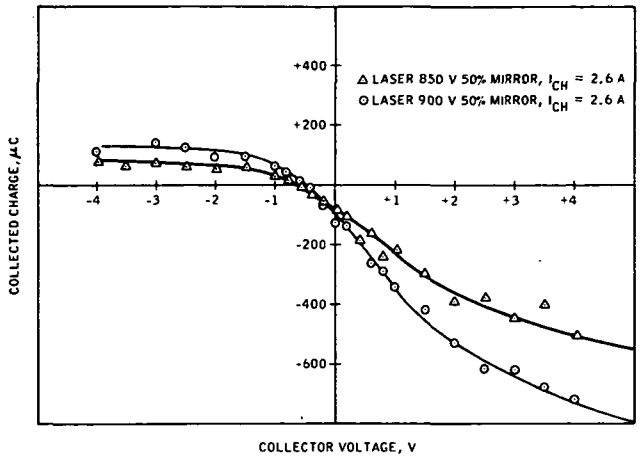

Figure 4.– Volt-coulomb curves with I_{CH} = 2.6A (T_c = 200° C).

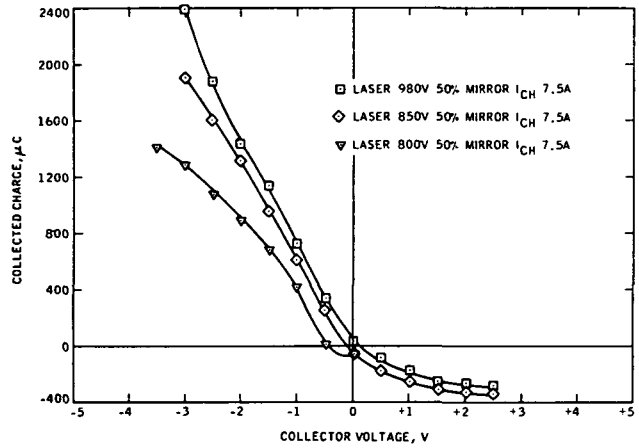

Figure 5.– Volt-coulomb curves with I_{CH} = 7.5A (T_c = 405° C).

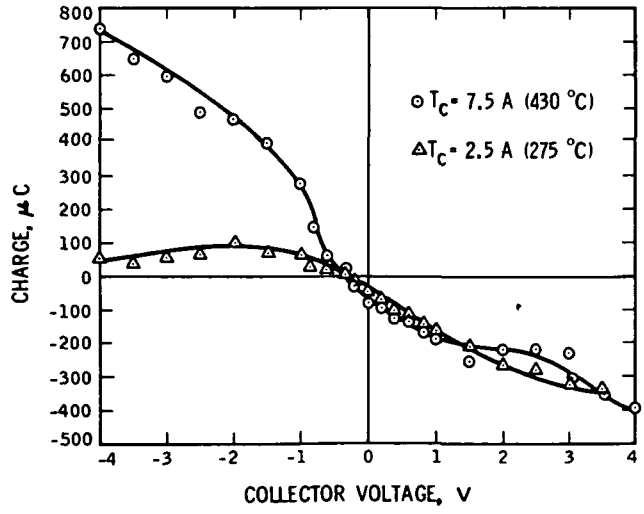

Figure 6.– Volt-coulomb curves with a Nd-glass laser.

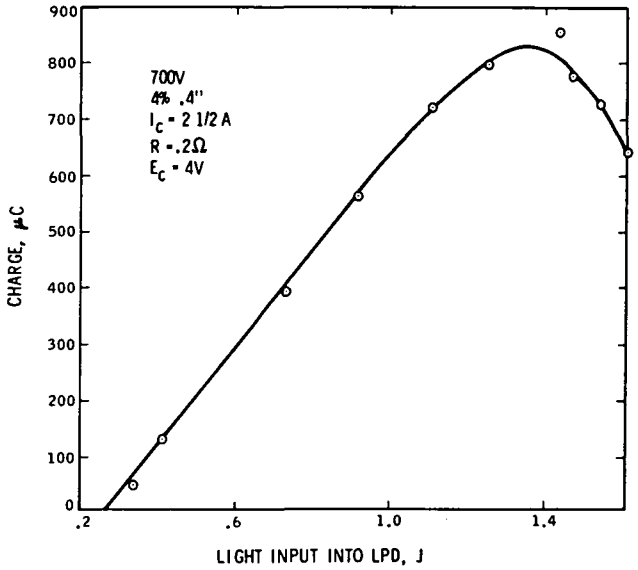

Figure 7.– Charge output *vs* light input.

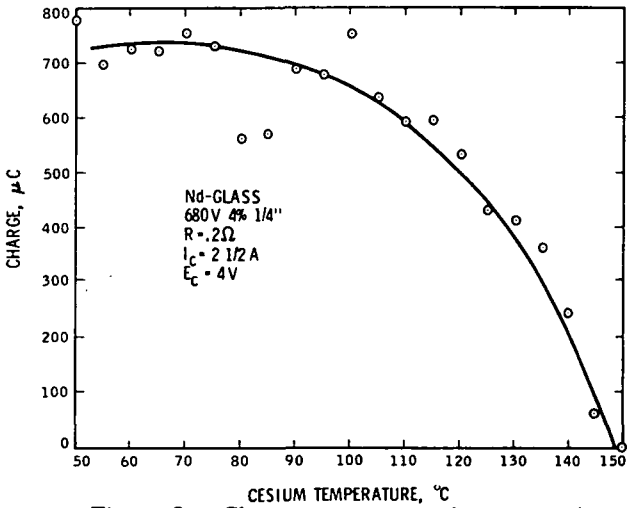

Figure 8.– Charge output *vs* cesium reservoir temperature.

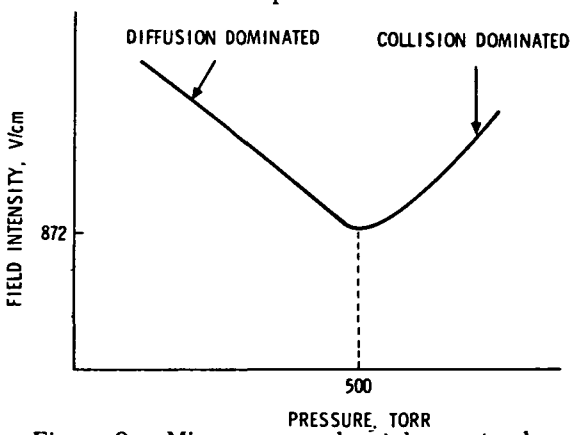

Figure 9.– Microwave gas breakdown at a laser frequency.

DISCUSSION

Malcolm Gower, NASA Ames Research Center – Are the ions produced by a multiphoton process?

Answer: Yes, that's one way. In that case it has to be three photons with ruby.

Malcolm Gower, NASA Ames Research Center – Well below 3000 Å the cesium dimer has a much, much larger cross section than the monomer.

Answer: Yes, we heard this very recently and we will be looking at it.

Max Garbuny, Westinghouse – How much energy goes into heat of vaporization – a lot? This system seems to lend itself to MHD.

Answer: Yes, a lot goes into vaporization. For MHD, however, we would rather have a gaseous phase than liquid, that is, we would use something more like Ned Rasor's talk.

Abe Hertzberg, University of Washington – Dr. Rasor, in the same connection, did you consider recombination effects in your theoretical work?

Ned Rasor, Rasor Associates – These are not important at the $10^{15} cm^{-3}$ densities we have considered.

K. Shimada: However, ours are much higher than that, where this *is* important.

CONVERSION OF LASER ENERGY TO GAS KINETIC ENERGY*

G. E. Caledonia

Physical Sciences, Inc.

INTRODUCTION

The use of a high intensity laser as a source of power can be advantageous in situations where it is either necessary or desirable to separate the sites of energy production and consumption by large distances. Such situations clearly arise in space applications where, for purposes of minimizing weight loading, it would be valuable to be able to supply various rocket or satellite power needs from Earth-based sites. Specific systems of this sort, which are presently under investigation, include (1) the novel idea of supplying rocket thrust via laser propulsion (ref. 1) and (2) direct Earth-based powering of satellites or space laboratories.

The successful development of such systems requires, among other things, efficient techniques for conversion of the incident laser radiation into other more useful forms of energy. This discussion is concerned with the direct gas phase absorption of laser radiation. The process envisioned is the heating of a high pressure reservoir gas via laser absorption followed by expansion of the heated gas through a sonic nozzle with subsequent conversion of the gas translational temperature to ordered kinetic energy. The resulting high velocity gas may then be used as specific impulse for rocket propulsion or alternately for the generation of shaft horsepower.

GAS PHASE ABSORPTION MECHANISMS

Inverse Bremsstrahlung

There are two basic techniques available for the gas phase absorption of laser radiation. The first of these is absorption by inverse bremsstrahlung. This technique is particularly suitable for absorption in high temperature gases and has been the subject of considerable research. The advantages of inverse bremsstrahlung are two fold: (1) the laser energy is converted directly to gas translational energy during the absorption process, that is, at a gas kinetic rate; and (2) the absorption process is spectrally continuous and thus lasers of any wavelength may be used.

The basic complication in the use of inverse bremsstrahlung is that the absorption coefficient scales either linearly or as the square of the electron density, depending on the ionization fraction, and thus under equilibrium conditions the absorption coefficient can be quite small at low temperatures. Even if a readily ionizable seed, such as cesium, is introduced into the gas, the absorption coefficient will still decrease exponentially with decreasing temperature below $\simeq 2500°K$ and be negligibly small at room temperature. This complication can be avoided by

*This research was supported by NASA-Lewis Research Center, Cleveland, Ohio, under Contract No. NAS3-18528.

producing non-equilibrium electron concentrations in the gas, for example, by laser induced gas breakdown or by an electric discharge; alternately, it can be avoided by introducing a different absorption mechanism that could be used to heat the gas to temperatures sufficiently high so that significant thermal ionization would occur.

Molecular Absorption

The second gas phase absorption technique, and the principal subject of this discussion, is the direct absorption by the vibrational rotation (V/R) bands of molecules. The main advantage in using V/R band absorption is that, unlike bremsstrahlung, the absorption process is as efficient in a cold gas as in a heated one. However, there are several compensating disadvantages:

1. A given molecule will have a finite number of absorbing transitions which will occur over a limited wavelength range.

2. The absorbed energy is deposited in the vibrational rather than translational modes of the molecule and efficient kinetic mechanisms are required to convert the absorbed energy into heat. In particular, when the upper state of an absorbing transition is populated more rapidly than it can be de-activated, gas "bleaching" can occur.

3. As the gas temperature increases undesirable chemical phenomena, such as dissociation, can degrade the absorption process.

This last point is particularly important for larger molecules. For example, SF_6, which is an efficient absorber of CO_2 laser radiation, will be significantly dissociated at temperatures above $\sim 1700°K$. Even a relatively stable triatomic such as CO_2 will dissociate at temperatures above $\sim 2500°K$. Generally speaking, only diatomic molecules with large dissociation energies can provide significant laser gas heating with minimal chemical effects. As will be discussed below, these disadvantages may be minimized by performing the absorption in a high pressure system. Although the discussion below will be limited to the absorption of diatomic molecules, much of what is said will also hold true for larger molecules.

High Pressure Absorption

The pressure broadened absorption coefficient for a given V/R transition with vibrational levels $v - 1 \rightarrow v$ and rotational level $J \rightarrow J \pm 1$ is defined by

$$\alpha_{v-1,\,J,\,\Delta J}(\nu),\ \mathrm{cm}^{-1} = \frac{\lambda^2_{v-1,\,J,\,\Delta J}\, A_{v,\,v-1,\,J,\,\Delta J}}{4\pi^2\, c\, \Delta\nu_L} \left(N_{v-1,\,J} - \frac{g_{v-1,\,J}}{g_{v,\,J\pm1}}\, N_{v,\,J\pm1} \right) \left[4 \left(\frac{\nu - \nu_{v,\,J,\,\Delta J}}{\Delta\nu_L} \right)^2 + 1 \right]^{-1} \tag{1}$$

where ν is wavenumber, c the speed of light, λ wavelength, A the Einstein coefficient of the transition, N the populations of the upper and lower states, g the degeneracy factor, and $\Delta\nu_L$ the full linewidth at half height in cm^{-1}. It can be seen from the first bracketed term on the right-hand side of equation (1) that the absorption coefficient decreases as the upper state population approaches the lower. This is the phenomenon of "bleaching" alluded to earlier. The number density dependence of the absorption coefficient is of some interest. The line width is directly proportional to number density and thus on line center ($\nu = \nu_{V,J,\Delta J}$) the absorption coefficient is independent of the total number density. On the other hand, on the wings of the line ($\nu - \nu_{V,\ J,\ \Delta J} > \Delta\nu_L$) the absorption coefficient scales as the square of the number density. Thus there can be a large variation in the pressure dependence of the absorption coefficient over the line shape.

For any given vibrational transition there are a large number of allowable rotational transitions. For example, the room temperature absorption spectrum for the $v = 0 \rightarrow 1$ transition of CO is shown in figure 1. It has been assumed here that the pressure is such that the line width is small compared to the spacing between lines ($\sim 3.8\ cm^{-1}$ for CO). The $v = 1 \rightarrow 2$ absorption spectrum will have a similar shape but will be shifted to somewhat longer wavelengths, as shown in figure 1, because of the molecular anharmonicity. As can be seen there is a considerable overlap between the $v = 0 \rightarrow 1$ and $v = 1 \rightarrow 2$ bands (and also with higher bands not shown); however if the line widths are small compared to the line spacing there will be essentially no wavelength coincidences between the various lines. Thus laser light of a given wavelength could at best be absorbed by only one of the manifold of possible absorbing transitions.

This constraint will not apply at sufficiently high pressures, $\gtrsim 30$ atm for self-broadening in CO, where the line width is $\gtrsim$ the line spacing. In this limit the molecule will absorb continuously over the wavelength region of the V/R band. The absorption coefficient at any given wavelength is no longer given directly by equation (1), but rather now involves a sum of the absorption coefficients of a number of overlapping transitions, and is independent of total number density depending only upon the mole fraction of the absorbing gas.

A band model has been developed for the prediction of the molecular absorption spectra in this high pressure limit and applied to the molecule CO. Predictions from this model are shown in figure 2 through 4. In figure 2 the room temperature absorption cross-section vs. wavelength is shown for the lowest three vibrational transitions of CO. The cross section increases with increasing vibrational level because of variation in the Einstein coefficient (a linear dipole moment function for CO was employed in the calculations (ref. 2)). The important feature is that, because of the large overlap between the absorption spectra for each vibrational transition, laser light of a given wavelength may be absorbed simultaneously by each vibrational level. This has the effect of minimizing bleaching phenomena because if a particular transition approaches the bleaching limit the upper state of that transition can also absorb the incident laser radiation.

Of more interest from the viewpoint of laser heating is the temperature variation of the absorption cross sections. This behavior will, of course, be quite sensitive to the choice of incident laser wavelength. Predictions for the absorption cross sections of the first five vibrational levels of CO over the temperature range of 200-3000°K are shown in figure 3. The incident laser radiation is taken to be at a wavelength of 4.755 μ, which would correspond to a P branch $v = 1 \rightarrow 0$, J = 10 CO laser. Although a high power CO laser of this type has not yet been developed, the results may be taken as generic for any diatomic molecule undergoing absorption at a wavelength near the center

of its fundamental V/R band. As can be seen, above 300°K the absorption cross sections for the various vibrational levels are all of the same order of magnitude. The absorption cross sections for individual transitions generally tend to decrease at the higher temperatures shown because of the effect of the rotational partition function. However absorption on the higher vibrational transitions ($V = 4 \rightarrow 5$ as well as higher transitions not shown) peak in the higher temperature region because absorption occurs in the high rotational wings of these bands. The net effect of this is that the overall molecular absorption coefficient can be relatively insensitive to temperature variations depending, of course, upon the vibrational distribution function.

A similar result is shown in figure 4 for an incident laser wavelength of 4.855 μ. This wavelength corresponds to an attainable P branch CO laser transition, $V = 3 \rightarrow 2$ $J = 8$. Since this wavelength occurs in the wing of the CO $V = 0 \rightarrow 1$ band (see figure 2), the absorption cross section for this initially increases rapidly with temperature. This is an important point since the upper vibrational states of CO are not significantly populated at room temperature. However, it is clear that as soon as ground state molecules are excited to the first vibrational state through absorption, excitation to higher states (including transitions to states higher than those shown in figure 4) will be quite rapid.

It would appear then that optimum absorption by diatomic molecules can be realized in the high pressure regime characterized by overlapping lines, since in this limit laser light of a given wavelength may be absorbed simultaneously on a number of different vibrational transitions. This multiline absorption should also have the effect of flattening out the temperature vibration of the total molecular absorption coefficient. It now remains to discuss techniques for the rapid conversion of the absorbed vibrational energy into translation.

Conversion of Vibrational Energy to Translation

The molecule CO was chosen as an example not only because its molecular properties are well defined, but also because it has a very high dissociation energy – 11.1 eV – and thus may be heated to relatively high temperatures (~ 6000°K) without introducing significant chemical effects. One disadvantage of this molecule, however, is that the rate constants for vibrational deactivation are quite small at temperatures below 1500°K. These small rate constants tend to preclude efficient coupling between the vibrational and translational modes. There are several atomic species such as Fe, H, and O that have been shown to be efficient ($k = 10^{-13}$ to 10^{-12} cc/sec) vibrational deactivators of CO (refs. 3 through 5); however, it is difficult to introduce such species into a cold gas flow.

One technique has been considered that, although not recyclable, may be of some interest for use in systems concerned with the development of thrust, etc. The technique involves the use of a rare gas seeded with iron pentacarbonyl, $Fe(CO)_5$. $Fe(CO)_5$ absorbs in the same wavelength region as CO, its vibrational modes will strongly couple with translation and, when dissociated, produces both the absorbing molecule CO and the efficient deactivator Fe. Unfortunately, detailed modeling of this system is complicated by the fact that the low temperature absorption spectra of $FE(CO)_5$ is not well defined.

To properly model gas laser heating by diatomic molecular absorption one requires a computer code that includes the phenomena of multiline absorption, vibration to translational (V–T) deactivation, and vibration-vibration (V–V) exchange between all vibrational levels. The resulting

vibrational distributions will not only be out of equilibrium with translation but can also be non-Maxwellian. Preliminary calculations, neglecting the V–V exchange processes, have been made for CO. A constant density gas was assumed at an initial pressure of 30 atm with 0.2 percent CO, 0.04% Fe in a helium diluent. A laser intensity of 10^6 W/cm^2 was assumed with a laser wavelength of 4.855 μ, corresponding to the absorption cross sections of figure 4.

The time histories of both gas absorption length and temperature for this case are shown in figure 5. As can be seen, the gas temperature increases essentially linearly from 400° to 3000°K and, more importantly, the absorption length remains approximately constant over this temperature range. The initial drop in the absorption length is caused by the early time increase in the vibrational populations of the upper states. The inclusion of V–V exchange in the calculations is not expected to produce a large change in these predictions.

It should be emphasized that this technique may be generally applied. In general, the radiation from most high power gas lasers which operate on vibrational transitions can be absorbed by several different diatomic molecules if the total gas density is sufficiently high to produce overlapping lines. The one major exception to this statement appears to be the 10.6-μ CO_2 laser. Although a number of the diatomic metal oxides can absorb radiation of this wavelength, these species are not readily produced under the conditions of interest. Of course this same line broadening phenomenon occurs for larger molecules. These could be reviewed to determine which species could optimally absorb CO_2 laser radiation with minimal chemical effects.

There are a number of candidate diatomic molecules that can be vibrationally deactivated relatively efficiently and that may be of interest in a closed cycle laser heating system. For example, the room temperature absorption spectra of the first two vibrational levels of NO are shown in figure 6. The middle peaks in these spectra arise because the NO ground state is a π state and thus the Q branch is allowed. (For simplicity in this calculation a linear dipole moment was assumed and the small wavelength shift between spin states was neglected). Shown at the top of the figure are the wavelength positions of several readily attainable CO laser lines. It would appear that NO would prove to be a viable absorber for CO laser radiation.

SUMMARY

Techniques for the gas phase absorption of laser radiation for ultimate conversion to gas kinetic energy have been discussed. Particular emphasis has been placed on absorption by the vibration rotation bands of diatomic molecules at high pressures. This high pressure absorption appears to offer efficient conversion of laser energy to gas translational energy. Bleaching and chemical effects are minimized and the variation of the total absorption coefficient with temperature is minimal. This latter feature is particularly advantageous from a systems design viewpoint.

REFERENCES

1. Pirri, A. N.; Monsler, M. J.; and Nebolsine, P. E.: Propulsion by Absorption of Laser Radiation. AIAA J., AIAA J., Vol. 12, no. 9, Sept. 1974, p. 1254-1261.

2. Young, Lee A.; and Eachus, James W.: Dipole Moment Function and Vibration-Rotation Matrix Elements for CO. J. Chem. Phys., Vol. 44, no. 11, 1 June 1966, p. 4195-4206.

3. von Rosenberg, C. W. Jr.; and Wray, K. L.: Vibrational Relaxation of CO by Fe Atoms. J. Chem. Phys., Vol. 54, no. 3, 1 Feb. 1971, p. 1406-1407.

4. von Rosenberg, C. W. Jr.; Taylor, R. L.; and Teare, J. D.: Vibrational Relaxation of CO in Nonequilibrium Nozzle Flow, and the Effect of Hydrogen Atoms on Co Relaxation. J. Chem. Phys., Vol. 54, no. 5, 1 Mar. 1974, p. 1974-1987.

5. Center, R. E.: Vibrational Relaxation of CO by O Atoms. J. Chem. Phys., Vol. 58, no. 12, 15 June 1973, p. 5230-5236.

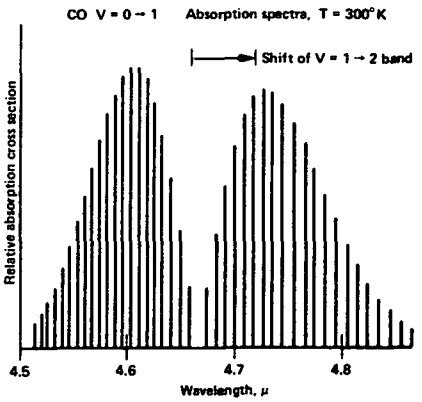

Figure 1.– Room temperature, low pressure absorption spectra of the V = 0 → 1 band of CO.

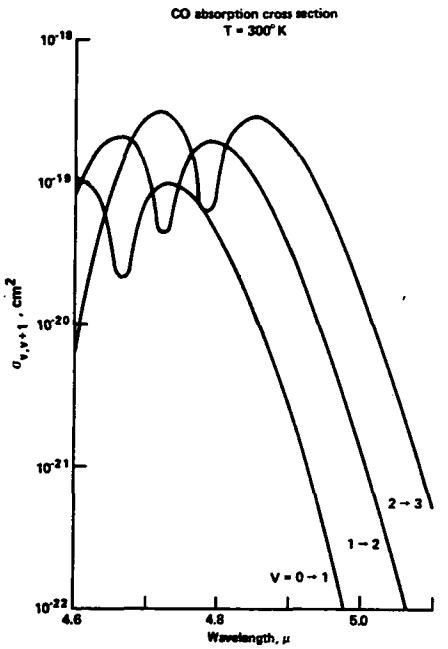

Figure 2.– Room temperature, high pressure absorption spectra of the V = 0 → 1, V = 1 → 2, and V = 2 → 3 bands of CO.

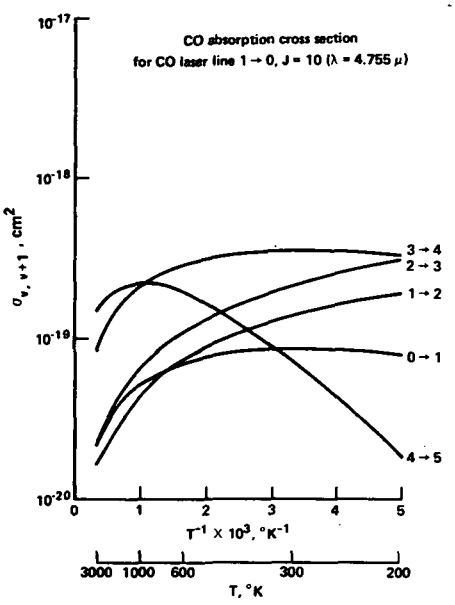

Figure 3.– Absorption cross section *vs* temperatures for the five lowest vibrational transitions in CO at a wavelength of 4.755 μm.

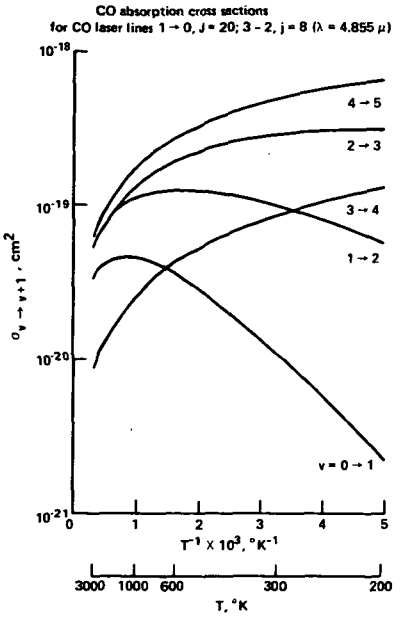

Figure 4.– Absorption cross section *vs* temperatures for the five lowest vibrational transitions in CO at a wavelength of 4.855 μm.

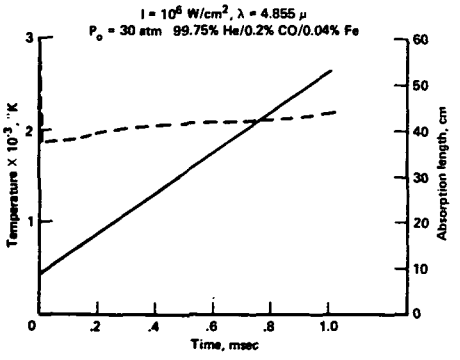

Figure 5.– Gas temperature and absorption length *vs* time; conditions as shown.

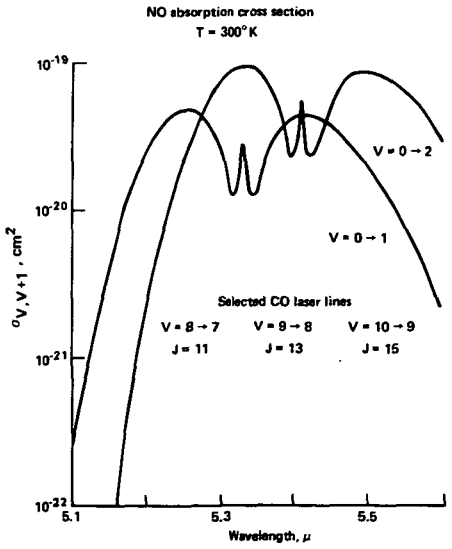

Figure 6.– Room temperature high pressure absorption spectra of the V = 0 → 1, V = 1 → 2 bands of NO.

DISCUSSION

Bob McKenzie, NASA Ames Research Center – Are the dissociation energies of the hydrogen halides too low for you to consider?

Answer: There are two problems there. One is that all these hydrogen bearing species have relatively large rotational spacings, so one has to go to pressures like 100 atm to get this line overlap. However, I won't rule them out. Secondly, you're right, the dissociation energies are lower.

Ernest Brock, Los Alamos Scientific Laboratory – I don't want to be too nit-picking, but perhaps I will be! Even in the very low pressure-low temperature CO, there are quite a large number of lines in the V – V manifold that overlap to 0.1 to 0.5 cm^{-1}.

Answer: Yes, as Lacina's recent publication indicates. Most of these are on higher vibrational levels, however. But your point's well taken – these accidental, rather than forced, overlaps do occur although the line centers don't match and hence the absorption can vary considerably.

Ernest Brock, Los Alamos Scientific Laboratory – The other comment I have, is that as one considers the uptake of energy in this system, one must keep in mind the relatively high cross sections for J – J transitions. In CO, for example, this is at 100 GHZ and one should be concerned about self-trapping of the 100 GHZ radiation.

Answer: I have assumed they are instantaneous in these calculations. One would have to do detailed kinetics to take it into account.

Abe Hertzberg, University of Washington – I would also note that the use of a Lorentzian is in error since there are indications that, if anything, it's super-Lorentzian.

Answer: Yes, that is correct.

Mark Wrighton, M. I. T. – What is the radiative probability from the upper excited state? That is, how long do they live?

Answer: The lifetime of the ground state, 1 – 0 transition, is like 33 msec, that might get down to 5 or 6 msec at high vibrational levels before it flattens out because of the energy dependence of the Einstein coefficient.

Mark Wrighton, M. I. T. – Is there any probability at all for a molecule to go from the fourth vibrational level down to the zeroth level?

Answer: Oh, that's very improbable. There is almost an order of magnitude between the fundamental and the first overtone. I might point out, however, about one-quantum transitions: anything radiated will be reabsorbed by the gas because all levels can absorb the wavelength.

Malcolm Gower, NASA Ames Research Center – Wouldn't you gain quite a bit by using a homonuclear molecule, like hydrogen and excite by stimulated Raman?

Answer: I would have thought the cross section was considerably lower.

Malcolm Gower, NASA Ames Research Center – Yes, except it becomes appreciable for high intensity laser sources.

Abe Hertzberg, University of Washington – Since inverse bremsstrahlung absorption works, and has a lot of nice properties, why not use it, in argon, say?

Answer: My point is that inverse bremsstrahlung under equilibrium conditions is very nonuniform in the first several thousand degrees of heating – that is, very temperature dependent.

Abe Hertzberg, University of Washington – Oh, I agree, but if I do have enough electrons, I could care less, I will absorb all the energy.

Answer: Well, it depends upon what the length of your system is. Of course at room temperature the absorption is zero. So, I'm saying that instead of using techniques which produce non-equilibrium electron concentrations, use this technique to get you to high enough temperatures so you can thermally ionize.

Abe Hertzberg, University of Washington – Well, being something of a practical engineer, I would suggest you use something like a flame thrower – the laser acts as the flame thrower.

ADVANCED PHOTON ENGINES

Abraham Hertzberg

University of Washington

Seattle, Washington 98195

At the University of Washington as part of studies relating to the conversion of laser energy into useful forms of work, it has been established that coherent radiation is a form of work. This study led to the design of concepts (ref. 1) which could convert coherent laser radiation into flow energy with a theoretical efficiency of unity. However, in examining the practical efficiencies that could be achieved, it was also found that the fraction of energy that was converted on each pass of the fluid was very small compared to the flow energy. Hence, only by extremely efficient design could successful photon engines of this class be created.

However, the coherent energy field of a laser can be concentrated into a small volume so that high energy densities and high gas temperatures are easily achieved. A normal thermodynamic engine working over this temperature range also produced efficiencies close to one. Nonetheless, this heat energy cannot be converted into work with a very high efficiency due to the well known limitations of high temperature materials.

A class of heat engines developed some years ago has proved capable of operation above normal material temperatures. Essentially, these heat engines use a device called the Energy Exchanger (ref. 2) which is related to principles developed by Claude Seippel of Brown Bovari (ref. 3). This principle has shown that energy can be directly exchanged between high temperature and low temperature gases so that the wall temperature of the machine sees only an average. An extension of this principle has shown that this energy exchange can in principle be also made highly efficient if an acoustic velocity match between the hot and cold gas is maintained. This ratio is easily maintained in working machinery by use of high molecular weight gases in contact with low molecular weight gases. Indeed, temperature ratios as high as 10 can be achieved. With these high temperatures the circulating power fraction becomes very small since the work available per unit of mass flow is correspondingly large. Indeed, in the limit of very high temperatures, it can be shown that for a simple cycle such as the Brayton cycle, the component inefficiency can be tolerated as shown in figure 1. When combined with recent studies showing that lasers can be used to heat gases to extremely high temperatures, such as has been proposed at this meeting for jet propulsion and as proposed for wind tunnel research (ref. 4), it is evident that very high thermal efficiencies are achievable. A reasonable extrapolation of this technology suggests that it is within engineering capabilities today to produce a practical engine that can convert coherent radiation back to work with efficiencies of approximately 60 percent. It is expected that further studies will show how this efficiency can be increased to 75 percent.

A proposed method of operating such a machine would involve the following operation as a Brayton cycle as shown in figure 2. We will consider here for simplicity only a simple regenerated Brayton cycle with the addition of an energy exchanger device. A compressor will be used, using a suitable intercooler, to bring the gas to a reasonably high compression ratio. The working gas could

be in this example argon or water vapor. The working gas would then be passed to the equivalent of the combustion chamber in a normal gas turbine cycle. However, rather than using combustion, heating would take place directly by laser energy addition. The laser heating techniques would closely follow those proposed by NASA in its program for space propulsion.

Roughly speaking the same problems of laser energy coupling and heating will be involved. After heating, however, the temperatures required in such a cycle would not be as high as that necessary for propulsion. The use of argon or water vapor of course would be necessary. After heating, the gas would be expanded into an energy exchanger device (ref. 2) as shown in figure 3 and give up its enthalpy directly to a gas of low molecular weight. For example, steam or hydrogen could prove interesting. The temperature of the driven gas would be limited to 1000°K, the conventional turbine inlet temperature. Since the molecular weight of argon is approximately 40 and that of hydrogen approximately 2, the temperature ratio for perfect acoustic impedance matching, which is required for efficient energy exchanger operation in this case, would allow a theoretical argon temperature of nearly 20,000°K. Hence the hydrogen temperature can either be made correspondingly low or gases of higher molecular weight can be used. This is of course an example of the extremes of operation. Steam might indeed be a very practical driver gas though the temperature ratios achievable for highest efficiency are not near as high.

The hydrogen or steam in the driven gas loop now has nearly the entire enthalpy of the laser heated gas at a much lower temperature. It then enters the turbine, expands through the turbine, and returns through the energy exchanger for recompression. The argon or steam, after it is discharged from the energy exchanger then passes through a conventional heat exchanger and is returned to the cycle. Thus we have the elements of a completely closed cycle as shown in figure 4. While the energy exchanger adds an element of inefficiency, the very high enthalpies involved mean a very small circulating power fraction which tends to reduce the effect of component inefficiencies and make it possible to achieve nearly ideal Brayton cycle efficiency.

We have yet to explore all of the problems involved in the optimal design of such a cycle. For example, the temperature limits on the argon could be such that they would involve a high radiative heat loss thus effectively limiting the advantages of laser heating. In addition there will be mixing of the driver and driven gas and hence some type of separation mechanism may have to be employed. This of course would be simplified by using steam in the driver or driven loop of the cycle since it could easily be condensed out as part of the operation and returned to the cycle. As pointed out previously, even when working with air, thermal efficiencies approaching 50 percent were achieved and certainly in this configuration we could expect to easily exceed this value. As a practical thermal-cycle this appears very appealing at this state, since it is capable not only of high conversion efficiency but involves concepts built around existing thermal machinery and has a capability for handling large amounts of power in principle.

In view of the potential of this approach, work in this area is continuing and studies of cycles of this type will be carried out to examine the limits of operation.

REFERENCES

1. Hertzberg, Abraham; Christiansen, Walter C.; Johnsont, Earl W.; and Alstrom, Harlow G.: Photon Generators and Engines for Laser Power Transmission. AIAA Journal, Vol. 10, no. 4, Apr. 1972, p. 394-400.

2. Weatherston, R. C.; and Hertzberg, A.: The Energy Exchanger, a New Concept for High-Efficiency Gas Turbine Cycles. Transactions of the ASME, Paper No. 66-GT-117.

3. Seippel, Claude: Pressure Exchanger. U. S. Patent No. 2,399,394, 30 Apr. 1946.

4. Buonadonna, Victor R.; Knight, Charles J.; and Hertzberg, Abraham: The Laser Heated Hypersonic Wind Tunnel. Aerospace Research Laboratories ARL 73-0074, May 1974.

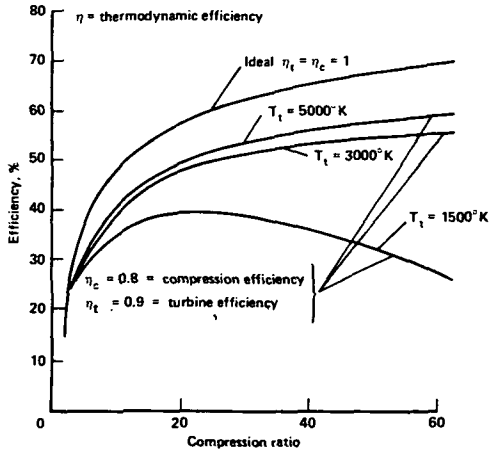

Figure 1.– Brayton cycle efficiency.

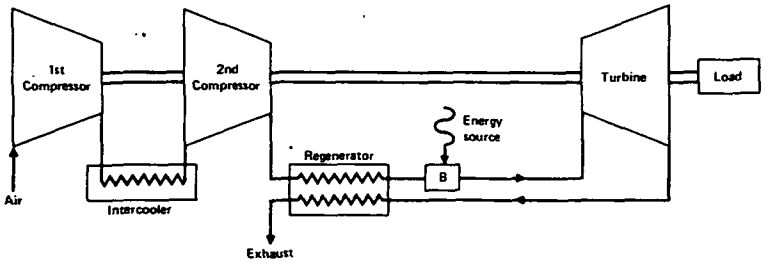

Figure 2.– Basic regeneration type gas turbine cycle.

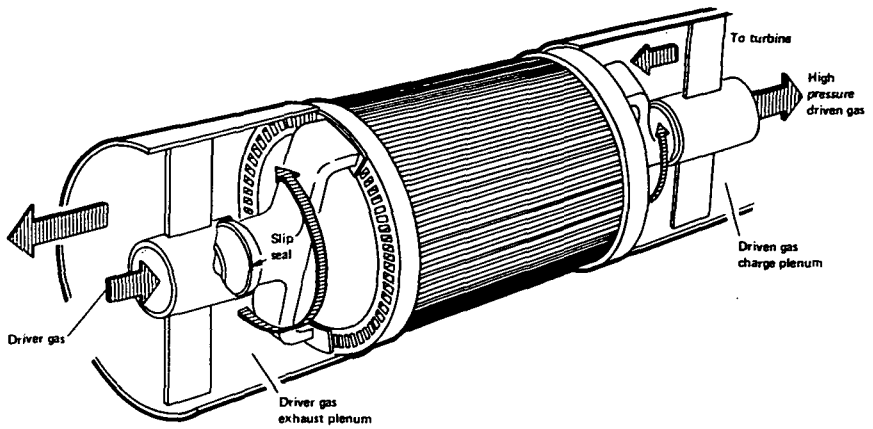

Figure 3.– Illustration of energy exchanger with fixed tubes.

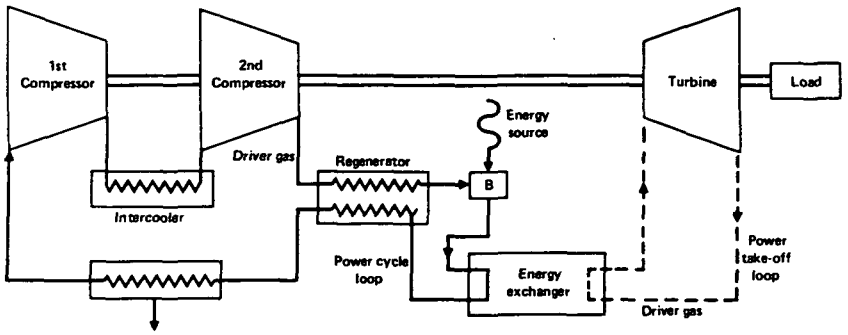

Figure 4.– Closed regeneration cycle with energy exchanger.

DISCUSSION

Ned Rasor, Rasor Associates – At what point do you add the heat from the laser to the cycle? At the high temperature?

Answer: That is where you want to add it to keep the entropy low. But look, between infinite temperature and 5000 degrees, there is enough ΔT to make heat transfer possible. Look, just imagine the rocket nozzle sitting in space and these tubes rotating by it. So we then use this as an energy exchanger, or really an enthalpy exchanger. The trick in getting it to be efficient is, if I can run this in two closed cycles, I can use gases of *vastly* different molecular weight which are commonly available and which are very compatible with real machinery. Argon is inert, helium is inert, the quantities needed are not large, and, finally, they are recyclable.

Arthur Cohn, Electric Power Research Institute – What is the efficiency of the gas-dynamic compressor like?

Answer: Well, in a widely unread paper (good thing you asked that question, sir!) we examined that. The machine is not for "smallies" – leakage and viscous losses will kill you. What we did is optimize it for several different cycles. The paper is "The Energy Exchanger – A New Concept for High Efficiency Gas Turbines" written in about 1966. Incidently, we found you could not sell, in those days, high efficiency gas turbines since people said, look at the cost of fuel compared with the capital cost! So it was unsaleable. But things have changed a little and that is why we are going back to look at it. We assumed just steam and air, not perfectly impedance matched, and found the efficiency of the exchanger to be 15 percent. So you add that loss; you optimize your cycle, adding a little turbine reheat, etc., and you find the cycle efficiency to be over 60 percent. So remember, if I apply it with perfect impedance matching, I would estimate, even at higher temperatures, I could keep the same 15 percent loss. But remember that those losses begin to disappear because the enthalpy per pound of gas going through there is so high that the inefficiencies working on it have less chance of being deadly. High temperatures are the salvation of almost any thermal machine. It even makes something like MHD which has a conversion of approximately 30 percent mechanical to electrical look more attractive (if things don't melt). So we continue to examine this. We wish it would work with coal but it's hard to believe that all that rotating machinery will live in such a dusty environment.

Ken Billman, NASA Ames Research Center – Abe, what was the exact reference of the paper?

Answer: It was presented at the Gas Turbine Conference at Zurich, Switzerland of 1966; American Society of Mechanical Engineers, Paper No. 66-GT-117. It is an archival reference.

Gerald Dzakowic, Lawrence Livermore Laboratory – How high a temperature difference can the Comprex machine tolerate across the unit? Will you eventually become radiation limited?

Answer: Yes, I'll become radiation limited at about 5000°K. Remember, when we expand the gas into the Comprex its ambient temperature, in the Comprex, is quite a bit lower. However, the time that the gas is at stagnation at 5000°K is very small and the radiation transfer will be significant at that temperature. We haven't done all the numbers yet, however. But a good point to mention is that at some temperature we are forbidden to use high molecular weight gases since they are great radiators.

Gary Russell, J. P. L. – Abe, as I remember, you applied that concept at Cornell to heat wind tunnels. Was the motivation the same or was it just an inexpensive approach to that problem?

Answer: Well, there was no other way to get air at 5000°K, 1500 psi total pressure. And, by the way, there still isn't – we've done better in an arc but not at those pressures. Nobody has been able to hit stagnation temperatures like that. In fact, we never found anything that would stand up to that blast coming out. Nothing!

OPTIMIZATION OF ENGINES OPERATED REMOTELY BY LASER POWER*

Max Garbuny and M. J. Pechersky

Westinghouse Research Laboratories

INTRODUCTION

The concept of converting electromagnetic energy, such as from solar or microwave power, remotely into work has been considered for several decades. Only recently, however, have such conjectures approached feasibility due to the availability of laser beams with aperture – limited directivity and enormous power flux densities. There exist three basic alternatives for the conversion of laser energy into mechanical work by an engine. These are, in ascending order of intricacy, as well in degree of utilization of the coherence properties of the laser, the following: (1) the boiler approach in which laser power is applied externally to a heat reservoir just as fossil fuel to a steam engine; (2) internal heating of a working fluid by resonance absorption of laser radiation admitted through a suitable window; and (3) selective resonance excitation of a single degree of freedom without increase of the translational temperature.

Clearly, aside from the optical beam tracking problem, the first approach reverts to the case of conventional engines. It should be noted that because thermal materials limitations and reradiation limit the temperature of the heat reservoir, an important advantage of laser radiation is forfeited. As will be shown, this disadvantage is, at least in principle, avoided in the second method (ref. 1). Furthermore, although this approach amounts to a mere modification of conventional engines, it lends itself to types of operation not achievable in ordinary heat-to-work converters. This leads to new considerations of engineering thermodynamics, and the scope of this paper is in the main limited to them. The third approach, first suggested in the concept of the *photon engine* (refs. 2 and 3) is conceptually more profound. However, it is a field by itself. Moreover, the practical realization of its various alternatives encounters obstacles which may prove insurmountable.

GENERAL FEATURES OF LASER ENGINES

Engines of the second type, that is, those in which laser radiation is absorbed by the molecular resonances of a gas, converted into translational heat, and thus used to perform mechanical work, are in the following referred to as laser engines. In principle, any conventional engine which can admit radiation through a window to a working fluid, can be modified for this purpose. There exist now several types of lasers that can deliver, or promise to deliver, high powers in pulsed, continuous, or shaped-pulse operation. Examples are the gas lasers based on CO_2 near 10 μ, CO near 5 μ, HCl near 3.5 μ, and HF near 2.8 μ. The wavelengths of these lasers can be matched with the resonances of many gases, cross sections of absorption varying from 10^{-19} to 10^{-17} cm^2 or more. Thus absorption is nearly complete at 1 atm over path lengths that may be as short as 0.1 mm or less or, admixed at 1 volume percent to a nonabsorbing gas, over 1 cm or less. The working fluid

*This study was supported by Ames Research Center, NASA, Moffett Field, California.

may therefore be a monoatomic gas with its $K = c_p/c_v = 1.666$. In addition, such gases as helium were found to have a fast quenching effect so that the time in which the vibrational excitation is dissipated into a thermal equilibrium is negligible compared with that of the pertinent engine cycle.

The maximum achievable temperature in such an engine deserves some discussion. The laser, in principle, is a source of infinite black body temperature. An absorbing gas, again in principle, could also reach an infinite temperature. There are, of course, material restraints, but these will be considerably less than in the boiler appraoch. A gas mixture, as described in the previous paragraph, has a negligible coefficient of thermal emission throughout the spectral range of interest, including the resonance line. Thus the temperature the gas can reach, or is allowed to reach, is determined by other factors. These are considered in the following:

1. Engine walls will not tolerate temperatures much in excess of about 2,000°K. However, in certain configurations, such as that of a piston cylinder, the laser radiation may be focused into a smaller space well shielded by the surrounding gas from the walls. Thus an effective temperature may be reached which is much higher than that which the walls can tolerate.

2. Bleaching, that is, the production of equal populations in the upper and lower levels of the absorbing transition occurs at sufficiently high radiant flux densities so that radiation is no longer absorbed. These power levels, however, increase with the rate of quenching and lead to a temperature limit much higher than that determined by the other factors.

3. Thermal saturation of the upper level leads to an effect similar to bleaching. Specifically, in thermal equilibrium, the ratio of upper level populations n_2 and lower level populations n_1 is given by $n_2/n_1 = (g_2/g_1) \exp(-h\nu/kT)$. One can thus define a limiting temperature T_s at which $h\nu = kT_s$ so that appreciable reduction of absorption occurs; (that is, neglecting the ratio of the statistical weights g. Except for the effect of the statistical weights, T_s is characteristic to some extent of the laser wavelength rather than of the absorbing molecule. Values of T_s for the lasers mentioned before and their wavelengths are listed in table I. As defined, the values of T_s provide only an approximate value for the temperatures at which absorption is significantly reduced. For example, for $g_1=g_2$, the absorption cross section of an ideal two-level system decreases to 0.46 of its value at low temperatures, but will be lower for a multi-level molecule.

4. Dissociation is a third cause for the reduction of absorption at elevated temperatures. The last column of table I shows the dissociation energies (ref. 4) of some gases resonant with the wavelengths of the four lasers cited. These values provide only a guide for the comparison of various gases. The rate, as well as the equilibrium value, of dissociation as a function of temperature still depend on other parameters, notably the collision rate and cross section.

Nevertheless, one can conclude on the basis of these considerations that laser engines can operate with effective temperatures between 2,000° and 3,000°K, if lasers with wavelengths shorter than about 5 μ are used as radiation sources. There are two additional features that set laser engines apart from ordinary heat-to-work converters, at least when applied in combination. The first is the application of an essentially monoatomic gas as working fluid. The second feature is the option of the pulse shape. In the internal combustion engine, for example, power is applied in pulses; but the working fluid is, of necessity, a polyatomic gas mixture.

THE LASER PISTON ENGINE AND THE OPTIMIZATION OF ITS OPERATION

Schematic diagrams of laser piston engines, including one for experimental use in a simplified version, are shown in figure 1. In addition, figure 2 shows certain optional features such as a change of absorption cross section, hence of depletion depth, by frequency shift as the laser pulse develops and also the method of focusing the laser radiation into a smaller space within the cylinder volume. The P–V diagram of the engine in figure 3 shows four steps of the simplified cycle: (1) isochoric pressure increase as the laser pulse arrives; (2) adiabatic expansion (2 – 3) performing external work; (3) isobaric compression which restores the initial temperature T_1; and (4) isothermal compression (4 – 1) which restores the initial volume V_1 at the starting point 1.

The performance of the engine depends, first of all, on its (theoretical) thermal efficiency η, defined by

$$\eta = 1 - \frac{\Sigma Q_{out}}{Q_{in}} \tag{1}$$

or, alternatively, by

$$\eta = \frac{\phi \delta W}{Q_{in}} = \frac{W_{out} - \Sigma W_{in}}{Q_{in}} \tag{2}$$

where Q_{in} represents the heat provided by the laser, ΣQ_{out} the heat rejected by the engine, and $\phi \delta W$ represents the sum of the positive and negative work terms.

The actual efficiency depends also on the efficiency of the work terms, that is, the losses encountered in isobaric and isothermal compression, as well as in the expansion step. A practical merit factor is given by the work ratio r_w, defined as

$$r_w = \frac{W_{out}}{\Sigma W_{in}} \tag{3}$$

Thermal efficiency and work ratio are best expressed in terms of the ratios $A = V_3/V_1$ (that is, the ratio of the volumes after, and before, the expansion step 2 – 3) and $B = T_2/T_1$ (that is, the ratio of the temperatures after, and before, the heating step 1 – 2). One has then

$$\eta = 1 - \frac{Q_{3-4} + Q_{4-1}}{Q_{in}} = \frac{C_p (A^{1-K} - B^{-1}) + RB^{-1} \ln (A^K/B)}{C_v (1 - B^{-1})} \tag{4}$$

and

$$r_w = \frac{(C_v/R)(1 - A^{1-K})}{A^{1-K} - B^{-1} + B^{-1} \ln (A^K/B)} \tag{5}$$

Once the maximum permissible temperature ratio B and a monoatomic gas are chosen, the only adjustable parameter is the compression ratio A. From equation (4) the maximum thermal efficiency is derived for the condition

$$A^{K-1} = B \tag{6}$$

It is easy to show that this amounts to the condition that $T_3 = T_1$, (that is, that the heat received by the engine in step 1 – 2 is equal to the work of expansion 2 – 3. By introducing equation (6) into equation (4), one obtains the maximum thermal efficiency

$$\eta_{max} = 1 - \frac{\ell n\, B}{B-1} \tag{7}$$

Conservative choices of T_1 and T_2 are, respectively, 300° and 2,000°K so that B = 6.67. We obtain then from equation (7), $\eta_{max} = 67$ percent.

Note that the maximum efficiency depends only on B and not even on the ratio K of specific heats. Thus this efficiency should be obtainable also for polyatomic gases. However, this can not be achieved for them because of equation (6). Since $A = B^{1/(K-1)}$, they require at least a compression ratio of 246, whereas monoatomic gases require only that A = 17.2.

The work ratio at maximum thermal efficiency follows from substitution of equation (6) in equation (5). In combination with equation (7), one obtains then the relationship between work ratio and maximum thermal efficiency

$$r_w = \frac{1}{1 - \eta_{max}} \tag{8}$$

One can quite generally show that equation (8) is equivalent to the condition $Q_{in} = W_{out}$. Since

$$W_{out} - \Sigma W_{in} = Q_{in} - \Sigma Q_{out} \tag{8}$$

one obtains then from equation (1):

$$\eta = 1 - \frac{\Sigma W_{in}}{W_{out}} = 1 - \frac{1}{r_w} \tag{9}$$

which is the statement of equation (8).

If we ask, independent of the thermal efficiency, for maximum work ratio r_w, one obtains a different value for A. Figure 4 shows a graph of r_w vs. A obtained with equation (5) for B = 6.666. One obtains a shallow maximum at A = 7 that is only about 10 percent larger than the value $r_w = 3$ at maximum thermal efficiency. Because r_w is nearly constant around that point, the optimized laser energy operates under the condition given by equation (6). The P–V and T–S diagram show then a particularly simple form, since the isobaric compression step has vanished (see figs. 5 and 6).

C-3

BRAYTON AND STIRLING CYCLES

We have performed a similar analysis for the laser powered turbine and Stirling engine. The conditions of the Brayton cycle are summarized in Figure 7. While the efficiency η is fixed for a given temperature ratio T_2/T_1, a maximum work ratio is obtained when

$$r_w = \frac{1}{1 - \eta} \tag{10}$$

as before.

The laser powered turbine operates with continuous wave (cw) radiation. The turbine, however, requires *a priori* larger powers than the piston engine.

The Stirling engine can be embodied in a variety of designs. One that appears particularly suitable for modification to laser power is shown in figure 8 and 9 (originally a Phillips, Eindhoven design). The theoretical thermal efficiency is that of the Carnot engine, and the work ratio is related to it by equation (10) see (fig. 10).

REFERENCES

1. Garbuny, M.: Laser Engine Operating By Resonance Absorption. NASA Ames Research Center. Laser Energy Conversion Symposium, NASA TM-X-62269, 18-19 Jan. 1973, p. 45-50.

2. Hertzberg, A.: The Photon Engine. ibid. p. 34-44.

3. Christiansen, Walter H.; and Hertzberg, Abraham: Gasdynamic Lasers and Photon Machines. Proc. IEEE, Vol. 61, no. 8, Aug. 1973, p. 1060-1072.

4. Gaydon, A. G.: Dissociation Energies and Spectra of Diatomic Molecules. 2nd rev. ed., Chapman and Hall LTD, London 1953.

TABLE 1. – VALUES OF T_s

Laser	Wavelength, μ	$h\nu$, eV	$T_s = h\nu/k$, °K	Absorbing gas	E_{diss}, eV
CO_2	10.6	0.11	1,300	SF_6	3.13
CO	4.7	0.26	3,000	CO	11.1
HCl	3.5	0.35	4,100	HCl	4.4
HF	2.8	0.44	5,100	HF	5.9

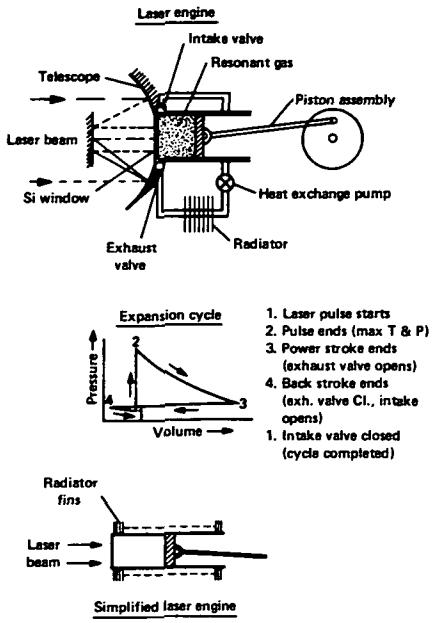

Figure 1.– The laser engine and PV diagram.

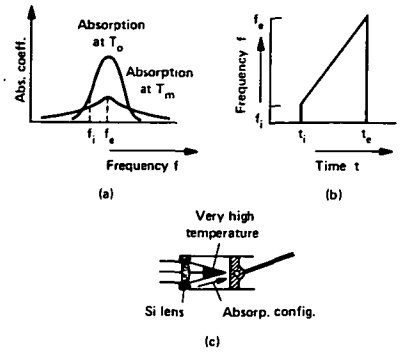

Figure 2.– Alternative details of operation.

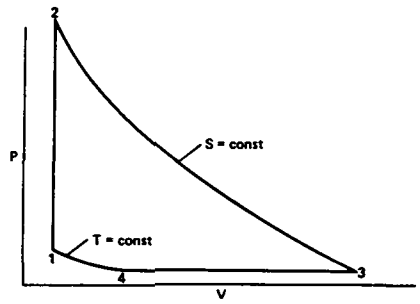

Figure 3.– Laser piston engine (not optimized).

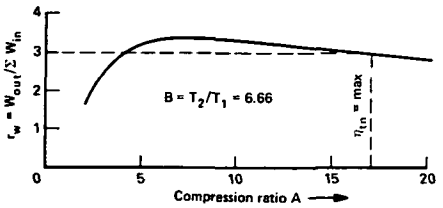

Figure 4.– Work ratio vs compression ratio in laser piston engine.

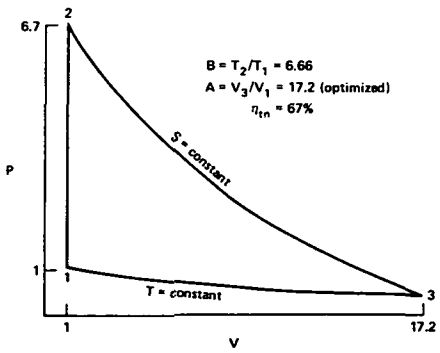

Figure 5.– PV diagram for the pulsed piston laser engine.

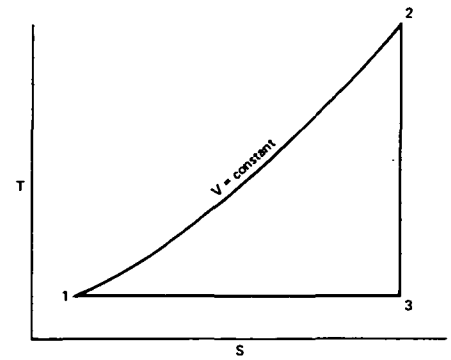

Figure 6.– Temperature-entropy diagram for the pulsed piston laser engine.

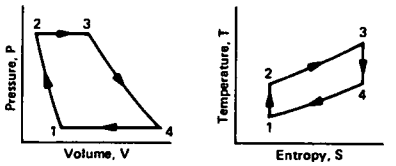

Figure 7.– The Brayton Cycle.

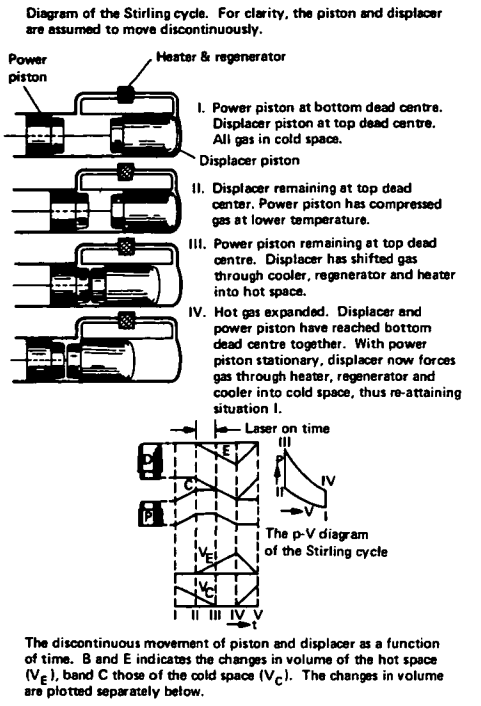

Figure 8.– The Stirling engine.

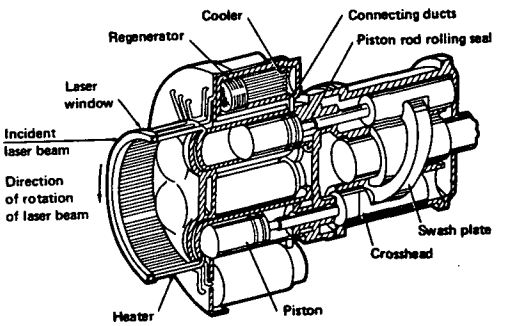

Figure 9.– Laser-driven Stirling engine.

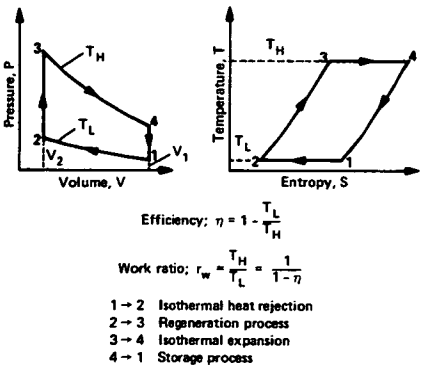

Figure 10.– Thermodynamic cycles for the Stirling engine.

DISCUSSION

Ken Billman, NASA Ames Research Center – Max, it was not apparent to me why you have concentrated on the piston engine. In other words, why is the turbine not a viable alternative?

Answer: Well, actually it is. In a long term approach, however, we are restricted with maximum turbine blade temperatures of 2000°K. In the near term approach, we looked into various turbines and found that they require much higher power than those around the laboratory, that is, 20 to 30 kW. But the real reason is, of course, that although they run CW, we will have to get around the turbine blade problem.

Ned Rasor, Rasor Associates – I think you showed a 67 percent thermodynamic efficiency. How does that translate into overall efficiency, or is that the overall efficiency?

Answer: No, we don't claim that we have achieved it – it will be the case when it is built. This is our hope and aim, if we can work at this temperature.

Dick Pantell, Stanford University – You described that the third approach, direct use of vibrational energy, suffered from the engineering problem of separating the upper and lower energy states?

Answer: Well, actually I must confess that I haven't considered using inhomogeneous fields for separation.

Dick Pantell, Stanford University – Yes, that is what I was going to suggest – to use inhomogeneous electrostatic fields.

Answer: Yes, it may work, but it seems to be beset with great complexity. I believe a wise man would not undertake such a scheme easily.

Abe Hertzberg, University of Washington – Let me comment! Piston engines actually scale down better than gas turbines. There are good large piston engines, however, such as a good diesel engine which could have a thermal efficiency of 60 percent and maybe you have been working on something closer to the Sargent cycle which will be a little higher. But the real efficiencies tend to be closer to 37 percent. This is due to the pumping work, friction, and so on.

Answer: Yes, but it's a "bird in the hand".

Abe Hertzberg, University of Washington – Oh yes, I agree.

Max Garbuny: Incidently, I might mention here something that I glossed over – the window problem. As was mentioned at the last meeting, it must handle these temperatures with good transmission and strength. Well if we go to CO wavelengths, we can solve this with the marvelous material: sapphire which can handle something like 170,000 lbs/in^2 pressure. So this problem can be solved.

INITIAL EXPERIMENTS WITH A LASER DRIVEN STIRLING ENGINE

Robert L. Byer

Stanford University

ABSTRACT

During the spring and summer of 1974 three students,* taking my Quantum Electronics Laboratory Course, and I set out to build a laser driven engine. To our delight we succeeded for a brief time in driving a Beale free piston Stirling engine with a 40-W CO_2 laser. I have no doubt that our initial experimental success is but a first step in efficient energy conversion of laser radiation by engines.

INTRODUCTION

The ability to transform energy from one form to another has fascinated engineers for over a century. Although our preliminary experiments were motivated by the thought of transmitting energy over great distances by a beam of light and then efficiently converting the received energy to electricity, we are not the first with such a dream. Figure 1 shows an early solar driven steam engine exhibited at the Paris World's Fair by Mouchot, nearly 100 years ago (ref. 1).

We became interested in the possibility of demonstrating a laser-driven engine following the pioneering work of A. Herzberg et al (ref. 2). Unfortunately, the photon engine in the form described by Herzberg proved to be unrealizable in practice (ref. 3). Thus the problem of actually constructing a laser driven engine remained unresolved. As sometimes happens, a chance remark by Max Garbuny of his work on the problem (ref. 4) renewed our interest and led to ideas about new ways to overcome the experimental difficulties. Our experimental constraints of low available CO_2 power and a requirement for closed cycle operation led to consideration of a Stirling engine. Fortunately, Stirling engines have been extensively reviewed recently (ref. 5) and a number of design alternatives are possible. The elegantly simple free-piston Stirling engine invented by Professor W. T. Beale of the University of Ohio seemed to meet our needs. A call to Professor Beale** led to the purchase of a single piston, closed-volume demonstration engine with drive power requirements between 30 and 50 W. After modifying the engine by adding a window to transmit CO_2 laser radiation we arranged to borrow a 40 W CO_2 laser and begin our investigation.

---

*Chuck Hawley, David Moore, and James Phillips, graduate students, Applied Physics Department, Stanford University.

**Professor W. T. Beale of Sunpower Incorporated, Athens, Ohio.

BEALE FREE PISTON STIRLING ENGINE

Figure 2 shows a schematic of a small free-piston Stirling engine designed to produce useful work by pumping water through a simple check valve arrangement. The engine consists of a displacer piston and an engine piston which is coupled to an inertia mass load which drives the pump ram. The expansion space at the end of the displacer piston is heated and the compression space between the displacer and engine piston is cooled for operation. The engine is filled with air or helium to between 2 and 4 atm. For the laser experiments, a transmitting window was added at the end of the displacer cylinder to allow direct heating of the gas in the expansion space volume by the laser radiation.

The operating cycle of the Beale free piston Stirling engine is shown in figure 3. The illustrated cycle is representative of the engine's performance as determined in detailed studies by Agbi (ref. 6). Figure 4 shows the oscillating frequency, power output and operating efficiency (percent) of our particular engine operating under the conditions indicated with air as the working gas. The 2.5 percent thermal efficiency is quite good for such a small engine with relatively large losses due to mechanical resistance and thermal conduction (ref. 7). However, it is by no means a limit as Agbi has obtained efficiencies of up to 8 percent with air and 13 percent with helium as working gases in a similar engine.

The oscillating frequency of the engine is given by (ref. 6)

$$f = 0.7 \left(\frac{A^2 P_o \gamma}{V M} \right)^{1/2} \qquad (1)$$

where A and V are the piston area and working space volume, M is the oscillating mass, P_o the charge pressure, and $\gamma = C_p/C_v$. Our engine operated at near 11 Hz but higher frequency operation is possible. Higher frequency oscillation would allow the use of a linear alternator in place of the water pump to efficiently couple power from the engine as direct electrical output.

The Beale engine operates with a sealed closed volume of gas. Furthermore, it is a simple mechanical device without gears, valves, or bearings and thus offers the possibility of lubrication-free long operating life. Finally, direct mechanical to electrical generation is possible with a simple linear alternator arrangement. These advantages make the Beale type engine ideal for conversion of small powers such as in solar power conversion or artificial heart pumps (ref. 6).

LASER EXPERIMENTS

Prior to operating the engine with a CO_2 laser source, we performed linear absorption measurements on helium – SF_6 gas mixtures. Our preliminary measurements showed that 100 torr of SF_6 in 1 atm of helium was adequate to absorb the CO_2 incident beam in less than a 1-cm path length. We arranged a gas manifold system that allowed introduction of SF_6, He, and CO_2 to the engine at a total pressure up to 4 atm.

Our initial irradiation of the engine with a 40-W CW CO_2 beam immediately broke the salt input window. After replacing the window we began more cautiously by first electrically heating the engine to near its operating temperature and then applying the CO_2 laser beam. Under these conditions the engine operated for a few minutes before the salt window again cracked. However, inspection of the window showed that the inner surface next to the engine's heated gas had melted and then cracked from thermal stress. Unfortunately, the CO_2 laser was available for only a very short time and there was no alternative but to continue with the experiments using salt windows.

These early results raised some questions about the engine's operation that prompted further study. The questions included whether the cylinder walls had to be hot for engine operation or whether a hot gas was sufficient. Also, was the SF_6 – He gas mixture being directly heated by the CO_2 laser radiation or being heated indirectly from a hot window or displacer piston? Finally, was the gas mixture optimum?

Further testing and then a call to Professor Beale verified our suspicion that the cylinder wall did have to be heated to a temperature near 200°C for engine operation. A cold wall leads to gas quenching and non-ideal circulation by the displacer piston. We therefore arranged to heat the cylinder wall.

To check whether the gas was being heated directly by absorption, we attempted to operate the engine without the SF_6 dopant in the helium. The engine did not run and furthermore, the displacer piston did not even respond to a sudden turn-on of the CO_2 laser beam. These results indicate that gas absorption was responsible for the engine's operation.

The ideal gas mixture was more difficult to determine given the short operating times between window failure and a lack of a quantitative engine performance measurement. However, the engine did seem to perform better with SF_6 dopant, 1 atm of CO_2, and the balance of helium up to a total pressure of 4 atm. The engine would also run without SF_6 at 1 atm of CO_2 plus 3 atm of helium. However, the engine would not run on CO_2 alone presumably due to the incorrect viscosity for the 0.010-in displacer piston to cylinder clearance.

As a final experiment, we operated the engine with a chopped CO_2 laser beam. A variable speed chopper allowed operation at a 50 percent duty cycle at chopping frequencies from above to below the engine's resonant frequency near 11 Hz. The engine showed a definite resonance when pumped by radiation chopped near its resonance frequency and operated poorly when pumped only slightly off resonance. It ceased to run when pumped at a very high chopping frequency or at a very low chopping frequency. These observations indicate that higher efficiency operation may be possible by driving the engine with pulsed laser radiation at a pulse rate nearer the engine resonant frequency.

The lack of time and also of salt windows prevented further, more quantitative work with the laser driven engine. However, for demonstration purposes the engine will operate with a 35 W average power alcohol lamp which heats a brass plate in place of the salt window.

CONCLUSION

It is interesting to speculate about the future of laser energy conversion by engines. If the initial negative reaction to energy conversion using such a mundane device as an eighteenth century engine is overcome, then the approach is seen to offer a number of advantages. First, a laser driven engine should operate at greater than the 40 percent conversion efficiency which is now obtainable from 160 hp (0.122 MW) conventional Stirling engines (ref. 5). Secondly, closed cycle operation allows optimization of the gas mixture for both absorption of the laser radiation and engine operation. Thirdly, the engines can be very simple in construction, small in volume and lightweight per unit of output energy.

There are limitations, however, that arise due to the use of the laser as the energy source. These include window damage problems, gas absorption, saturation and dissociation, and mechanical vibration due to engine operation.

High power infrared window materials have been extensively investigated and their power and energy density limits are now known (ref. 9). With the exception of diamond and sapphire, infrared windows of salt or semiconductor materials withstand up to $1 - 10\ kW/cm^2$ of continuous power density. The small size of available diamond windows may limit their use, but diamond can withstand over $2\ MW/cm^2$ of continuous intensity at $10.6\ \mu$ (ref. 10). Sapphire is nearly an ideal window material for wavelengths less than $5.5\ \mu$, because of its mechanical strength as well as optical quality.

If higher intensities could be handled by the window materials, such intensities would probably not be useful anyway because saturation and dissociation become important at intensities even less than $10\ kW/cm^2$. For example, Karlov et al. (ref. 11), have shown that $BC\ell_3$ and SF_6 are more than 97 percent dissociated at an incident CO_2 laser intensity of $10\ kW/cm^2$. In this regard CO may prove to be an optimum engine fluid due to its high dissociation energy. Finally, at high gas temperatures absorption bands begin to become transparent due to the reduced population. For example, CO_2 absorption coefficients for the $9.6\ \mu$ and $10.6\ \mu$ bands peak at $0.04\ cm^{-1}$ at 900°K and fall to approximately $0.01\ cm^{-1}$ by 1500°K (ref. 12).

In spite of these limitations the laser-driven engine does offer the possibility of efficiently converting absorbed laser energy to either mechanical or electrical energy. The efficient operation of a heat engine through laser heated gas is not accidental. Under most circumstances of interest, the heat engine cycle times are long enough to allow vibrational to translational energy conversion but short enough to prevent excessive heat losses due to thermal conduction to the walls.

With very high average power lasers now available, remote power transmission and conversion are indeed possible. Stirling, or perhaps Brayton cycle engines, offer an attractive alternative to efficient remote energy conversion. Closed-cycle operation, long life, inexpensive construction, and size scalability to 100 MW are significant potential advantages. Our preliminary experimental results show that nineteenth century heat engines may fulfill a twentieth century energy conversion need.

Acknowledgement – We wish to express our gratitude to Coherent Radiation Laboratory of Palo Alto, California, for providing the CO_2 laser.

REFERENCES

1. Wolf, Martin: Solar Energy Utilization by Physical Methods. Science, Vol. 184, 19 Apr. 1974, p. 382-386.

2. Hertzberg, Abraham; Christiansen, Walter H.; Johnston, Earl W.; and Ahlstrom, Harlow G.: Photon Generators and Engines for Laser Power Transmission. AIAA Journal, Vol. 10, no. 4, Apr. 1972, p. 394-400.

3. Begley, R. F.: A Thermodynamic Analysis of a Closed Cycle, Gas Dynamic CO_2 Laser. Department of Applied Physics, Ph.D qualifying orals, 8 Jan. 1973.

4. Garbuny, M.: Laser Engine Operating by Resonance Absorption. NASA Ames Research Center. Laser Energy Conversion Symposium, 18-19 Jan. 1973, NASA TM-X-62269, Jan. 1973.

5. Walker, Graham: Stirling Cycle Machines. Clarendon Press, Oxford 1973.

6. Agbi, Babatunde O: Theoretical and Experimental Performance of The Beale Free-Piston Stirling Engine, M. Sc. Thesis, University of Calgary, Canada, Faculty of Engineering, Dept. of Mechanical Engineering, 1971.

7. Scott, David: Flame Powered Push-Pull Generator. Popular Science, Vol. 206, no. 2, Feb. 1975, p. 82, 134.

8. Glass, Alexander J.; and Guenther, Arthur H.: Laser Induced Damage in Optical Materials. Washington, National Bureal of Standards, 1972. (NBS Special Publication, 372).

9. Douglas-Hamilton, D. H.; Hoag, E. D.; and Seitz, J. R. M.: Diamond as a High-Power-Laser Window. Journ. Opt. Soc. Am., Vol. 64, no. 1, Jan. 1974, p. 36-38.

10. Karlov, N. V.; Karpov, N. A.; Petrov, Yu. N.; and Stel'makh, O. M.: Dissociation and Bleaching of a Multilevel Molecular Gas by High Power CO_2 Laser Radiation, Soviet Physics: JETP, Vol. 37, no. 6, Dec. 1973, p. 1012.

11. Strilchuk, A. R.; and Offenberger, A. A.: High Temperature Absorption in CO_2 at 10.6 μm, Applied Optics, Vol. 13, no. 11, Nov. 1974, p. 2643-2646.

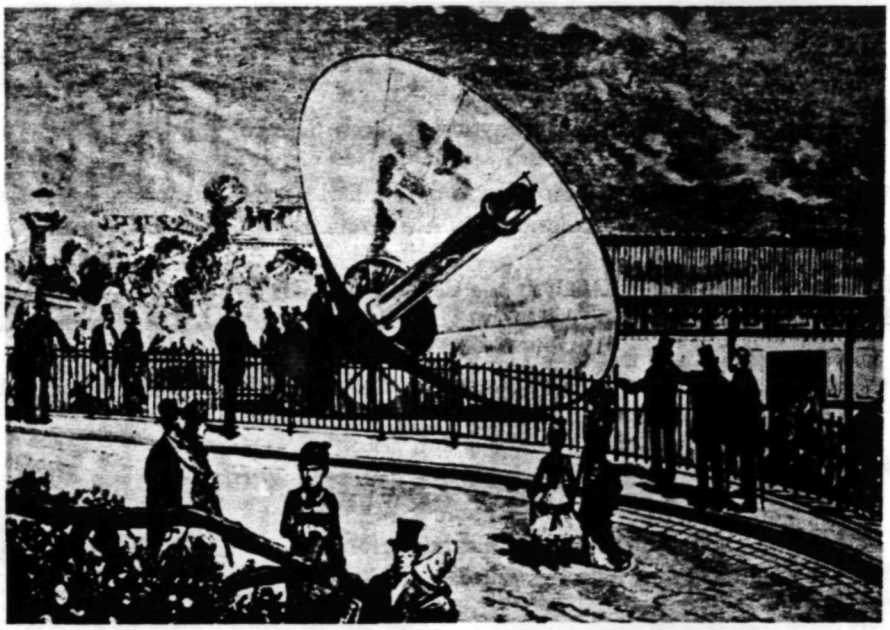

Figure 1.– A solar driven steam engine exhibited at the 1878 Paris World's Fair by Mouchot.

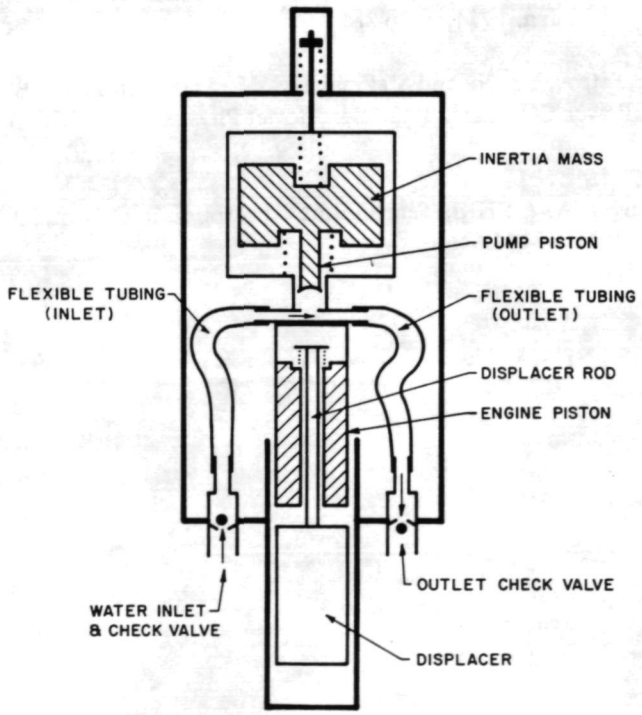

Figure 2.– A schematic of the Beale free piston Stirling engine.

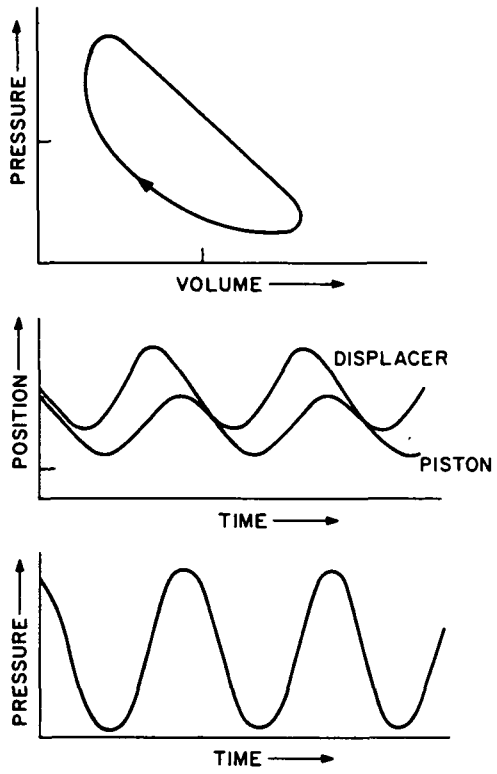

Figure 3.– Operating cycle, displacement of piston and pressure *vs* time for the Beale engine.

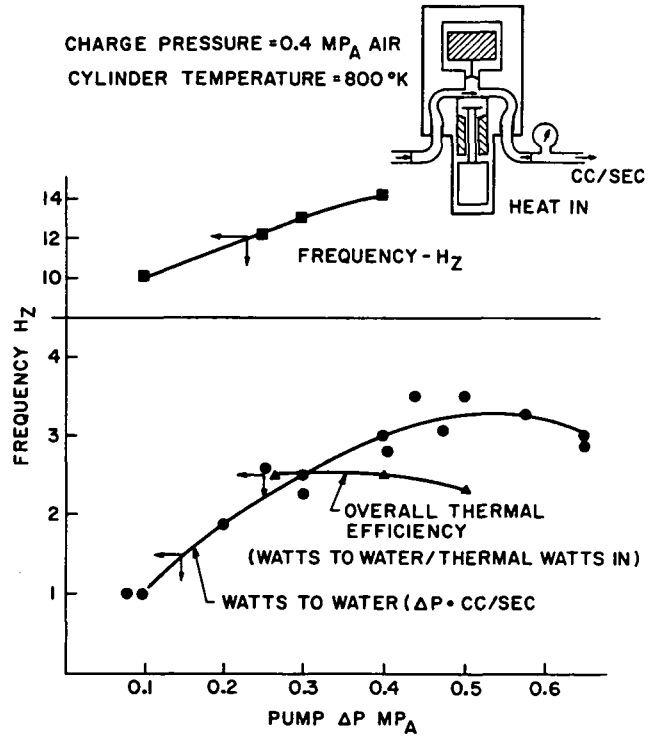

Figure 4.– Oscillating frequency, power output, and operating efficiency (percent) of our engine.

DISCUSSION

Ned Rasor, Rasor Associates – Are you familiar with the engine they worked on at McDonald-Douglas for the artificial heart program?

Answer: Yes, that is a closed cycle Stirling engine also. It differs a little from ours. The general schematic of this type of a Stirling engine has three volumes: a volume between your displacement piston and your heat source, which is your compressor volume, a volume between your working piston and your displacer piston, which is the cooled volume, and then you need the bounce space.

Ned Rasor, Rasor Associates – His engine puts out about 5 to 10 W and they are pushing 20 percent efficiency now.

Answer: Yes, that's about what the best of these run at. I should mention that 2 years ago, NASA, in conjunction with the Navy, did a very detailed study on engines to operate in closed environments, such as in submarines. They looked at 1 to 10 kW Stirling engines versus diesel engines versus other types of cycles. That is where I got the number of 40 percent loaded efficiency for the Stirling engine. And, indeed, engines have been built such as the work by the Phillips Company in the Netherlands, where 40 percent efficiency has been attained.

Don Nored, NASA Lewis Research Center – Just a comment on the thermodynamic diagram you showed where you said that sharp corners could not be attained in practice. We have worked on concepts, such as switching valves, which can help get rid of that.

Answer: Yes. The one thing I liked about the Beale engine is its utter simplicity but it does, therefore, suffer in efficiency. But for the type of device that you can consider sealing up in a stainless steel can and carrying it anywhere in the world you want, bouncing it in the Sahara, etc., and all you have to do is put helium in one end and it works – I think he has a lot of thought behind this type of construction.

Dick Pantell, Stanford University – You mentioned that Professor Beale designed this engine to work on solar energy. How does it operate in that mode? And does it have high efficiency?

Answer: Exactly like it's set up here. Right now, he has not yet produced an actual engine to fit that market. There is a capital cost problem. That is, a couple of square meters of collector are needed which together with an engine like this, to pump water in the desert, would cost approximately $1000. For those in India or the Sahara, this is an enormous investment. So as of yet there is not a market for this device.

Gary Russell, J. P. L. – I think its a sobering thought that it has taken us 4 years to get 30 W of green light that your alcohol burner, which you used to demonstrate the operation of the Stirling engine for us, puts out!

Abe Hertzberg, University of Washington – Gentlemen, I would like to suggest that we members of the panel make brief statements and then see if we can start a dialogue with the floor.

Max Garbuny, Westinghouse – In looking through the proceedings, I had a few surprises. Many things have moved along beautifully. One thing, for example, that is of personal interest, is the possibility of remote laser chemistry. One idea might be, for example, a laser dissociation engine. I imagine that I have a gas such as $Fe(CO)_5$ which dissociates with low energy IR photons. Thus by remote laser action we can increase the gas pressure by dissociation and we do not need high temperatures or conversion to translational molecular energy. I should point out, of course, the need for narrow bandwidth lasers for these laser chemistry processes. Perhaps on another occasion we should discuss this interesting field further! There were other interesting things on the agenda, such as the harmonic and sum frequency generation which may allow new converters to be used. I was particularly impressed by the laser-electron beam interaction work. Although it is not yet to the point of giving useful power, conceptionally it is a very interesting idea. I was also particularly impressed by the laser talks. Tunable IR lasers, such as proposed by Drs. Hess and Javan, where high pressure broadens the lines into bands, is of notable interest since it leads to tunable IR and at high powers. These things, and of course it goes without saying – the work on conversion to translational energy – were of great interest.

Ned Rasor, Rasor Associates – Being an engineering physicist I have an interest on both sides on all these interesting effects discussed. But my engineer side prompts me to say that perhaps someone is *really* going to need laser energy conversion someday! In fact, I think this feeling also hit Ken Billman when he wrote the letter of invitation to the authors saying that he wanted hard engineering data this time. If you look at the things that are ready for engineering – for example, if you would be on a wartime basis where, like the needs of the British in the radar area during World War II, and you had to use them very quickly – just how many things are like that at this conference? Of course there are conventional engines – you can get the Phillips Stirling engine or get a Brayton cycle engine from NASA Lewis, etc. But suppose those didn't do the job, for some reason, and you needed tomorrow's work today. What could you really push into use? Well, solar cells, if they could work at high temperatures and you used large arrays, are indeed a "bird in the hand", as are the conventional engines. I look over the rest of the things and, strangely, I find only the thermionic converter to really be in this category, if you really had to do it! Thermionic converters *are* producing power right now in a Russian reactor, as we would also be doing if the funding hadn't been lost when NASA dropped its nuclear energy program. But what are other alternatives. Fortunately, in the laser energy conversion program we have, as we have done in this meeting, the option of looking at all the possibilities. It seems that at each meeting people come up with a rediscovery of another old principle. Dr. Garbuny, Dr. Hertzberg, and I were talking about the fact that what you really want to do, if you cannot use a photon effect, that is, you are going to have to live with the Carnot theorem, is that you have to add the heat at high temperatures. In the thermionic case that's saying you are working with the electron gas rather than heating a metal.

At the conference 2 years ago, there was an interesting experiment explained in which a Russian scientist generated radiation to attract bugs by placing metal whiskers in a jar of silicon oil and applying an oscillating electric field. This aligned the whiskers and they radiated as simple diodes. Now the worry I have about printing up millions of optical diodes for laser energy

conversion is that it will be impossible on that scale and especially since they will have to be done in depth to achieve high cross section. But this whisker device might be worked in the inverse – using whiskers round on one end and pointed on the other, aligned by the electric field. When irradiated they will field emit for one direction of the optical field but not the other and thus you have a high voltage converter. I bring this up because the kinds of things I heard here stimulated me to think of such things. I hope everyone else here had the same thing happen to them. Furthermore, I hope the people who can affect the money will read the proceedings and similarly be stimulated.

Dick Stirn, J.P.L. – Well, I would like to say that I was pleasantly surprised. We heard about adaptive optics and Abe showed us that he was adaptive also! I have to agree with Ned, that, compared with 2 years ago, we have generated some more ideas and, for Ken, there has been some hard engineering data. In fact, it is much more than I had expected to see in 2 years. I do think we are getting to the point where the Centers have to begin sharing this data and, for example, Don should tell us some of the parameters that are necessary to optimize certain applications. For example, what is the energy density we must operate with? This is important – photovoltaics may work in one region but other techniques are necessary for higher intensity. Are there applications that demand each of these? I think that the photovoltaics can work in the short term with a little more engineering. For latter applications, perhaps some of the more esoteric ideas will be useful. So the main point I would like to make is that we need to define more closely the operating parameters of the device. When the power density is defined, we can begin to engineer our devices to a potential mission.

Joe Lundholm, NASA Headquarters – I believe Dick's comment about now needing more coordination between the Centers is well taken. In the last 2 years the program has moved forward and now we have moved from the organization stage to an accomplishment stage. Carl Schwenk, incidentally, agrees and believes more meetings between the Centers would be very useful.

I believe the type program that Ken put together was a good one – covering the gamut from far out concepts to operating laser devices. Again, I would like to remind you to keep your eye on the timetable I showed yesterday. I should say that the philosophy of the Research Division at NASA Headquarters, which supports this work, is that we will work on research and technology and do everything possible to keep from getting bogged down in expensive systems development at this stage of the game. A lot of programs have been wrecked when they took off prematurely to get into systems. Fortunately, our philosophy appears to be followed by all of you.

Some new ideas have been introduced here. We look to the Centers to decide on which areas should continue to be funded or dropped and which should be added. Of course, they are operating on a pretty well fixed funding level. So they must make the hard decisions on what concepts are funded or deleted.

In the near future we are going to *consider* whether we should be making systems and applications studies. Again, the Centers will guide us on this.

Again, I would like to urge you to keep a sense of urgency in mind and keep our major objectives in mind; to develop the technology required to provide the knowledge that we hope we will be needing to make some major decisions around the 1980 time frame. Hopefully some NASA missions will be identified at that time; perhaps 10 years will then be necessary to develop a prototype system and then in 1990 the flyable system will begin construction. Thus, perhaps in 1990 we can actually begin the use of our high power laser systems.

Abe Hertzberg, University of Washington – How to sum all this up! First, in reviewing the progress made in the last 2 years, I can't really say that we are there! But our technology base, and our understanding of what we can and cannot do has increased significantly. For example, consider adaptive optics. In the early days, when we realized that laser beams were more akin to searchlights than diffraction limited beams, the suggestion that we put a phase correction plate in the beam was rejected as being too complicated. Now we have gone a step beyond that and are talking about the reality of actual adaptive optics that vastly will extend the capabilities. We are starting to narrow down what can and cannot be done. But let me play the devil's advocate. Suppose we had a perfectly good laser today, running at 75 percent efficiency, reasonably compact, and we had a good converter running at 75 percent efficiency. Would we use it? I'm not sure I can answer that question. I can only point to the future and say that it's probable, and perhaps inevitable, that we will use it. A historical analogy is the repeating rifle in the Civil War. The concept was there, the technology was there, but the frame of mind of the engineers and military were against it. One general argued that too much ammunition would be wasted with a repeating rifle! Here we are also dealing with the future and developing its technology, but we are going to have to build also a readiness and need to accept it. I would like the audience to help us think of a way to "slide" into application. Of course war is always a hot house for technology – witness the development and universal usage of the gas turbine for aircraft during the war. But, in the absence of that, we will have to "slide" this new technology into usage in some simple way so as not to encounter the attitude that this is too radical – too new. We could, of course, set up laser power transmission systems to transmit significant amounts of energy with not intolerable efficiency. But who is going to buy it?

Joe Lundholm, NASA Headquarters – I reviewed with Dick Stirn recently the progress in the solar cell area. If you are a program manager for a spacecraft you will probably stick with solar cells because you know you can get them without a cost overrun. Only when enough engineering is done will a program manager risk something new, since in these days of tight money any overrun usually means that the spacecraft will just not fly.

I should also mention that we are getting some requests at Headquarters on what these systems will be able to do. That's a two-edged sword. If we maintain a low profile, an overall budget cut could end up eliminating the laser program. If we take a high profile, then when funds get short they might ask what are the attainable efficiencies? If the current value is low then, of course, again the program could be dropped. So we have to take the middle path.

Bob Hess, NASA Langley Research Center – Isn't one possibility to combine the laser energy experiments with other experiments which NASA wants to do anyway? For example, the shuttle is looking for experiments. Both atmospheric absorption measurements and communications experiments could, for example, also be used to study power transmission. This would gradually bring power transmission to the public.

Fred Hansen, NASA Ames Research Center – I think I can give an answer to Abe. Even if we had a good system right now, 80 percent efficient laser, 80 percent efficient converter, the present climate is that it would just not be used.

Abe Hertzberg, University of Washington – Yes, that is just my point.

Fred Hansen, NASA Ames Research Center – But some of the things that interest me in the program are the spin-offs. Two years ago we heard the beginnings of optical diodes and frequency

conversion. Now we are making such progress in these areas that we can see that they will revolutionize some of the basic physics that we do. Two similar things which we heard about at this meeting, and we may hear more about in 2 years, are high voltage ceramics and the electron-laser interactions. Both of these are very exciting and offer great possibilities. Although neither of these may be directly applicable to laser energy conversion, a program like this allows such ideas to have a focus, to percolate for awhile, and to develop. I'm not sure how we can get this across to administrators, however.

Tom Karras, General Electric – I might just comment that the military will probably apply some of these concepts – this will get NASA going. This has always been the case.

Abe Hertzberg, University of Washington – Yes, history shows that to be the case. For example, the nitrogen fixation process was developed to make explosives for World War I. But the ultimate use was for peaceful fertilizer production.

Ned Rasor, Rasor Associates – Actually there is a very real, and almost wartime like requirement now if you want to latch on to it – the energy requirement. One of the best insurances of this program, when someone asks "What are we going to cut?" is that you have "energy" as your middle name! I've seen a lot of this happening here already. When people gave their talks they said "Incidentally, this device or process could use solar radiation". An analogy is the semiconductor industry. Only one device coming out of Bell Labs. was able to guarantee the long-lived existence of the industry. Similarly, if one useful application in the area here were found, possibly in the energy area, it would quite likely guarantee the continued existence of the whole program.

Abe Hertzberg, University of Washington – I think you're right. Energy application is taking on a new importance. Ultimately we may use lasers for this purpose. For example, I don't see anything intrinsically wrong with the concept of a space borne nuclear reactor with a laser energy transmission system to the ground. But I just wonder about the mechanism of bringing into use a new technology – a technology that we are really not that far away from. Maybe sliding in through the military is the only way.

Don Nored, NASA Lewis Research Center – I think the propulsion area may offer a way to slide into it. The orbit to orbit application is one that could be done with foreseeable lasers. The military should be interested in another – the orbital drag make-up. As far as power transmission to satellites goes this faces a good competitor – solar cells. Most satellites want 1 to 2 kW and solar cells will do this. There is one thing, however, if you examine the NASA flights up through approximately 1990, there will be a total of about 419 flights. This will require about 1.8 billion dollars worth of solar cells – a very large amount of money just to build solar cells. So a low-cost converter could be attractive. There are all sorts of trade-offs – cost, weight, etc. We don't know all the answers yet.

Bob Hess, NASA Langley Research Center – Of course NASA is looking for Shuttle experiments. Wouldn't it just be possible to do a demonstration experiment? The efficiency would not have to be high – it would just demonstrate, with low profile – the possibilities in this approach.

Abe Hertzberg, University of Washington – I do agree, just because of NASA politics, we've got to tie it to the Shuttle.

Ned Rasor, Rasor Associates – Just so you are not riding on the anchor chain of the Titanic! Just remember what happened with thermionics. It was dropped because it was intuitively tied to the space nuclear program, which was dropped. So one has to show application in a number of areas.

Abe Hertzberg, University of Washington – Well, I have a high opinion of NASA management. They will attempt to keep the good parts of any program alive. But look, the first application of the laser will probably be in isotope separation. Its competition – diffusion separation – was a wartime emergency need which, if proposed today, would not be acceptable on energy considerations. So the laser will win this competition. It is an idea whose time has come. I think the laser power transmission will find that point in time. But I sure would like to know the way of edging it in. You must remember that a pure engineer is a very conservative fellow – ask him to change his viewpoint on anything he learned beyond his freshman year and you have an impasse. The aircraft industry is a classic example. Although the 747 was thought of as a tremendous advance, its swept wings, etc. are just scaled up from the 707.

Ned Rasor, Rasor Associates – Yes, remember the difficulty in getting commercial aircraft designers to accept the jet engine? They failed to see the advantages, such as extremely long, maintenance free, lifetimes of these devices. But your point is well taken, somebody has to take a risk.

Dick Stirn, J.P.L. – As Joe said, of course, project managers make conservative engineers look like liberals. Part of the problem is cost –you usually do not have ten backup vehicles. A trivial example is the case of solar cells. The first units were made p on n and they were flown in the early years. Then it was shown that n on p solar cells were a factor of 10 better in radiation resistance. But it took 3 years before these much superior cells were used on a flight.

Joe Lundholm, NASA Headquarters – Fred, you made the comment that NASA wouldn't use the system now, even if we had it. Of course NASA is spending much of its money now on Shuttle development. Assuming the budget remains at, say, 3.2 billion beyond this development, it will become available to *use* the Shuttle for experiments. And I believe that there will develop so many interesting Shuttle experiments that we will look back and say, "Weren't we naive and narrow in our predictions, back in 1975, on the uses of space?"

Fred Hansen, NASA Ames Research Center – I agree, Joe. I believe our best hope is to continue to have Headquarter managers that will keep programs like ours alive until the time comes. But in the meantime we must develop our technology so that when the moment arrives we are ready.

Joe Lundholm, NASA Headquarters – Yes, that is why I keep stressing 1980. Horizontal flights will take place at that time and then a great push for experiments should begin.

Fred Hansen, NASA Ames Research Center – As Ned said, however, we need some caution relative to Shuttle which has some rough periods ahead. If it goes, then one can imagine a large number of satellites being launched from it per year – but if it doesn't go we will probably only launch about five Apollo type units per year. This has to influence our applications thinking.

Ned Rasor, Rasor Associates – There is an extremely important point to be made here. What you want to do is to establish some kind of equilibrium situation so that it is not necessary to

continually need to dredge up new reasons to justify your existence. Has the Government, and in particular NASA, learned the value of maintaining a good research base independent of big programs? Do we always need some national emergency, like an astronaut about to die in orbit, to make research programs sell? You speak of the need of exciting the public – will a demonstration of laser energy transmission really get the attention of the public? Are we on the track of getting away from this continual justification need or do you detect no change in that attitude in NASA?

Joe Lundholm, NASA Headquarters – Well, the Shuttle is a big program, taking most of the money. There are significant other programs going on, however, such as Earth resources technology satellites, the Viking launches, etc.

Ned Rasor, Rasor Associates – But can there be an energy conversion category that exists regardless of all these missions?

Joe Lundholm, NASA Headquarters – Well, I think it's a sobering thought that we are funding about one-half of the country's total effort, with ERDA supplying the other half, on gas core reactor design and thermionic convertors. But NASA management has decided, and probably wisely so, that our main effort will be in space rather than in energy development.

Ned Rasor, Rasor Associates – I didn't mean to tie my question simply to energy. In other words, can there be, in NASA, an equilibrium situation where one can investigate, say, basic photon-plasma interactions without tying it to a mission? Does OAST have that kind of charter?

Joe Lundholm, NASA Headquarters – Yes, I think OAST has the tradition of having this.

Fred Hansen, NASA Ames Research Center – Of course there may be a change in NASA budgeting as a result of the energy research necessary. Maybe the situation will change.

Abe Hertzberg, University of Washington – We have been watching research budgets go down during the last decade. But they have bottomed during the last 2 years. There is a general realization by Congress that long-range research is an indispensable part of our economy. Even military thinkers are coming to this viewpoint. If you think about the green revolution, which makes our country the Saudi Arabia of food, you realize that this research has been a long one. But in terms of the effect on our country's economy, the return on the small research investment has been at least a thousandfold.

Max Garbuny, Westinghouse – Of course the military has had the relevance clause which has had a very depressing effect on individual creativity resulting in a depression of both quantity and quality of research. Now, there are some exceptions and one of them has been NASA. It has been willing to support non-mission relevance and this is good and important to national survival.

Ned Rasor, Rasor Associates – I hope they also realize that not only money is important, but that continuity is equally important. That is, one needs approximately 3 years for a good study and about 10 years for final results.

Kurt Wray, Physical Sciences, Inc. – Earlier a statement was made by Fred Hansen that we had better be ready or we may be passed over. It seems to me that when the time comes to be ready for

something, we are not going to be ready for it if we don't know what the something is. I don't know how many of these schemes we have discussed will be a good way to go or a bad way to go. But we're not going to find out until a mission is defined. In the meantime, all we can hope to do is continue these investigations on a very basic level, that is, keep bringing them along until a mission is defined and then scramble to design a system. I really haven't heard anyone define such a system yet, toward which we can design.

Abe Hertzberg, University of Washington – I essentially agree with you. But oftentimes you design the device that creates the mission, you take it to the people, who should be sensitized to it, but they don't know how to put it in. I think *that* is really our problem, that is, how to insert this into the system. Well, by clever timing, I have so arranged things that the time has run out, and I have had the last word on the subject!

Well, gentlemen, thank you. It has been a fascinating meeting and we owe sincere thanks to our hosts, NASA Ames, and especially to Ken Billman who single handedly put the meeting together, for providing us with a fabulous forum.

*U.S. GOVERNMENT PRINTING OFFICE: 1976 - 635-275/82